

**Applied Battery Research for Transportation
(B&R No. VT-1102000)**

**Progress Report
for
Third Quarter FY 2012**

**Contributions from
Argonne National Laboratory
Army Research Laboratory
Brookhaven National Laboratory
Idaho National Laboratory
Jet Propulsion Laboratory
Lawrence Berkeley National Laboratory
National Renewable Energy Laboratory
NAVSEA Carderock
Oak Ridge National Laboratory
Sandia National Laboratories**

August 2012

Applied Battery Research for Transportation Program Third Quarter Progress Report for FY 2012

This quarterly progress report describes the activities being conducted in support of DOE's Applied Battery Research for Transportation (ABR) Program. This program focuses on helping the industrial developers to overcome barriers for Li-Ion batteries for use in plug-in hybrid electric vehicles (PHEVs). In its goal of developing low-emission high fuel economy light-duty HEVs and PHEVs, the DOE and U.S. DRIVE established requirements for energy storage devices in these applications. The Vehicle Technologies Program at DOE has focused the efforts of this applied battery R&D program on the PHEV application.

Through the U.S. DRIVE Partnership, DOE is currently supporting the development of advanced Li-Ion batteries with industry for HEV, PHEV, and EV applications. The industrial developers have made significant progress in developing such batteries for HEV applications and there are new challenges associated with developing viable battery technologies for the PHEV application, especially when targeting the 40-mile all electric range. In addition to the calendar life, abuse tolerance, and cost challenges that exist for Li-Ion batteries in the HEV application, now the issue of providing sufficient energy within the weight and volume requirements becomes a huge challenge, as does cycle life. Also, the abuse tolerance and cost challenges become even greater. The Applied Battery Research for Transportation program is directed at assisting the industrial developers to identify the major factors responsible for the technical barriers and to find viable cost-effective solutions to them. The goal is to facilitate the development of low-cost cell chemistries that can simultaneously meet the life, performance, abuse tolerance, and cost goals that have been established by the U.S. DRIVE Partnership.

The ABR Program is organized into three main technical tasks to address these issues for PHEVs:

- (1) Battery Cell Materials Development—focuses on research, development, and engineering of advanced materials and cell chemistries that simultaneously address the life, performance, abuse tolerance, and cost issues.
- (2) Calendar & Cycle Life Studies—deals with understanding the factors that limit life in different Li-Ion cell chemistries, which are used as feedback to Task 1. This task also deals with the establishment and operation of in-program cell fabrication capabilities for use in these life studies.
- (3) Abuse Tolerance Studies—deals with understanding the factors that limit the inherent thermal and overcharge abuse tolerance of different Li-ion cell materials and chemistries, as well as developing approaches for enhancing their abuse tolerance.

As part of a restructuring of the ABR program Argonne initiated in March a crosscutting project focused on enabling the Argonne high energy composite layered cathode $x\text{Li}_2\text{MnO}_3 \cdot (1-x)\text{LiMO}_2$ ($M = \text{Ni, Mn, Co}$), also referred to as lithium and manganese rich NMC material (LMR-NMC), for the 40-mile PHEV (PHEV-40) application. This class of

materials offers the potential for capacities exceeding 250mAh/g, excellent cycle and calendar life, and outstanding abuse tolerance. However, the material currently possesses a voltage fade issue (and other related issues) that affects its long-term cycle life and needs to be resolved. The voltage fade project results are reported under Task 1 although they cover activities in Task 2 also.

A list of the projects is given in the table, with the individual reports compiled in the Appendix.

Organization	AMR Project ID	AOP Project ID	Title	PI/Contact Point	Page Number
			Task 1: Battery Cell Materials Development		
ANL	ES161		Voltage Fade in the LMR-NMC Materials	Anthony Burrell	6
ANL	ARRA VT076		Materials Scale-Up Facility	Gregory Krumdick	29
ANL	ES167	IV. E.1.1	Process Development and Scale up of Advanced Cathode Materials	Gregory Krumdick	33
ANL	ES168	IV. E.1.2	Process Development and Scale up of Advanced Electrolyte Materials	Gregory Krumdick	38
ANL	ES016	1.1B	New High Energy Gradient Concentration Cathode Material	Khalil Amine	42
ANL	ES019	1.1G	Development of High-Capacity Cathode Materials with Integrated Structures	Michael Thackeray	47
ANL	ES020	1.1C	Developing High Capacity, Long Life anodes	Ali Abouimrane	51
ARL	ES024	A	High Voltage Electrolytes for Li-ion Batteries	Richard Jow	54
ARL	ES024	B	High Voltage Electrolytes for Li-ion Batteries	Kang Xu	57
ANL	ES025	1.1D	Development of Advanced Electrolyte Additives	Zhengcheng Zhang	63
JPL	ES026		Electrolytes for Use in High Energy Li-Ion Batteries with Wide Operating Temperature Range	Marshall Smart	71
INL	ES027		Novel Phosphazene Compounds for Enhancing Electrolyte Stability and Safety of Lithium-ion Cells	Kevin Gering	79

Organization	AMR Project ID	AOP Project ID	Title	PI/Contact Point	Page Number
			Task 1: Battery Cell Materials Development		
ANL	ES028	1.1E	Streamlining the Optimization of Lithium-Ion Battery Electrodes	Wenquan Lu	86
ANL	ES028	1.3	Screen Electrode Materials, Electrolytes, and Additives	Wenquan Lu	88
LBNL	ES029	1.2.2	Scale-up and Testing of Advanced Materials from the BATT Program	Vincent Battaglia	91
ANL	ES113	1.1L	Development of High Voltage Electrolyte for Lithium Ion Battery	Zhengcheng Zhang	93
ANL	ES114	1.2D	High Capacity Composite Carbon Anodes Fabricated by Autogenic Reactions	Vilas Pol	99
ANL	ES115	1.1V	Synthesis and Development of High-Energy and High-Rate Cathode Materials from Ion-Exchange Reactions	Christopher Johnson	103
NAVSEA-Carderock	ES038		High Energy Density Ultracapacitors	Patricia Smith	106
ORNL	ES164	18502	Overcoming Processing Cost Barriers of High Performance Lithium Ion Battery Electrodes	David Wood	109
NREL	ES162		Development of Industrially Viable Battery Electrode Coatings	Robert Tenent	114
			Task 2: Calendar & Cycle Life Studies		
ANL	ES030	2.1B	Fabricate PHEV Cells for Testing and Diagnostics in Cell Fabrication Facility	Andrew Jansen	117
ANL	ES031	2.2B	Model Cell Chemistries	Kevin Gallagher	122
ANL	ES032	2.3A	Diagnostic Evaluations - Electrochemical	Dan Abraham	126
ANL	ES032	2.3B	Diagnostic Evaluations - Physicochemical	Dan Abraham	131

Organization	AMR Project ID	AOP Project ID	Title	PI/Contact Point	Page Number
			Task 2: Calendar & Cycle Life Studies		
LBL	ES033	1.1.1 and 2.4	Strategies to Enable the Use of High-Voltage Cathodes and Diagnostic Evaluation of ABRT Program Lithium Battery Chemistries	Robert Kostecki	135
BNL	ES034	2.4 and 3.3	Life and Abuse Tolerance Diagnostic Studies for High Energy Density PHEV Batteries	Xiao-Qing Yang	138
ORNL	ES165	18502	Online and Offline Diagnostics for Electrodes for Advanced Lithium Secondary Batteries	David Wood	141
ANL	ES111	2.2A	Battery Design Modeling	Kevin Gallagher	149
			Task 3: Abuse Tolerance Studies		
ANL	ES035	3.1	Develop & Evaluate Materials & Additives that Enhance Thermal and Overcharge Abuse	Zonghai Chen	153
SNL	ES036	3.2	Abuse Tolerance Improvements	Chris Orendorff	157
LBL	ES037	3.3	Overcharge Protection for PHEV Batteries	Guoying Chen	162

APPENDIX

Individual Project Progress Reports

TASK 1

Battery Cell Materials Development

Project Number: ES161

Project Title: Voltage Fade in the LMR-NMC Materials

Project PI, Institution: Anthony Burrell, Argonne National Laboratory

Collaborators (include industry): Ali Abouimrane, Daniel Abraham, Khalil Amine, Mahalingam Balasubramanian, Javier Barena Garcia-Ontiveros, Ilias Belharouak, Roy Benedek, Ira Bloom, Zonghai Chen, Dennis Dees, Kevin Gallagher, Hakim Iddir, Brian Ingram, Christopher Johnson, Wenquan Lu, Nenad Markovic, Dean Miller, Yan Qin, Yang Ren, Michael Thackeray, Lynn Trahey, and John Vaughey all from Argonne National Laboratory

Project Start/End Dates: March 2012 / September 2014

Objectives: The objective of the work is to enable the Argonne high energy composite layered cathode $x\text{Li}_2\text{MnO}_3 \cdot (1-x)\text{LiMO}_2$ ($M = \text{Ni, Mn, Co}$), also referred to as lithium and manganese rich NMC material (LMR-NMC), for the 40-mile PHEV (PHEV-40) application. This class of materials offers the potential for capacities exceeding 250mAh/g, excellent cycle and calendar life, and outstanding abuse tolerance. This material currently possesses a voltage fade issue (and other related issues) that effects its long-term cycle life and this issue needs to be resolved.

Approach: Bring together a diverse technical team that will share data and expertise to “fix” voltage fade in the LMR-NMC cathode materials. This will be a single team effort (i.e. not multiple PI’s working independently on the same problem).

- Definition of the problem and limitations of the composite cathode materials.
- Data collection and review of compositional variety available using combinatorial methods.
- Modeling and Theory.
- Fundamental characterization of the composite cathode materials.
- Understand the connections between electrochemistry and structure.
- Synthesis.
- Post treatment/system level fixes.

Milestones:

- (a.) Define voltage fade. September 2012, (Complete)
- (b.) Establish test protocols. September 2012, (Complete)
- (c.) Benchmark materials properties using different synthesis techniques. September 2012, (On schedule)

- (d.) Initiate detailed structural analyses of composite electrode structures at the Advanced Photon Source (APS) by X-ray diffraction, X-ray absorption and pair-distribution-function (pdf) analyses. September 2012, (On schedule)
- (e.) Initiate measurement of entropy changes in standard composite cathode material. September 2012, (On schedule)

Financial data: \$2500 in FY12 (\$4000K/year)

PROGRESS TOWARD MILESTONES

The last quarter represents the initiation of this program and as such much of the work (below) represents early state development and experimental design. Significant data has been generated but at this state it is too preliminary to enable unambiguous interpretations.

This is a large project with many contributions which are heavily interconnected. The organization of this report creates artificial separations in the work in an attempt to portray an incomplete story in a somewhat systematic fashion. At the inception of this project we made out several critical determinations, including defining a baseline material, establishing uniform testing and reporting procedures, and generating a data base. Concurrently, work is underway to characterize the LMR-NMC materials, using both theory and extensive spectroscopy, as well as chemically modify the material. For the propose of this report we will break these activities into separate sections.

Section 1 Underpinning data collection and methodology.

1.1 Baseline materials selection.

While there cannot be a “perfect” baseline material in the LMR-NMC class due to the breath of potential materials compositions and almost infinite processing variations we selected a commercial batch of HE5050 ($0.5\text{Li}_2\text{MnO}_3 \cdot 0.5\text{LiMn}_{0.375}\text{Ni}_{0.375}\text{Co}_{0.25}\text{O}_2$) as our initial reference point. We have 10kg of well characterized material which has been validated in our Materials Validation Facility and electrodes prepared in the Cell Fabrication Facility (CFF). The Toda HE5050 electrodes have also been sent to ARL, JPL, LBNL, BNL, ORNL, NREL and INL and as such present the most well characterized sample of an LMR-NMC material known. This baseline material will be used to validate any post formation modifications (coating for example).

Materials and experimental details:

The “TodaHE5050”. Table 1 summarizes the chemistry and formulation of the positive electrode tested. Galvanostatic cycling is conducted in 2032-type coin cells (1.6 cm² area electrodes) with Li-metal counter electrodes. They are assembled in an Ar-atmosphere glove box (O₂ < 10 ppm, H₂O < 1 ppm) and cycled at exactly 30°C. A standard cycling protocol is used to allow all future work to be directly compared to this LMR-NMC baseline. The protocol uses a cycling current of 10.3 mA-g_{oxide}⁻¹ (~C/13 rate) between 2.0

and 4.7 V vs. Li⁺/Li. The protocol also measures cell resistances via a current interrupt technique at various cell voltages during charging and discharging. The current is stopped for 10 minutes and voltages are recorded before and after the stopping period to estimate the cell resistance. Resistances are recorded during charging at 3.5, 3.9, 4.3, 4.7 V, and during discharging at 4.0, 3.6, 3.2, 2.0 V.

Table 1. Chemistry and Formulation of positive electrode

Active material	86 wt.% Li _{1.2} Ni _{0.15} Mn _{0.55} Co _{0.1} O ₂ (Toda HE5050)
Binder	8 wt.% PVdF (Solvay 5130)
Additives	4 wt.% SFG-6 graphite (Timcal) 2 wt.% SuperP (Timcal)
Current collector	Al, 15 μm
Electrolyte	1.2 M LiPF ₆ in ethylene carbonate : ethyl methyl carbonate (3:7 by wt.)
Separator	25 μm thick (Celgard 2325)
Active loading density	6.64 mg-cm ⁻²
Electrode porosity	37%
Laminate thickness	35 μm

Results and discussion:

Fig. 1 shows charge and discharge voltage profiles of the first 20 cycles. Some capacity loss is apparent. Most of this occurs during and after the activation cycle (0th cycle). A gradual capacity loss from then on is related to a variety of degradation processes, including surface structural changes of the oxide particles, transition-metal ion dissolution from them, particle isolation, as well as cell resistance increase (apparent at the end of charging). Electrochemical cycling and impedance spectroscopy of three-electrode cells show that cell resistance predominantly originates from the positive side, and is related to surface film formation between the active oxide and electrolyte which impedes Li-ion motion, as well as a degrading electronic network.

Capacity loss and cell resistance increase are plotted versus cycle number in Figs. 2 and 3, respectively. Capacity loss proceeds at about 0.5% per cycle for about 20 cycles. Over the same cycle period, the cell resistance at 3.9 V increases by a factor of three. Extended cycling (ongoing in a separate study) shows that capacity loss and resistance increase continue and even accelerate after 20 cycles.

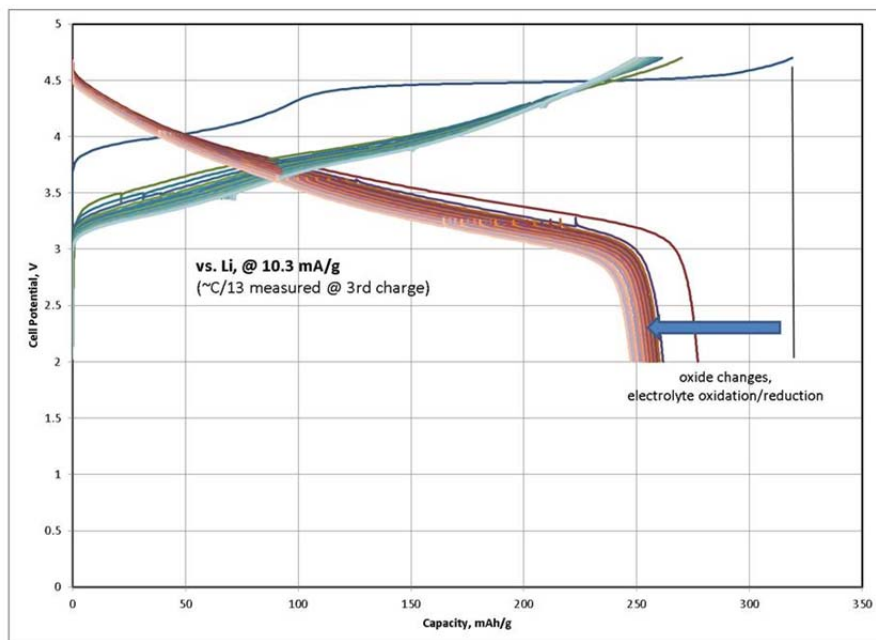


Fig.1 Charge and discharge voltage profiles of the LMR-NMC $0.5\text{Li}_2\text{MnO}_3 \cdot 0.5\text{LiMn}_{0.375}\text{Ni}_{0.375}\text{Co}_{0.25}\text{O}_2$ cycled against metallic Li for 20 cycles.

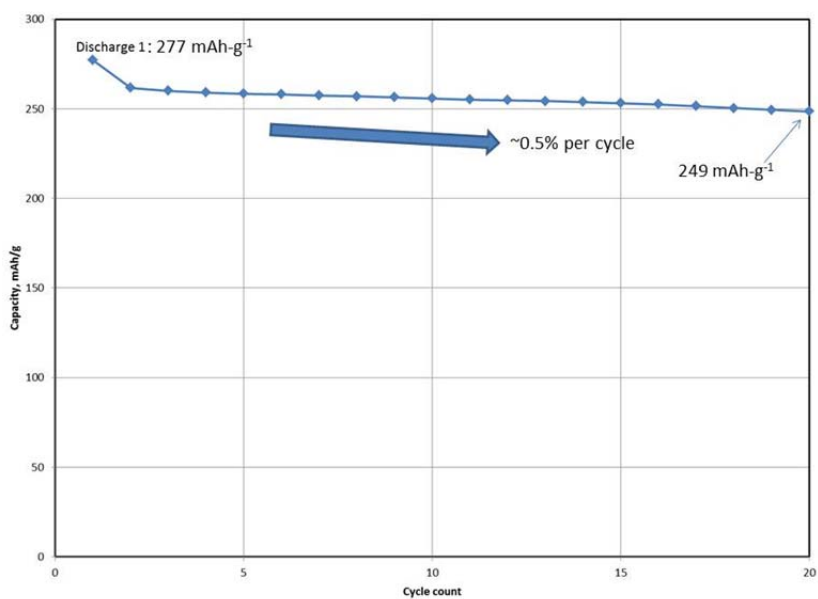


Fig. 2 Discharge capacity during first 20 cycles, measured after initial the activation cycle (cycle 0). The average capacity fade is $\sim 0.5\%$ per cycle with respect to the capacity after the 1st discharge (277 mAh-g^{-1}). Gravimetric capacities are based on the mass of the active oxide.

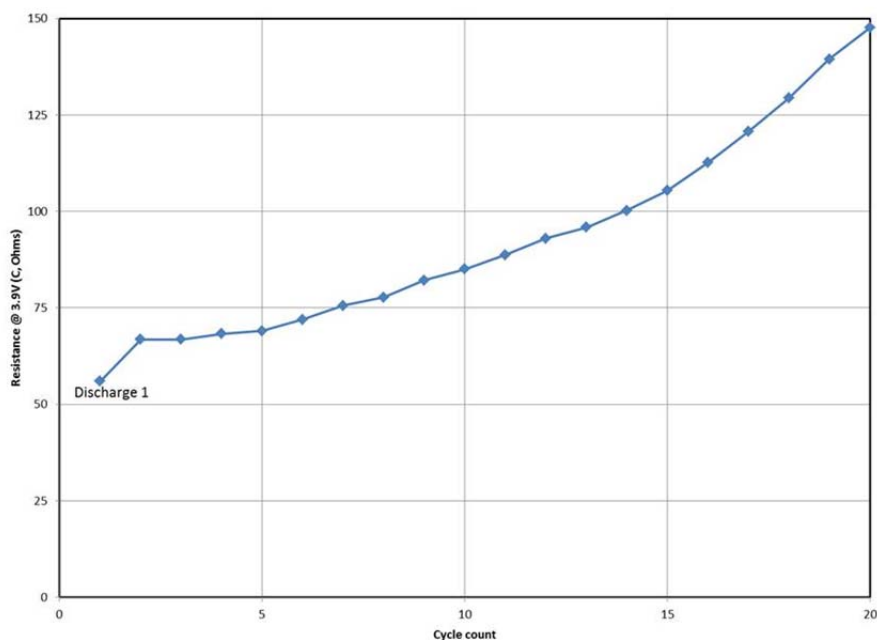


Fig. 3 Cell resistance measured by the current interrupt technique at 3.9 V during charge which corresponds to the lowest cell resistance during one cycle [Gallagher2011]. Cell resistance rises dramatically during cycling. The electrode area is 1.6cm^2 .

To identify voltage fade, capacity loss and increasing cell resistance need to be factored out. One way of doing this is to show capacity-normalized voltage profiles *during charging*. This is shown in Fig. 4. If the normalized charge profiles drop in voltage, despite an increase in cell resistance, the oxide material experiences severe voltage fade. Fig. 4 also shows normalized profiles during discharging. Here, however a drop in voltage is also partly related to increasing cell resistance. Nevertheless, it is clear that cell potentials drop over a wide range of charge states and discharge depths throughout cycling.

Another way of identifying voltage fade is to calculate average charge and discharge voltages and plot them versus cycle number, shown in Fig. 5 where voltage fade is clearly evident: The average charge voltage decreases from 3.95 V to 3.77 V ($\sim 0.24\%$ per cycle, excluding 0th and 1st cycles); and the average discharge voltage decreases from 3.65 V to 3.53 V ($\sim 0.17\%$ per cycle) after 20 cycles. Note, that the biggest drop in average voltage within one cycle occurs after the activation charge. Also, the average charge potential drops faster than the average discharge potential. Extended cycling (ongoing in a separate study) shows that the average voltage still continues to decay after 20 cycles, but possibly at a slower rate.

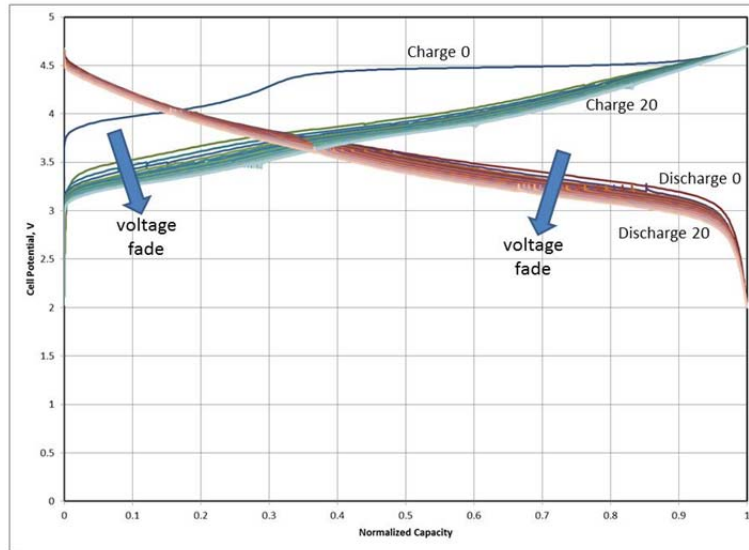


Fig. 4 Voltage profiles during charge and discharge versus normalized capacity. Voltage fade is evident.

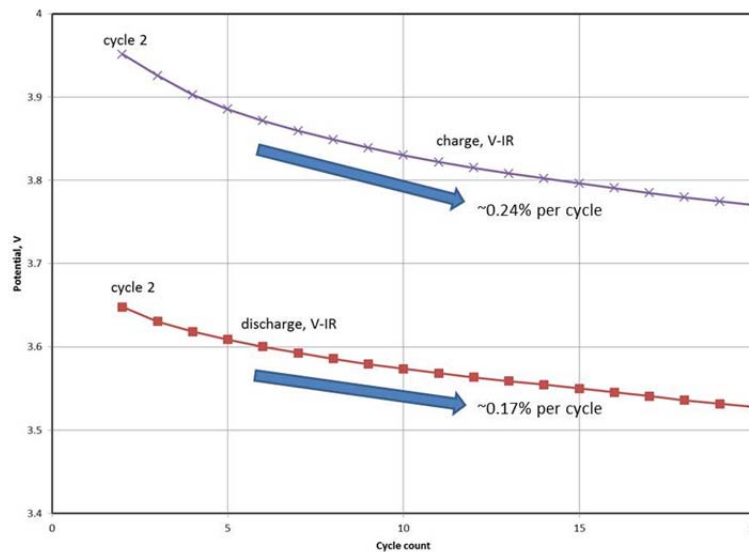


Fig. 5. Resistance-corrected average cell potentials plotted versus cycle number. A continuous drop in average potential exceeding 0.1 V is apparent during charging and discharging. The drop in average charge potential is larger than the drop in the average discharge potential. The average potential is calculated by dividing the measured total energy (current x time x voltage) by the measured cell capacity (current x time).

Voltage fade, along with capacity losses and resistance increases result in suboptimal energy efficiencies and decreasing energy densities, as shown in Fig. 6. The gravimetric energy density drops by approximately 0.7% per cycle with energy efficiencies around 91% for the first 20 cycles.

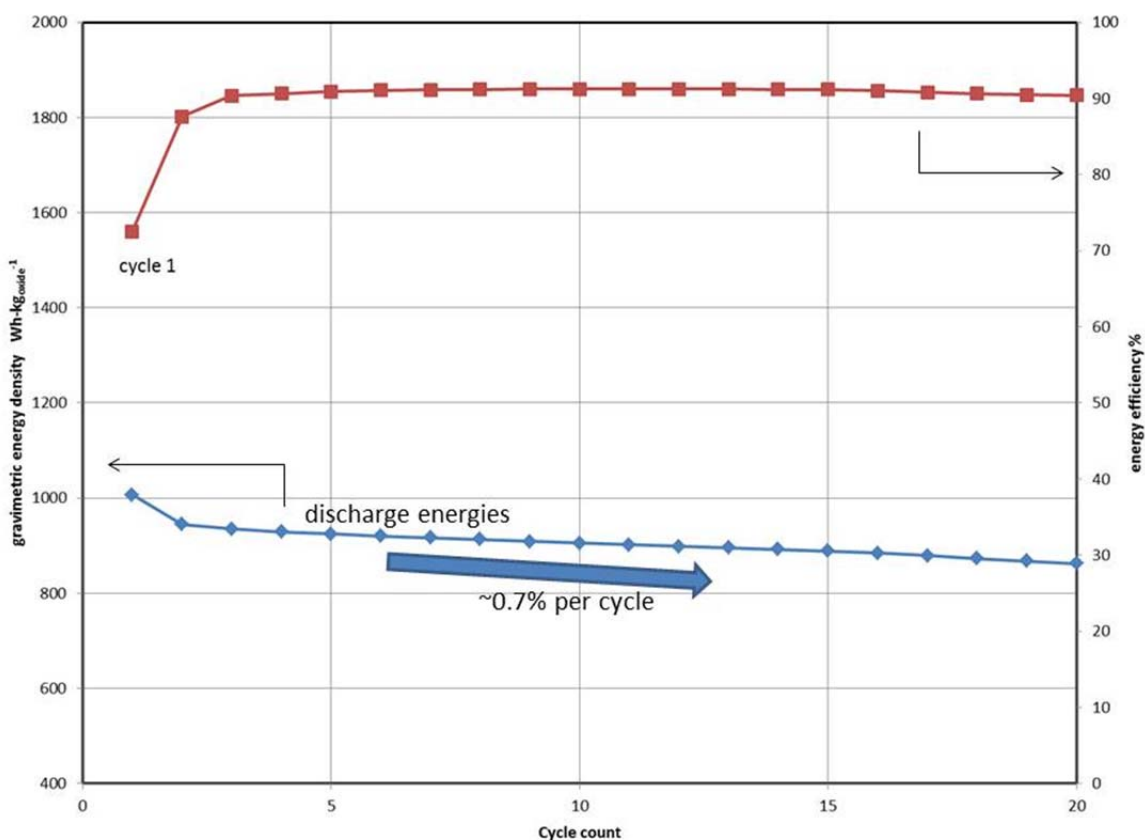


Fig. 6 Gravimetric energy density during discharge and energy efficiency plotted versus cycle number. Voltage fade, along with capacity loss and cell resistance increase, contribute to suboptimal cycling efficiencies and an overall loss in deliverable energy for a given amount of active oxide.

This work provides a baseline for HE5050 that can be used to evaluate the effectiveness of future strategies addressing the problem of voltage fade.

1.2 Modeling Cost targets for LMR-NMC

Using the Battery Performance and Cost model (BatPaC: www.cse.anl.gov/batpac), we have created an initial set of performance metrics to guide materials developers. The most significant value of the LMR-NMC cathodes is realized when they are paired with an advanced Li-ion anode. Thus using the study presented at the AMR (1300 mAh/g GrSi Composite), we evaluated the pack price to the OEM for various cathode material performances. The metrics for cathode performance of a minimum voltage and capacity that still results in pack goals are the following:

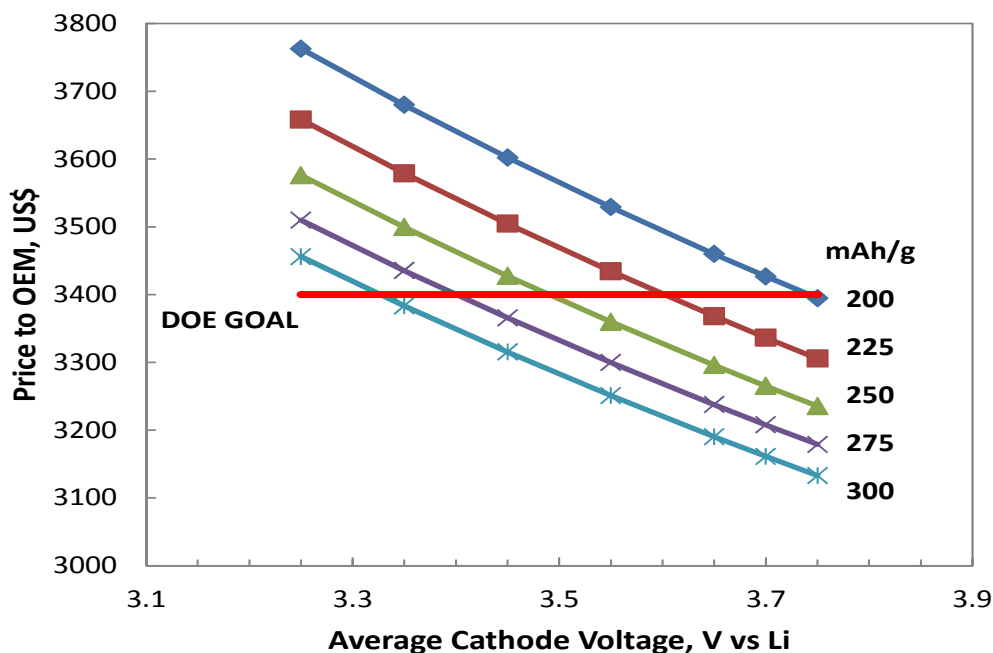


Fig 7. Change in battery pack price to OEM as a function of average voltage and capacity.

Cathode performance target

- For a half cell at C/3 (or C/10)
- 225 mAh/g and $V_{avg} > 3.55$ V (3.60 V) vs Li
- 250 mAh/g and $V_{avg} > 3.45$ V (3.50 V) vs Li
- 275 mAh/g and $V_{avg} > 3.35$ V (3.40 V) vs Li
- $avg\ mV_{ocv}/cycle = 0$?

Ongoing work: Two main factors remain to be determined. First, what is the penalty for operating over a wide voltage window? Current power electronics used in vehicle powertrains have specific voltage and current windows for operation. The LMR-NMC material spans over a much larger voltage window particularly when it is coupled to an advanced Li-ion anode (steep OCV curve). Conversations with an OEM suggest an additional \$500 charge for a DC/DC converter may be necessary to boost the battery's voltage at lower SOC's thus penalizing the use of these advanced materials. We continue to examine this issue. Second, the same OEM has concurred that no voltage fade is acceptable from a battery management perspective. If the voltage changes with time, tracking the SOC is only possible if one can predict the voltage fade reliably and easily over the entire life of the battery.

1.3 Testing: Establishment of a uniform testing protocol to determine voltage fade

The establishment of a standardized protocol for electrochemical testing was critical to the determining success metrics. In the past quarter the first version of a standardized test

protocol was created and distributed to the Argonne voltage fade team. We have created a macro that enabled the quick and reliable processing of the data collected using the protocol. This enables a rapid integration of the cycle data into the database (below) An example output is both the average voltage and IR corrected average voltage versus cycle number. Ongoing work: Further testing protocols will be added as understand and our models indicate more sophisticated protocols.

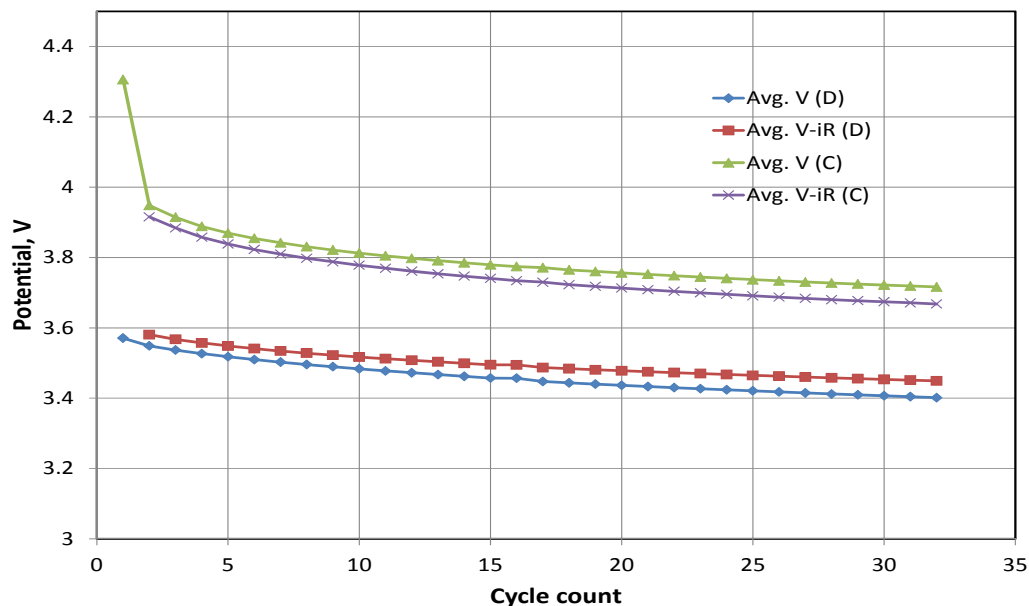
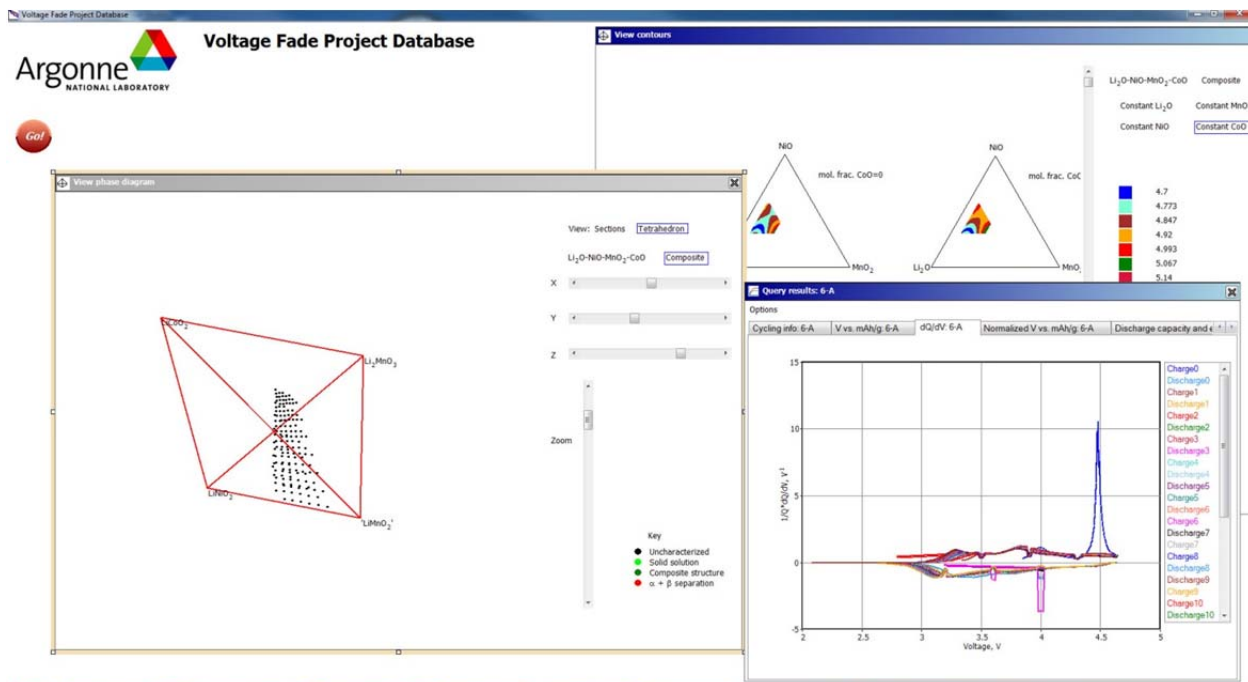


Fig 8. Average voltage vs. cycle for HE5050 tested at C/10 2-4.6V at 55C.

1.4 Database.

We have developed a database, where all data generated in this project will be stored, which is in the process of being populated. Data that is collected using the standard protocols will be included and directly comparable. Other data will be added as it becomes relevant. Once there is sufficient data available mining other factors and correlations will begin.



2.0 Materials characterization.

2.1 Population of the database and examination of materials compositional variation as it relates to voltage fade.

While many different compositions for LMR-NMC have been described no systematic study of how chemical composition affects voltage fade has been undertaken. We have taken advantage of the combinatorial equipment newly available at ANL to synthesize 147 different samples to explore wide range of composition of LMR-NMC material. We expect to get an overview of how the chemical composition, such as Li, Ni, Mn and/or Co concentration affects the voltage fade. There are many synthetic methods available for the formation of cathode materials we selected sol-gel as the most convenient and as the focus of this study is only comparing chemical composition effects and the internal consistency of the synthesis will provide the data required.

Initially the precursors have been prepared and composition is listed in Table 2 with 21 groups, and then each group has seven samples with varied Li content from 1 to 1.6 with 0.1 as the interval. In the past quarter we selected groups 6 and 7 as it has the composition closest to HE50505. The materials have been prepared and laminates made. These materials are under electrochemical evaluation.

Table 2 List of sample compositions from combinatorial synthesis

Group	Li	Ni	Co	Mn	Group	Li	Ni	Co	Mn
1	1~1.6	0.15	0	0.85	12	1~1.6	0.25	0.2	0.55
2	1~1.6	0.15	0.05	0.85	13	1~1.6	0.3	0	0.7
3	1~1.6	0.15	0.1	0.75	14	1~1.6	0.3	0.05	0.65
4	1~1.6	0.2	0	0.8	15	1~1.6	0.3	0.1	0.6
5	1~1.6	0.2	0.05	0.75	16	1~1.6	0.3	0.15	0.55
6	1~1.6	0.2	0.1	0.7	17	1~1.6	0.35	0	0.65
7	1~1.6	0.2	0.15	0.65	18	1~1.6	0.35	0.05	0.6
8	1~1.6	0.25	0	0.75	19	1~1.6	0.35	0.1	0.55
9	1~1.6	0.25	0.05	0.7	20	1~1.6	0.4	0	0.6
10	1~1.6	0.25	0.1	0.65	21	1~1.6	0.4	0.05	0.55
11	1~1.6	0.25	0.15	0.6					

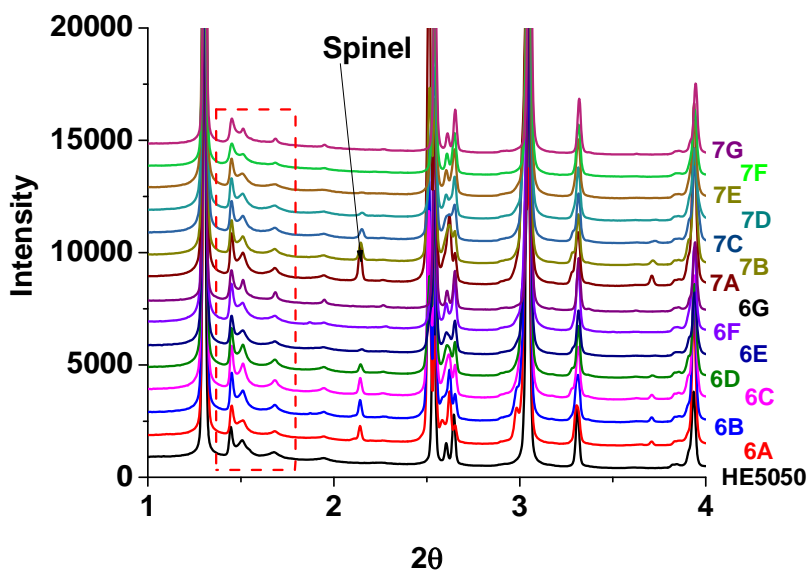


Figure 8 XRD patterns for Group 6 & 7 between 1° and 4° 2θ.

The cycling performance for group 6 is shown in Figure 9. The specific capacity has the following trend: 6F>6E>6G>6D,6A,6B>6C. As expected excess lithium is required to give the enhanced capacity in the LMR-NMC system. Much more experimental data needed before any real conclusions can be reached.

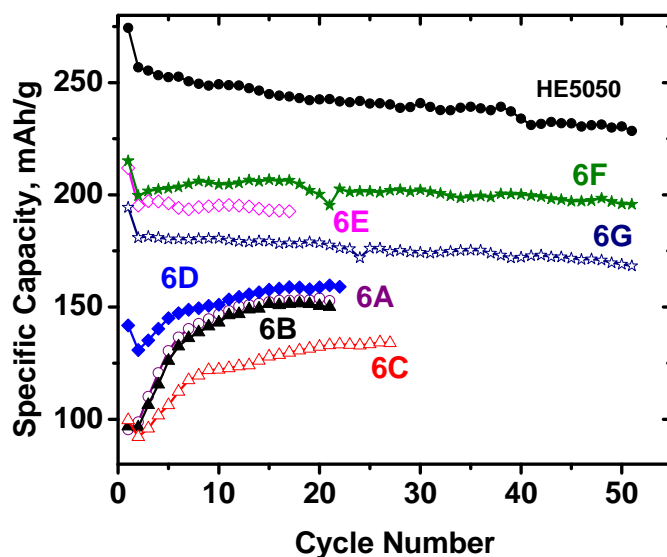


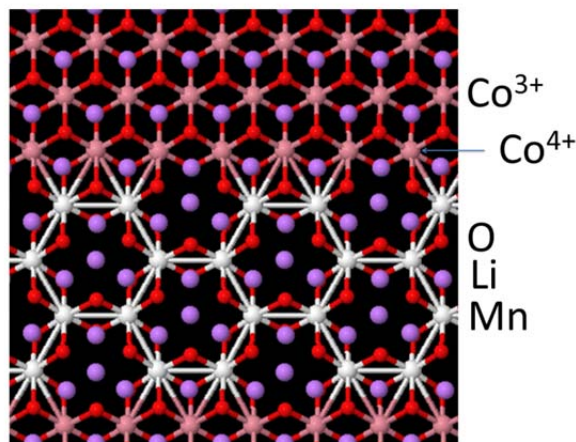
Figure 9 Cycling performances for Group 6 samples with C/10 rate.

2.2 Atomic-scale models of voltage-fade materials

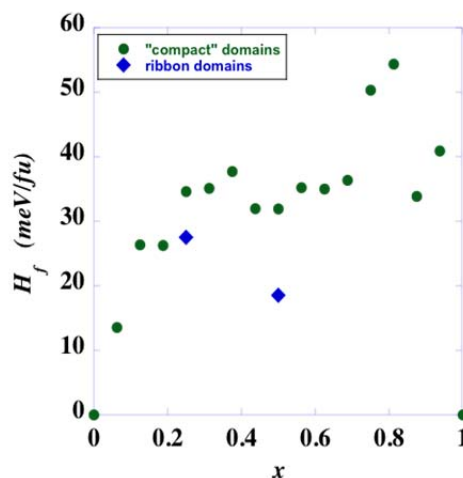
Atomic-scale simulation is one of the diagnostic tools being applied at ANL to gain insight into characteristic atomic arrangements and transformations that occur in materials that exhibit voltage fade. During the first reporting period (03-2012 to 06-2012), first principles DFT calculations at the GGA+U level were performed, with the VASP code, for a set of lithium-excess materials. We have focused initially on the pseudo-binary system $x\text{Li}_2\text{MnO}_3 \cdot (1-x)\text{LiCoO}_2$. The enthalpy of formation has been calculated as a function of x , for Li_2MnO_3 domains with different shapes within the LiCoO_2 matrix. The calculations employed 192-atom supercells, with each layer containing 6×8 ions. 15 different domain sizes were considered, in addition to the endpoints $x=0$, and $x=1$. The preliminary calculations allowed us to extract few heuristic rules with respect to the atomic arrangements within the materials. The formation energy (relative to phase separated Li_2MnO_3 and LiCoO_2) is found positive for all domain sizes, which indicates that phase separation is favored. Furthermore, no critical nucleus size exists below which energy increases with increasing domain size, so that agglomeration is favored for all domain sizes.

A positive surface energy exists between domains (of any size and shape) and the matrix, which is proportional to the under-coordination of the Li ions at the periphery of the domains. Ribbon-shaped domains are lower in energy, for given composition x , than compact domains, owing to their smaller Li under-coordination. Although phase separation and large domains are thermodynamically favored, real cathode materials are expected to contain a distribution of domains that span the full range of sizes; the actual domain size distribution reflects the temperature at which defect mobility and transition-metal atomic transport become negligible upon cooling, following the annealing step employed in most synthesis routes. Preliminary calculations for domains in

$\text{Li}(\text{Mn}_{0.5}\text{Ni}_{0.5})\text{O}_2$ and $\text{Li}(\text{Mn}_{1/3}\text{Ni}_{1/3}\text{Co}_{1/3})\text{O}_2$, along similar lines to those for LiCoO_2 , suggest similar behavior, with slightly lower domain formation energies than in $x\text{Li}_2\text{MnO}_3 \cdot (1-x)\text{LiCoO}_2$, owing to shielding of the Li at domain peripheries by Mn. Finally, simulations were performed of the initial delithiation of $x\text{Li}_2\text{MnO}_3 \cdot (1-x)\text{LiCoO}_2$. It was found that the thermodynamically favorable sites for removing Li and creating $\text{Co}(4+)$ lie at the periphery of the Li_2MnO_3 domains, which enables the $\text{Co}(4+)$ to shield the domain Li ions.



Example of ribbon Li_2MnO_3 domain within LiCoO_2 matrix



Calculated formation enthalpy vs. domain size for $x\text{Li}_2\text{MnO}_3 \cdot (1-x)\text{LiCoO}_2$

Based on these predictions we are looking into experiments that can determine the effect of domain size on voltage fade.

2.3 Thermodynamics

Thermodynamically, the voltage of LMR-NMC is directly related to the entropy change of the composite cathode material. Investigation on thermodynamics of composite electrode should help to shed a light on the root cause of its voltage fade during cycling. In addition, lithium ion diffusion and electronic conductivity of LMR-NMC will be studied to better understand the thermodynamics and kinetics role in voltage fading.

The heat generation of electrode materials during charge and discharge process is generally related the phase transition. Two components, Li_2MnO_3 and LiMO_2 (M denoted as Ni, Co, and Mn), in LMR-NMC material contribute differently to heating, which will be monitored using Isothermal Micro Calorimetry (IMC). The standard HE5050 ($0.49\text{Li}_2\text{MnO}_3 \cdot 0.51\text{LiNi}_{0.37}\text{Co}_{0.24}\text{Mn}_{0.39}\text{O}_2$, Toda) electrode was chosen for in-situ heat generation measurement using 2032 coin type cells.

Using a total voltage window of 2.0V-4.6V, broken in to three segments (low: 2.0V~3.66V; middle: 3.6V~4.3V; and high: 4.2V~4.6V), the electrochemical behavior of HE5050 was characterized in detail. The heating rate of the Li/HE5050 half cells was determined. In Fig. 10, the hysteresis present in the voltage profile is clearly apparent. It is possible that the voltage hysteresis is caused by the activation asymmetry of Li_2MnO_3 component, which appears to be activated throughout whole charging process. Surprisingly the Li_2MnO_3 makes a significant capacity contribution only at the lower voltages. Further work is required to confirm this preliminary observation.

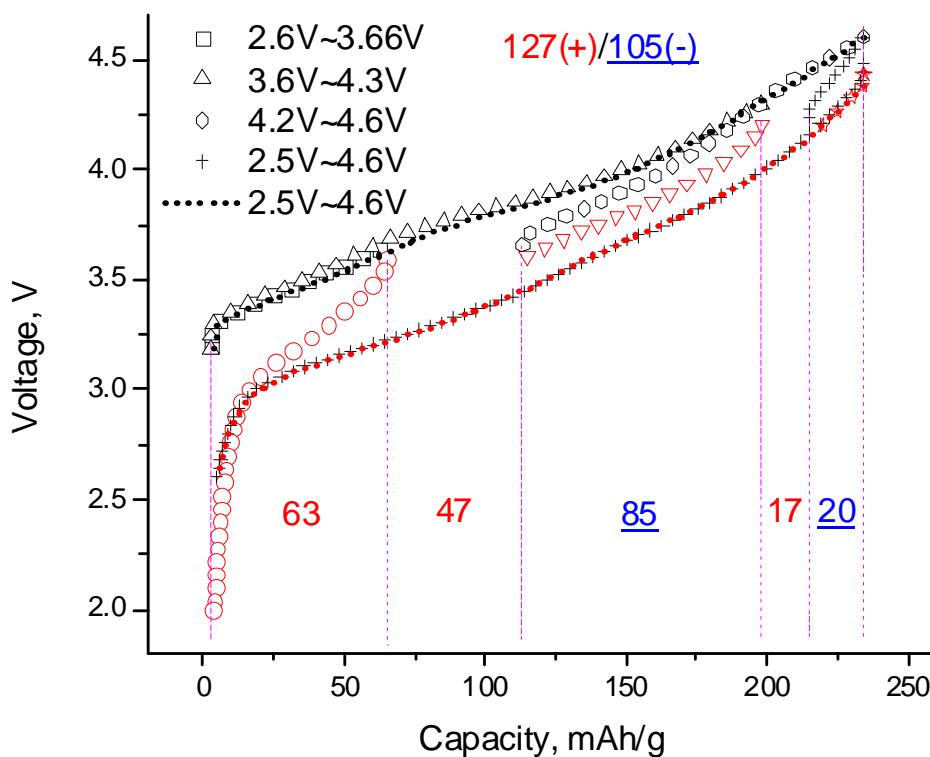


Fig. 10. Voltage profile of HE5050 with various voltage window.

2.4 High-resolution synchrotron x-ray diffraction

The HE5050 raw material shows the typical superlattice reflections in the diffraction pattern due to the ordering of Li and transition metals (TMs) in the TM layers. The main features of the XRD pattern can be well described by a layered structure with the R-3m symmetry. The composition can be written as $\text{HE5050} = \{\text{Li}_{1-x}\text{Ni}_x\}^{3a}[\{\text{Li}_{0.2+x}\text{Ni}_{0.15-x}\text{Mn}_{0.55}\text{Co}_{0.1}\}^{3b}]\text{O}^{6c}$, with 1.0(1)% of Li/Ni exchange between Li in the Li layers and Ni in the TM layers. The lattice parameters are $a_h=b_h=2.85518(2)$ Å, $c_h=14.2479(2)$ Å, and $V_h=100.589(2)$ Å³. If the monoclinic structure (C2/m) is used for profile fits (Fig. 11, left), one gets lattice parameters $a_m=4.94610(8)$ Å, $b_m=8.56459(9)$ Å, $c_m=5.02830(6)$ Å and $\beta_m=109.178(3)$ deg, $V_m=201.184(3)$ Å³ (in comparison with $a_m=4.937(1)$ Å, $b_m=8.532(1)$ Å, $c_m=5.030(2)$ Å and $\beta_m=109.46(3)$ deg, $V=201.137(1)$ Å³ from single

crystal study by Strobel et al.). Note that $b_m/a_m=1.732=\sqrt{3}$. One can see the relationship between the two symmetries: $b_m \sim \sqrt{3} * a_m \sim 3 * a_h$, and $c_m * \cos(\beta_m-90) \sim c_h/3$.

The HE5050 cathode was charged to 4.3 V and 4.7 V, respectively, and then discharged to 2.0 V. The diffraction patterns of the two cathode materials after first cycle were plotted together with the original HE5050 in Fig. 11 (right). The material that was charged to 4.3 V and discharged to 2.0 V (HE5050_4.3V-2V) showed almost identical XRD pattern to the HE5050, except slightly broadened peaks. But the materials that was charged to 4.7 V and discharged to 2.0 V (HE5050_4.7V-2V) has a pattern quite different from the raw HE5050, indicating a clear irreversible structural change. At first glance, the XRD can be well fitted using the layered structure with lattice parameters of $a_h=b_h=2.86370(2) \text{ \AA}$, $c_h=14.3315(2) \text{ \AA}$, and $V_h=101.784(2) \text{ \AA}^3$. There is 3.2(1)% of Li/Ni exchange between Li in the Li layers and Ni in the TM layers, indicating a slightly more Ni moved to the Li layers after the activation. The activated HE5050 (4.7V-2V) has a lattice expansion of 0.30% along a, and 0.59% along c and a volume expansion of 1.19%, in comparison to the raw HE5050.

However, close inspections revealed that all peaks become broad and, especially, (001) peaks are split. This indicated that after the activation (charged above 4.5V), the materials become structurally heterogeneous, or phase separated. One possibility for the phase separation could be that two similar layered structures interconnected (the inset drawing in Fig. 11 (right)), but with a misfit (lattice strain) of 0.26% along the c axis (perpendicular to the layers) and 0.16% within the layers. But there might be other possibilities for the structural inhomogeneity.

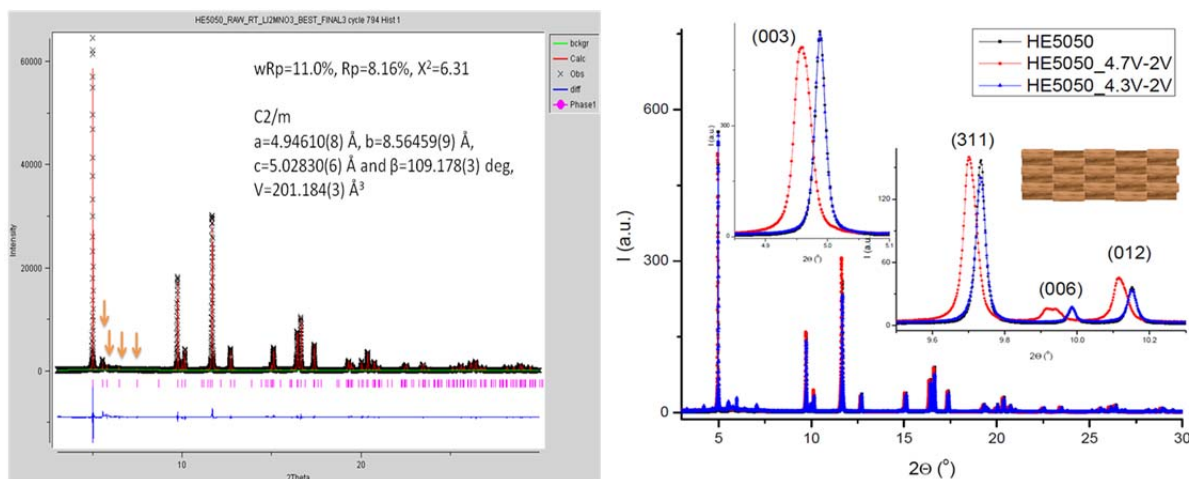


Fig. 11. (left) HR-SXRD pattern of HE5050 shows the super-reflections (020), (110), (11-1), (021), etc. due to the presence of Li/M ordering and associated monoclinic phase (C2/m). (right) HR-SXRD patterns of HE5050, HE5050_4.3V-2V_1cycle, and HE5050_4.7V-2V_1cycle. The inset drawing shows a possible interconnected layered structure for the heterogeneous structure after the activation.

2.5 Electron Microscopy

With electrochemical cycling, the cathode particles undergo structural changes. In this specific work we studied samples harvested from a coin cell that had been cycled 1500 times. Transformations to spinel or “spinel-like” phases are commonly reported and were the dominant transformation observed in this work. However, a transformation to a rock-salt-related structure was also observed. Examples of each of the structures observed are shown in Figure 12, for which Li_2TMO_3 and the layered phases were recorded from the as-prepared material and the spinel and rock-salt structures were recorded from cycled material.

The spinel-like phase is the dominant transformation product observed. This is illustrated in Figure 13, which shows representative electron diffraction and high-resolution images for fresh, as-prepared oxide (Figs. 13 a,c) and for oxide harvested from the coin cell after 1500 cycles (Figs. 13 b,d). Figure 14 shows a region of cycled material that reveals the rather uniform transformation to spinel-like phase over a larger region.

With respect to the ideal layered phase, the transformation to spinel-like involves reordering of both lithium and TM (with a corresponding relaxation of oxygen) as can be seen by comparing Figs. 12b and 12c. The relaxation of TM to “Li positions” likely takes place during lithium extraction, induced by local structural distortions as Li moves out of the structure. This leaves TM-vacancy planes within the crystal in the delithiated state. However, it is important to note that the as-prepared oxide includes domains of both the layered $\text{Li}(\text{Mn},\text{TM})\text{O}_2$ phase and $\text{Li}_2(\text{Mn},\text{TM})\text{O}_3$, the latter already incorporating mixed layers containing both Li and TM (Fig 12a). The presence of these pre-existing mixed layers is important – extraction of Li from these layers also leaves TM-vacancy layers. Thus, when Li is reintroduced, it faces an array of planes that begin to look more and more alike. In essence, the “pure” Li planes are lost and the structure tends towards a more uniform distribution of mixed TM-Li planes. From Fig. 12d, one can see that in the limit the rock salt structure may be a natural terminal phase.

While our observations show this reordering of TM, comparing the degree of cation mixing observed experimentally with structural models suggests that the reordering on the cation positions generally is not going as far as a mixing on every second or every cation position mixing (which would yield simple rock salt) even for many cycles, but it is moving in that direction. Rock salt is indeed one of the phases we observe in highly cycled material although only as a minority phase.

In future work we will study the delithiated structures to confirm our model for TM rearrangement. Studies of cathode oxides with other TMs may also be studied in order to identify the correlation of e.g. cation reordering, structural and valence changes on capacity and voltage fade.

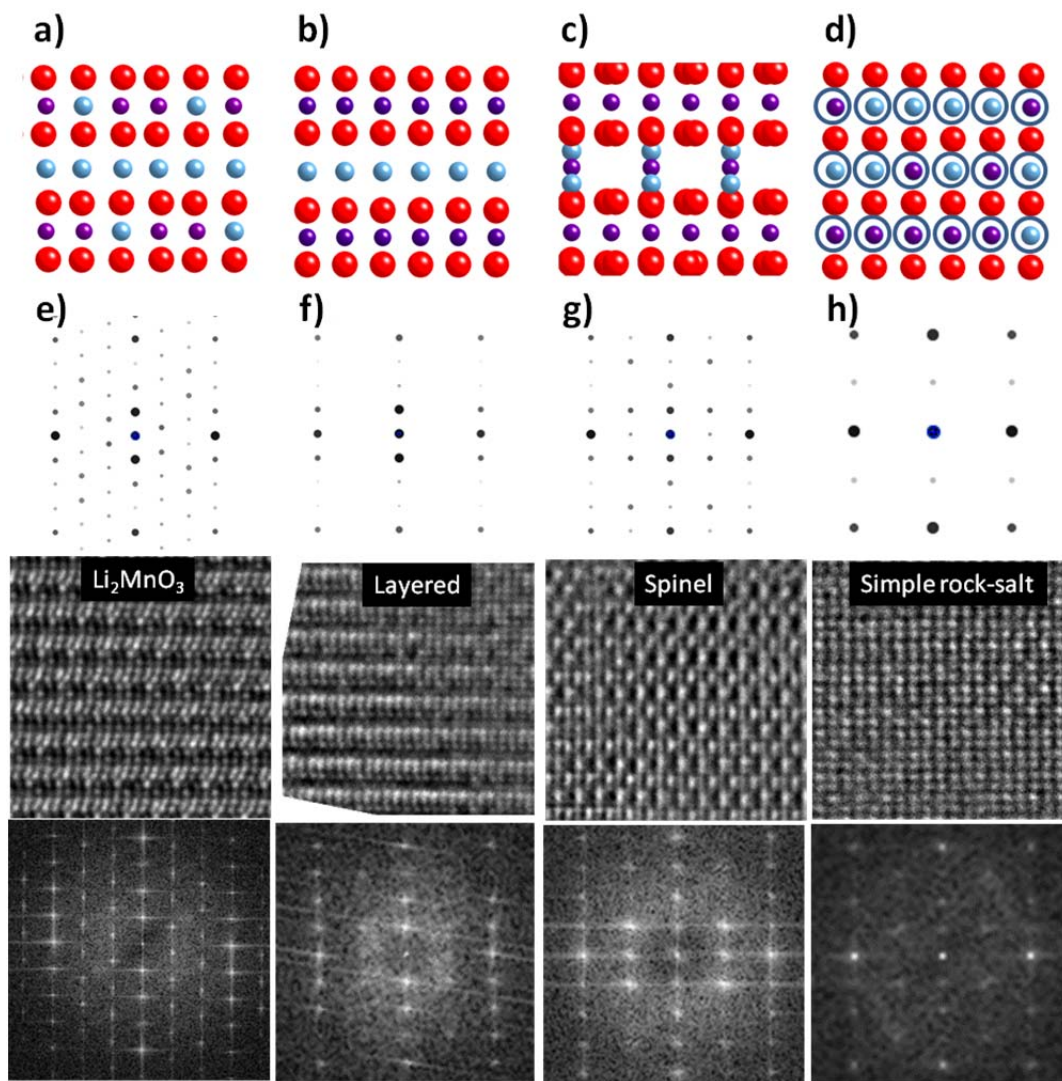


Figure 12: Crystal structure models for Li_xTMO_2 phases: (a) Li_2TMO_3 (110 plane), (b) layered (1-100), (c) spinel (112) and (d) simple rock-salt (112). Oxygen is drawn as red, TM as purple, and Li as blue. The atom columns with circles represent randomly mixed Li/TM columns. The corresponding experimental electron diffraction patterns, high resolution images, and Fourier transform patterns from the high-resolution images are shown under each crystal model (e-h)

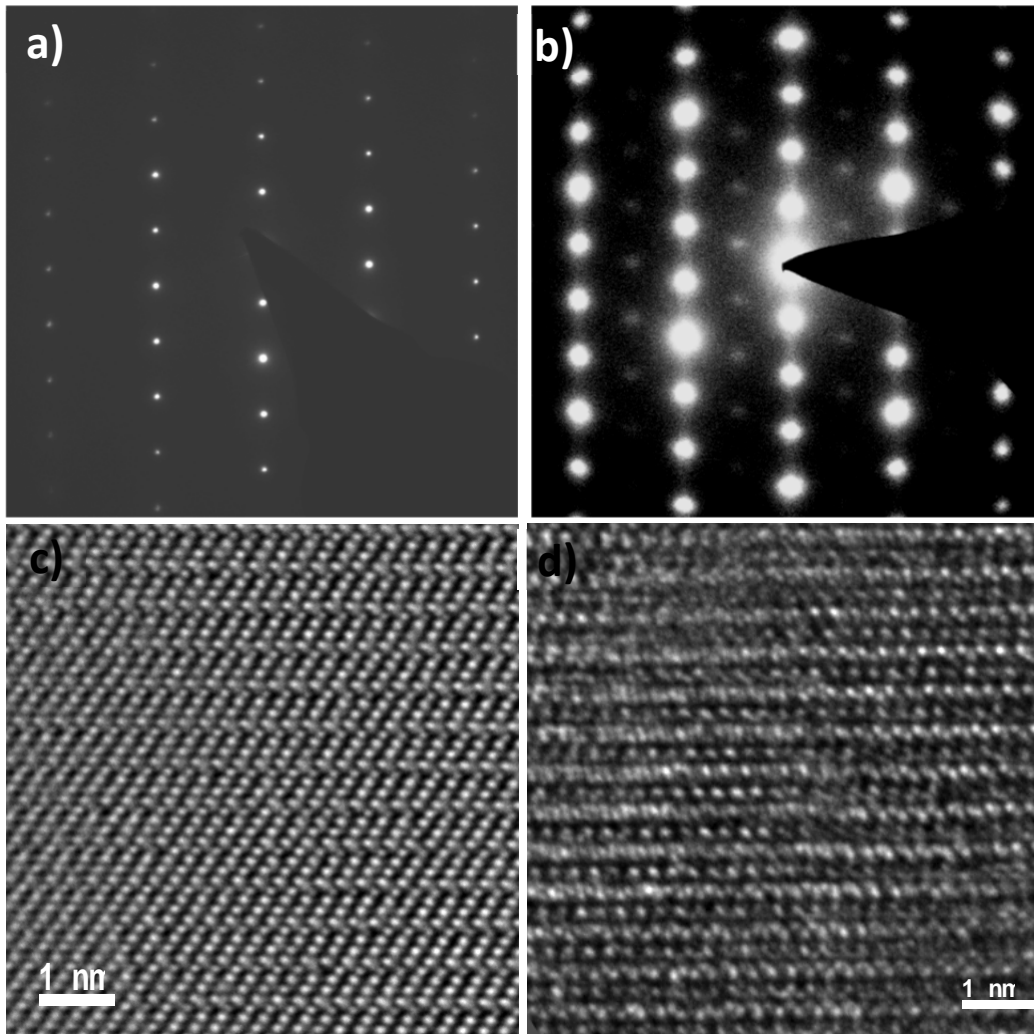


Figure 13: Electron diffraction patterns from (a) fresh and (b) 1500 times cycled $\text{Li}_{1.2}\text{Ni}_{0.15}\text{Mn}_{0.55}\text{Co}_{0.1}\text{O}_2$ showing the transformation from layered to spinel-like structure. Corresponding high resolution images are presented in (c) and (d).

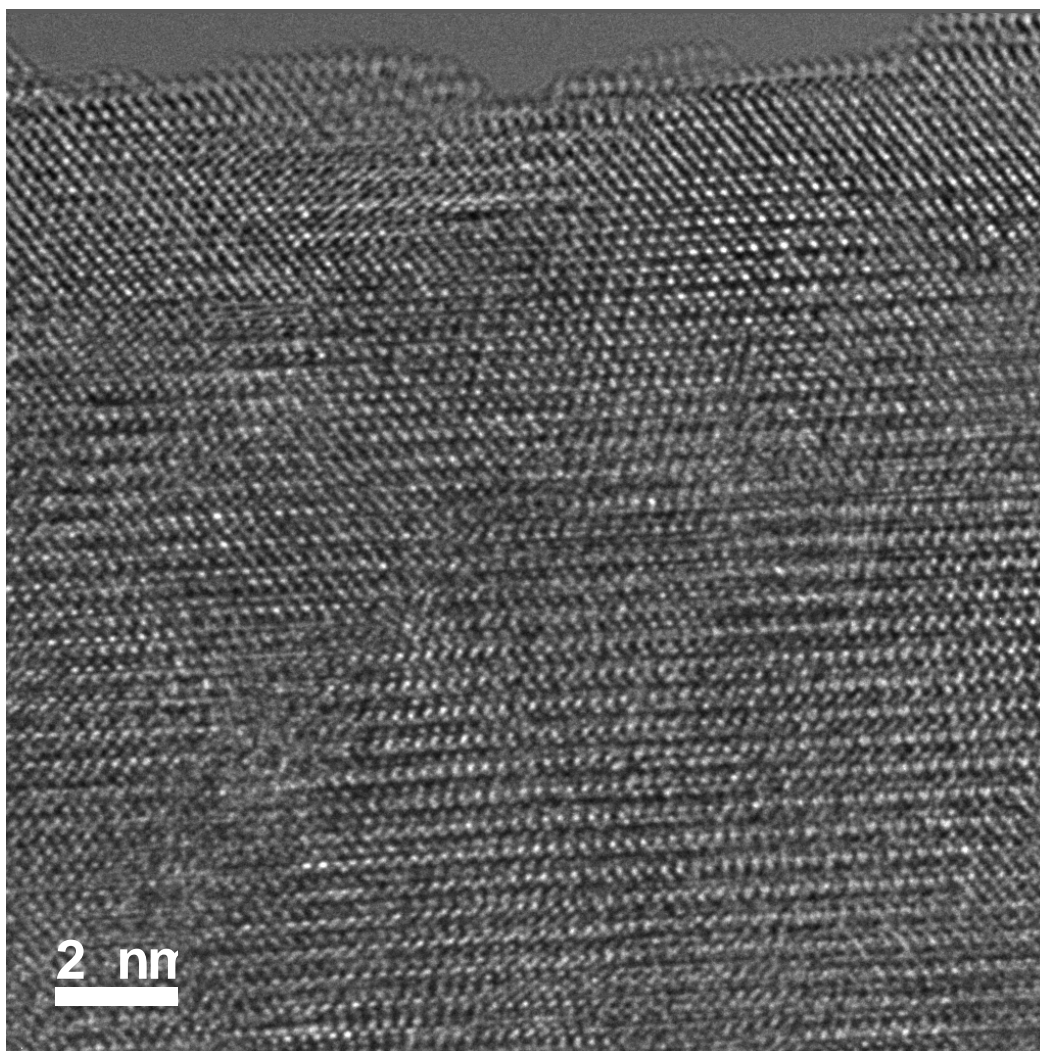
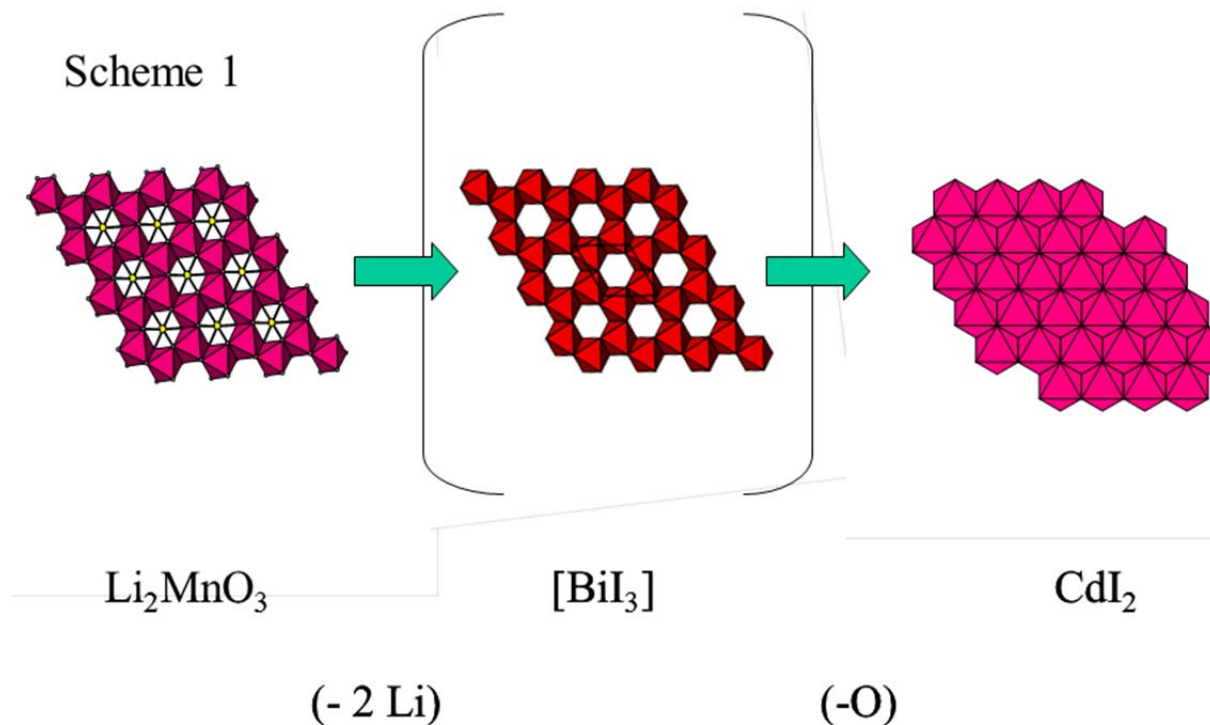


Figure 14: High resolution image of $\text{Li}_{1.2}\text{Ni}_{0.15}\text{Mn}_{0.55}\text{Co}_{0.1}\text{O}_2$ after cycling (1500x) showing the uniform transformation to spinel-like phase.

3.0 Synthetic activities

In this synthesis project, our objective is to evaluate structure-function property relationships in the composite $x\text{Li}_2\text{MnO}_3 \bullet (1-x)\text{LiMO}_2$. Based upon our theory work (above), the domain size of Li_2MnO_3 component has a pronounced effect on the total energy of the system: the smaller the domain size distribution, then the higher energy it takes to remove lithium from the host matrix. This is because the charge on the Li is less screened by adjacent tetravalent Mn (i.e. Li_2MnO_3 component). Conversely, the voltage of reinsertion of lithium cations into the matrix would also be lower. If this is the case and the *domains become smaller with cycling, then voltage fade occurs*. Our approach thus is to systematically manipulate the initial size of the domains in the composite and consequently observe the rate of change in voltage fade.



First we are studying single phase Li_2MnO_3 as a model system for the composite $x\text{Li}_2\text{MnO}_3 \bullet (1-x)\text{LiMO}_2$. During this past quarter we have synthesized three large batches of single phase Li_2MnO_3 with different particle sizes and subjected the materials to acid-treatment to exchange lithium for protons, then continuing to oxygen removal. XRD shows that simple proton insertion causes a shearing of the layers and a phase change from octahedral to prismatic layer stacking. In one case, all Li and oxygen was removed, the TM ordering in the transition metal layer was lost, and Li vacancies were filled by rearrangement of Mn. This process therefore mimics electrochemical removal of Li and oxygen from the $x\text{Li}_2\text{MnO}_3 \bullet (1-x)\text{LiMO}_2$ composite during high-voltage activation with rearrangement of transition metals in the TM layer. We have assembled a structural model to describe this process (Scheme 1). The structural prototypes involve an intermediate $[\text{BiI}_3\text{-type structure}]$ with its vacancies, and finally vacancy-condensation to leave layered CdI_2 . hcp MnO_2 (Li_2O removal from Li_2MnO_3) therefore has the CdI_2 structure with direct O-O interactions above and below the layer which may cause severe crystal distortions, and by analogy, severe distortions in delithiated ‘activated’ composite $x\text{Li}_2\text{MnO}_3 \bullet (1-x)\text{LiMO}_2$.

One of the key issues in the voltage fade materials is the formation of spinel like domains in the cycled product (see TEM data above). We have been deliberately embedding a spinel component in composite $x\text{Li}_2\text{MnO}_3 \bullet (1-x)\text{LiMO}_2$ ($\text{M}=\text{Mn}, \text{Ni}, \text{Co}$) ‘layered-layered’ structures to improve their electrochemical properties and cycling stability. In general, efforts are being focused on the preparation of three-component ‘layered-layered-spinel’ electrodes by lowering the lithium content of a parent ‘layered-layered’ $x\text{Li}_2\text{MnO}_3 \bullet (1-x)\text{LiMO}_2$ material (and substituted derivatives) while maintaining a constant Mn:M ratio. Such ‘layered-layered-spinel’ compounds are located on the tie-line between selected $x\text{Li}_2\text{MnO}_3 \bullet (1-x)\text{LiMO}_2$ and $\text{LiM}'_2\text{O}_4$ spinel compositions, as shown

schematically in a compositional phase diagram (Fig. 15). With a constant Mn:M ratio, these systems can be normalized to a simpler notation; for example, the $0.5\text{Li}_2\text{MnO}_3 \cdot 0.5\text{LiMn}_{0.5}\text{Ni}_{0.5}\text{O}_2$ ('layered-layered') – $\text{LiMn}_{1.5}\text{Ni}_{0.5}\text{O}_4$ ('spinel') system, in which the Mn:Ni ratio remains constant at 3:1, reduces simply to $\text{Li}_x\text{Mn}_{0.75}\text{Ni}_{0.25}\text{O}_y$, with the end-members having x and y values of 1.5 and 2.5 ($\text{Li}_2\text{MnO}_3 \cdot 0.5\text{LiMn}_{0.5}\text{Ni}_{0.5}\text{O}_2$) and 0.5 and 2.0 ($\text{LiMn}_{1.5}\text{Ni}_{0.5}\text{O}_4$), respectively.

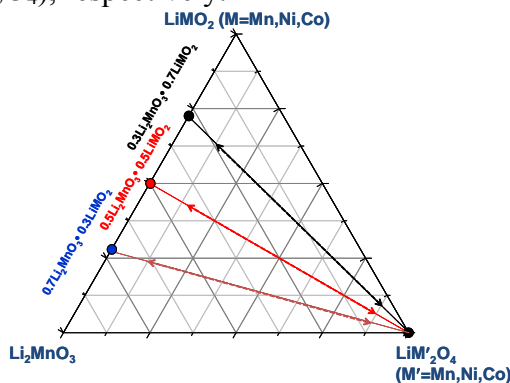


Fig. 15. Compositional phase diagram of a 'layered-layered-spinel' system with $x\text{Li}_2\text{MnO}_3 \cdot (1-x)\text{LiMO}_2$ (layered-layered) and $\text{LiM}'_2\text{O}_4$ (spinel) components.

During the past quarter, emphasis was placed on a targeted composition $\text{Li}_{1.30}\text{Mn}_{0.75}\text{Ni}_{0.25}\text{O}_{2.40}$ in which $x = 1.30$ and $y = 2.40$ (or $0.8[0.5\text{Li}_2\text{MnO}_3 \cdot 0.5\text{LiNi}_{0.5}\text{Mn}_{0.5}\text{O}_2] \cdot 0.2\text{Li}_{0.5}\text{Mn}_{0.75}\text{Ni}_{0.25}\text{O}_2$ in 'layered-layered-spinel' notation) with 20% spinel, and a targeted composition $\text{Li}_{1.40}\text{Ni}_{0.22}\text{Co}_{0.12}\text{Mn}_{0.66}\text{O}_{2.42}$ in which $x = 1.40$ and $y = 2.42$ (alternatively, $0.95[0.44\text{Li}_2\text{MnO}_3 \cdot 0.56\text{LiNi}_{0.39}\text{Co}_{0.22}\text{Mn}_{0.39}\text{O}_2] \cdot 0.05\text{Li}_{0.50}\text{Mn}_{0.75}\text{Ni}_{0.25}\text{O}_2$) with 5% spinel. (Note: for these calculations, the formula of spinel was $\text{Li}_{0.5}\text{Mn}_{0.75}\text{Ni}_{0.25}\text{O}_2$ rather than $\text{LiMn}_{1.5}\text{Ni}_{0.5}\text{O}_4$). The electrochemical data of a $\text{Li}/\text{Li}_{1.30}\text{Ni}_{0.25}\text{Mn}_{0.75}\text{O}_{2.40}$ cell, when charged and discharged between 4.6 – 2.0 V at 15 mA/g, are provided in Figure 16. The cycling data in Fig. 16a shows that the Li_2MnO_3 component of the composite cathode is slowly and continuously activated during the charge process at 4.6 V until a stable reversible capacity of approximately 225 mAh/g is reached after 20 cycles with a steady voltage profile, which is particularly noticeable between 25 and 33 cycles (Fig. 16b).

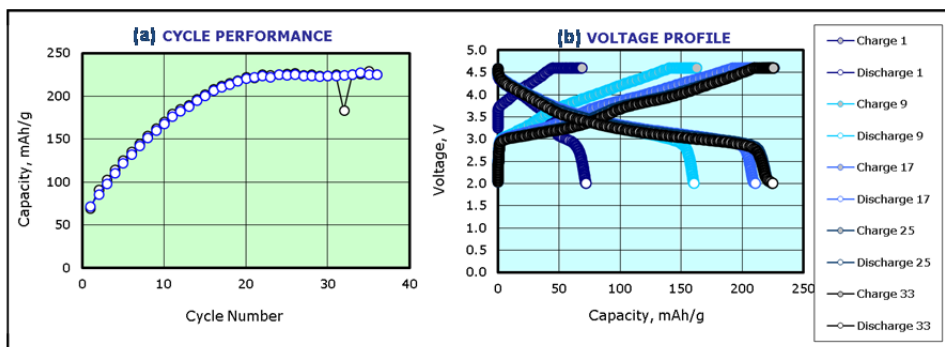
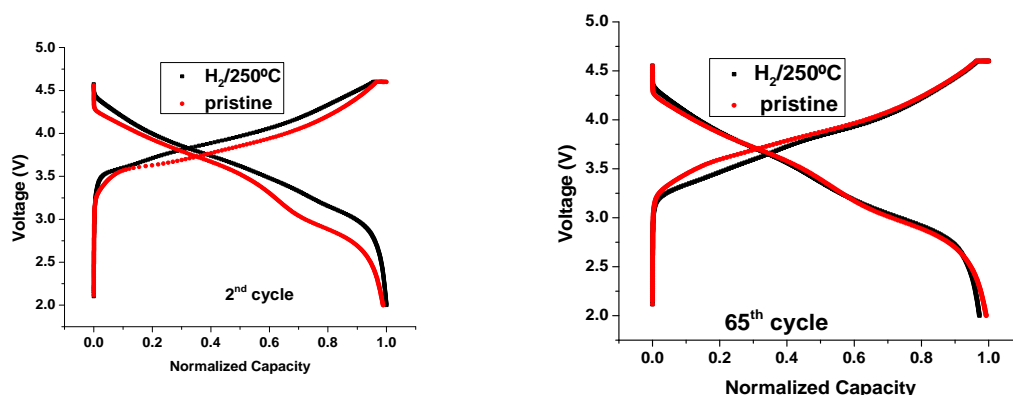


Fig. 16. Electrochemical data of a $\text{Li}/\text{Li}_{1.3}\text{Ni}_{0.25}\text{Mn}_{0.75}\text{O}_{2.40}$ cell (4.6-2.0 V; 15 mA/g): a) capacity vs. cycle number plot, and b) charge/discharge profiles.

One of the alternatives to changing the synthesis of the material is some form of post treatment that may stabilize the structure during cycling. During this quarter, we studied the effect of mild thermal reducing treatment under H_2 on the voltage profile of the Toda He5050. This material was heated for 3 h at 250°C under a flow of H_2 gas (3.5% H_2 in He) in a tube furnace. XPS shows a partial reduction of Mn^{4+} to Mn^{3+} . Significant voltage fade was observed with cycling and after 65 cycles the heated and pristine material provide similar discharge voltage plateau. *Hydrogen reduction does appear to have a significant effect and this work is discontinued.* The evaluation of coated electrodes, for example with AlF_3 , is on-going; the coating results will be presented and discussed in a subsequent report.



4.0 New capabilities

4.1 Application of Electrochemical Quartz Crystal Microbalance

A new electrochemical quartz crystal microbalance (EQCM), capable of detecting nanogram mass changes on electrode surfaces, has been purchased from Q-Sense and is in the process of being set-up in an inert atmosphere glove box. A postdoctoral appointee, Zhenzhen Yang, has been hired and starts on July 23rd 2012. Dr. Yang has a strong background in nanoscale materials characterization and electroanalytical chemistry and will be in charge of executing these experiments for half of her time.

4.1 Solid State NMR

A purchase order was finalized and submitted to ANL Purchasing in May 2012 for a 300 MHz Solid State NMR dedicated magnet and spectrometer with high spinning speed capability; submission to Bruker Inc. expected July 2012. A static probe is also included to initiate additional in-situ studies.

TASK 1

Battery Cell Materials Development

Project Number: ARRAVT076 **2012 Q3 update**

Project Title: Materials Scale-Up Facility

Project PI, Institution: Gregory Krumdick, Argonne National Laboratory

Collaborators (include industry):
Barton Malow, Design Build Subcontractor

Project Start/End Dates: start: 4/1/2010; end: 3/31/2012

Objectives: The objective of this project is to design and build a pilot-scale battery-materials production facility (Materials Engineering Facility) to scale up bench-scale battery chemistries and produce bulk quantities of new materials for evaluation in prototype cells to enable quick turnaround validation of new materials chemistries. Such a facility is a key missing link between the bench-scale development of battery technology and high-volume manufacturing of large-format advanced batteries for transportation applications. One of the primary contributing factors to the lack of a significant domestic Li-ion battery manufacturing capability is the lack of adequate facilities to enable the research community to produce quantities of materials for prototype cells to enable quick-turnaround validation screening of new materials chemistries throughout the R&D process.

Approach: To enable the process development and scale-up of new battery materials, the facility is planned to have:

- Suitable space – The Materials Engineering Facility will contain high hazard Group H-Occupancy labs to accommodate the larger volumes of hazardous materials used as processes are scaled up.
- Modular process equipment – The facility and equipment design will incorporate modular equipment to enable quick change out of unit operations, as required for a range of materials process R&D.
- Analytical lab for materials analysis – A dedicated analytical lab to characterized materials during scale up allows for rapid process optimization and can also provide materials quality assurance analysis.
- Staff experienced in process scale-up R&D – Scientists and engineers trained and experienced in process development and scale up are a critical component to the program.

The approach to achieve the facility plan is to:

- Establish conceptual design of facility (CDR), Establish Design Build contract for facility.
 - Following the principals of the DOE Project Management Process.
- Establish interim scale-up labs during the design and construction of the facility.

- To allow for the scale up of battery materials to begin now.
- Prepare the environmental and safety plans and NEPA for the facility construction and interim labs.
- Begin work in interim labs to demonstrate that scaling is possible.

Milestones:

Materials Engineering Facility Construction – All Milestones have been completed

Milestone / Deliverable	Description	Date	Status
Milestone 1	Complete full facility design (CDR)	10/1/2010	COMPLETED 8/19/2010
Milestone 2	Award full facility construction contract	2/1/2011	COMPLETED 11/22/2010
Deliverable 1	Open interim facility (3 facilities) 2 opened 9/17/10, 1 opened 6/13/11	9/30/2010	COMPLETED 9/17/2010
Deliverable 2	Complete full facility construction	2/1/2012	COMPLETED 1/31/2012
Deliverable 3	Open full facility	3/31/2012	COMPLETED 3/30/2012

Interim Facilities and Equipment – All Milestones have been completed

Milestone / Deliverable	Description	Date	Status
Milestone 1	Interim facility equipment purchased & installed (3 facilities)	12/31/2010	COMPLETED 9/17/2010
Milestone 2	Production scale-up facility equipment purchased & accepted	12/31/2011	No Funding Allocated
Deliverable 1	Interim facility open (3 facilities) 2 opened 9/17/10, 1 opened 6/13/11	9/30/2010	COMPLETED 9/17/2010
Deliverable 2	Full facility open	3/31/2012	COMPLETED 3/30/2012

Financial data:

Total project duration: 24 mo.

Construction funds for facility: \$3.3M

Capital equipment for process and analytical equipment: \$2.5M

Progress towards construction milestones:

- The environmental and safety plans and NEPA for the facility construction and interim labs have been approved.
- First Construction milestone completed – 8/19/2010
 - Jacobs Engineering drafted the Conceptual Design Report and Fire Protection Assessment
- Second Construction milestone completed – 11/22/2010
 - Design Build contract was awarded to Barton Malow
- Construction deliverable #1 completed – 9/17/2010
- Construction deliverable #2 completed – 2/1/2012
 - **Beneficial occupancy was issued on 1/31/2012**
- Construction deliverable #3 completed – 3/31/2012
 - **Final occupancy was issued on 3/30/2012**



Figure 1. Materials Engineering Research Facility Construction Site – March 28, 2012

During the last quarter, we have relocated our interim electrolyte materials scale-up lab and interim analytical lab to the new facility and have begun work in the labs.



Figure 2. Electrolyte materials process development lab.



Figure 3. Electrolyte materials scale-up lab.



Figure 4. Analytical lab.

TASK 1

Battery Cell Materials Development

Project Number: IV.E.1.1 (ES167)

2012 Q3 update

Project Title: Process Development and Scale up of Advanced Cathode Materials

Project PI, Institution: Gregory Krumdick, Argonne National Laboratory

Collaborators (include industry):

Young-Ho Shin, Argonne National Laboratory

Kaname Takeya, Argonne National Laboratory

Project Start/End Dates: start: 10/1/2011; end: 9/30/2013

Objectives: Next generation cathode materials have been developed at the bench scale by a number of researchers focusing on developing advanced lithium ion battery materials. Process engineers will work with these researchers to gain an understanding of the materials and bench-scale processes used to make these materials and then scale-up and optimize the processes.

The objective of this task is to conduct process engineering research for scale-up of Argonne's next generation high energy cathode materials. These materials will be based on NMC chemistries and may include lithium rich technology, layered-layered and possibly layered-spinel classes of cathode materials. The current multistep batch processes, capable of producing approximately 2 kg of material per week using a 4L reactor will be optimized and scaled up. Scaling up the process involves modification of the bench-scale process chemistry to allow for the semi-continuous production of material, development of a process engineering flow diagram, design of a mini-scale system layout, construction of the experimental system and experimental validation of the optimized process. The design basis for scale-up will be based on a 20L reactor capable of producing a 10 kg batch of cathode materials per week.

During Q1, it was reported that process optimization of $\text{Li}_{1.14}\text{Mn}_{0.57}\text{Ni}_{0.29}\text{O}_2$ on the 4L system was completed and work had begun on scaling the process to the 20L system. A primary issue identified on the 4L system was the fact that prior to reaching steady state, particles continued to grow past the optimal size forming a mixture of sized particles both larger and smaller than optimal. A technique was identified and tested to overcome this issue to allow for continuous processing. During Q2, the method for the prevention of plugging was revised to improve control of particle size, distribution and morphology and was tested on the 20L system.

Approach: Integrity of particle growth control technology on the 20L system without plugging was achieved after several system revisions. Desired precursor particle size and its distribution were obtained with spherical morphology for $\text{Li}_{1.35}\text{Ni}_{0.33}\text{Mn}_{0.67}\text{O}_{2.35}$. Using this precursor (#2012-07-11), re-optimization of Li excess and calcination condition will

be carried out to achieve high C-rate performance and long cycle life. Optimized 1 kg #2012-07-11 cathode will be tested by the cell fabrication facility during the next quarter. Upon validation of the material, a 10kg cathode batch with optimal particle size will be synthesized next quarter.

Schedule and Deliverables: Deliverables will include scaled materials for independent testing, publications and a topical report.

Financial data:

Total project duration: 12 mo.

Staff and M&S: \$1.0M

Progress towards deliverables:

(a) Process development for 20L scale co-precipitation system was completed. Integrity of 20L system without plugging was achieved after several system revisions. 24hr continuous operation of 20L co-precipitation system was successfully completed (Figure 1).

(b) Desired precursor particle size and its distribution were obtained with spherical morphology. Modifications to the 20L system enabled small spherical precursor with sharp size distribution. D50 was decreased greatly from 29 μ m to 8 μ m by several test operations (Figure 2).

(c) To minimize of cathode fracture during calendar process and maximize high C-rate capability, small-sized spherical cathode with narrow particle distribution was synthesized (Table 1 and Figure 3).

(d) Re-optimization of Li excess and calcination condition based on #2012-07-11 precursor is being carried out to achieve high C-rate capability and long cycle life. Figure 4 shows good cycle life and high C-rate capability (C/3 = 215mAh/g, 1C = 200mAh/g for $\text{Li}_{1.35(\text{est})}\text{Ni}_{0.33}\text{Mn}_{0.67}\text{O}_{2.35}$)

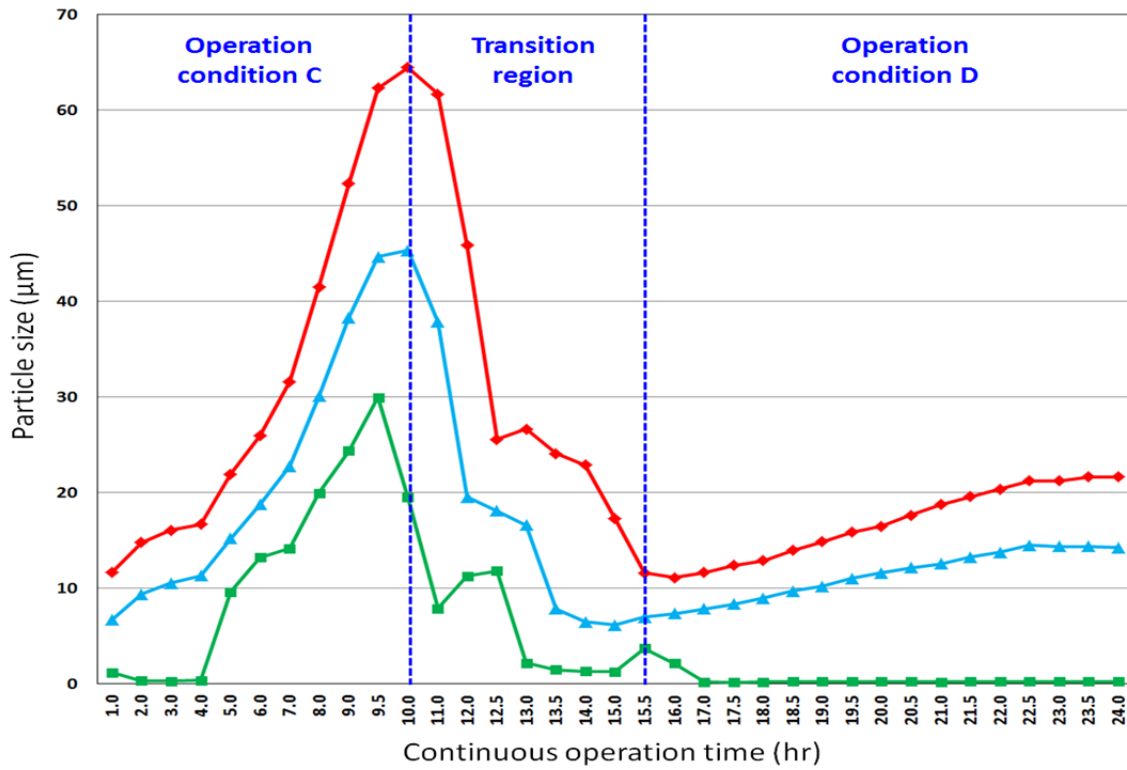


Figure 1. 20L 24hr continuous operation (#2012-06-14).

Table 1. Particle size analysis.

PSA for cathode	6th 20L operation #2012-07-11	4th 20L operation #2012-06-14	3rd 20L operation #2012-04-12	4L operation #2011-09-21
D10	6.0	8.3	11.7	17.2
D50	8.1	13.9	20.6	28.7
D90	11.2	23.8	36.0	48.4

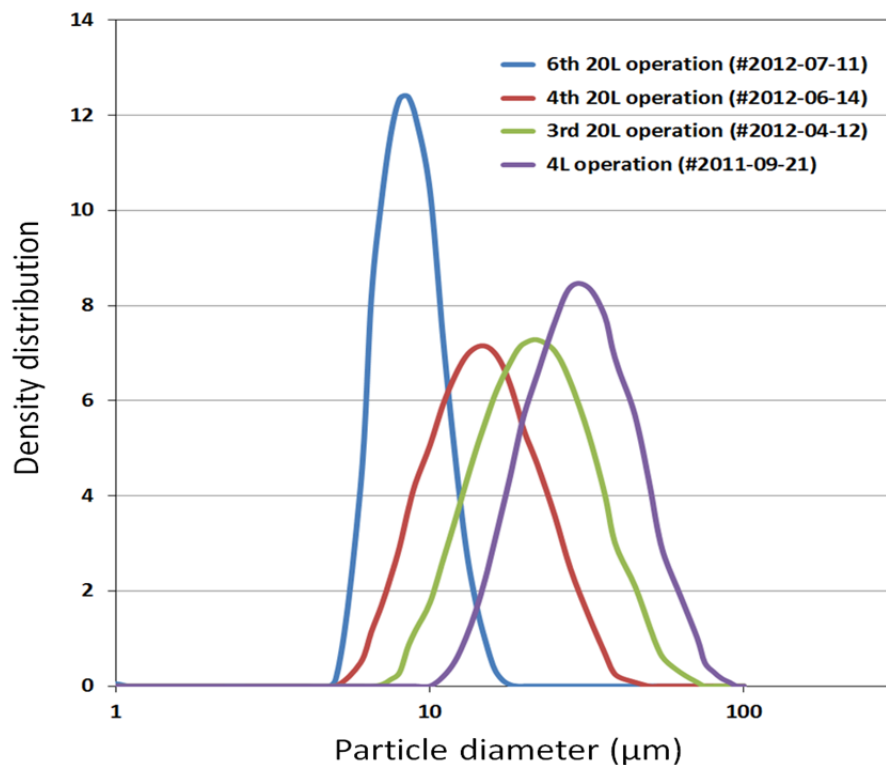


Figure 2. Particle size distribution comparison plots.

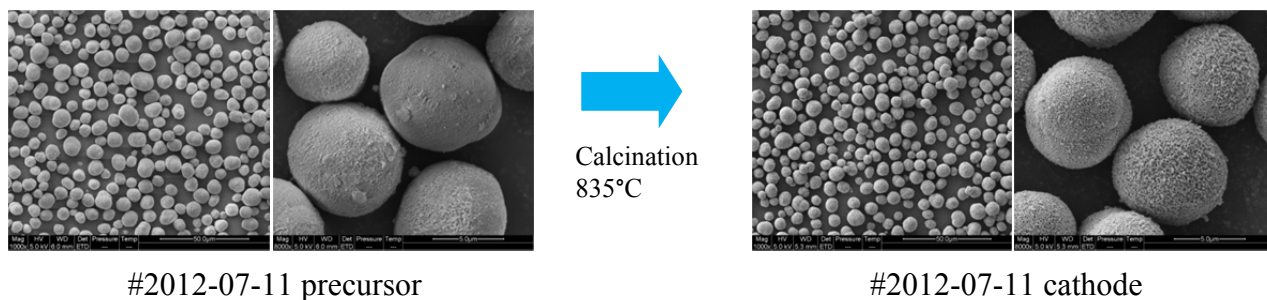


Figure 3. Precursor and cathode material from 20L run #2012-07-11.

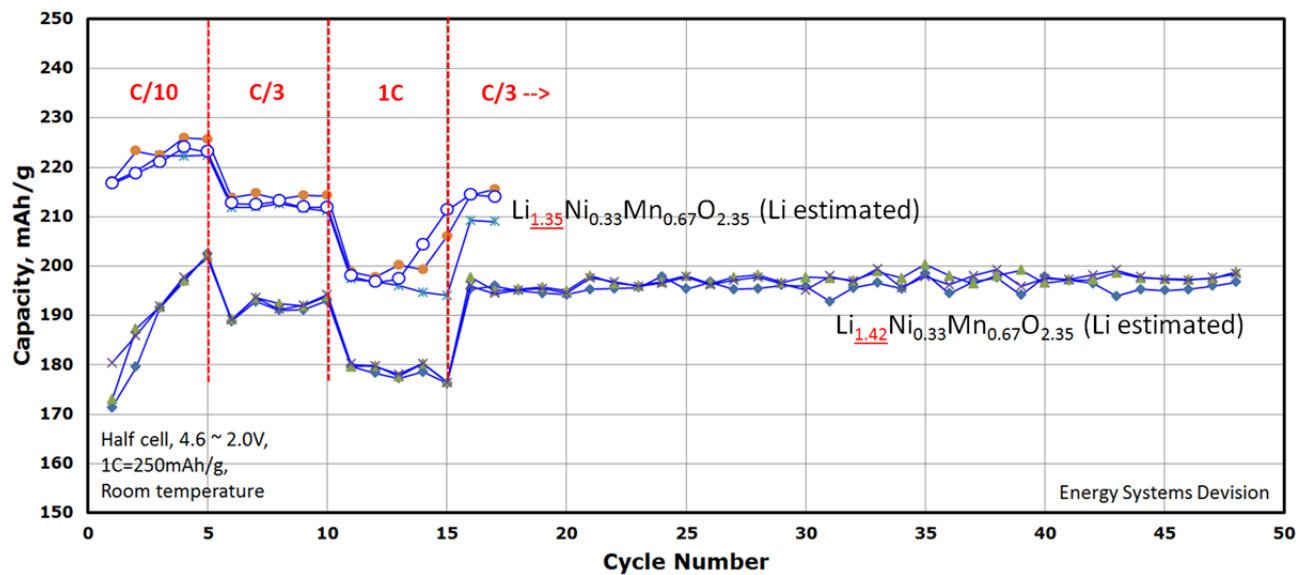


Figure 4. Coin cell results for #2012-07-11 cathodes (Li excess and calcination condition are under re-optimization to achieve high C-rate capability and long cycle life).

TASK 1

Battery Cell Materials Development

Project Number: IV.E.1.2 (ES168)

2012 Q3 update

Project Title: Process Development and Scale up of Advanced Electrolyte Materials

Project PI, Institution: Gregory Krumdick, Argonne National Laboratory

Collaborators (include industry):

Krzysztof Pupek, Argonne National Laboratory

Trevor Dzwiniel, Argonne National Laboratory

Project Start/End Dates: start: 10/1/2011; end: 9/30/2013

Objectives: The objective of this task is to conduct process engineering research for scale-up of Argonne's new electrolyte and additive materials. Advanced electrolytes and additives are being developed to stabilize the interface of lithium ion batteries by forming a very stable passivation film at the carbon anode. Stabilizing the interface has proven to be key in significantly improving the cycle and calendar life of lithium ion batteries for HEV and PHEV applications. Up to this point, these advanced electrolytes and additives has only been synthesized in small batches. Scaling up the process involves modification of the bench-scale process chemistry to allow for the semi-continuous production of materials, development of a process engineering flow diagram, design of a mini-scale system layout, construction of the experimental system and experimental validation of the optimized process. The mini system will be assembled utilizing an existing synthesis reactor system. Electrolyte materials produced will be analyzed to confirm material properties and for quality assurance. The electrochemical properties of the material will be validated to confirm a performance match to the original materials.

Approach: A formal approach for the scale-up of electrolyte materials has been defined. This approach starts with the initial discovery of a new electrolyte material and an initial electrochemical evaluation. This determines if the material is to be added to the inventory spreadsheet, ranked and prioritized. At this point, the scale-up process begins with the initial feasibility study, proof of concept testing, 1st stage scale-up and 2nd scale scale-up. Go/No go decisions are located after feasibility determination and electrochemical validation testing. See Figure 1 for more details.

Schedule and Deliverables: The schedule of electrolyte materials to scale will be determined once the scale-up spreadsheet has been ranked and prioritized. This will be reflected in the project milestones. Deliverables will include scaled materials for independent testing and a technology transfer package of information on each material scaled.

Financial data:

Total project duration: 12 mo.

Staff and M&S: \$1.0M

Progress towards deliverables:

Work on the passivation additive LiDFOB has ended. Work on the solvent 1S1M3 has been completed. Work on the passivation additive HFiPP for the Army Research Lab has been completed. The interim labs have been relocated to the MERF and are fully operational. Two additional materials have been assigned for scale-up (ANL-1NM2 and RS2') and have been added to the list of milestones.

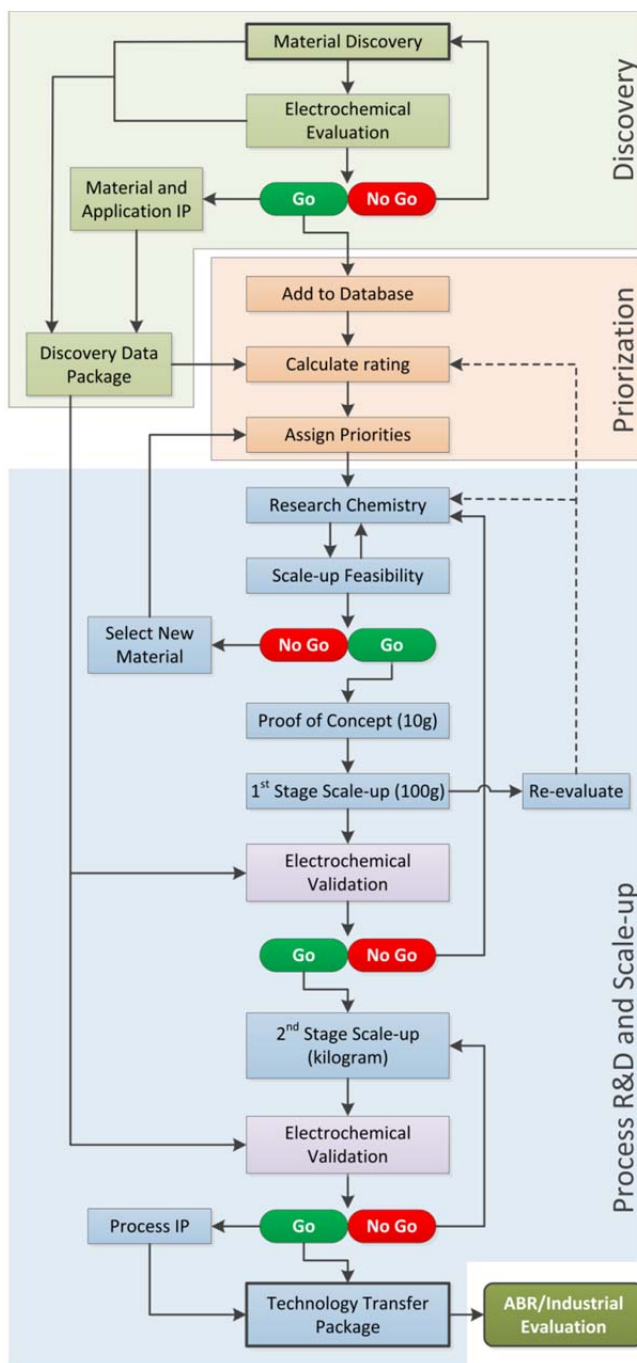


Figure 1. Electrolyte Materials Process R&D Flowchart

Milestones:

MILESTONE	DATE	STATUS	COMMENTS
LiDFOB (Continued from FY11) - COMPLETED			
Select CSE material to scale	01/07/2011	Completed	
Assess scalability of CSE process	08/12/2011	Completed	
WP&C documentation approved	06/22/2011	Completed	
Develop and validate scalable process chemistry (10g scale)	08/26/2011	Completed	
First process scale-up (100g bench scale)	11/07/2011	Completed	The material (~150 g) was synthesized, purified and analyzed.
Second process scale-up (1000g pilot scale)	March 2012	Ended	The usefulness and need of this material were re-evaluated and determined to be insufficient to justify further work
1S1M3 (Continued from FY11) - COMPLETED			
Select CSE material to scale	01/04/2011	Completed	
Assess scalability of CSE process	08/03/2011	Completed	
WP&C documentation approved	02/22/2011	Completed	
Develop and validate scalable process chemistry (10g scale)	09/02/2011	Completed	The reaction was successfully run in several 2 g-scale batches
First process scale-up (100g bench scale)	11/04/2011	Completed	The material was synthesized, purified and analyzed (80 g, >99%)
Second process scale-up (1000g pilot scale)	02/28/12	Completed	The material was synthesized, purified and analyzed (1327 g, 99.63%)
HFiPP, tris(1,1,1,3,3,3-hexafluoro-2-propyl) phosphate - COMPLETED			
Assess scalability of disclosed process	10/07/2011	Completed	
WP&C documentation approved	10/21/2011	Completed	
Develop and validate scalable process chemistry (10g scale)	11/30/2011	Completed	
First process scale-up (100g bench scale)	12/22/2011	Completed	
Second process scale-up (1000g pilot scale)	01/27/2012	Completed	1230g produced in a single batch, purity >99.5%.

MILESTONE	DATE	STATUS	COMMENTS
Relocation to Materials Engineering Research Facility - COMPLETED			
Decommission Interim Lab	04/06/2012	Completed	
Transfer Equipment	April 2012	Completed	
Electrolyte Lab Operational	May 2012	Completed	
Set up Equipment in MERF	July 2012	Completed	
MILESTONE	DATE	STATUS	COMMENTS
1NM2 - ONGOING			
Assess scalability of disclosed process	7/20/12	Scheduled	Process not yet disclosed
WP&C documentation approved	N/A	Completed	Approved under existing documentation
Develop and validate scalable process chemistry (10g scale)	8/20/12	Scheduled	
First process scale-up (100g bench scale)	8/31/12	Scheduled	
Second process scale-up (1000g pilot scale)	9/20/12	Scheduled	
Interim name RS2' - ONGOING			
Assess scalability of disclosed process	7/20/12	Scheduled	Process not yet disclosed
WP&C documentation approved	9/31/12	Scheduled	
Develop and validate scalable process chemistry (10g scale)	10/30/12	Scheduled	
First process scale-up (100g bench scale)	11/12/12	Scheduled	
Second process scale-up (1000g pilot scale)	11/31/12	Scheduled	

TASK 1

Battery Cell Materials Development

Project Number: 1.1B (ES016)

Project Title: New High Energy Gradient Concentration Cathode Material

Project PI, Institution: Khalil Amine, Argonne National Laboratory

Collaborators (include industry): H. Wu, D. Carter, Ilias Belharouak, Argonne National Laboratory; Prof. Yang-Kook Sun, Hanyang University; and ECPRO

Project Start/End Dates: October 1, 2008-September 30, 2014

Objectives: Develop a high energy cathode material for PHEV applications that provides over 200 mAh/g reversibly capacity, good rate capability, excellent cycle and calendar life, and good abuse tolerance. The cathode material capacities being investigated have capacities exceeding 200 mAh/g, which exceeds that of the NMC baseline.

Approach: Our approach is to develop a general synthetic method to tailor the internal composition gradient in cathode particles. This will be achieved by depositing a gradual composition gradient throughout particles to suppress stress during lithium intercalation and diffusion. We also aim to further enrich materials in Mn at the surface to enhance safety.

Milestones:

- a) Develop a model to predetermine the concentration gradient in particles produced via co-precipitation. This is necessary to have reproducibility of synthesized cathode materials. Complete.
- b) Develop a process for precursors with a gradient in transition metal composition that was enriched in manganese. Manganese enriched materials have shown excellent safety and cycle life. Complete.
- c) Demonstrate in a proof-of-principle experiment that precursors could be synthesized with predetermined compositional profiles. Complete.
- d) Demonstrate high capacity (>200 mAh/g) in final materials produced using the gradient precursors. On schedule
- e) Demonstrate that a tailored relative transition metal composition at the surfaces of gradient particles influences safety and cycle life. Complete.

- f) Develop hydroxide co-precipitation process at Argonne and implement gradient concentration materials in hydroxide process to achieve higher tap density particles and larger relative core nickel concentrations for increased rate capability and high level of Mn concentration at the outer layer. On schedule.

Financial data: \$300K/year

PROGRESS TOWARD MILESTONES (e,f)

In the past, we reported on the core-shell approach that resulted in a nickel-rich bulk that delivered high capacity at high voltage, and a manganese-rich shell that stabilized the surface of the material. However, due to the structural mismatch and the difference in volume change between the core and the shell, a large void forms at the core/shell interface after long-term cycling, leading to a sudden drop in capacity. We also demonstrated that this structural mismatch could be mitigated by nano-engineering of the core/shell material, where the shell exhibits a concentration gradient. However, because of the short shell thickness, the manganese concentration at the outer layer of the particle is low; therefore, its effectiveness in stabilizing the surface of the material is moderate, especially during high temperature cycling (55 °C).

The nickel-rich lithium transition metal oxide investigated here has a nominal composition of $\text{LiNi}_{0.75}\text{Co}_{0.10}\text{Mn}_{0.15}\text{O}_2$, and the concentration gradient of transition metals shown in Figure 1; the concentration of nickel decreases gradually from the center toward the outer layer of the particle, while the concentration of manganese increases gradually so that the manganese-rich and nickel-poor outer layer can stabilize the material, especially during high voltage cycling. The full concentration gradient (FCG) cathode material was prepared by a newly developed co-precipitation method involving the precipitation of transition metal hydroxides from the precursor solutions, where the concentration ratio of Ni:Mn:Co changes continuously with the reaction time.

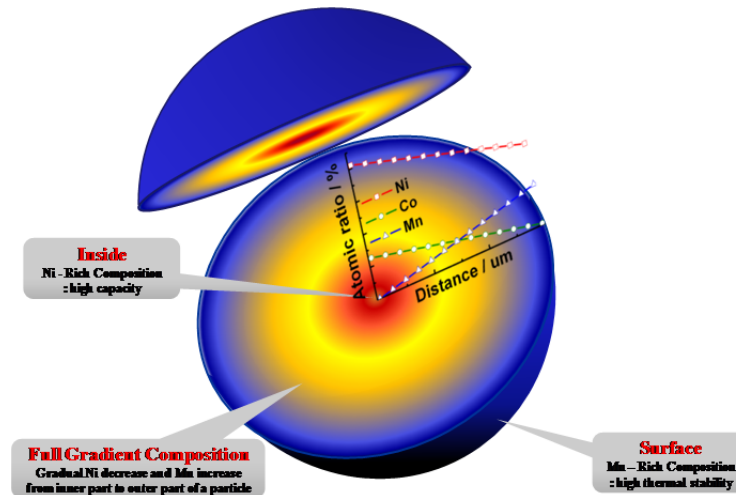


Figure 1. Schematic diagram of the full concentration gradient lithium transition metal oxide particle with the nickel concentration decreasing from the center toward outer layer and the concentration of manganese increasing accordingly.

Figure 2 shows scanning electron microscopy images and elemental distribution of Ni, Co, and Mn within a single particle of both the precursor ($(\text{Ni}_{0.75}\text{Co}_{0.10}\text{Mn}_{0.15})(\text{OH})_2$) and the final lithiated product ($\text{LiNi}_{0.75}\text{Co}_{0.10}\text{Mn}_{0.15}\text{O}_2$) having concentration gradient. The atomic ratio between Ni, Co, and Mn was determined by integrated 2D electron probe micro-analysis (EPMA). Figure 2 clearly demonstrates that the atomic percentage of Co remained constant at about 10% in both the precursor and the lithiated particles as originally designed, while the concentration of Ni decreased and Mn increased continuously from the center toward the outer layer of the particle. Note that the slopes representing the metal (Ni and Mn) concentration change of the precursor are greater than those of the lithiated material because of the directional migration of the metal elements during the high temperature calcination to increase the entropy.

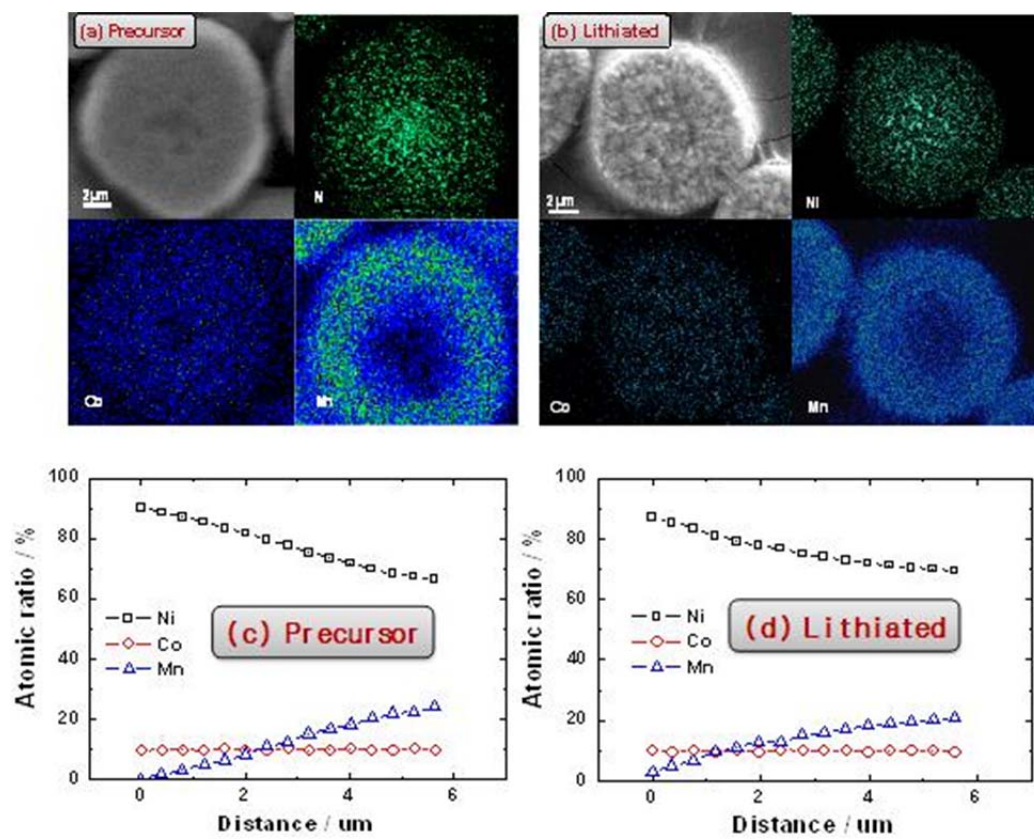


Figure 2 Scanning electron microscopy images and electron-probe X-ray micro-analyzer mapping of (a) a precursor particle and (b) a lithiated particle; and integrated atomic ratio of transition metals as a function of the distance from the center of the particle for (c) the precursor and (d) the lithiated material

The long-term electrochemical stability of the FCG material was further characterized in tests using half cells having lithium metal as the counter electrode (cycling between 2.7 V and 4.5 V vs. Li⁺/Li at constant current of C/5). The inner composition (IC) and the outer composition (OC) materials were also tested by the same procedure for comparison. Figure 3b shows that the IC material (highest nickel content) had the highest initial capacity, but the reversible capacity decreased dramatically with cycling. This rapid capacity fade was mainly caused by the direct exposure of a high content of Ni(IV)-based compound to non-aqueous electrolyte at high potential; this exposure led to the chemical decomposition of both the electrode material and the electrolyte. By contrast, the OC material had higher manganese content and lower oxidizing capability toward non-aqueous electrolyte. Therefore, this material had a lower reversible capacity, but much better capacity retention. Figure 3 shows that the FCG material had combined advantages of high capacity from the high nickel content in the bulk and high electrochemical stability from the high manganese content on the surface. Further investigation is underway to characterize further this material using Hard X-ray nano-tomography to

determine the 3D distribution of Ni and Mn in a single lithiated particle. Also further testing by varying the upper cutoff voltage of the test cells is underway to establish the effectiveness of this full gradient approach is stabilizing the material at voltages as high as 4.5V.

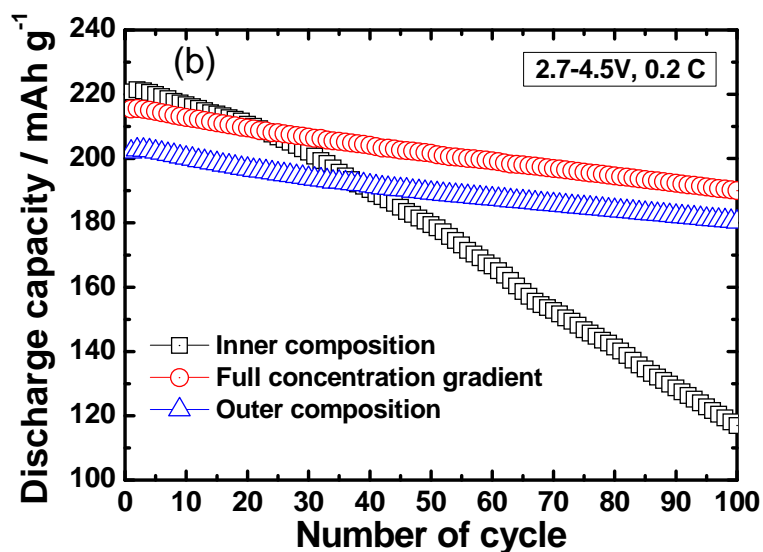


Fig. 3. cycling performance of half cells using the full concentration gradient material, inner composition $[\text{Li}(\text{Ni}_{0.86}\text{Co}_{0.10}\text{Mn}_{0.04})\text{O}_2]$ and the outer composition $[\text{Li}(\text{Ni}_{0.72}\text{Co}_{0.10}\text{Mn}_{0.18})\text{O}_2]$ materials cycled between 2.7 V and 4.5 V vs. Li+/Li using a constant current of $C/5$ (about 44 mA g⁻¹).

Publications, Reports, Intellectual property or patent application filed this quarter.
High energy cathode material for lithium battery.
Nature Material, 2012, (accepted, 2012)

TASK 1

Battery Cell Materials Development

Project Number: 1.1G (ES019)

Project Title: Development of High-Capacity Cathode Materials with Integrated Structures

Project PI, Institution: Michael Thackeray, Argonne National Laboratory

Collaborators (include industry):

Donghan Kim, Giselle Sandí, Zonghai Chen, Jason Croy, Argonne National Laboratory
Peter Chupas, Karena Chapman, Matthew Suchomel, APS, Argonne National Laboratory
Roy Benedek, Hakim Iddir, Argonne National Laboratory
Yang Shao-Horn, Massachusetts Institute of Technology

Project Start/End Dates: October 2009/September 2014

Objective: The objective of this work is to develop low cost Li- and Mn-rich cathode materials with integrated structures that offer good thermal stability, high capacity (~240 mAh/g), good rate capability (≥ 200 mAh/g at C/1 rate) and high first-cycle efficiency. The targeted performance values are 240 mAh/g of reversible capacity and a first-cycle efficiency of at least 85%. If successfully developed, the energy density of a cell coupled with graphite would be ~460 Wh/kg (assuming 300 mAh/g graphite, 3.7 V nominal).

Approach: ‘Layered-layered’ composite cathode materials, $x\text{Li}_2\text{MnO}_3 \cdot (1-x)\text{LiMO}_2$ (M=Ni,Co,Mn) can deliver a high capacity of 240-260 mAh/g. However, these materials have drawbacks such as low first-cycle efficiency, voltage fade on cycling, transition metal dissolution and poor power performance. The concept of embedding a spinel component into ‘layered-layered’ structures is being exploited to improve their electrochemical properties and cycling stability. Studies of blending $x\text{Li}_2\text{MnO}_3 \cdot (1-x)\text{LiMO}_2$ with high-power cathode materials, such as LiFePO_4 , are being continued to improve impedance at low states of charge.

Milestones:

- (a) Optimize the chemical composition of ‘layered-layered-spinel’ electrodes, including coatings such as AlF_3 ;
- (b) Characterize ‘layered-layered-’ and ‘layered-layered-spinel’ electrodes to determine, in particular, the causes for the voltage fade phenomenon;
- (c) Identify performance degradation mechanisms, particularly voltage fade phenomena in structurally-integrated ‘layered-layered-spinel’ electrodes;

Financial data: \$300K

PROGRESS TOWARD MILESTONES

Summary of work related to milestone (a)

The concept of embedding a spinel component in composite $x\text{Li}_2\text{MnO}_3 \cdot (1-x)\text{LiMO}_2$ ($M=\text{Mn, Ni, Co}$) ‘layered-layered’ structures to improve their electrochemical properties and cycling stability is being exploited. In general, efforts are being focused on the preparation of three-component ‘layered-layered-spinel’ electrodes by lowering the lithium content of a parent ‘layered-layered’ $x\text{Li}_2\text{MnO}_3 \cdot (1-x)\text{LiMO}_2$ material (and substituted derivatives) while maintaining a constant Mn:M ratio. Such ‘layered-layered-spinel’ compounds are located on the tie-line between selected $x\text{Li}_2\text{MnO}_3 \cdot (1-x)\text{LiMO}_2$ and $\text{LiM}'_2\text{O}_4$ spinel compositions, as shown schematically in a compositional phase diagram (Fig. 1). With a constant Mn:M ratio, these systems can be normalized to a simpler notation; for example, the $0.5\text{Li}_2\text{MnO}_3 \cdot 0.5\text{LiMn}_{0.5}\text{Ni}_{0.5}\text{O}_2$ (‘layered-layered’) – $\text{LiMn}_{1.5}\text{Ni}_{0.5}\text{O}_4$ (‘spinel’) system, in which the Mn:Ni ratio remains constant at 3:1, reduces simply to $\text{Li}_x\text{Mn}_{0.75}\text{Ni}_{0.25}\text{O}_y$, with the end-members having x and y values of 1.5 and 2.5 ($\text{Li}_2\text{MnO}_3 \cdot 0.5\text{LiMn}_{0.5}\text{Ni}_{0.5}\text{O}_2$) and 0.5 and 2.0 ($\text{LiMn}_{1.5}\text{Ni}_{0.5}\text{O}_4$), respectively.

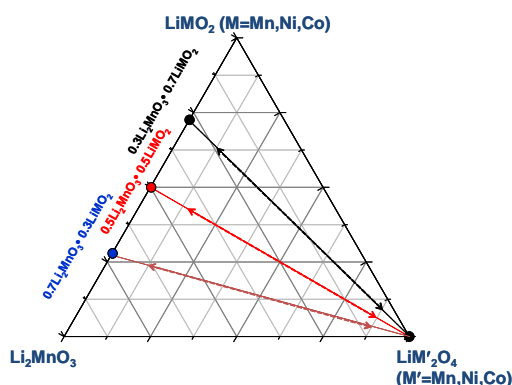


Fig. 1. Compositional phase diagram of a ‘layered-layered-spinel’ system with $x\text{Li}_2\text{MnO}_3 \cdot (1-x)\text{LiMO}_2$ (layered-layered) and $\text{LiM}'_2\text{O}_4$ (spinel) components.

During the past quarter, emphasis was placed on a targeted composition $\text{Li}_{1.30}\text{Mn}_{0.75}\text{Ni}_{0.25}\text{O}_{2.40}$ in which $x = 1.30$ and $y = 2.40$ (or $0.8[0.5\text{Li}_2\text{MnO}_3 \cdot 0.5\text{LiNi}_{0.5}\text{Mn}_{0.5}\text{O}_2] \cdot 0.2\text{Li}_{0.5}\text{Mn}_{0.75}\text{Ni}_{0.25}\text{O}_2$ in ‘layered-layered-spinel’ notation) with 20% spinel, and a targeted composition $\text{Li}_{1.40}\text{Ni}_{0.22}\text{Co}_{0.12}\text{Mn}_{0.66}\text{O}_{2.42}$ in which $x = 1.40$ and $y = 2.42$ (alternatively, $0.95[0.44\text{Li}_2\text{MnO}_3 \cdot 0.56\text{LiNi}_{0.39}\text{Co}_{0.22}\text{Mn}_{0.39}\text{O}_2] \cdot 0.05\text{Li}_{0.50}\text{Mn}_{0.75}\text{Ni}_{0.25}\text{O}_2$) with 5% spinel. (Note: for these calculations, the formula of spinel was $\text{Li}_{0.5}\text{Mn}_{0.75}\text{Ni}_{0.25}\text{O}_2$ rather than $\text{LiMn}_{1.5}\text{Ni}_{0.5}\text{O}_4$). The electrochemical data of a $\text{Li}/\text{Li}_{1.30}\text{Ni}_{0.25}\text{Mn}_{0.75}\text{O}_{2.40}$ cell, when charged and discharged between 4.6 – 2.0 V at 15 mA/g, are provided in Figure 2. The cycling data in Fig. 2a shows that the Li_2MnO_3 component of the composite cathode is slowly and continuously activated during

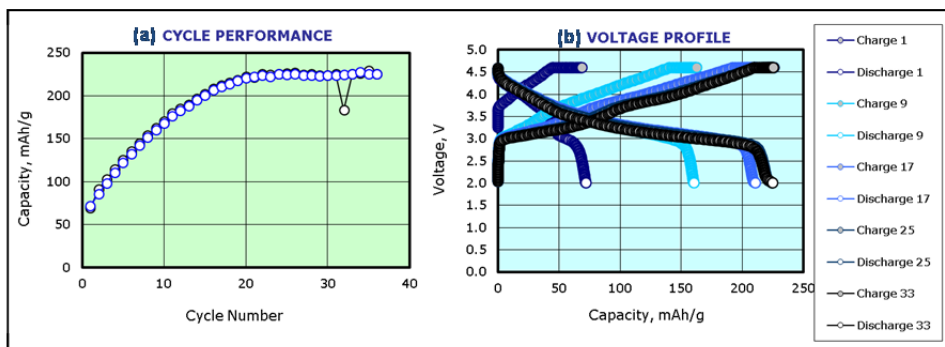


Fig. 2. Electrochemical data of a $\text{Li}/\text{Li}_{1.3}\text{Ni}_{0.25}\text{Mn}_{0.75}\text{O}_{2.40}$ cell (4.6-2.0 V; 15 mA/g): a) capacity vs. cycle number plot, and b) charge/discharge profiles.

the charge process at 4.6 V until a stable reversible capacity of approximately 225 mAh/g is reached after 20 cycles with a steady voltage profile, which is particularly noticeable between 25 and 33 cycles (Fig. 2b). The evaluation of coated electrodes, for example with AlF_3 , is on-going; the coating results will be presented and discussed in a subsequent report.

Summary of work related to milestone (b)

The electrochemical properties of ‘layered-layered-spinel’ $\text{Li}_{1.4}\text{Ni}_{0.22}\text{Co}_{0.12}\text{Mn}_{0.66}\text{O}_{2.42}$ electrodes (alternatively, $0.95[0.44\text{Li}_2\text{MnO}_3 \bullet 0.56\text{LiNi}_{0.39}\text{Co}_{0.22}\text{Mn}_{0.39}\text{O}_2] \bullet 0.05\text{Li}_{0.5}\text{Mn}_{0.75}\text{Ni}_{0.25}\text{O}_2$) with 5% spinel were evaluated in lithium half cells between 4.6 and 2.0 V at constant current (15 mA/g), as shown in Figure 3. Note that the composite formula assumes that the cobalt is associated with the ‘layered-layered’ component and that the spinel component is $\text{LiMn}_{1.5}\text{Ni}_{0.5}\text{O}_4$; in practice, there are likely to be variations in the cation distribution and formulae of the layered and spinel component structures. Nevertheless, the data in Fig. 3(a-c) show that there appears to be a suppression of the voltage decay process, as highlighted by the voltage profiles over the first 12 cycles (Figure 3a); more importantly, the dQ/dV plots in Figure 3b reveal that, after 10 cycles, the predominant electrochemical processes occurs above 3 V during discharge, implying the existence of spinel-like cation arrangements, not ideal spinel arrangements, in the composite structure because a pure Mn-based spinel structure would be expected to show a reduction peak around 2.8 V. Of particular interest is that, after the initial break-in cycles, the dQ/dV plots show that the dominant reduction of the composite electrode occurs at approximately 3.1 V, which is tentatively attributed to lithium insertion into octahedral sites; in contrast, Figure 3b reveals that oxidation occurs in three discrete steps, two between 3.1 and 3.4 V, tentatively attributed to lithium extraction from two crystallographically independent octahedral sites, and one at about 3.8 V, which is attributed to lithium extraction from tetrahedral sites.

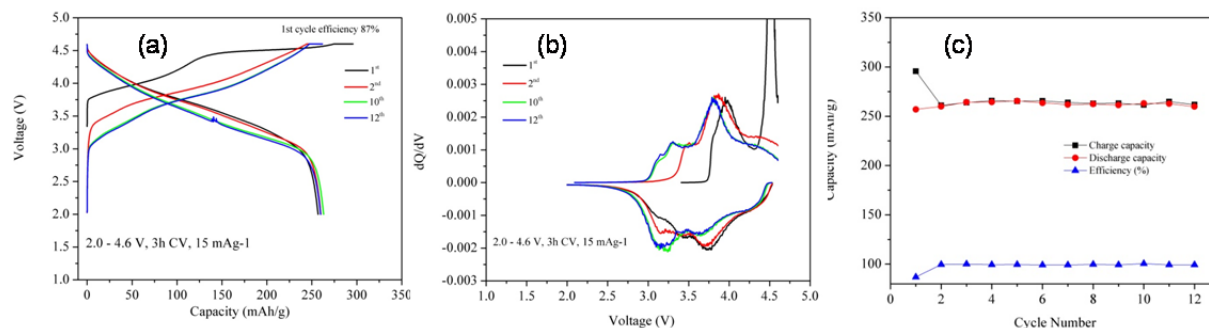


Fig. 3. Electrochemical data of a $\text{Li}/\text{Li}_{1.40}\text{Ni}_{0.22}\text{Co}_{0.12}\text{Mn}_{0.66}\text{O}_{2.42}$ cell (4.6-2.0 V; 15 mA/g): a) charge/discharge profiles; b) dQ/dV plots; and c) capacity vs. cycle number plot.

Summary of work in the past quarter related to milestone (c)

The voltage decay phenomenon exhibited by ‘layered-layered’ cathode materials is being studied from a structural standpoint using high-resolution X-ray diffraction and pair-distribution function (pdf) analysis with collaborators at the Advanced Photon Source with $0.5\text{Li}_2\text{MnO}_3 \cdot 0.5\text{LiCoO}_2$ as an initial baseline system. Structural evolution of the end-member LiCoO_2 was monitored from 450 to 950 °C. A spinel-like structure is first formed up to about 650 °C, which subsequently transforms to a layered structure, reaching a highly crystalline single-phase material at 750 °C. A similar study will be performed for Li_2MnO_3 , and then for the composite series $x\text{Li}_2\text{MnO}_3 \cdot (1-x)\text{LiCoO}_2$ using pdf analyses to gather more detailed structural information. A collaboration with Roy Benedek and Hakim Iddir, who are performing first principle calculations of $x\text{Li}_2\text{MnO}_3 \cdot (1-x)\text{LiCoO}_2$ composite structures, has been established (see separate report).

TASK 1

Battery Cell Materials Development

Project Number: 1.1C (ES020)

Project Title: Developing High Capacity, Long Life anodes

Project PI, Institution: A. Abouimrane and K. Amine Argonne National Laboratory

Collaborators (include industry):

- B. Liu, D. Dambournet (CSE/ANL).
- P. Chupas, K. Chapman, Y. Ren Advanced Photon Source, (APS/ANL).
- Z. Fang (University of Utah).
- FMC, Northwestern University,

Project Start/End Dates: October ^{1st}, 2009/September 2014

Objectives:

- Develop new advanced high energy anode materials with long life and improved Safety for PHEV and EV applications
- Develop a low cost synthesis methods to prepare high energy anodes
- Full structural and electrochemical characterizations of the prepared anode materials.
- Demonstrate the applicability of these anodes in half and full cells systems.

Approach:

- MO-Sn_xCo/Fe_yC_z (MO=SiO, SiO₂, SnO₂, MoO₂, GeO₂) anode materials were selected for investigation as high energy anode based on the following criteria:
 - Sn_xCo/Fe_yC_z alloys are known to provide a capacity of 400-500mAh/g for hundreds of cycles.
 - MO anodes are known to provide more than 1000 mAh/g with poor cycleability.
 - The formation of Sn_xCo/Fe_yC_z and MO composite could lead to the increase in the capacity, reduce the amount of cobalt in the material and improve the cycleability as Sn_xCo/Fe_yC_z play the role of buffers against the volume expansion of MO.
 - This anode system is more safer than the graphite and possess low potentials in the range of 0.3-0.75V (expect high voltage cells when combined with high cathodes)

Milestones:

- 1- Make full cells of SiO-SnCoC anode coupled by commercial cathodes using stabilized lithium metallic powder technique. (2013);
- 2- Use iron powder instead of cobalt to cut the cost for industrial application. (2013);

- 3- Characterize the as-milled SiO-SnFeC to optimize the electrochemical performance. (2013);
- 4- Study on the different composition of SiO-SnFeC electrochemical performance. And screen out the optimum combination. (2013)

Financial data: 300K/year

PROGRESS TOWARD MILESTONES

(a) Summary of work in the past quarter related to milestone (1)

Ball-milled SiO-Sn₃₀Co₃₀C₄₀ electrode was coupled with different commercial cathode (Li_{1.2}Ni_{0.3}Mn_{0.6}O_{2.1}, 5V Spinel and Toda HE5050). Small amount of lithium powder (from SLMP) was added to the anode. Promising cycleability (100 cycles) and coulombic efficiency demonstrate the feasibility of our anode material shown in Fig.1. This millstone is achieved now at 75%.

(b) Summary of work in the past quarter related to milestone (2)

We have successfully taken the place of cobalt using metallic iron. SiO-Sn₃₀Fe₃₀C₄₀ was prepared by ball milling method. Iron can cut the cost for industrial application. Good electrochemical performance was obtained (900 mAh/g upon C/6, 700 mAh/g upon C/2). The various current densities were loaded on the composite electrode shown in Fig.4. The composite electrode maintains 600 mAh/g upon a high current density (1200 mA/g). It exhibits excellent recoverable performance after switching back to a low current density (100 mA/g). This millstone is achieved now at 75%.

(c) Summary of work in the past quarter related to milestone (3)

Three phases, FeSn₂, Fe₃Sn and Fe can be observed in the high resolution XRD pattern. The structures of the intermetallic compounds affect the electrochemical reaction of the phases with Li. Therefore, FeSn₂ exhibits a larger capacity but poorer cycleability, while FeSn presents the better cycle performance but has lower capacity. This millstone is achieved now at 50%.

(d) Summary of work in the past quarter related to milestone (4)

Through changing the amount of Fe, we try to avoid FeSn₂ phase after ball milling. That is the key point to have a better cycle life. (En schedule) “The progress to this milestone is achieved at 10%”.

FY 2012 Publications/Presentations

1. 2011 DOE Annual Peer Review Meeting Presentation, May 9th-13th 2011, Washington DC.
2. Provisional patent application A. Abouimrane & K. Amine “Anode materials for lithium batteries: ANL-IN-10-013”
3. “A new anode material based on SiO-Sn₃₀Co₃₀C₄₀ for lithium batteries” B. Liu, A. Abouimrane, D. Wang, Y. Ren, Z. Fang and K. Amine (submitted paper).

4. New anode materials based on $\text{MO-Sn}_{30}\text{Co}_{30}\text{C}_{40}$ ($\text{MO}=\text{SiO}, \text{SiO}_2, \text{SnO}_2, \text{MoO}_3, \text{GeO}_2$) for lithium batteries Materials Challenges in Alternative & Renewable Energy, Clearwater FL, Feb. 28th 2012.

5. New anode materials based on $\text{MO-Sn}_{30}\text{Co}_{30}\text{C}_{40}$ ($\text{MO}=\text{SiO}, \text{SiO}_2, \text{SnO}_2, \text{MoO}_3, \text{GeO}_2$) for lithium batteries. IBA meeting, Waikoloa Village, HW, Jan.

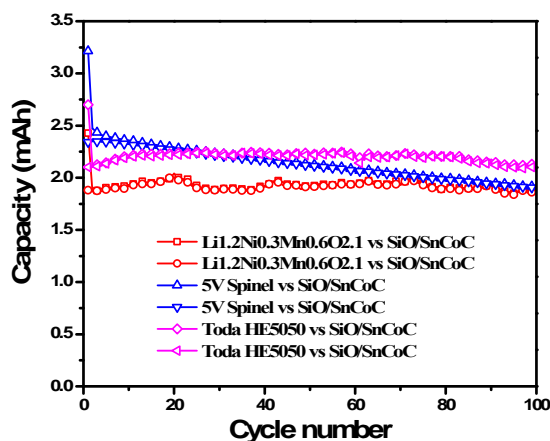


Fig.1 Room temperature cycling performance of Full cell using SiO-SnCoC (Li-SLMP) anode and 5V, HE5050, and $\text{Li}_{1.2}\text{Ni}_{0.3}\text{Mn}_{0.6}\text{O}_{2.1}$ cathode materials under C/3 current rate.

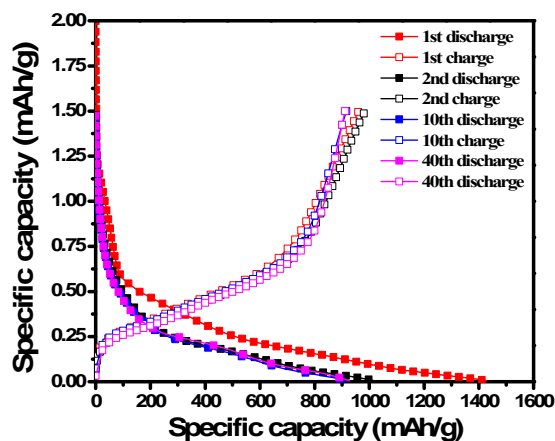


Fig.2 Voltage profile of as-milled $\text{SiO-Sn}_{30}\text{Fe}_{30}\text{C}_{40}$ composite.

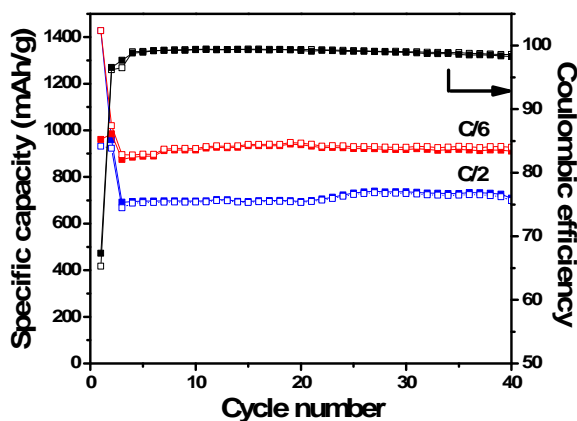


Fig.3 Cycling performance of as-milled $\text{SiO-Sn}_{30}\text{Fe}_{30}\text{C}_{40}$ composite

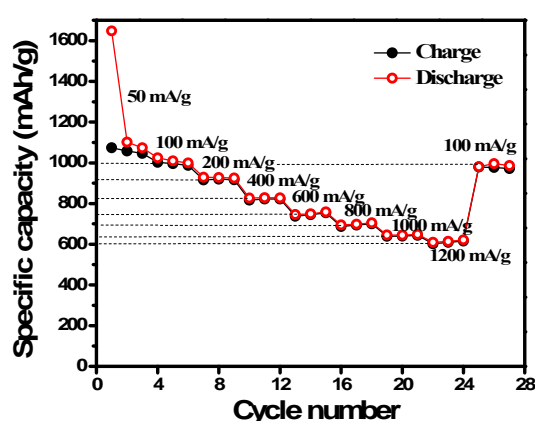


Fig.4 Rate performance of as-milled $\text{SiO-Sn}_{30}\text{Fe}_{30}\text{C}_{40}$ composite.

TASK 1

Battery Cell Materials Development

Project Number: ES024-A

Project Title: High Voltage Electrolytes for Li-ion Batteries

Project PI, Institution: T. Richard Jow, U.S. Army Research Laboratory

Collaborators (include industry): Dr. Jan L. Allen, Dr. Oleg Borodin, Dr. Arthur von Cresce, Dr. Wishvender Behl, Army Research Laboratory; Y. F. Lam, U. of Maryland; Lidan Xing, U. of Utah; K. Amine, D. Abraham, D. Dees, ANL

Project Start/End Dates: June 2011 / May 2014

Objectives: Develop high voltage electrolytes that enable the operation of 5 V Li Ion Chemistry. With a 5-V high voltage electrode materials and a capacity similar to that of the state-of-the-art cathode, the energy density will be increased more than 25% than that of the state-of-the-art Li-ion batteries for HEV/PHEV. Our other objective is to understand the surface chemistry at the high voltage cathode and electrolyte interface through surface characterization and computational effort. With better understanding, better electrolyte components and cathode materials can be developed.

Approach: Three approaches were taken.

- 1. Develop additives for carbonate based solvents for high voltage cathodes**
 - a. Search additives that would decompose and form protective interface on cathode
 - b. Formulate electrolytes using fluorinated phosphate ester as additives for the state-of-the-art electrolytes
- 2. Characterize interfacial chemistry at the cathode/electrolyte interface**
 - a. Use high resolution XPS
 - b. Use mass spectroscopy method, NMR, AFM, etc
- 3. Computational effort**
 - a. Understand oxidative stability of solvents/electrolytes
 - b. Understand reactive pathways of additives and electrolytes
 - c. Develop ability to predict and design electrolyte components

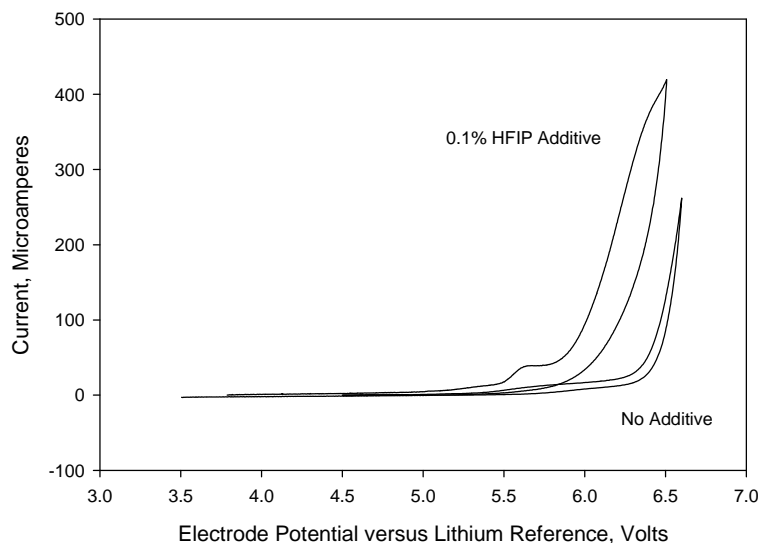
Milestones:

- (a) Explored new additives for high voltage cathodes (June 2012)
- (b) Evaluate electrolytes with additives in both half cells and full cells (Dec 2012)
- (c) Diagnostic studies: surface characterization and SEI chemistry (Dec 2012)
- (d) Understand reactive pathways of electrolyte components through computational effort (June 2012)
- (e) Develop stable high voltage cathodes and understand their electronic structures (Dec 2012)

Financial data: \$250,000/year

PROGRESS TOWARD MILESTONES

(a) Oxidation limits of HFiP



Cyclic voltammograms at glassy carbon electrodes in 1.2 M LiPF₆-EC-EMC solution at a scan rate of 10 mV/s (Electrode Area: 0.0792 cm²)

HFiP [tris(hexafluoro-iso-propyl) phosphate, (C₃HF₆O)₃PO] has been demonstrated as an effective additive in 1.2 M LiPF₆ in EC:EMC (3:7) baseline electrolyte for the operation of high voltage spinel, LiNi_{0.5}Mn_{1.5}O₄, at voltages close to 5 V. The mechanism of how HFiP works is under intensive investigation. HR-XPS results indicate that phosphorus content on the cathode is 5 to 10 times more than that on the graphite anode surface. Here we report our observation of the oxidation limits of HFiP using cyclic voltammetry (CV) technique with glassy carbon (GC), platinum (Pt), aluminum (Al) as working electrodes and Li metal as a counter and a reference electrodes in an electrolyte made of 1.2 M LiPF₆ in EC:EMC (3:7) baseline solution at a scan rate of 10 mV/sec. The representative cyclic voltammograms at glassy carbon electrodes for 0.1% HFiP in the baseline solution comparing that in the baseline electrolyte without HFiP are shown in the figure above. At voltages below 5 V, there is no significant oxidation currents at the GC electrodes observed in both the baseline electrolytes with and without HFiP. However, at voltages above 5.4 V, oxidation current at the GC electrode started to increase with significant amount at voltages of above 5.8 V. In comparison to the baseline electrolyte, HFiP containing electrolyte is oxidized at voltages lower than that of the baseline electrolyte on GC electrode. The CV of LiNi_{0.5}Mn_{1.5}O₄ as a working electrode in both electrolytes is under investigation and to be reported in the coming quarter.

(b) New additives development

New additives are being synthesized. The evaluation of these new additives is in progress.

(c) Modeling of oxidation reactions of EC

The study of the oxidation induced decomposition of EC, EC₂ and EC₄ and decomposition products was completed using DFT, MP4 and G4 levels. The polarized continuum model (PCM) was used to implicitly include the rest of the surrounding solvent. The oxidation potentials of EC₂ and EC₄ were found to be significantly lower than the intrinsic oxidation potential of an isolated EC and also lower than the oxidation potential of EC-BF₄⁻. The exothermic proton abstraction from the ethylene group of EC by the carbonyl group of another EC was responsible for the decreased oxidative stability of EC₂ and EC₄ compared to EC. The most exothermic path with the smallest barrier for EC₂ oxidation yielded CO₂ and ethanol radical cation. The reaction paths with the higher barrier yielded oligo(ethylene carbonate) suggesting a pathway for the experimentally observed poly(ethylene carbonate) formation of EC-based electrolytes at cathodes surfaces. The decomposition products and oxidation potentials obtained from these calculations are summarized in Xing & Borodin *Phys. Chem. Chem. Phys.* 2012, DOI 10.1039/c2cp41103b.

Publications

1. Jow, T. R.; Marx, M. B.; Allen, J. L., Distinguishing Li⁺ Charge Transfer Kinetics at NCA/Electrolyte and Graphite/Electrolyte Interfaces, and NCA/Electrolyte and LFP/Electrolyte Interfaces in Li-Ion Cells. *J. Electrochem. Soc.* **2012**, 159(5), A604-A612.
2. Xing, L.; Borodin, O. "Oxidation induced decomposition of ethylene carbonate from DFT calculations – importance of explicitly treating surrounding solvent" *Phys. Chem. Chem. Phys.* **2012**, DOI 10.1039/c2cp41103b

Presentations

1. Cresce, A.; Borodin, O.; Ho, J.; Xu, K., Electrolyte/Electrode Interphases in Li Ion Batteries, 16th International Meeting on Lithium Batteries, June 17-22, 2012, Jeju, Korea, p. 79.
2. Allen, J. L.; Johannes, M. D.; Jow, T. R., Stabilized Lithium Cobalt Phosphate for High Voltage Lithium-Ion Batteries, 16th International Meeting on Lithium Batteries, June 17-22, 2012, Jeju, Korea, p. 172.

TASK 1

Battery Cell Materials Development

Project Number: ES024-B

Project Title: High Voltage Electrolytes for Li-ion Batteries: Part B: Additive Synthesis and Characterization

Project PI, Institution: Arthur Cresce, J. Ho, O. Borodin, Kang Xu, U.S. Army Research Laboratory

Collaborators (include industry): Y. F. Lam, Y. Li (U. of Maryland); K. Amine, D. Abraham, D. Dees (ANL); X. Yu, X. Yang (BNL).

Project Start/End Dates: June 2011/May 2014

Objectives: This part of the report concerns the design and synthesis of high voltage electrolyte additives. Both Al- and B-based additives were designed so that an electron-deficiency will be created in the resultant additives. After synthesis and thorough purification, structural characterization and preliminary electrochemical evaluation were conducted using various high voltage electrochemical couples. The effect on the additives' behavior on cathode surface will be evaluated by both computational and experimental approaches.

Approach:

4. Design and Synthesis

- a. Rationale of electron-deficient center
- b. Synthesis, purification and structural characterization by NMR, MS and FTIR

5. Electrochemical evaluation

- a. CV and CCCV cyclings in half and full cells

6. Surface Characterizations

- a. Investigation of the electrochemical fate of these additives on surfaces of LMNO, NMC and graphite.

7. Computational evaluation

- a. Understanding of how electron-deficiency would impact on the oxidation stability of additives

Milestones:

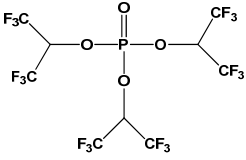
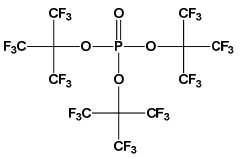
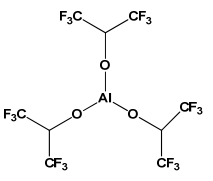
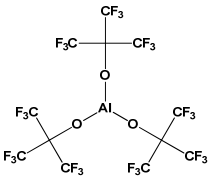
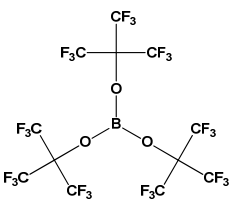
- (a) Synthesized three new additives (two Al-based and one B-based), purified, and fully characterized their structures (June 2012)
- (b) Evaluated these additives in electrochemical cells (August 2012)
- (c) Surface characterizations: surface characterization and SEI chemistry (Dec 2012)
- (d) Understand reactive pathways of electrolyte components through computational effort (Dec 2012)

Financial data:

PROGRESS TOWARD MILESTONES

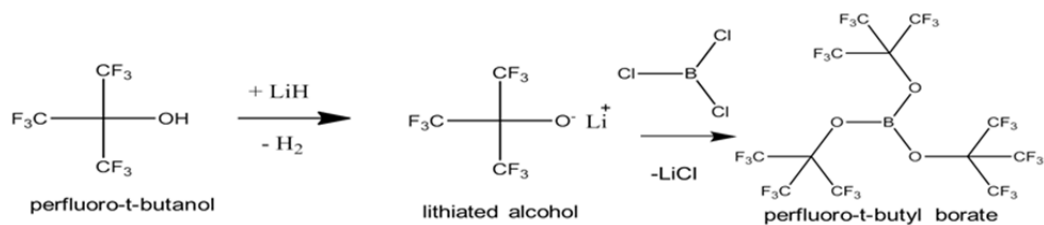
(b) Design and synthesis rationale

Previously we have found that phosphate-based additives (HFiP, PFBP) showed positive effect on anodic stability of electrolytes on high voltage cathode surfaces. Surface studies by HR-XPS also showed that fragments of HFiP ends up mostly on cathode instead of anode. Considering that phosphate is an ester that should be more related to reduction rather than oxidation, this new surface chemistry is apparently counter-intuitive. Therefore we decided to explore, if we make the additives even more electron-deficient than phosphate, whether effectiveness of those additives would be improved. Hence we choose Aluminum and Boron as the electron-deficient centers to constitute the skeleton of the new additives. Also, since HR-XPS revealed fluorinated alkyl moieties might play a key role in passivating the cathode surfaces, we designed the following Al- and B-based additives (Table 1). HFiP and PFBP were listed as references.

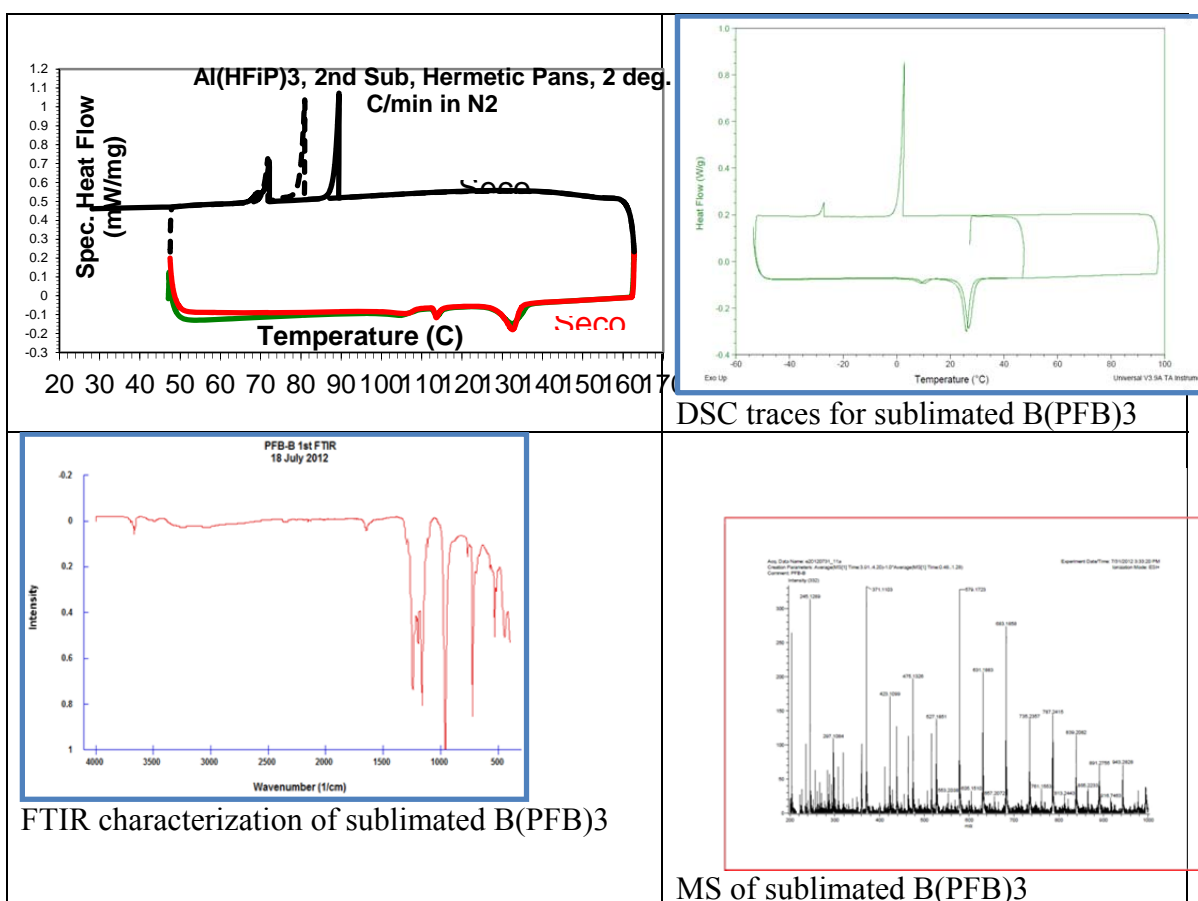
Additive Acronyms	Structures
HFIP	
PFBP	
Al(HFiP)3	
Al(PFB)3	
B(PFB)3	

(b) Purification and structural characterization

All three additives were synthesized in dryroom following established deprotonation/esterification pathway as reported earlier. B(PFB) was exemplified in the following route.



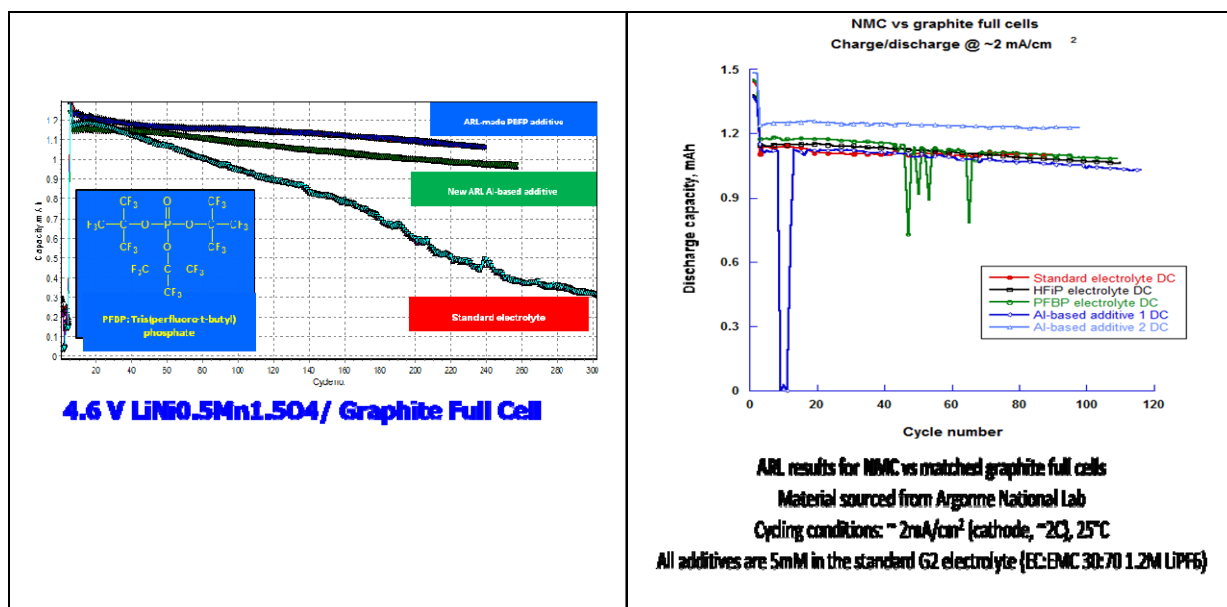
After filtration to remove inorganic species (LiCl), the liquid remnant was subject to evaporation, distillation and eventually sublimation under vacuum. Then following figures showed selected results for physical properties and structural spectra.



All Al- and B-based additives are molecular compounds that have low to medium melting points. Some of them sit on the border between liquid and solid. The solubility of all three additives are especially high in low polar solvents.

(c) Electrochemical evaluation

NMC vs. graphite and LMNO vs. A12 graphite electrochemical couples were used to evaluate those additives. The following figures showed preliminary results.



These additives demonstrated varying effects on cycling stability on both NMC/graphite and LMNO/A12 graphite electrochemical couples. Detailed investigations are underway to determine their oxidative surface chemistry. Emphasis will be placed on their fate on these cathode materials. Computational studies will assist our understanding about the structure-property relation.

Publications

- (1) “Correlating Li⁺-solvation sheath structure with interphasial chemistry”, A. v. Cresce, O. Borodin, and K. Xu, to be published
- (2) “Multifunctional structural composite batteries and supercapacitors”, J. F. Snyder, E. Gienger, E. D. Wetzel, and K. Xu, *SPIE Proceedings*, March 2012
- (3) “Genetically Programming the Interfaces between Bio-templated Cathode Nanoparticles and Current Collector in Li Ion Batteries”, K. Xu, D. Oh, H. Yi, J. Qi, A. Xu, J. Snyder, and A. Belcher, submitted to *Electrochemical Society Transaction*, **2012**, *41*, 55~64
- (4) “Tailoring an Ideal Interphases for Faster Li Ion Transport with Ionic Additives”, J. Ho, and K. Xu, submitted to *Electrochemical Society Transaction*, **2012**, *41*, 159~166
- (5) “Li⁺-Solvation Structures Directs Interphasial Processes at Graphitic Anodes”, K. Xu, and A. v. Cresce, submitted to *Electrochemical Society Transaction*, **2012**, *41*, 187~193
- (6) “Phosphate-based compounds as additives for 5-volt lithium ion electrolytes”, A. v. Cresce, and K. Xu, submitted to *Electrochemical Society Transaction*, **2012**, *41*, 17~22

- (7) “Li⁺-solvation/desolvation dictates Interphasial Process at Graphitic Anode in Li Ion Cells”, K. Xu, and A. v. Cresce, **invited contribution** to *J. Mater. Research*, **2012**, in press

Presentations

- (1) “Interfacing Electrolytes and Electrodes in Li Ion Batteries”, K. Xu, **invited speech** at the 16th International Meeting on Lithium Batteries, Jeju Island, Korea (June 18, 2012)
- (2) “Correlating Li⁺-solvation with Interphase”, A. v. Cresce, O. Borodin, and K. Xu, at 45th Power Source Conference, Las Vegas, NV (June, 2012)
- (3) “Phosphate and phosphazene electrolyte additives for high voltage cathodes in Li ion batteries”, A. v. Cresce, J. Ho, and K. Xu, at 45th Power Source Conference, Las Vegas, NV (June, 2012)
- (4) “Interphasial Chemistry on Graphitic Anode Directed by Li⁺-Solvation Sheath”, K. Xu, **invited speech** at Gordon Research Conference on Batteries, Ventura, CA (March 5, 2012)
- (5) “Li⁺-solvation structure directs interphasial processes on graphitic anodes”, K. Xu and A. v. Cresce, at 221st ECS Meeting, Seattle, WA (May, 2012)
- (6) “Metallizing graphite/electrolyte interface for faster Li⁺-transport”, J. Ho, A. v. Cresce and K. Xu, at 221st ECS Meeting, Seattle, WA (May, 2012)
- (7) “Phosphate and phosphazene electrolyte additives for Li ion batteries”, A. v. Cresce and K. Xu, at 221st ECS Meeting, Seattle, WA (May, 2012)
- (8) “Li Battery Materials Research at Army Research Lab”, K. Xu, **invited speech** at Israeli-US Defense Departments P&E Workshop, Bar Ilan University/Tel Aviv (Feb, 2012)
- (9) “Interphasial Chemistry and Processes in Li ion Devices”, K. Xu, **invited speech** at American Ceramic Society Meeting, Orlando, FL (Jan 18, 2012)

TASK 1

Battery Cell Materials Development

Project Number: 1.1D (ES025)

Project Title: Development of Advanced Electrolyte Additives

Project PI, Institution: Zhengcheng (John) Zhang, Argonne National Laboratory

Collaborators (include industry): Khalil Amine, Lu Zhang, Libo Hu

Project Start/End Dates: 10/01/2008~09/30/2014

Objectives: The objective of this work is to develop new electrolytes and associated additives that could bring additional features to the state-of-the-art lithium-ion battery electrolyte to meet the requirements of EV and PHEV applications.

Approach: The approach for development novel electrolyte and additives consists of three phases. The first phase is to screen and evaluate novel electrolyte and additive candidates using DFT theory and relative sample test procedures. Certain criteria are needed to make the screening list. In the second phase, thorough evaluation and mechanism analysis will be conducted to the promising candidates to gain the insights of their superior performance. In the third phase, based on the knowledge earned, new design of promising electrolytes and additives should be proposed and organic synthesis will be involved to make these compounds. Evaluations will certainly give feedback to our designs and thus leading to modifications and even more new designs.

Milestones

(a) Establish screening system that could continuously generate promising candidates for this project. To meet this goal, the semi-empirical rule and theoretical computation were constantly involved and modified based on the feedbacks from the experimental evaluation, Sep. 2013 (On schedule).

(b) Establish valid and efficient evaluation procedures to confirm the electrochemical performance of promising additive candidates. Different chemistries are chosen to serve different purposes, such as NCA/MCMB for anode improvements and $\text{LiNi}_{0.5}\text{Mn}_{1.5}\text{O}_4/\text{LTO}$ for cathode improvements, Sep. 2013 (On schedule).

(c) Understand connections between chemical structures and electrochemical performance by looking into the mechanism of promising additives. Progress is based on various characterization, mechanism analysis, and experimental reconfirmations, Sep. 2013, (On schedule).

(d) Design novel SEI additives based on the knowledge gained through previous studies. Incorporation of UD containing functional groups is one important approach, and computational simulation is also involved for quick evaluation of feasibility, Sep. 2013, (On schedule).

Financial data: \$400K/FY2012

PROGRESS TOWARD MILESTONES

(a) Summary of work in the past quarter related to milestone (a).

Degree of Unsaturation (DU) was utilized as the criterion for screening electrolyte additives, which is valid in our study cases. DU can derive from cyclic and double bond structures, based on which various types of additives can be developed. As shown in **Figure 1**, the additive A3 and A4 are built with bicyclic structures, which are expected to be reduction type additives. On the other hand, additive A12 and A29 are built with multiple double bonds, which are regarded as polymerization type additives. In both cases, the computational method is employed to estimate the reduction potentials. **Figure 2** shows the mechanism of the SEI formation using A3 additive during reduction process which is supported by the DFT calculation.

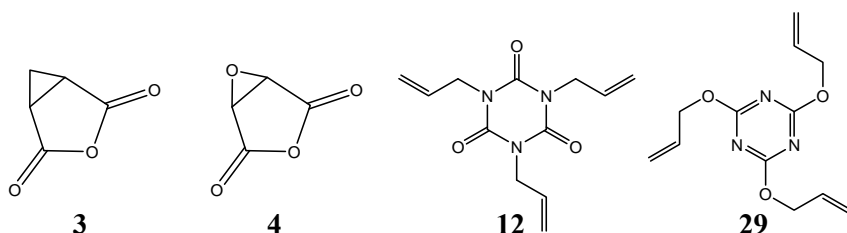


Figure 1. New additive candidates containing unsaturated bonds.

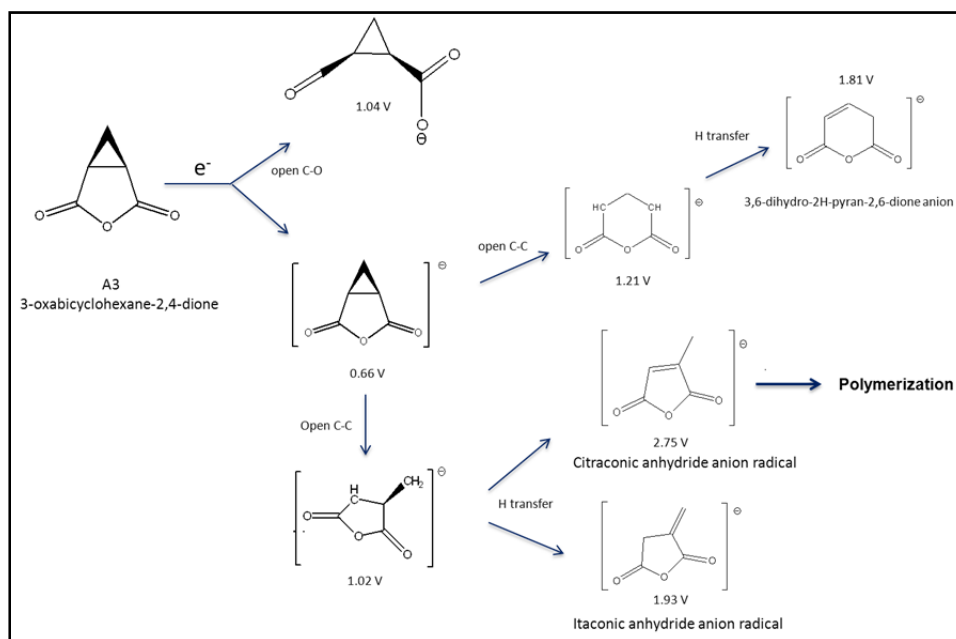


Figure 2. SEI formation mechanism by the reductive decomposition of A3 additive. This proposed pathway was supported by the DFT calculation results.

(b) Summary of work in the past quarter related to milestone (b)

NMC/MCMB chemistry was employed for anode additive study. The capacity retention and ac impedance profiles were collected to evaluate the performance improvement. To accelerate the evaluation process, the elevated temperature (55°C) and high C-rate (1C) were adopted as efficient screening procedures. For cathode additive study, $\text{LiNi}_{0.5}\text{Mn}_{1.5}\text{O}_4/\text{LTO}$ was used as standard chemistry. The capacity retention profiles were obtained under different conditions. Some electrochemical measurements are also conducted for quick evaluation, such as cyclic voltammetry.

Using this procedure, quite a few additives have been evaluated and showed promising performance. Additive A3 was one example that was screened out from our screening procedure. **Figure 3** (a) shows the differential capacity profiles of the cells with and without additive A3. As the A3 concentration increases, EC decomposition peaks at 2.8V was significantly depressed and a new peak at around 2.2 V showed up, indicating A3 was effectively involved in the SEI formation process. With 0.2 w% of additive, the cell showed dramatic improvements in capacity retention at 55°. More interestingly, the impedance of the cell with A3 additive (**Figure 4**) remains the same to that without additive. This result is very encouraging since the SEI formed during the polymerization of A3 is thin but yet very effective.

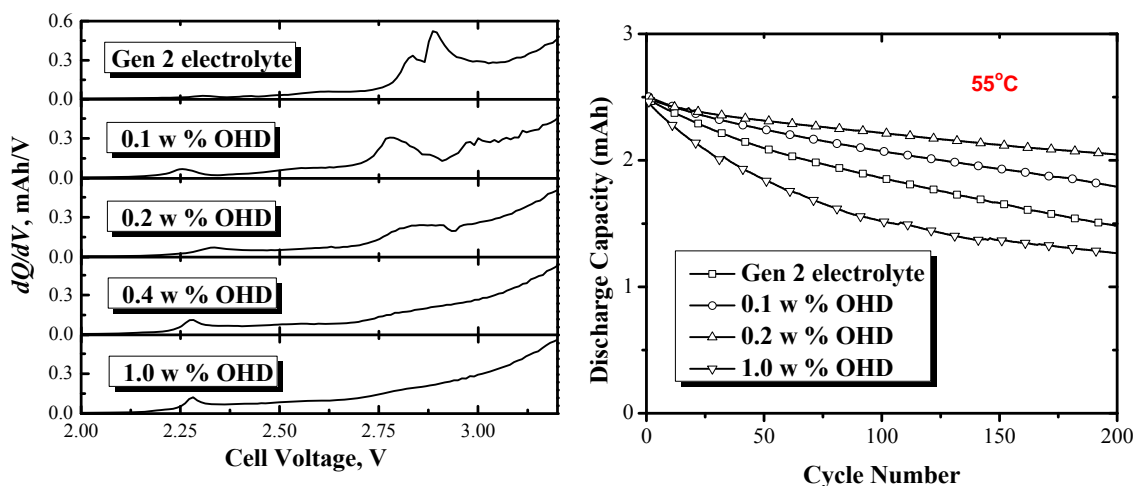


Figure 3. (a) Differential capacity profiles of MCMB/NCM cells, electrolyte: 1.2M LiPF_6 EC/EMC 3/7 with and without A3; (b) Capacity retention of MCMB/NCM cells cycled between 2.7 and 4.2V at 55 °C in electrolyte of 1.2M LiPF_6 EC/EMC 3/7 with no and various amount of additive A3.

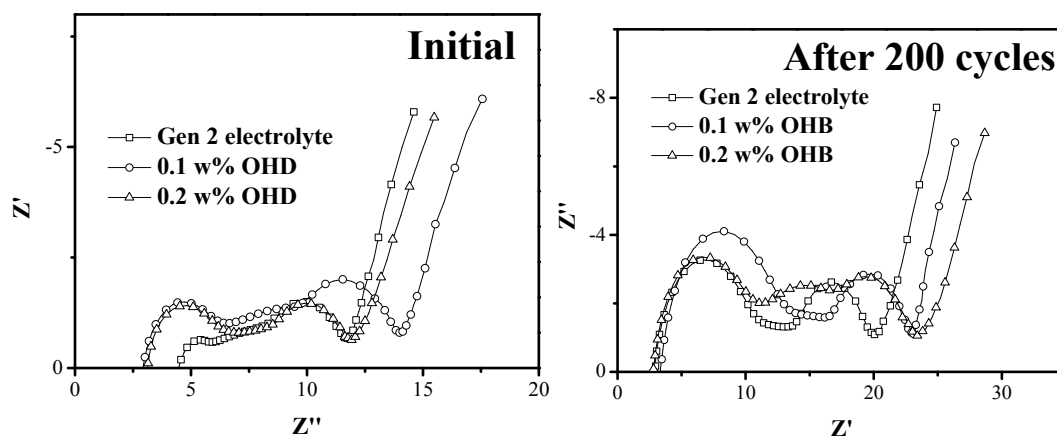


Figure 4. (a) Initial ac impedance profiles and (b) after 200 cycles of MCMB/NCM cells with and without various amount of A3 additive in 1.2M LiPF₆ EC/EMC 3/7.

(c) Summary of work in the past quarter related to milestone (c)

Understanding the connection between chemical structures and electrochemical performance is of tremendous importance to this project, which will certainly help develop new additives. One approach we took is to utilize surface characterizations to study the interfaces within cell system. For instance, the mechanism of A3 was investigated using various techniques, such as FT-IR, SEM and XPS. Unlike the maleic anhydride derivatives, A3 additive shows no significant increase the initial interfacial impedance of the cell. **Figure 5** shows the FT-IR spectra of MCMB electrodes harvested from cells containing different amount of A3 after formation process. Based on our previous study, peaks around 1622, 1396 cm⁻¹ should be attributed to C=O asymmetric stretch and symmetric stretch vibration, and 1074 and 813 cm⁻¹ peaks are identified as C-O stretch vibration and OCO₂⁻ bending vibration. As the concentration of A3 increased, both 1622 and 1396 peaks decreased in intensity, indicating the decrease of C=O double bonds. Peaks at 1074 and 813 cm⁻¹ increased slightly as additive amount increased, indicating the accumulation of Li₂CO₃ in the SEI layer

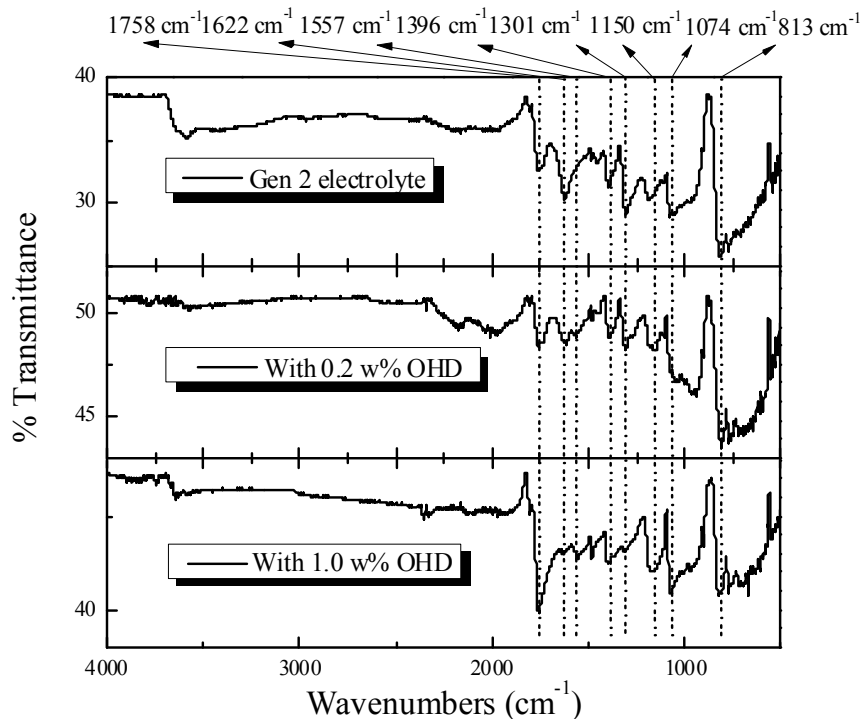


Figure 5. FTIR spectra of MCMB electrodes obtained from the MCMB/NCM cells containing various amount of A3 after formation.

(d) Summary of work in the past quarter related to milestone (d)

Based on our screening results, we identified novel compounds that have potential to be excellent SEI additives. One example presented here is ethylene phosphate-based compounds, whose chemical structures are shown in **Figure 6**. As discussed above, cyclic and double bond structures are promising SEI additives. Cyclic ethylene phosphate, with a DU of 2, was chosen as the base structure to build novel SEI additives. In addition, P-based compounds are known to be good flame retardants, which bring an additional feature to SEI additives. Functional groups with higher DU, such as ester, ring, double bond structures, were also proposed in building novel additives, which could increase the activities and add extra benefits to the electrolyte system. Other groups include heteroatoms, such as silicon, and ether chain, allowing us to tune the SEI properties.

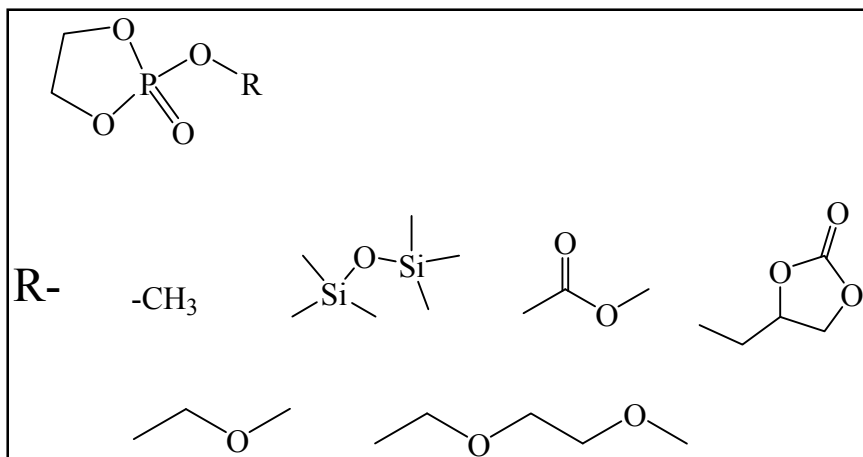


Figure 6. Proposed ethylene phosphate-based compounds as potential SEI additives.

Currently, ethylene methyl phosphate (EMP) is being synthesized. Some difficulties in separation and purification were met and are being addressed. **Figure 7** is the nuclear magnetic resonance (NMR) spectrum of this compound.

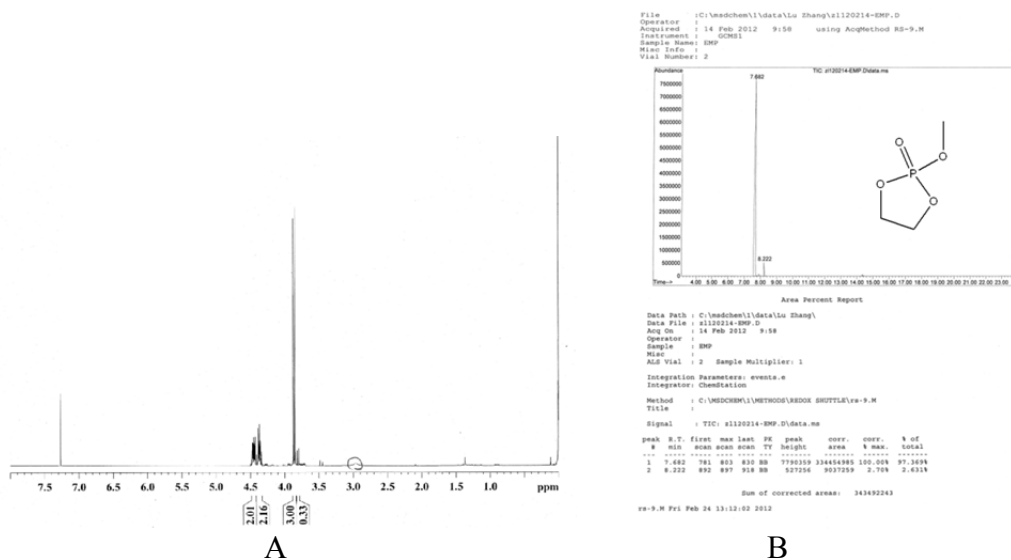


Figure 7. $^1\text{H-NMR}$ (A) and GC spectra (B) of synthesized ethylene methyl phosphate (EMP).

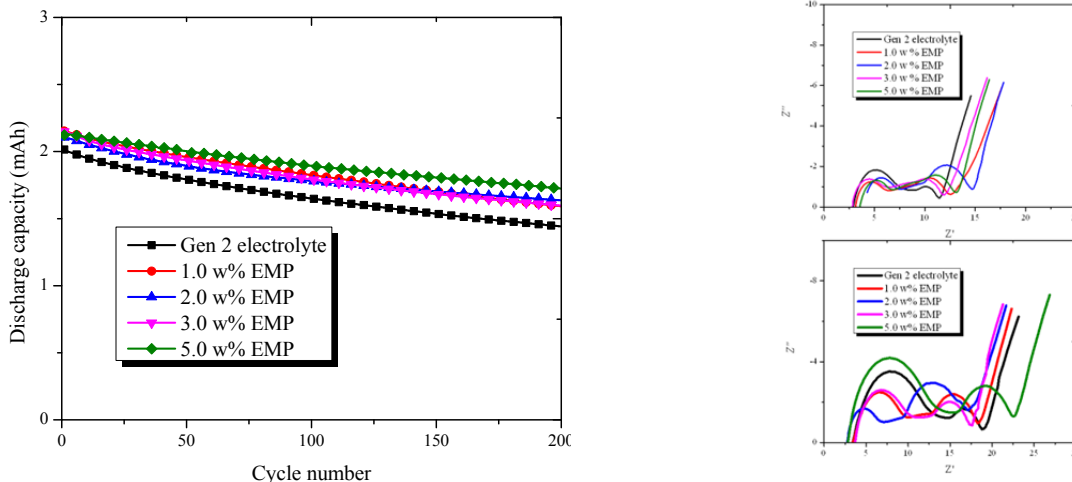


Figure 8. (a) Capacity retention of MCMB/NCM cells cycled between 3 and 4V at 55 °C in electrolyte of 1.2M iPF₆ EC/EMC 3/7 with no and various amount of additive EMP. (b) impedance profiles of MCMB/NCM cells after formation (up) and after 200 cycles (bottom) containing no and various amount of additive EMP.

Initial electrochemical results indicate EMP (Figure 8) is an effective additive for the MCMB/NMC chemistry. Its mechanism and characterization of the SEI identification are in progress.

Publications, Reports, Intellectual property or patent application filed this quarter. (Please be rigorous, include internal reports--invention records, etc.)

Inventions:

Lu Zhang, Zhengcheng Zhang, Khalil Amine, “NON-AQUEOUS ELECTROLYTE FOR LITHIUM-ION BATTERIES”, invention report, ANL-IN-10-39;

Zhengcheng Zhang, Lu Zhang, Khalil Amine, “Non-Aqueous Electrolyte for Lithium-Ion Batteries”, (internal # ANL-IN-12-022).

Lu Zhang, Zhengcheng Zhang, Lu Zhang, Khalil Amine, “Functional Electrolyte for Lithium-Ion Batteries”, (internal # ANL-IN-12-023).

Peer review paper:

Lu Zhang, Zhengcheng Zhang, Paul C. Redfern, Larry A. Curtiss, and Khalil Amine, “Molecular engineering towards safer lithium-ion batteries: a highly stable and compatible redox shuttle for overcharge protection”, Energy & Environmental Science, 2012, **5**, 8204.

Book Chapter:

Lithium Ion Batteries - New Developments.

Chapter 7, “Redox Shuttle Additives for Lithium-Ion Battery”, Published on 2012-02-24.

Authors: Lu Zhang, Zhengcheng Zhang and Khalil Amine.

Presentations:

Zhang, Lu; Zhang, Zhengcheng; Amine, Khalil “Recent Development of Redox Shuttles for Li Ion Batteries at Argonne National Laboratory”, invited talk, THE 29TH INTERNATIONAL BATTERY SEMINAR & EXHIBIT, March 12 - 15, 2012, Fort Lauderdale, Florida.

Zhang, Lu; Zhang, Zhengcheng; Amine, Khalil, “Redox shuttles for overcharge protection of lithium-ion batteries”, Oral presentation, 221st ECS Meeting in Seattle, Washington.

Zhang, Zhengcheng; Zhang, Lu; Kyrrilos Youssef; and Amine, Khalil “Advanced Electrolyte Additives for PHEV/EV Lithium-ion Battery”, ES025, DOE ABR annual merit meeting, Washington D. C., May 14th~18th, 2012.

TASK 1

Battery Cell Materials Development

Project Number: ES026

Project Title: Electrolytes for Use in High Energy Li-Ion Batteries with Wide Operating Temperature Range

Project PI, Institution: Marshall Smart, Jet Propulsion Laboratory, California Institute of Technology

Collaborators (include industry): (1) University of Rhode Island (Prof. Brett Lucht) (Analysis of harvested electrodes, on-going collaborator), (2) Argonne Nat. Lab (Khalil Amine) (Source of electrodes, on-going collaborator), (3) LBNL (John Kerr, Li Yang) (Evaluation of novel salts), (4) Loker Hydrocarbon Institute, USC (Prof. Surya Prakash) (Fluorinated Solvents and novel salts), (5) A123 Systems, Inc. (Electrolyte development, on-going collaborator), (6) Quallion, LCC. (Electrolyte development, on-going collaborator), (7) Yardney Technical Products (Electrolyte development, on-going collaborator), (8) Saft America, Inc. (Collaborator, industrial partner under NASA program), (9) NREL (Smith/Pesaran)(Supporting NREL in model development by supplying data), (10) Sandia National Laboratory (Safety testing of low flammability electrolyte and supplier of electrode materials), and (11) Hunter College (Prof. Greenbaum) (Ex-situ NMR measurements).

Project Start/End Dates: Start Date: Oct 1, 2009, Projected End Date: September 30, 2014

Objectives:

- Develop a number of advanced Li-ion battery electrolytes with improved performance over a wide range of temperatures (-30 to +60°C) and demonstrate long-life characteristics (5,000 cycles over 10-yr life span).
- Improve the high voltage stability of these candidate electrolyte systems to enable operation up to 5V with high specific energy cathode materials.
- Define the performance limitations at low and high temperature extremes, as well as, identify life limiting processes.
- Demonstrate the performance of advanced electrolytes in large capacity prototype cells.

Approach: The development of electrolytes that enable operation over a wide temperature range, while still providing the desired life characteristics and resilience to high temperature (and voltage) remains a technical challenge. To meet the proposed objectives, the electrolyte development will include the following general approaches: (1) optimization of carbonate solvent blends, (2) use of low viscosity, low melting ester-based co-solvents, (3) use of fluorinated esters and fluorinated carbonates as co-solvents, (4) use of novel “SEI promoting”

and thermal stabilizing additives, (5) use of alternate lithium based salts (with USC and LBNL). Many of these approaches will be used in conjunction in multi-component electrolyte formulations (i.e., such as the use of low viscosity solvents and novel additives and salts), which will be targeted at improved operating temperature ranges while still providing good life characteristics.

The candidate electrolytes are characterized using a number of approaches, including performing ionic conductivity and cyclic voltammetry measurements, and evaluating the performance characteristics in experimental ~ 200-400 mAh three-electrode cells. In addition to evaluating candidate electrolytes in spirally-wound experimental cells, studies will be performed in coin cells, most notably in conjunction with high voltage cathode materials. Cells will be fabricated using a number of electrode couples: (a) MCMB/LiNi_{0.8}Co_{0.2}O₂, (b) graphite/LiNi_{0.8}Co_{0.15}Al_{0.05}O₂, (c) graphite/LiNi_{1/3}Co_{1/3}Mn_{1/3}O₂, (d) Li₄Ti₅O₁₂ (LTO)/LiNi_{0.5}Mn_{1.5}O₂ (LMNO), and (e) graphite/LiNiCoMnO₂ (lithium excess, layered-layered composite). Other chemistries can be evaluated depending upon availability from collaborators. In addition to performing charge/discharge characterization over a wide range of temperatures and rates on these cells, a number of electrochemical characterization techniques will be employed, including: (1) Electrochemical Impedance Spectroscopy (EIS), (2) DC linear (micro) polarization, and (3) Tafel polarization measurements. The electrochemical evaluation in proven three-electrode test cells enables electrochemical characterization of each electrode (and interface) individually and the identification of performance limiting mechanisms for each electrode and for the cell. Electrodes are easily harvested from these test cells and samples will be delivered to collaborators (i.e., URI and Hunter College).

Performance testing of prototype cells containing candidate advanced electrolytes will be performed and evaluated under a number of conditions, i.e., assessment of wide operating temperature capability and life characteristics. JPL has on-going collaborations with several battery vendors and also has the capabilities to perform extensive testing. Typical prototype cell designs that will be considered include (i) Yardney 7 Ah prismatic cells, (ii) Quallion prismatic cells (0.250Ah size and 12 Ah size), and (iii) A123 2.2 Ah cylindrical cells. Cells will be procured and/or obtained through on-going collaborations

Milestones:

Month/Year	Milestone
Sept. 2012	Milestone A: Prepare and characterize experimental laboratory cells containing Gen-3 electrolytes, designed to operate over a wide temperature range in high voltage systems (i.e., Li(NiMnCo)O ₂ and LiNi _{0.5} Mn _{1.5} O ₂), and identify performance limiting characteristics (Sep. 12)
Sept. 2012	Milestone B: Demonstrate improved performance of second generation electrolytes over a wide temperature range (-30° to +60°C) compared with baseline electrolytes, in experimental and prototype cells (Sep. 12)

Financial data:

Total project funding:

- 875K total (~ 175K/year)
- Contractor share = 0K

Funding received:

- FY'10 = 175K (Start Date = Oct 1, 2009)
- FY'11 = 175K
- FY'12 = 170K

Accomplishments and Progress toward Milestones:

In the recent quarter, we have subjected a number of large capacity 12 Ah cells (MCMB Carbon/LiNiCoAlO₂) that contain wide operating temperature range electrolytes to cycle life testing to determine the life characteristics and the extent to which the low temperature capability degrades with time. These cells have been obtained from our collaborator (Quallion, LCC) and contain electrolytes that have been demonstrated to have excellent low temperature capabilities in experimental and prototype cells, namely (i) 1.20M LiPF₆ in EC+EMC+MP (20:20:60 v/v %) and (ii) 1.20M LiPF₆ in EC+EMC+MP (20:20:60 v/v %) + 4% FEC. In addition to JPL developed electrolytes, the group of cells contain a Quallion developed wide operating temperature range electrolyte and the DOE baseline electrolyte (i.e., 1.2M LiPF₆ in EC+EMC (30:70 v/v %)). After completing extensive low temperature discharge rate testing, the cells were placed on partial depth of discharge cycling (approximately 50% DOD) consisting of one cycle performed each day using a variable load profile with low to moderate rates. Once 100 days of operation under this cycling regime was completed (100 cycles), the cells were re-characterized to determine the capacity, impedance, and low temperature discharge rate capability. As shown in Table 1, good capacity retention was observed with all of cells after completing initial characterization and low temperature testing (~100 cycles) and the life testing, representing approximately one year of testing. The best capacity retention observed was with the cell containing the methyl propionate-based electrolyte that contains FEC as an additive (4%), slightly outperforming the baseline electrolytes, suggesting that the additive has produced a desirable, protective SEI layer. In addition to performing 100% DOD capacity and impedance determination, the cells were subjected to discharge rate testing at low temperature (-20° to -50°C) over a range of rates (C/10 to 2C) to determine the extent to which the low temperature capability has degraded. As shown in Table 2, good retention of low temperature capability was observed at -20° and -40°C when evaluated at C/5 and 2C rates, with generally 2-4% loss in capacity and energy under these conditions, with the cells containing the methyl propionate-based cells delivering the highest capacity and energy. It is interesting to note that under certain conditions (i.e., 2C rate at -40°C) high capacity was observed after life testing, which is attributed to the increased impedance leading to enhanced internal cell heating during discharge.

		Cell QP-49							Cell QP-65					Cell QP-66				Cell QP-46					
		1.20 M LiPF ₆ in EC+EMC (30:70 v/v %)							Quallion Electrolyte A1					1.20 M LiPF ₆ in EC+EMC+MP (20:20:60 v/v %)				1.20 M LiPF ₆ in EC+EMC+MP (20:20:60 v/v %) + 4% FEC					
	Temperature	Discharge Rate	Discharge Current (A)	Discharge Capacity (Ah)	Percent C10 Capacity	Percent C10 Capacity at 20°C	Discharge Watt-Hr (Wh)	Discharge Energy (Wh/Kg)	Discharge Capacity (Ah)	Percent C10 Capacity	Percent C10 Capacity at 20°C	Discharge Watt-Hr (Wh)	Discharge Energy (Wh/Kg)	Discharge Capacity (Ah)	Percent C10 Capacity	Percent C10 Capacity at 20°C	Discharge Watt-Hr (Wh)	Discharge Energy (Wh/Kg)	Discharge Capacity (Ah)	Percent C5 Capacity	Percent C5 Capacity at 20°C	Discharge Watt-Hr (Wh)	Discharge Energy (Wh/Kg)
Initial Capacity	20°C	C/5	2.400	13.6031	100.00	100.00	49.5323	93.74	12.5561	100.00	100.00	45.6779	88.83	14.1289	100.00	100.00	51.3849	97.25	13.2675	100.00	100.00	48.3083	91.42
After Low Temperature Testing	20°C	C/5	2.400	13.4195	98.65	98.65	48.7900	92.34	12.3607	98.44	98.44	44.9340	87.39	13.4466	95.17	95.17	48.9430	92.62	13.2637	99.97	99.97	48.1530	91.13
After Completing 100 Cycles	20°C	C/5	2.400	13.1084	96.36	96.36	47.6936	90.26	11.9451	95.13	95.13	43.4942	84.59	13.0794	92.57	92.57	47.6478	90.17	12.8422	96.79	96.79	46.6732	88.33

Table 1: Capacity determination of 12Ah MCMB-LiNiCoAlO₂ cells (Quallion, LCC) containing various electrolytes after low temperature characterization and partial DOD cycle life testing , using C/5 rates over a voltage range of 2.75V to 4.10V.

		Cell QP-49							Cell QP-65					Cell QP-66				Cell QP-46					
		1.20 M LiPF ₆ in EC+EMC (30:70 v/v %)							Quallion Electrolyte A1					1.20 M LiPF ₆ in EC+EMC+MP (20:20:60 v/v %)				1.20 M LiPF ₆ in EC+EMC+MP (20:20:60 v/v %) + 4% FEC					
	Temperature	Discharge Rate	Discharge Current (A)	Discharge Capacity (Ah)	Percent C10 Capacity	Percent C10 Capacity at 20°C	Discharge Watt-Hr (Wh)	Discharge Energy (Wh/Kg)	Discharge Capacity (Ah)	Percent C10 Capacity	Percent C10 Capacity at 20°C	Discharge Watt-Hr (Wh)	Discharge Energy (Wh/Kg)	Discharge Capacity (Ah)	Percent C10 Capacity	Percent C10 Capacity at 20°C	Discharge Watt-Hr (Wh)	Discharge Energy (Wh/Kg)	Discharge Capacity (Ah)	Percent C5 Capacity	Percent C5 Capacity at 20°C	Discharge Watt-Hr (Wh)	Discharge Energy (Wh/Kg)
Initial Capacity	-20°C	C/5	2.400	11.5647	85.02	85.02	40.0224	75.74	11.1605	88.88	88.88	38.5397	74.95	11.9173	84.35	84.35	41.1668	77.91	11.4780	86.51	86.51	39.4647	74.69
		2.0C	24.00	11.2530	82.72	82.72	35.2471	66.71	11.1740	88.99	88.99	35.9119	69.84	11.9768	84.77	84.77	38.2553	72.40	11.3029	85.19	85.19	35.2538	66.72
After Completing 100 Cycles (100 Days)	-20°C	C/5	2.400	11.2645	82.81	82.81	38.7449	73.32	10.7899	85.74	85.74	36.6991	71.28	11.3759	80.52	80.52	38.8384	73.50	11.3547	85.58	85.58	39.1845	74.16
		2.0C	24.00	11.2025	82.35	82.35	34.8236	65.90	10.8943	86.08	86.08	34.4055	68.91	11.5607	81.82	81.82	36.3958	68.88	11.4050	85.96	85.96	34.8383	65.93
Initial Capacity	-40°C	C/5	2.400	9.4562	69.52	69.52	27.9256	52.85	10.1802	81.08	81.08	31.3574	60.98	10.8938	77.10	77.10	33.5327	63.46	10.1753	76.69	76.69	31.3902	59.41
		2.0C	24.00	9.7003	71.31	71.31	26.3924	49.95	10.7160	85.35	85.35	31.6800	61.61	11.4353	80.94	80.94	33.5327	63.46	10.4989	79.13	79.13	30.3517	57.44
After Completing 100 Cycles (100 Days)	-40°C	C/5	2.400	9.6569	70.99	70.99	28.2589	53.48	9.8088	78.03	78.03	28.7043	55.82	10.1014	71.49	71.49	30.4018	57.54	10.0273	75.58	75.58	30.3270	57.39
		2.0C	24.00	10.0405	73.81	73.81	27.3641	51.79	10.4199	82.99	82.99	30.0334	58.39	11.0347	78.10	78.10	31.7327	60.05	10.7799	81.25	81.25	29.9095	56.60

Table 1: Discharge rate testing at low temperature of 12Ah MCMB-LiNiCoAlO₂ cells (Quallion, LCC) containing various electrolytes after low temperature characterization and partial DOD cycle life testing (cells were charged at 20°C prior to low temperature discharging).

We are also continuing to evaluate a number of cells (0.25Ah MCMB/LiNiCoAlO₂ cells manufactured by Quallion, LCC) that contain a number of electrolytes that are permutations of this approach, consisting of methyl propionate with varying amounts of mono-fluoroethylene carbonate (4, 10, and 20%) and 1.20M LiPF₆ in EC+EMC+MP (20:20:60 vol %) + 0.10M LiBOB. The use of LiBOB as an additive has been previously identified to result in improved low temperature performance coming mainly from improved cathode kinetics. These electrolytes were envisioned to have improved high temperature resilience compared to the baseline MP-containing electrolyte. A number of performance tests are currently being implemented on these cells, including discharge rate characterization as a function of temperature, charge rate characterization, and cycle life performance under various conditions (including cycling at high temperatures). Of

these electrolytes, the formulation containing LiBOB has been observed to have the best low temperature performance and cycle life performance at high temperature. As illustrated in Figure 2, excellent discharge rate capability has been observed at -40°C (delivering 49 Wh/kg at a 5C discharge rates) and at -50°C (delivering over 40 Wh/kg at a 4C discharge rate).

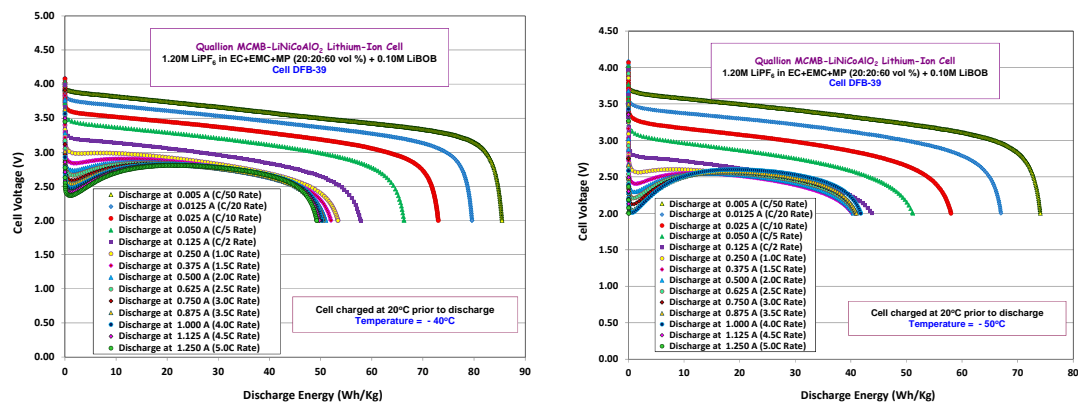


Figure 1: Discharge performance of a 0.25Ah MCMC-LiNiCoAlO₂ cell (Quallion, LCC) containing a methyl propionate-based electrolytes with LiBOB at -40°C (Fig. 1A) and at -50°C (Fig. 1B). (Cell was charge at room temperature prior to low temperature discharging).

We also continue to evaluate the life characteristics of a number of A123 cells that possess methyl butyrate-based electrolytes previously investigated under this program (i.e., specifically 1.20M LiPF₆ in EC+EMC+MB (20:20:60 vol %) + 4% FEC and 1.20M LiPF₆ in EC+EMC+MB (20:20:60 vol %) + 2% VC). As reported previously, these cells have exhibited excellent rate capability over a wide temperature range (-60°C to $+20^{\circ}\text{C}$) being able to support up to 10C rates at temperatures as low as -50°C and C rates at -60°C . As illustrated in Fig. 2, excellent cycle life has been obtained with the cells exhibiting over 6,000 cycles to-date (on test for over two years) and displaying comparable performance to the baseline electrolyte (over 85% of the initial capacity). We also continue to evaluate the high temperature resilience of these systems by implementing variable temperature cycling tests, in which the cells are continuously cycled between temperature extremes (i.e., at -20° and $+50^{\circ}\text{C}$) with charging and discharging at the respective temperature, as shown in Fig 2B. Although the electrolyte variant with FEC was observed previously to be less resilient to high temperature exposure compared to the VC-containing electrolyte, good performance was observed over the temperature with only modest loss in capacity.

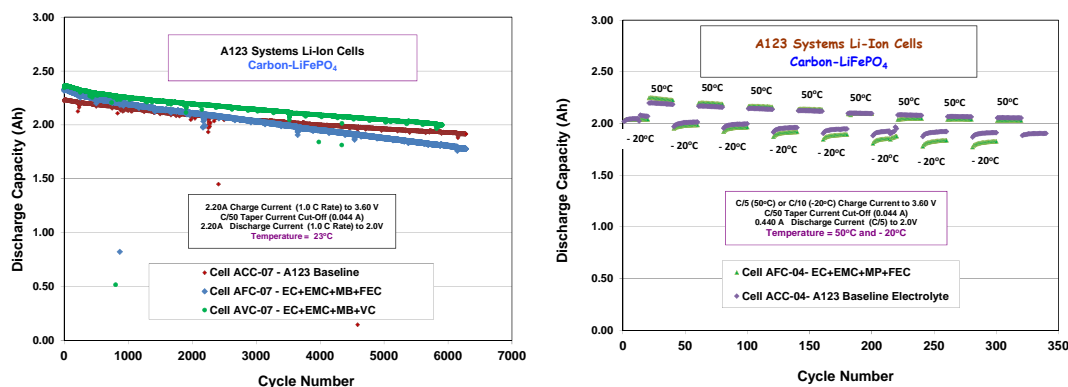


Figure 2: Cycle life performance of LiFePO₄-based A123 cells containing various electrolytes at +23°C (Fig. A) and variable temperature cycling between +50°C and -20°C.

In the last quarter, we have also continued to focus upon investigating ester-based wide operating temperature range electrolytes with high voltage systems, including LiNi_{1/3}Co_{1/3}Mn_{1/3}O₂ and the excess lithium layered-layered composite oxides Li(NiCoMn)O₂ (NMC) (from two sources). We continue to study a number of methyl butyrate-based electrolytes (with various additives, including vinylene carbonate, lithium oxalate, FEC and LiBOB) in larger three-electrode cells consisting of Conoco graphite anodes and NMC cathodes supplied by Argonne National Labs. Being equipped with lithium reference electrodes, these cells enabled us to study the lithium kinetics of the respective electrodes by electrochemical techniques. In particular, both anodes and cathodes were subjected to a number of electrochemical measurements, including Electrochemical Impedance Spectroscopy (EIS), Tafel polarization, and linear micro-polarization measurements. As reported previously, upon performing Tafel polarization measurements on each electrode (which possess relatively heavy loadings), it was observed that the NMC-based cathode displayed poor lithium kinetics (limiting electrode) compared to the anode. EIS measurements support these findings and suggest that the charge-transfer kinetics of the cathode is particularly slow and contributes significantly to the overall cell impedance and poor rate capability. We have recently characterized the discharge rate of these cells as a function of temperature (down to 0°C) and all of the methyl butyrate-based electrolytes (with various additives) displayed improved low temperature capability compared with the baseline, with 1.20M LiPF₆ in EC+EMC+MB (20:20:60 vol %) + 0.10M LiBOB delivering the best performance which is attributed to improved cathode kinetics, as substantiated by the Tafel polarization measurements, and improved ionic conductivity. Although improved low temperature performance has been demonstrated, it should be noted that the rate capability of the system (which is dominated by the NMC) is much poorer than comparable NCA-based systems, which is magnified at low temperatures.

Electrolyte Type		1.0M LiPF ₆ + 0.10M LiBOB EC+EMC+MB (20:20:60 vol%)			1.0M LiPF ₆ EC+EMC+MB (20:20:60 vol%) + 1.5% VC			1.0M LiPF ₆ EC+EMC+MB (20:20:60) + lithium oxalate			1.2M LiPF ₆ EC+EMC (30:70 vol%)		
Temperature	Current (mA)	Capacity (Ahr)	Capacity (mAh/g)	Percent (%)	Capacity (Ahr)	Capacity (mAh/g)	Percent (%)	Capacity (Ahr)	Capacity (mAh/g)	Percent (%)	Capacity (Ahr)	Capacity (mAh/g)	Percent (%)
23°C	C/20	0.1100	243.87	100.00	0.1018	224.33	100.00	0.1168	257.10	100.00	0.1211	266.57	100.00
	C/10	0.1059	234.95	96.34	0.1001	220.53	98.31	0.1130	248.60	96.69	0.1108	243.84	91.47
	C/5	0.0973	215.91	88.54	0.0947	208.66	93.01	0.1039	228.57	88.90	0.1029	226.42	84.94
	C/2	0.0843	186.92	76.65	0.0840	185.03	82.48	0.0900	197.97	77.00	0.0896	197.16	73.96
10°C	C/20	0.0972	215.59	88.40	0.0829	182.73	81.45	0.0974	214.33	83.37	0.1037	228.15	85.58
	C/10	0.0911	201.99	82.82	0.0798	175.82	78.37	0.0894	196.81	76.55	0.0858	188.84	70.84
	C/5	0.0798	177.06	72.60	0.0717	158.05	70.46	0.0798	175.55	68.28	0.0599	131.77	49.43
	C/2	0.0636	141.14	57.88	0.0526	116.01	51.71	0.0585	128.72	50.07	0.0335	73.81	27.69
0°C	C/20	0.0848	187.98	77.08	0.0668	147.14	65.59	0.0808	177.86	69.18	0.0748	164.70	61.78
	C/10	0.0745	165.15	67.72	0.0559	123.14	54.89	0.0670	147.33	57.30	0.0349	76.85	28.83
	C/5	0.0646	143.21	58.72	0.0467	102.91	45.88	0.0559	123.02	47.85	0.0250	55.12	20.68
	C/2	0.0491	108.92	44.66	0.0235	51.71	23.05	0.0334	73.53	28.60	0.0130	28.57	10.72

Table 2: Discharge rate performance of Conoco A12 graphite/Toda HE 5050 LiNiCoMnO₂ cells in contact with various methyl butyrate-based electrolytes at 20°, 10° and 0°C.

We also continued our efforts to evaluate a number of low flammability electrolytes in cells consisting of Conoco graphite anodes and LiNi_{1/3}Co_{1/3}Mn_{1/3}O₂ cathodes (electrodes supplied by Sandia National Laboratory). These electrolytes were previously developed under a NASA-funded project and possess triphenyl phosphate (TPP) as a flame retardant additive (10 to 15%). As a result of interest that DOE has expressed, cells containing some of these low flammability electrolytes developed at JPL are being subjected to safety testing by collaborators at Sandia National Laboratory. A number of TPP-containing electrolytes have been shown to result in comparable reversible capacities compared with the baseline electrolytes (approximately 2-4% decrease in capacity). Due to the lower conductivity of the TPP-containing electrolytes, somewhat lower discharge rate capability is observed, as illustrated in Fig. 3, as one would expect. Good cycle life has been obtained thus far, as shown in Fig. 4, which is consistent with results that we have obtained traditional chemistries (i.e., NCA-based).

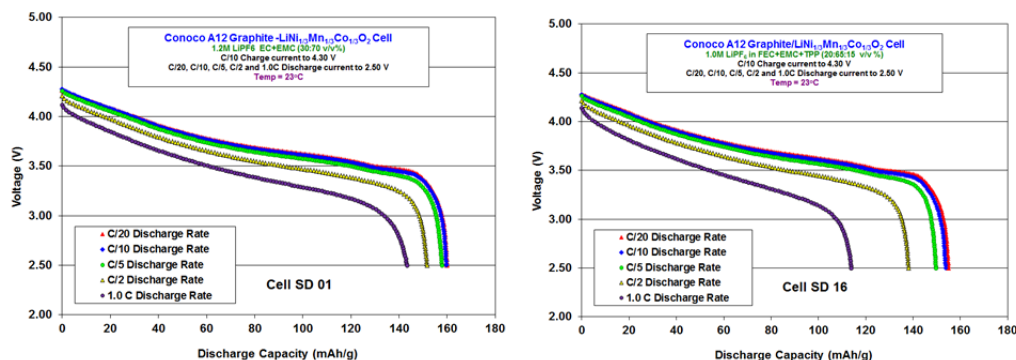


Figure 3: Discharge rate capability of graphite/ and LiNi_{1/3}Co_{1/3}Mn_{1/3}O₂ coin cells for the baseline electrolyte (Fig. 3A) and a TPP-containing formulation (Fig. 3B).

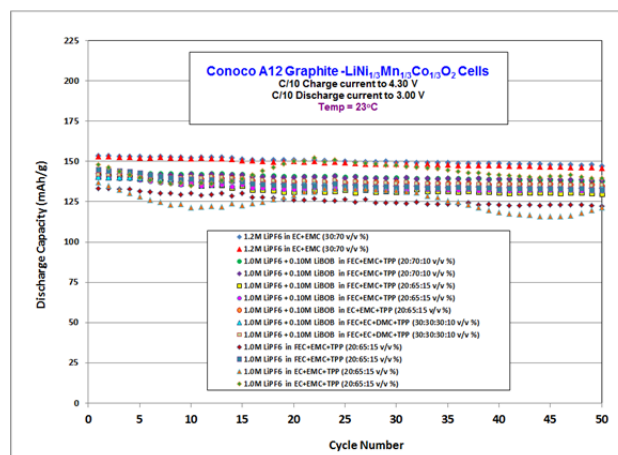


Figure 3: Discharge rate capability of graphite/ and $\text{LiNi}_{1/3}\text{Co}_{1/3}\text{Mn}_{1/3}\text{O}_2$ coin cells for the baseline electrolyte (Fig. 3A) and a TPP-containing formulation (Fig. 3B).

Future work will involve continuing the investigation of the use of additives in conjunction with ester-based, wide operating temperature range electrolytes evaluated with different electrode chemistries, with a focus upon (i) assessing other candidate electrolyte additives, including new lithium-based salts (ii) studying the high temperature and cycle life degradation modes, (iii) correlating electrochemical trends with performance, and (iv) identifying performance limiting aspects at extreme temperatures. Future work will also focus upon demonstrating these systems in prototype cells.

Publications:

1. M. C. Smart, B. L. Lucht, S. Dalavi, F. C. Krause, and B. V. Ratnakumar, “The Effect of Additives upon the Performance of MCMB/ LiNiCoO_2 Li-Ion Cells Containing Methyl Butyrate-Based Wide Operating Temperature Range Electrolytes”, *J. Electrochem. Soc.*, **159** (6), A739-A751 (2012).
2. S. DeSilvan, V. Udinwe, P. Sideris, S. G. Greenbaum, M. C. Smart, F. C. Krause, K. A. Smith and C. Hwang, “Multinuclear NMR Studies of Electrolyte Breakdown Products in the SEI of Lithium-Ion Batteries”, *ECS Trans.* **41** (41), 207 (2012).
3. M. C. Smart, M. R. Tomcsi, C. Hwang, L. D. Whitcanack, B. V. Ratnakumar, M. Nagata, V. Visco, and H. Tsukamoto, “Improved Wide Operating Temperature Range of LiNiCoAlO_2 -Based Li-ion Cells with Methyl Propionate-Based Electrolytes”, 221st Meeting of the Electrochemical Society, Seattle, WA, May 6-10, 2012.

The work described here was carried out at the Jet Propulsion Laboratory, California Institute of Technology, under contract with the National Aeronautics and Space Administration (NASA).

TASK 1

Battery Cell Materials Development

Project Number: ES027

Reporting Period: FY 2012 Q3

Project Title: Novel Phosphazene Compounds for Enhancing Electrolyte Stability and Safety of Lithium-ion Cells

Project PI, Institution: Kevin L. Gering, INL

Collaborators (include industry): Michael T. Benson (INL), Mason K. Harrup (INL), Harry W. Rollins (INL), Sergiy V. Sazhin (INL), Khalil Amine (ANL), Chris Orendorff (SNL), Princess Energy Systems, Dow Chemical

Project Start/End Dates: Jan. 2009/Ongoing

Objectives: Our focus is to understand stability of our new classes of phosphazene materials and to establish viability for their use in lithium-ion cell electrolytes, considering both conventional voltage ranges (4.2V) and higher voltage electrode couples (4.5-5V). Comprising this overall work are the following focus areas:

- ◆ Synthesize novel solvents for Li-ion cells that are safer alternatives to volatile organics.
- ◆ Gain understanding of molecular-scale interactions between phosphazenes and other electrolyte components.
- ◆ Determine what phosphazene structures are more tolerant to high and low voltage, and to high temperatures.
- ◆ Determine the effect of phosphazenes on SEI films, cell performance, and cell aging in general, using ABR-relevant electrode couples.
- ◆ Synthesize and engineer novel phosphazene polymers that would serve as safe and robust alternatives to carbon-based anodes. Linked with our electrolyte research, this enhances overall compatibility of cell chemistry.

This collective effort will enable us to engineer advanced materials for more robust lithium-ion cells and move us closer to the overall goal of a carbon-reduced cell chemistry.

Approach: The INL is leveraging this work based on interdepartmental synergy between a well-established battery testing program and its foremost experts in phosphazene chemistry that are producing new classes of novel compounds for use in lithium-ion batteries. As such, the INL is strongly positioned to approach primary targets for ABR electrolyte development while maintaining historical knowledge of phosphazene chemistry and related applications.

This work is split under four primary tasks: solvent synthesis, characterization, DFT modeling, and lithium-ion cell testing. Upfront issues are

- ◆ voltage stability (CV)
- ◆ temperature stability
- ◆ flammability (flash point)
- ◆ lithium salt solubility
- ◆ transport properties (viscosity, conductivity)
- ◆ chemical compatibility with the cell environment
- ◆ molecular interactions (solvent-ion)

Coin cell testing covers issues of formation, interfacial impedance, polarization testing, and aging, using our compounds as electrolyte additives (1-10%). In previous quarters we investigated our electrolytes with ABR electrode couples LNMO/LTO, NMC(3M)/Carbon, and HE5050/Carbon. We test our novel polymeric anodes against ABR-relevant cathodes such as NMC. For most coin cell testing the general protocol is: formation cycling (C/10 @ 3), EIS, followed by a matrix of C/10, C/3, C/1, and 3C, all at 30 °C. Testing concludes with 3C cycling at 45-55 °C to determine electrolyte effect on high temperature tolerance. Final EIS is optional.

Milestones (cumulative over FY 2011-2012):

	= Activity completed in reporting period
--	--

Milestone	Status	Date
a. Synthesis of Fluorinated Phosphazene series (FM1,2,3)	completed	March 2011
b. Synthesis of Gen1 Ionic Liquid Phosphazene (PhIL-1)	completed	Feb. 2011
c. Synthesis of newer SM series (SM 5,6,7)	completed	October 2010
d. Development of improved voltammetry techniques for SEI characterization.	completed	December 2010
e. DFT simulations of selected phosphazenes regarding interaction with lithium ions	completed	Feb./March 2011
f. Thermal stability testing of blends with SM6 and SM7	completed	March 2011
g. Cell testing using LNMO/LTO and NMC/Carbon* couples: characterization of capacity and impedance attributes	completed	March 2011
h. Cell testing using LNMO/LTO and NMC/Carbon* couples: aging studies	completed	October 2011
i. Phase 1 concept validation for alternative anode materials	completed	October 2011
j. Cell testing using HE5050/Carbon couple: characterization of capacity and impedance attributes	completed	December 2011
k. DFT study on complete FM Series (fluorinated cyclics)	completed	February 2012
l. Cell testing using HE5050/Carbon couple: aging studies	completed	March 2012
m. Phase 2 concept validation for alternative anode materials	completed	March 2012
n. Initial PALS measurements of alternative anode materials	completed	March 2012
o. Synthesis of newer FM series and second-generation Ionic Liquid Phosphazenes	In Progress	
p. Abuse testing of INL electrolyte additives at SNL	In Progress	
q. Collaboration with ANL regarding scale-up of INL electrolyte compounds	In Progress	
r. Cell testing using NCA (Toda)/Carbon couple: characterization of capacity and impedance attributes	In Progress	
s. Phase 3 Alternative Anode materials with improved electronic conductivity	In Progress	
t. NMR evaluation of electrolyte fate at elevated temperatures (Washington State Univ.)	In Progress	

Financial data: Funding Received: FY 10: \$ 400K; FY 11: \$ 400K ; FY 12: \$500K (under subcontract, a small portion of this might go to Washington State University for specialized NMR measurements).

PROGRESS TOWARD MILESTONES

(a, b) Completed 2011 Q2.

(c) Completed 2011 Q1.

(d) Completed 2011Q1.

(e) Completed 2011 Q2.

(f) Completed 2011 Q2.

(g) Completed 2011 Q2.

(h) Completed 2012 Q1.

(i) Completed 2012 Q1.

(j) Completed 2012 Q1.

(k) Completed 2012 Q2.

(l) Completed 2012 Q2.

(m) Completed 2012 Q2.

(n) Completed 2012 Q2.

(o) Our synthesis targets during this quarter are newer generations of FM and phosphazene-based ionic liquid (PhIL) compounds. We are reviewing synthesis routes to arrive at a streamlined and more economical path toward production of these compounds. In previous quarters our voltammetry studies clearly showed that our phosphazene compounds can triple the voltage window of the baseline electrolyte while at moderate levels (20%), and small amounts of phosphazenes (1%) can dramatically improved the temperature stability of the electrolyte. We will confirm and quantify such benefit for lesser amounts of our newer compounds. These compounds will also be tested with our novel electrode materials in (m) and (s) to further enhance cell voltage stability at 5V. *A key driver of our work is to move toward an “inorganic cell chemistry” that has a common chemical basis throughout the cell. The next step in this progression is to test phosphazene-containing electrolytes against an electrode couple comprised of a phosphazene-based anode and a high voltage cathode.*

(p) Abuse testing (ARC) of INL Phosphazene compounds at SNL started January 2012, using 18650 cells containing the NMC (3M)/carbon (A10) couple. INL additives include FM-2, SM-6, and PhIL-2 at one and three percent levels. The focus of this work is to determine how INL additives help mitigate (delay) the onset of thermal runaway. Initial results from this work indicate overall benefit of INL phosphazene additives in terms of thermal stability, in the order of {SM-6 > PhIL-2 > FM-2}. For example, at 3% levels SM-6 decreases the peak heating rate by over 100 degrees C per minute, while PhIL-2 cuts the gas evolution to one-third that of the baseline system. *ARC and flammability testing at SNL was expected to conclude in Q3, but was delayed to Q4.*

(q) We have continued our efforts to collaborate with ANL regarding the synthesis of INL phosphazene electrolyte compounds in the ANL materials scale-up facilities. The top candidate for scale-up will be the best compound(s) that emerges from the final results of the SNL abuse testing, which are not yet available as of this writing.

(r) Cell testing using NCA (Toda)/Carbon couple. Characterization of capacity and impedance attributes is ongoing for coin cells made with phosphazene-doped electrolytes and the NCA (Toda)/Carbon couple provided by ANL. Discharge capacity over cycling rate is shown (**Fig. 1**), wherein electrolyte formulations contained one or three percent phosphazenes additives SM-4, SM-6, FM-2, or PhIL-2 in a baseline of EC-EMC (2:8) with 1.2M LiPF₆. Electrolyte performance is on par with that seen for earlier testing with LNMO/LTO, HE5050/Carbon, and NMC/Carbon couples. In some cases the electrolytes with FM-2 and PhIL-2 performed better than the baseline system. These early results suggest that the INL additives are compatible with the NCA (Toda)/Carbon couple. Our testing is currently looking at thermal stability of the cells represented in Fig.1 while they cycle at 45 °C.

(s) Phase 3 Alternative Anode materials with improved electronic conductivity and safety. We are performing a third phase matrix of our alternative anode materials investigation, using a polymeric approach toward engineering new carbon-reduced anode materials. Phase 1 and 2 studies showed cycling to 5V (full cell) was achieved, yet we determined that the observed capacity was being impacted by low electronic conductivity of the 3D polymer framework. While capacities of Phase 1 and 2 materials were approaching that of conventional carbon systems, and we concluded that enhancing the electronic conductivity of these materials will allow us to improve capacity to achieve competitive levels. Efforts to enhance the conductivity of INL cyclophosphazene-based anode materials have pursued two different routes. New cyclophosphazene molecules with substituents that when cross-linked either electrochemically or using a chemical oxidant can become conducting have been synthesized. Second, copolymer systems have been prepared which include high performing tert-butyl hydroquinone cyclophosphazene (tbu-HQCP) materials and a second conducting polymer. To facilitate more rapid evaluation of the anode films a four point probe has been purchased and is being employed to monitor the thin film resistivity of prepared samples. The resistivities are also being correlated with electrochemical performance.

We are also seeing correlations between polymer type and lithium uptake, indicating further information regarding the 3D framework of these materials. Lastly, the presence of the phosphazenes in the electrode composition adds to the overall flame resistance of the cell chemistry.

(t) NMR evaluation of electrolyte fate at elevated temperatures (Washington State Univ.). Sub-contracted work with WSU (contact: Prof. Bill Hiscox) performs advanced NMR studies in two areas of our new materials development. The first area employs high resolution multi-dimensional solution NMR. The thrust here is to attempt to identify early degradation fragments from conventional electrolytes and determine the primary mechanisms of thermal degradation. Then electrolyte formulations containing INL phosphazene additives will be studied using the same techniques in an attempt to elucidate the mechanisms by which the phosphazene additives prevent the organic carbonate degradation. The value added in using WSU instead of INL facilities is their NMR center has more NMRs at various field strengths and a greater instrumental capability than currently possessed at INL. Further, their resident NMR experts have greater concentrated expertise in these types of complex multi-dimensional analyses.

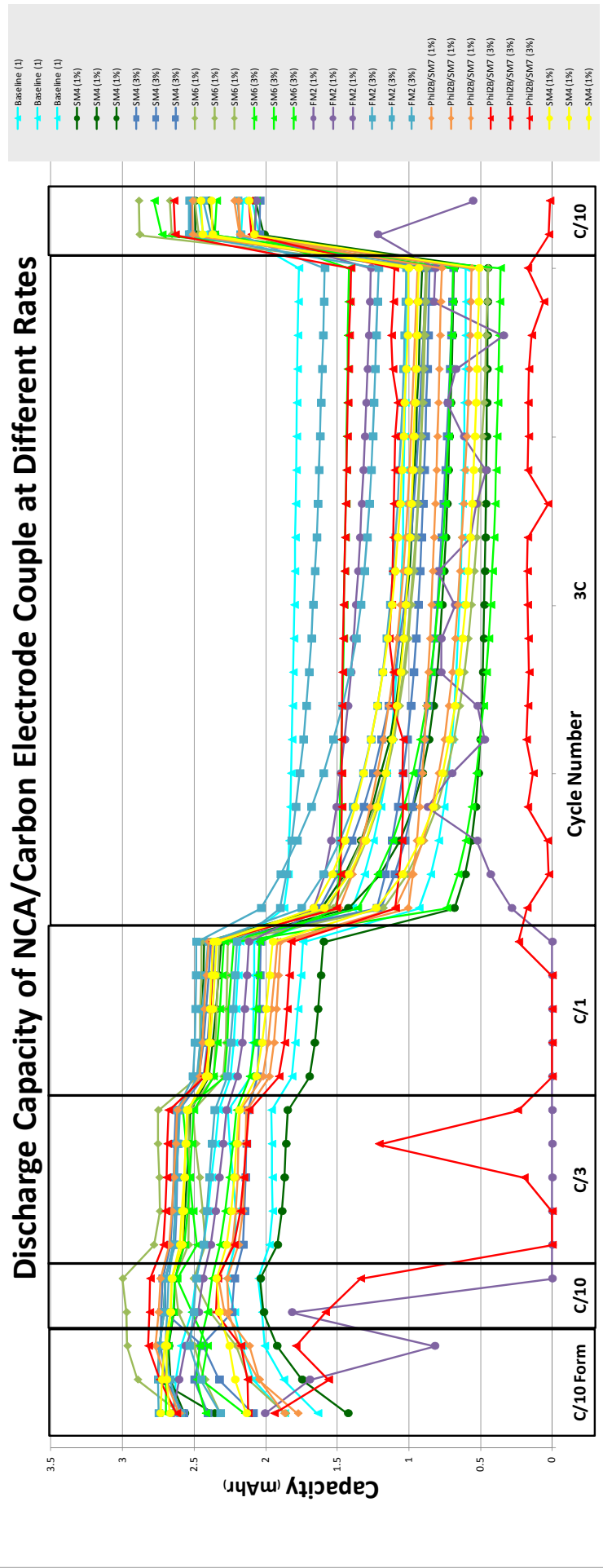
From initial WSU findings, the baseline sample, having no protection from the phosphazene, formed a gel at the bottom of the tube as time progressed at 60°C. The sample has become much more viscous overall than Sample 1 (having the protective cyclic phosphazene), which has not undergone a perceptible viscosity increase. The evidence of phosphorus-proton coupling in the reaction products of the baseline sample suggest that phosphorus is reacting with the solvent, which is a mixture of ethyl and methyl carbonates. These NMR-observable product species may be intermediates in polymerization of the carbonates, leading to a polycarbonate formation. This would account for the viscosity change in the baseline sample. However, formation of dimers, trimers, etc. of solvent molecules containing PF₂ linking units, may explain why the new PF₂ signals have continued to increase in intensity with respect to PF₆⁻ signals, and why they appear to be stable products in the mixture. However, the final fate of these species is not known from the present preliminary aging study. Continued monitoring of the two samples, and further studies of starting materials and products will be necessary to sort this out. The complexity of this system (5+ observable nuclei with spin-spin coupling interactions among at least 4 of them) will require a number of approaches to fully elucidate the mechanisms of degradation in the unprotected system, and the mode of protection of the cyclic phosphazenes.

The second area employs solid-state 1- and 2-dimensional analyses of the phosphazene anode materials under development. The value added in this area is that the INL recently lost its 300 MHz spectrometer (acquired in 1999) due to age and terminal malfunction. This was the only instrument at INL with solids capability.

Publications, Reports, Intellectual property

- “Lithium binding in fluorinated cyclic triphosphazenes” M. T. Benson, M. K. Harrup, K. Gering, *J. Phys. Chem. A*, submitted.

Fig. 1



TASK 1

Battery Cell Materials Development

3rd Quarter Report, Apr. ~ Jun. 2012

Project Number: 1.1E (ES028)

Project Title: Streamlining the Optimization of Lithium-Ion Battery Electrodes

Project PI, Institution: Wenquan Lu, Argonne National Laboratory

Collaborators (include industry):

Qingliu Wu, Argonne National Laboratory

Khadija Yassin-Lakhsassi, Argonne National Laboratory

Miguel Miranda, Argonne National Laboratory

Dennis Dees, Argonne National Laboratory

Jai Prakash, Illinois Institute of Technology

Project Start/End Dates: October 2008 / September 2012

Objectives:

To establish the scientific basis needed to streamline the lithium-ion electrode optimization process.

- To identify and characterize the physical properties relevant to the electrode performance at the particle level.
- To quantify the impact of fundamental phenomena associated with electrode formulation and fabrication (process) on lithium ion electrode performance.

Approach:

The initial focus of this effort will be on optimizing the electronic conductivity of the electrode. The factors affecting the distribution of binder and conductive additive throughout the composite matrix will be systematically investigated at the particle level, as well as their effect on overall electrode performance. Modeling simulations will be used to correlate the various experimental studies and systematically determine their impact on the overall electrode performance.

Milestones:

- (a) Optimum composition of LiFePO_4 by modeling and experimental.

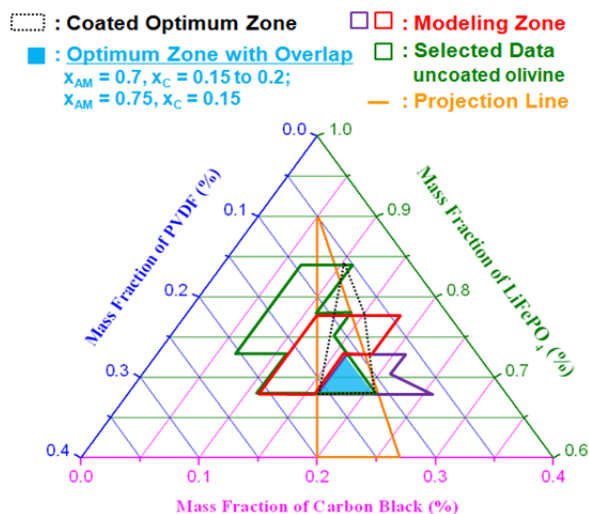
Financial data: \$300K carryover fund

PROGRESS TOWARD MILESTONES

(a) Summary of work in the past quarter related to milestone (a).

For optimization studies, the objective of this project is to determine the optimum electrode composition that will provide high energy and high power with minimum carbon and binder loadings. Our approach was to locate the optimum composition using modeling and experimental techniques. In the porous electrode modeling studies as described in the last report, the physical parameters such as electrical conductivity and electrode porosity were used for a variety of compositions to predict the corresponding electrochemical performance. Coin cells were fabricated for the same range of electrode compositions and the corresponding electrochemical performances of the cells were also measured. The porous electrode model along with cell design parameters such as cathode thickness, electrode delamination, and brittle nature of the electrode were also used to screen the optimum composition zone for high energy and high power. The results of the optimization studies of LiFePO_4 are presented in the figure below.

Electrode optimization:



The optimum electrode composition determined by experiments and modeling was found to be between 70/20/10 and 75/15/10 (Active material/Carbon/Binder).

Publications, Reports, Intellectual property or patent application filed this quarter. (Please be rigorous, include internal reports--invention records, etc.)

TASK 1

Battery Cell Materials Development

3rd Quarter Report, Apr. ~ Jun. 2012

Project Number: 1.3 (ES028)

Project Title: Validation of Electrode Materials, Electrolytes, and Additives

Project PI, Institution: Wenquan Lu, Argonne National Laboratory

Collaborators (include industry):

Qingliu Wu, Argonne National Laboratory
Khadija Yassin-Lakhsassi, Argonne National Laboratory
Miguel Miranda, Argonne National Laboratory
Thomas K. Honaker-Schroeder, Argonne National Laboratory
Steven Trask, Argonne National Laboratory
Bryant Polzin, Argonne National Laboratory
Andrew Jansen, Argonne National Laboratory
Ilias Belharouak, Argonne National Laboratory
Dennis Dees, Argonne National Laboratory
Gregg Krumdick, Argonne National Laboratory
Jai Prakash, Illinois Institute of Technology
James Banas, JSR Corporation
Rick Jansen, SWeNT
Toda Kogyo

Project Start/End Dates: October 2008 / September 2014

Objectives:

- To identify and evaluate low-cost cell chemistries that can simultaneously meet the life, performance, abuse tolerance, and cost goals for Plug-in HEV application.
- To enhance the understanding of advanced cell components on the electrochemical performance and safety of lithium-ion batteries.
- Identification of high energy density electrode materials is the key for this project.

Approach:

Base upon battery design model developed by Argonne, the specific capacities of cathode and anode materials should be above 200mAh/g and 400mAh/g, respectively, to meet PHEV requirements set by USABC.

Since there is no commercial available electrode materials can meet PHEV energy requirements, the electrode material candidates will be required from both battery materials companies and research institutes. The promising materials will be evaluated under the controlled process and standard test procedures derived from the “Battery Test

Manual for Plug-in Hybrid Electric Vehicles” by INL 2010. In addition, thermal properties of the electrode materials will be studied.

Other battery components for lithium ion batteries, such as electrolyte and additives, separators, binder, conductive additives, and other relevant materials, will also be investigated accordingly.

Milestones:

Materials have been investigated in 2nd Quarter:

- a) Complete material validation on FEC additive for silicon composite
- b) Complete material validation of $\text{Li}_{1+x}\text{Ni}_{0.5}\text{Co}_{0.2}\text{Mn}_{0.3}\text{O}_2$ (NCM523) from Toda
- c) Complete material validation of LiDFOB additive for LMR-NCM
- d) Complete material validation of LMR-NCM from Argonne (I. Belharouak)
- e) Complete material validation of carbon nanotube as conductive additive

Financial data: \$450K

PROGRESS TOWARD MILESTONES

This quarter, the performance of several materials was validated, including fluorinated ethylene carbonate additive for silicon composite anode and LiDFOB additive for LMR-NCM cathode. The cycle performance was dramatically increased by adding these additives in to the cell system. The additive will be considered for the future cell build at CFF. One LMR-NCM cathode material developed in Dr. Belharouak’s group was tested. This material showed high energy density, good rate performance and cycleability.

In order to support CFF, validation of NCM523 from Toda was completed and the report was delivered. We also looked at carbon nanotube as conduction additive. Its impact on cell performance was completed and reported to vendor.

(a) Summary of work in the past quarter related to milestone (a).

Due to its high energy density, silicon composite is viewed as next generation anode material. However, this material has poor cycleability in addition to its well-known volume expansion issue. The poor cycle performance is attributed to the unstable SEI formation. Fluorinated ethylene carbonate (FEC) has been studied recently and shows promising result. In this work, 10% FEC was added into 1.2M LiPF₆ in EC/EMC. The electrolyte was used in the Li/Si-C half cell. The excellent cycling performance was obtained. Moreover, the FEC was found out to work with other Silicon composite. The good cycling performance is attributed to the better SEI formation.

(b) Summary of work in the past quarter related to milestone (b)

$\text{Li}_{1+x}\text{Ni}_{0.5}\text{Co}_{0.2}\text{Mn}_{0.3}\text{O}_2$ (NCM-523) cathode material was received from Toda. This material is going to be used at CFF to build library. The general test procedure was applied to both lithium half cell and graphite full cells. By cycling half cell between 3.0V and 4.3V, this material shows 675Wh/kg, 10% irreversible capacity loss. In the graphite full cell, excellent rate and cycle performance was obtained. The information was delivered to CFF group for electrode preparation and cell fabrication.

(c) Summary of work in the past quarter related to milestone (c)

In this work, we demonstrate that more than 90% of the initial capacity was preserved with LiDFOB additive even after 100 cycles at relatively high rate (C/2), while less than 50% of initial capacity remained in cells without LiDFOB. The analysis on the electrochemical behavior of cells during the initial stage, SEM observations of cycled electrodes, and EIS of cells suggested that the enhancement of cell performances could be ascribed to the thin and stable SEI films form on the surface of anode in the presence of LiDFOB, which might prevent the lithium consumption during the cycling.

(d) Summary of work in the past quarter related to milestone (d)

In this work, one composite material developed in Dr. Belharouak's group was tested. When cycled between 2.0V and 4.6V in the half cell, 250mAh/g capacity was obtained with 23% irreversible capacity loss. After three cycles, this material can deliver 890Wh/kg. C rate test results of full cell against graphite anode indicate that there is still 96% capacity at C/2 rate. After 100 cycles, the electrode can still deliver more than 200 mAh/g capacity.

(e) Summary of work in the past quarter related to milestone (e)

Carbon nanotube developed at SWeNT was tested as conductive additive in both cathode and anode. The test results indicate that the additive has little impact on graphite anode. By replacing 4%+4% graphite and carbon with carbon nanotube, the electrodes show relatively high impedance. However, rate and cycle performance of the electrode with carbon nanotube is comparable to that of the electrode with 8% graphite and carbon combined additive.

Publications, Reports, Intellectual property or patent application filed this quarter. (Please be rigorous, include internal reports--invention records, etc.)

Carbon Nanotube Conductive Additive for Lithium Ion Battery, May 2012.

ANL Composite from I. Belharouak, Jun. 2012.

TASK 1

Battery Cell Materials Development

Project Number: 1.2.2 Electrode Material Development (ES029)

Project Title: Scale-up and Testing of Advanced Materials from the BATT Program

Lead PI and Institution: Vince Battaglia, Lawrence Berkeley National Laboratory

Support PI and Institution: None

Barrier: Cost is too high (energy density needs to be increased.)

Specific Objectives: (i) Identify materials in the BATT Program that are ready for enhanced screening diagnostics, (ii) Procure *ca.* 10 grams of new material to make laminates for coin cell or pouch cell testing, (iii) Work with BATT researchers to improve their materials by identifying shortcomings.

General Approach: Work with BATT PIs in deciding what materials are ready for scale-up and enhanced testing and diagnostic evaluation in full cells. Once materials are identified, decide on the best approach for increasing the quantity of the material to approximately 10 g. Make laminates of the material and test in coin cells against Li. Based on initial test results, decide on best automotive application for material, design the electrodes for the application, and perform long-term cycling tests. Provide a comparison to state-of-the art materials and cells.

Current Status as of October 1, 2011: Eight materials were identified for scale-up and further testing. Three of the materials showed significant problems during preliminary testing: two exhibited large first-cycle irreversible capacity losses, and the other displayed low specific capacity. Four materials continue on long-term cycling, and one material has recently begun preliminary testing. This last material, from MIT, was scaled-up and its claimed high-rate capability has been confirmed.

Expected Improvement by September 30, 2012: Will have identified at least three more BATT Program materials that should undergo further testing. Will have developed some basic principles for the optimal scale-up of the MIT material.

Schedule and Deliverables: Attend review meetings and present interim results on the scale-up of BATT Program materials (November 2011, February 2012, August 2012.)

Deliverable: Battery design, performance, and cycling characteristics of three BATT materials will be reported on at the DOE Merit Review (May 2012.)

Quarter 3 Report

Dan Scherson of Case Western Reserve University has been developing salts for Li-ion batteries that improve the flame retardance of a Li-ion electrolyte but without sacrificing performance. The material they send for this exercise was not identified. They requested that it be used in a baseline electrolyte at a level of just 0.5% with 1.5 % VC. Their material arrived as a powder that was moved immediately to a glovebox upon receipt. We acquired VC from Aldrich and added it to our 1M LiPF₆ in 1:2 EC:DEC (Daikin, America).

We built four full cells of graphite/NCM. In two of the cells was added the baseline electrolyte, in the other two the baseline with 1.5 % VC and 0.5 % CaseX salt. The cells were all cycled in the same manner: between 3 and 4.2 V at C/20 for 5 cycles and C/2 after that. The cells of the same demonstrated similar cycleability; the results of just one cell of each chemistry is provided in the two graphs below.

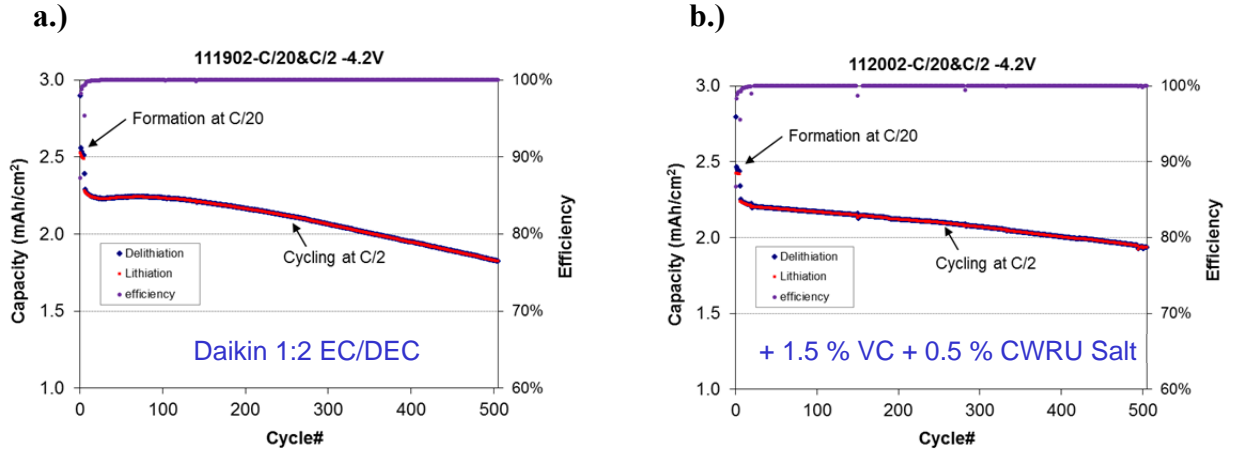


Figure: 1. Cycling results of Graphite/NCM cells between 3 and 4.2 V with a.) 1 M LiPF₆ in EC:DEC, and b.) same electrolyte with VC and CaseX salt.

These preliminary cycling tests indicate that the addition of the CaseX salt to the baseline electrolyte does not negatively affect the cycle life of this chemistry and, if anything, appears to improve it. Now, it is not clear whether the improvement is coming from the addition of the VC, however, these results are showing better results than previously obtained by our group using VC alone.

In some of the BATT quarterlies, CWRU has reported that the addition of their salt to the electrolyte has resulted in the reduction of the flammability of the electrolyte. This test has indicated that it does not negatively impact cycleability. A follow-on test would be to make enough of this electrolyte to put into an 18650 and have the cell evaluated at Sandia National Laboratory for safety testing. This might make for a good proposal for the ABR RFP that is to be issued in July.

TASK 1

Battery Cell Materials Development

Project Number: 1.1L (ES113)

Project Title: Development of High Voltage Electrolyte for Lithium Ion Battery (High Voltage Electrolyte for Lithium Batteries)

Project PI, Institution: Zhengcheng Zhang, Khalil Amine, Argonne National Laboratory

Collaborators (include industry):

Libo Hu, Argonne National Laboratory
Huiming Wu, Argonne National Laboratory
Wei Weng, Argonne National Laboratory
Kevin Gering, Idaho National Laboratory
Daikin Industry

Project Start/End Dates: October 2010 / September 2014

Objectives: The objective of this work is to develop an electrolyte with wide electrochemical window that can provide stable cycling performance for cathode materials that can charge above 4.5 V.

FY12's objective is to enable the LNMO/LTO and LNMO/graphite cell using fluorinated electrolyte solvents as high voltage electrolyte.

Approach: Investigate new solvents as high voltage electrolyte applications. Based on the theoretical calculation, the introduction of electron-withdrawing group on the carbonate structure will increase the oxidation stability. We will continue the fluorinated carbonate based electrolyte study in the new fiscal year. We will also design and synthesize new solvents to further explore other possibilities for high voltage application. Exploring a hybrid electrolyte made of the mixture of the above solvents is the general approach.

Milestones:

- (a.) Material evaluation in the graphite cell system, December, 2012 (Complete)
- (b.) New material synthesis and purification, March, 2012 (Complete)
- (c.) Physical properties of the new high voltage electrolyte candidates (March, 2012 (Complete)
- (d.) Complete evaluation of high voltage electrolyte using LNMO/LTO and LNMO/Graphite chemistries, September 2012 (On schedule)

Financial data: \$400K (FY2012)

PROGRESS TOWARD MILESTONES

(1) Summary of work in the past quarter related to milestone

Studies using the previously synthesized fluorinated carbonates (Table 1) were continued in this quarter. Previous study using LNMO/LTO chemistry suggested that the electrolyte E5, all fluorinated components FCC-1, FLC-1 and FE-1, is the most stable electrolyte formulation on the LNMO cathode surface. However, when used in a graphite cell, E5 electrolyte showed inferior performance compared with Gen 2 electrolyte, suggesting the possible inability of FCC-1 to form a stable SEI on the anode surface. To test this theory, Li/A12 anode (ConocoPhillips) half cells with different electrolytes were fabricated to investigate the SEI formation capability of these electrolytes.

Table 1. Theoretical Oxidation and Reduction Potential of Some Fluorinated Carbonate Solvents.

Code Name	Chemical Structure	P_{ox}/V	P_{red}/V
EC		6.91	1.43
PC		6.80	1.35
EMC		6.63	1.30
FCC-1		6.97	1.69
FEC		7.16	1.63
FCC-3		6.93	1.50
FLC-1		7.10	1.58
FE-1		7.29	1.82

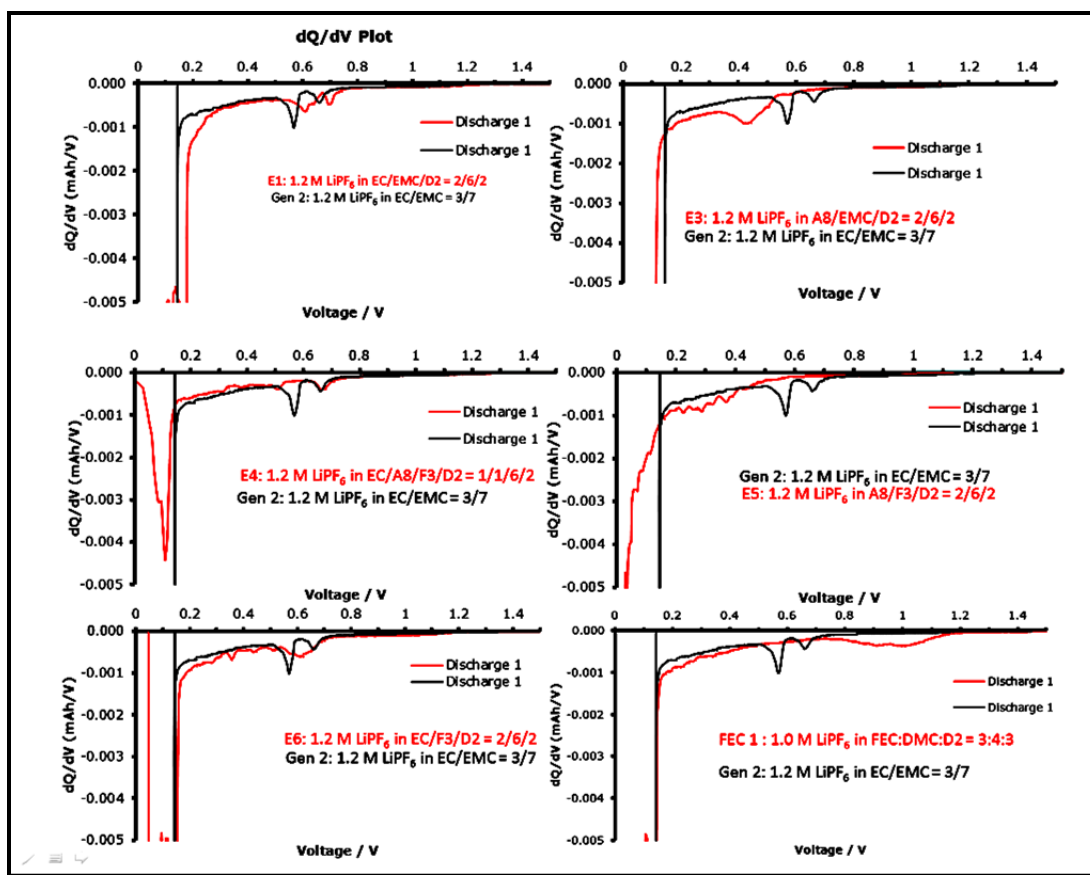


Figure 1. dQ/dV plots of Gen2 electrolyte fluorinated electrolytes with Gen2 electrolyte in Li/A12 cells.

The dQ/dV profiles of the high voltage electrolytes compared with Gen 2 electrolyte were summarized in Figure 1. The electrolytes that employed EC as the cyclic carbonate such as E1 and E6 all show similar SEI formation peaks as Gen 2 does at around 0.6 V. However, when EC was substituted with FCC-1 as in E5 and E3, the peaks were either gone or shifted to a lower potential. When EC was reintroduced into the system as in E4, the peaks reappeared but to a lesser intensity. All these data point out that FCC-1 is unable to form stable SEI. The inability of FCC-1 to form a stable SEI explains the poor performance of E5 in A12/LNMO full cells in comparison with its excellent performance in LTO/LNMO full cells where no SEI is needed. In a more interesting case, when EC was substituted with FEC, the SEI formation peak shifted to a much higher potential at around 1.0 V, which suggests a more stable SEI might be formed.

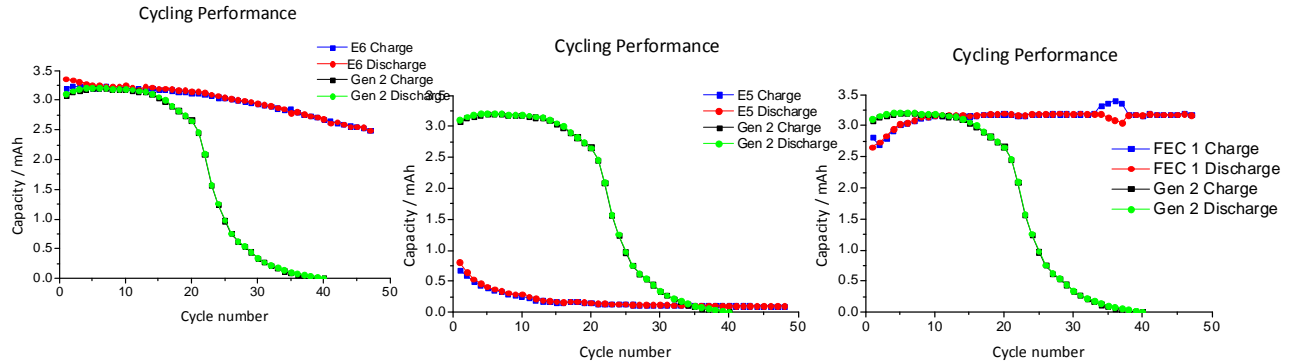


Figure 2. Cycling performance of Gen2 electrolyte and fluorinated electrolytes in Li/A12 anode half cells at 55 °C (cycling rate at C/3 and cut off voltage 1.5-0.01 V).

To further study the electrochemical stability of the electrolytes on the anode surface at elevated temperature, selected anode half cells were subjected to cycling at 55 °C (**Figure 2**). Gen 2 electrolyte showed an initial plateau in the first 20 cycles and then the capacity dropped sharply afterwards. This observation is in accordance with literatures reporting the SEI formed with EC is unstable at elevated temperature. The SEI will keep breaking down and new SEI forms and the lithium metal will be slowly consumed. When the excess lithium metal is used up, the capacity of the cell will drop sharply. In the case of E6, it seems the introduction of FLC-1 and FE-1 slowed down this process, as the capacity did not drop as sharply as Gen 2 did. E5 showed much inferior performance than any other electrolytes, which was expected due to the SEI formation problem. The even lower capacity in the anode half cell than in the full cell of E5 suggests a possible compatibility issue of E5 with Li metal as well. The electrolyte that performed the best was the FEC-based electrolyte, with minimal capacity loss over the 50 cycles. The observation is in agreement with the empirical rule that SEIs formed above 1.0 V are more high temperature tolerant.

(2) Summary of work in the past quarter related to milestone

The electrochemical stability of the electrolytes on the cathode was also studied in a similar manner. Cathode half cells using Li metal and LNMO electrode were made with different electrolytes and subjected to cycling test at 55 °C. The results were summarized in **Figure 3**. When subjected to the same cut off voltage, E5 and E6 showed much inferior capacity retention than Gen 2 electrolyte, which is contradictory to the results obtained from both the LTO/LNMO and A12/LNMO full cells. A detailed investigation at the voltage profile revealed that the overpotential of the fluorinated electrolytes are higher than that of the non-fluorinated Gen 2 electrolytes, so when the cut off voltage was set at 4.9 V, the potential is too low for E5 and E6 cells to be fully charged and as the overpotential kept building up, the cells were charged to an even less extent. When the cut off voltage was raised to 5.3 V, such problem no longer exists so E5 and E6 electrolyte showed a similar behavior as Gen 2 electrolyte, having a plateau at beginning cycles and then the capacity faded quickly. The reasoning behind this is similar to the Gen 2 anode half cell. The decomposition of the electrolyte on the cathode surface is also

a process that consumes active lithium in the cell, so when the excess Li metal was consumed, the capacity faded quickly. The observation of the capacity of E5 cells fading quickly is not a necessary indication of the instability of the electrolyte on the cathode, as the compatibility issue of E5 with Li metal observed in the anode half cells may also present in the cathode half cells and cause problems. The plateau in all the data also suggests that despite the decomposition of the electrolyte, the structure of the cathode materials is not affected.

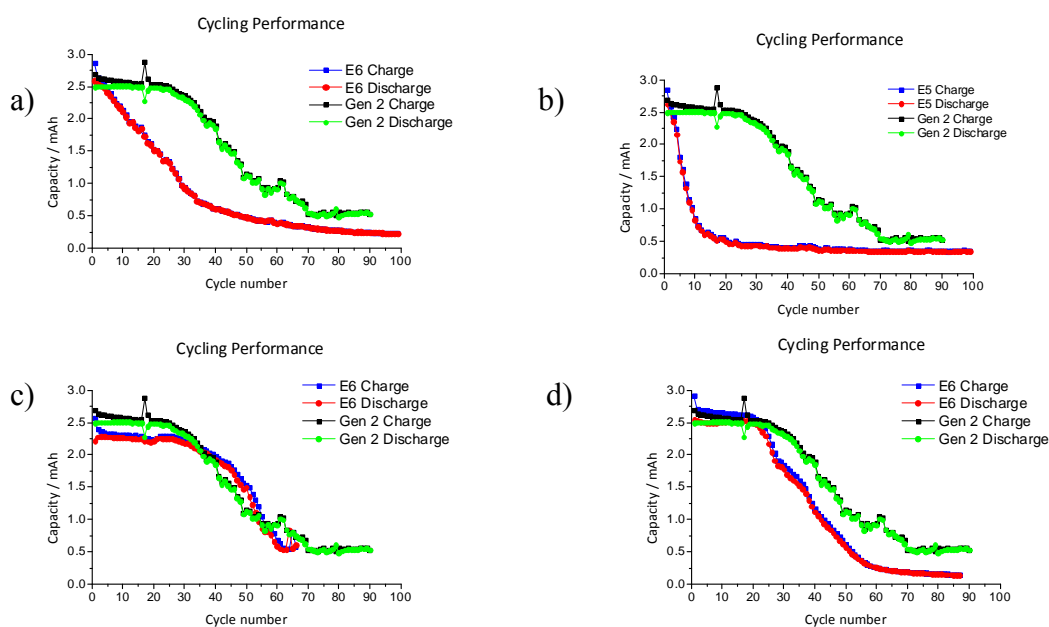


Figure 3. Cycling performance of Gen2 electrolyte and fluorinated electrolytes in Li/LNMO cathode half cells at 55 °C, cycling rate at C/3 and cut off voltage for a) and b) 3.5-4.9 V. c) and d) 3.5 – 5.3 V for E5 and E6.

(3) Summary of work in the past quarter related to milestone

Due to the overpotential and cut off voltage issue observed in the cathode half cell study, the charging conditions for the A12/LNMO full cells were reinvestigated. Two types of adjustments were tested. First, the cut off potentials were increased gradually to see if more capacity could be realized. The results were summarized in **Figure 4**. Second, the cutoff potential remained at 4.9 V, but a constant voltage charging step with a cutoff current and no time limit was added into the charging protocol to realize the full capacity of the electrodes. These testing are in progress and will be reported in next quarter.

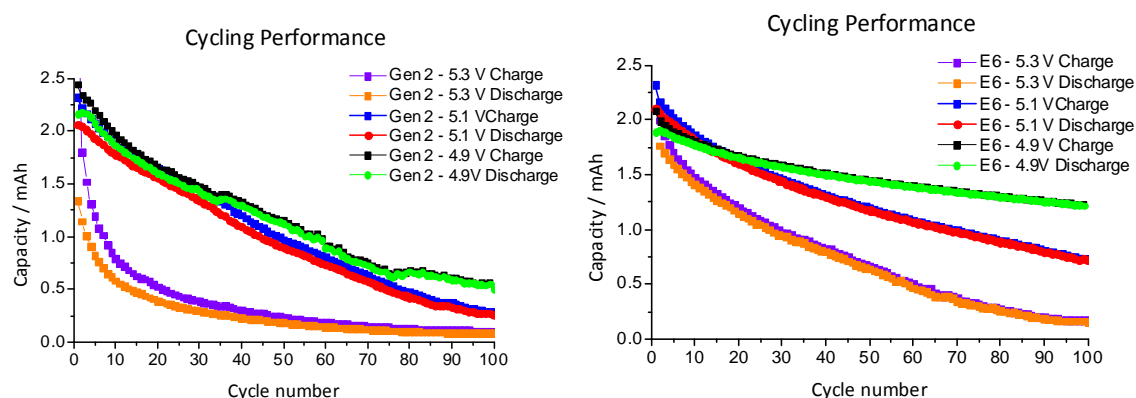


Figure 4. Changing charging conditions for Gen 2 and E6 A12/LNMO full cells from 4.9 V to 5.1 V and 5.3 V, C/3 at 55 °C.

Publications, Reports, Intellectual property or patent application filed this quarter. (Please be rigorous, include internal reports--invention records, etc.)

Argonne-Daikin Joint Workshop on High Voltage Electrolyte, Feb. 25, 2012.

Electrolyte for electrochemical cells. US patent application ANL-IN-09-039.

Recent development of high voltage electrolytes, oral presentation on USABC-ABR-BATT Electrolyte Workshop, Aug.18-19, 2011, Southfield, MI, US.

Advanced Electrolyte and Electrolyte Additive for lithium ion batteries, invited talk on 4th International Conference on Advanced Lithium Batteries for Automotive Application (ABAA-4), Sep. 20-23, 2011, Beijing, China.

Advanced Battery Materials for EV Applications, invited talk on EV Battery Tech: 5th Global Cost Reduction Initiative, Feb. 28-29, 2012 London, United Kingdom

TASK 1

Battery Cell Materials Development

Project Number: 1.2D (ES114)

Project Title: High Capacity Composite Carbon Anodes Fabricated by Autogenic Reactions

Project PI, Institution: Vilas G. Pol, Argonne

Collaborators (include industry): Michael M. Thackeray (Co-PI, Argonne), ConocoPhillips, Superior Graphite

Project Start/End Dates: 1 October 2011/30 September 2012

Objectives:

The objectives of this project are to evaluate *high capacity*, spherically-shaped carbon particles, combined with lithium-alloying elements as anode materials for HEVs, PHEVs and EVs and to compare their electrochemical behavior with commercial carbon-composite electrode materials.

Approach:

- 1) Exploit autogenic reactions to prepare spherical carbon quickly, cost-effectively and reliably;
- 2) Collaborate with industry to access high-temperature furnaces to increase the graphitic component in spherical carbon;
- 3) Increase the capacity of the carbon spheres by combining them with lithium alloying elements to form carbon-composite anode materials;
- 4) Study and compare the electrochemical, chemical, physical and thermal properties of Argonne's carbon-composite products with commercially available carbon-composite materials;
- 5) Optimize processing conditions and evaluate the electrochemical properties of pristine and carbon-composite materials in collaboration with industry;

Milestones:

- (a) Consolidate industrial collaboration for this project (January 2012);
- (b) Prepare carbon samples for industrial partner for heat-treatment; prepare carbon-composite samples from Argonne's carbon materials and from industrial products (April 2012);
- (c) Evaluate and optimize the electrochemical properties of carbon-composite samples in lithium half cells and full cells (September 2012);
- (d) Determine the chemical, physical and thermal properties of Argonne's carbon-composite anodes with commercial carbon-composite materials (September 2012);

Financial data: \$300K/year

PROGRESS TOWARD MILESTONES

Milestone (a). Consolidate industrial collaboration for this project

Commercial carbon (ConocoPhillips) samples were coated with high capacity alloying materials by sonochemical methods to enhance their specific capacity and to compare their electrochemical properties against Argonne's carbon sphere materials. Samples of the carbon spheres were sent to an industrial collaborator, ConocoPhillips, for high temperature treatment at 2400 °C/8h and at 2800 °C/2h under inert conditions; these samples are currently under electrochemical investigation. The carbon spheres prepared at 700 °C were coated with Sn and Sb to form carbon-composite materials to increase the reversible capacity of the electrodes.

Milestone (b). Prepare carbon samples for industrial partner for heat-treatment; prepare carbon-composite samples from Argonne's carbon materials and from industrial products

Pure spherical carbon electrodes typically offer a stable rechargeable capacity of 250 mAh/g. To further enhance their electrochemical properties, carbon microspheres, prepared at 700 °C were used as a support to decorate a mixture of electrochemically active SnO₂ and Sb nanocrystals by sonochemical surface modifications. To synthesize these materials, as-prepared carbon spheres were dispersed in an ethanol solution, using ultrasonic irradiation for 1 minute. Appropriate amounts of SnCl₂ and SbCl₃ as tin and antimony precursors, respectively, were added to the carbon sphere-ethanol dispersion. Sonication of the above slurry was carried out with high-intensity ultrasonic radiation for about 5 to 7 minutes by direct immersion of the titanium horn (20 kHz, 20W/cm²) in a glass sonication cell, under a flow of argon gas. After separating the ethanol component, the product was dried at about 100 °C and further heated in an inert argon filled glove box at about 500 °C for about 3 hrs. The final heat-treated, SnO₂/Sb-coated carbon sphere products were evaluated for their morphological, compositional, structural and electrochemical properties.

Milestone (c). Evaluate and optimize the electrochemical properties of carbon composite samples in lithium half cells and full cells

Electrochemical evaluations were carried out in coin cells using a lithium metal foil electrode, a SnO₂/Sb-decorated carbon sphere counter electrode, and an electrolyte consisting of 1.2M LiPF₆ in a 3:7 mixture of ethylene carbonate (EC) and ethylmethyl carbonate (EMC). Figure 1 (left panel, inset) shows the discharge/charge behavior of a Li/carbon sphere-SnO₂/Sb cell during the first two cycles at a current density of 75 mA/g (~C/5.5 rate) when cycled between 1.5 and 0.01 V). The first-cycle discharge and charge capacities of a SnO₂/Sb-carbon sphere composite electrode are 612 mAh/g and 394mAh/g, respectively. The first cycle irreversible capacity loss is about 35%, which is significantly lower than that delivered by a pure carbon sphere electrode (60%). A steady reversible capacity of 425 mAh/g, obtained at a C/5.5 rate for 40 cycles, is significantly higher than the capacity delivered by the carbon spheres alone (Figure 1, left). The

coating of ~11 wt% nanosized tin oxide/antimony therefore significantly improves the discharge and charge capacities of the SnO₂/Sb-carbon sphere composite electrode when compared to the respective capacities of a bare carbon sphere electrode. The variation in discharge capacity as a function of current rate in Li/SnO₂-Sb-carbon sphere cells was also monitored. More than 400 mAh/g was delivered at a C/6 rate, about 315 mAh/g at a C/1.5 rate, and more than 200 mAh/g at a C rate. Efforts to increase the capacity above 400 mAh/g by tailoring the loading of lithium-alloying elements on the surface of commercial carbon products are in progress.

Milestone (d). Determine the chemical, physical and thermal properties of Argonne's carbon-composite anodes with commercial carbon-composite materials

The powder X-ray diffraction patterns of as-prepared, SnO₂-Sb coated carbon spheres showed that the coating was essentially amorphous to X-rays, whereas, after drying and heating the product to about 500 °C for about 3 hours, it was apparent that crystalline phases of body centered tetragonal SnO₂ and hexagonal Sb were formed by these thermal processes. Scanning and transmission electron micrographs of the SnO₂/Sb-coated carbon spheres (Figure 1, right panel) and energy dispersive X-ray analysis indicated that the surface of the carbon particles was uniformly covered by <10 nm diameter SnO₂/Sb nanoparticles. The thin SnO₂/Sb layer of particles on the surface of the carbon spheres remains intact after the heat-treatment process. EDX analysis showed that the SnO₂ and Sb accounted for approximately 11% by weight of the carbon sphere-SnO₂/Sb composite product. It appears that, under similar experimental conditions, Sn is more sensitive to oxidation than Sb. Note that in these SnO₂/Sb-coated carbon sphere electrodes, all three components (SnO₂, Sb and the carbon spheres) are electrochemically active.

This project is a work-in-progress and is being extended to investigate the effects of sonochemical deposition of Sn, Cu₆Sn₅ and other alloying materials on industrially-prepared and commercially available carbon products. Initial results on various alloying elements coated on numerous carbon samples from industry have been obtained; these data will be presented in a subsequent report, once the results have been discussed with our industrial partner.

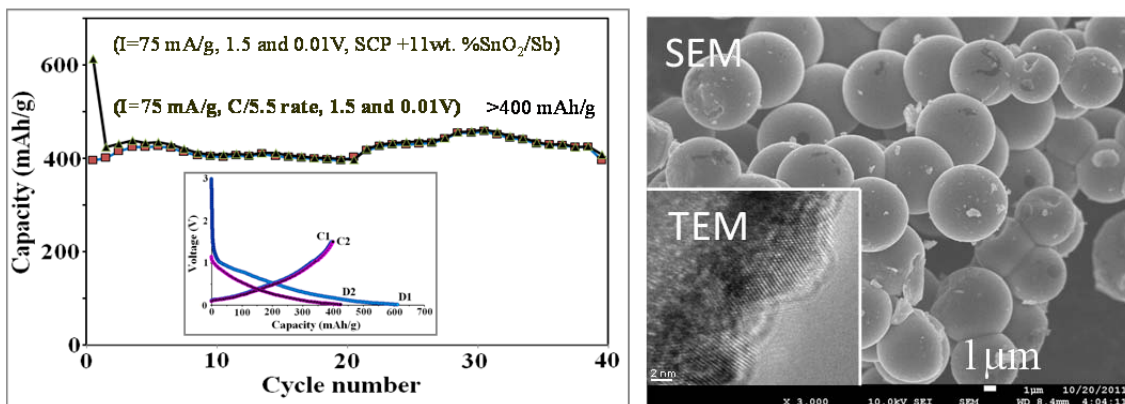


Figure 1. Left: First and second discharge-charge- profiles (inset) and capacity vs. cycle number plot of a lithium half cell with a SnO_2/Sb -carbon sphere electrode cycled between 1.5 and 0.01 V at a C/5.5 rate; Right: SEM and TEM (inset) images of SnO_2/Sb -coated carbon spheres.

Publications, reports, talks, invention reports, patent applications.

1. V. G. Pol, High Capacity Composite Carbon Anodes Fabricated by Autogenic Reactions, Annual Merit Review, Arlington, Virginia, Washington, D.C. May 14-18 (2012).
2. M. M. Thackeray and V. G. Pol, Electrochemical Performance of Spherical Carbon Particles, 16th International meeting on Lithium Batteries, (IMLB) Jeju, Korea. June 17-22, 2012.

TASK 1

Battery Cell Materials Development

Project Number: 1.1V (ES115)

Project Title: Synthesis and Development of High-Energy and High-Rate Cathode Materials from Ion-Exchange Reactions (Novel Composite Cathode Structures)

Project PI, Institution: Christopher Johnson, Argonne National Laboratory

Collaborators (include industry):

Michael Slater, Argonne National Laboratory
Donghan Kim, Argonne National Laboratory
Shawn Rood, Argonne National Laboratory
Eungje Lee, Argonne National Laboratory
Wenquan Lu, Argonne National Laboratory
Stephen Hackney, Michigan Technological University

Project Start/End Dates: October 2010 / September 2016

Objectives: Ion-exchange reactions are used to make new cathode materials with high-energy and high-rate. The objective is to produce an optimized material that shows an improvement over the drawbacks of Argonne high-energy cathodes. These ion-exchange cathodes should thus demonstrate <10% irreversible capacity in the first cycle, > 200 mAh/g at a C rate, no alteration in voltage profile during cycling, lower cost, and improved safety.

Approach: We will synthesize, characterize, and develop new cathode materials that exploit the difference in sodium versus lithium cation radii and their respective coordination properties. Cathodes will be derived from layered sodium transition metal oxide precursors that contain modest amounts of lithium in the transition metal (TM) layer. The sodium in the precursor materials is then ion-exchanged with lithium to form layered composite oxide cathodes for lithium batteries. We will focus on electrode materials that contain redox active Ni, and low cost Mn and Fe transition metals

Milestones: Materials will be produced and tested that will show progressively improved properties as the project moves forward.

- (a) Synthesize new materials, September 2011, (completed)
 - Optimize ion-exchange reaction conditions, April 2012 (on-going)
- (b) Characterize electrochemical properties of synthesized materials, March 2012, (on-going)
 - Demonstrate high-rate of 205 mAh/g @ 2C rate, March 2012, (completed)
- (c) Characterize structure of materials, April 2012, (on-going)
 - Examine morphology of starting materials, and ion-exchange products, June 2012, (on-schedule)

- (d) Continue optimization of Na, Li and transition metal content ratios in materials, September 2012, (on-schedule)
- (e) Initiate measurement of thermal properties of charged cathode materials that have been compositionally optimized using DSC, September 2012, (on-schedule)

Financial data: \$500K; \$50K subcontracted to Prof. S. Hackney (Michigan Technological University)

PROGRESS TOWARD MILESTONES

An objective of the project (milestone (d) for Sept. '12)) is to pursue varied transition metal (TM) precursor compositions other than the standard $\text{Na}_x\text{Li}_{1-x}(\text{Ni}_{0.25}\text{Mn}_{0.75})\text{O}_2$ (which is subsequently ion-exchanged). In this past quarter we synthesized the following compositions: $\text{Na}_x\text{Li}_{1-x}(\text{Ni}_{0.5}\text{Mn}_{0.5})\text{O}_2$, $\text{Na}_x\text{Li}_{1-x}(\text{Ni}_{1/3}\text{Mn}_{1/3}\text{Co}_{1/3})\text{O}_2$, and $\text{Na}_x\text{Li}_{1-x}(\text{Ni}_{0.225}\text{Mn}_{0.65}\text{Co}_{0.125})\text{O}_2$ (TM is the ANL-NMR composition) precursors and did ion-exchange on them. The $\text{Na}_x\text{Li}_{1-x}(\text{Ni}_{0.5}\text{Mn}_{0.5})\text{O}_2$ precursor ($x=0$) was single phase (P2), and retains a single phase in the ion-exchanged product (O3) (see Fig. 1). The electrochemical performance of the Li cell is shown in Fig. 2. The capacity is about $\sim 170 \text{ mAhg}^{-1}$ (14th cycle), with a reasonably flat voltage profile (inset).

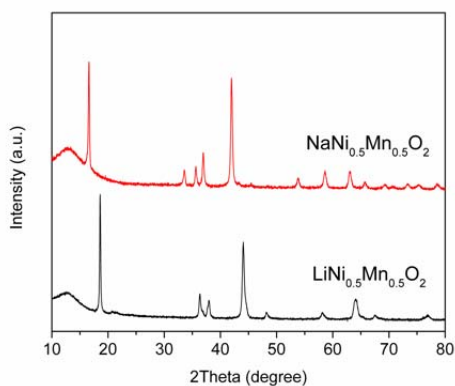


Fig. 1 XRD patterns of samples (product) cell

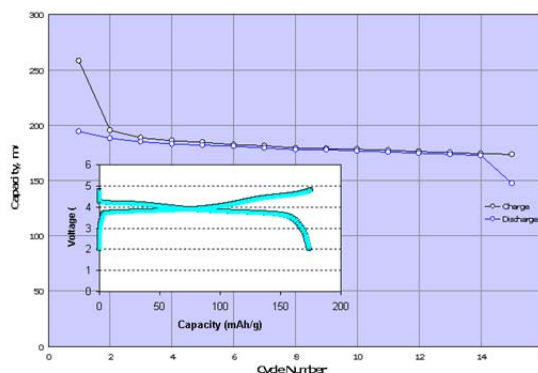


Fig. 2. Capacity Li/LiNi_{0.5}Mn_{0.5}O₂ (IE)

It turns out that the other compositions: $\text{Na}_x\text{Li}_{1-x}(\text{Ni}_{1/3}\text{Mn}_{1/3}\text{Co}_{1/3})\text{O}_2$, and $\text{Na}_x\text{Li}_{1-x}(\text{Ni}_{0.225}\text{Mn}_{0.65}\text{Co}_{0.125})\text{O}_2$ do not yield single phase precursor layered materials, as there is both Na layered phases and Li layered phases. After ion-exchange, there were still multiple phases present and the electrochemical performance is poor.

In milestone (c) the morphology of the $\text{Na}_x\text{Li}_{1-x}(\text{Ni}_{0.25}\text{Mn}_{0.75})\text{O}_2$ ion-exchanged product was studied. Fig. 3 shows that there are exposed crystal plates which maintain a hexagonal symmetry and that the edges can provide entry points for Li insertion and fast diffusion. However, the rough edges also can lead to deterioration of the crystal during long-term cycling.

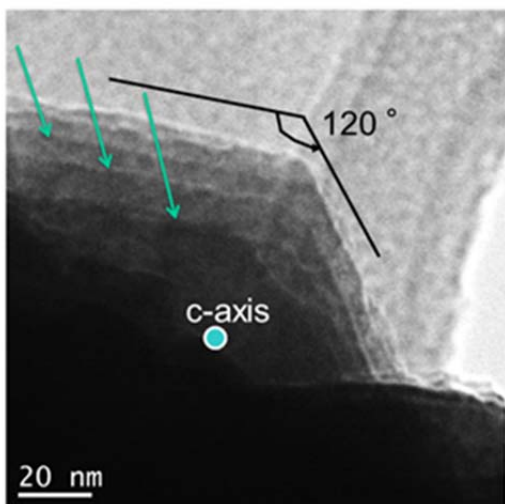


Fig. 3. TEM of $\text{Na}_x\text{Li}_{1-x}(\text{Ni}_{0.25}\text{Mn}_{0.75})\text{O}_2$ ion-exchanged product

The next reporting period will focus on running mixed Na- and Li- layered phases together in a Li cell.

Publications, Reports, Intellectual property or patent application filed this quarter.

Oral Presentations

- “Novel Composite Cathode Structures”, Christopher Johnson, DOE-EERE VTP Annual Merit Review, 16 May 2012.

TASK 1

Battery Cell Materials Development

Project Number: ES038

Project Title: High Energy Density Ultracapacitors

Project PI, Institution: Patricia Smith, NAVSEA-Carderock

Collaborators: Thanh Tran and Thomas Jiang (NAVSEA-Carderock), Michael Wartelsky (SAIC), Deyang Qu (University of Mass., Boston)

Project Start/End Dates: FY09 to FY12

FY12 Objectives: Assess safety and electrochemical performance of LIC technology. Improve low-temperature energy density of lithium ion capacitor (LIC) by 25% (in comparison to 1st generation LIC cells).

Approach:

Identify candidate high-performance electrolyte compositions via technical discussions with battery/capacitor manufacturers, DOE investigators and from literature reports. Evaluate most promising systems by fabricating and cycling pouch cells in the temperature range from 25°C to -30°C. Investigate the effect of negative electrode carbon graphitization on cell performance and thermal stability. Identify optimal carbon pore size for low temperature performance. Evaluate the thermal stability of electrode materials, electrolytes, and cell design using differential scanning calorimetry (DSC) and accelerating rate calorimetry (ARC). Evaluate the effect of temperature and discharge rate on experimental LIC cell performance.

Milestones:

- (a) Safety and performance evaluation of 1st generation LIC cell technology (March 2011). Status: Complete
- (b) Identification of negative electrode material that exhibits high reversible capacity, high power capability, and good low temperature performance. (September 2012). Status: In progress
- (c) Identification of high-performance, low-temperature electrolyte (July 2011). Status: Complete
- (d) Safety and performance evaluation of 2nd generation LIC cell technology (September 2011). Status: Complete
- (e) Evaluation of the effect of temperature and discharge rate on the electrochemical performance of 1,000F experimental cells (January 2012). Status: Complete
- (f) Evaluation of the self-discharge behavior of LIC cells. Comparison to lithium ion batteries and electrochemical double layer capacitors (June 2012). Status: Complete

Financial Data: Funding Expensed 3Q FY12: \$61,200

Progress Toward Milestones:

Task f was completed. The self-discharge behavior of double-layer capacitors is an important factor when considering their suitability for electric vehicle applications. There are three distinguishable self-discharge mechanisms that can attribute to capacity deduction in a capacitor. These include: cell overcharge, Faradaic impurity reactions and leakage currents. During this quarter, we measured the difference in capacity of a lithium-ion and a double-layer capacitor that were discharged immediately after being charged, to capacities of cells that were discharged after remaining at open circuit for three days (72 hours) after their charge. Experiments were conducted over a wide range of temperatures. Similar experiments were performed with a lithium ion battery for comparison.

Figure 1 shows that cell self-discharge increases as the temperature rises, regardless of the cell electrochemistry. The lithium ion capacitor's percentage capacity loss was determined to be in between that of a lithium ion battery and a double layer capacitor. This is understandable as it is well known that the self-discharge behavior of a two-electrode cell is the sum of the self-discharge which takes place at the individual electrodes recorded against a reference electrode. Faradaic electrodes, where the potentials are thermodynamically based, are usually more stable than charged capacitor electrodes that have no thermodynamically defined electrode process and that would be self-stabilizing. The self-discharge of the asymmetric, lithium ion capacitor should therefore be less than that of the symmetric, capacitive counterpart, but greater than a cell containing two faradaic electrodes.

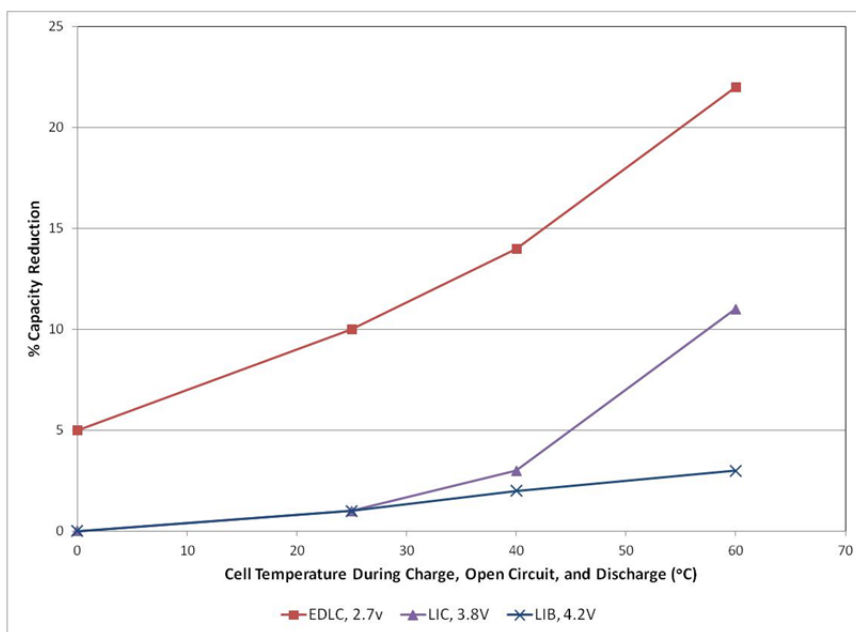


Figure 1. Percentage of capacity loss for cells stored at open circuit (OC) for three days at the noted temperatures. The electrochemical double layer capacitor (EDLC) was charged to 2.7V, the lithium ion capacitor (LIC) to 3.8V and the lithium ion battery (LIB) to 4.2V prior to OC.

Investigations continued to identify a high capacity, highly reversible carbon for the negative electrode. Emphasis was placed on the heat treatment of an activated carbon to improve its Li^+ diffusivity while maintain high capacity. A series of samples were heated at temperatures ranging from 900°C to 2100°C for 1 hour under a blanket of argon. Powder X-ray diffraction measurements were made and the R value, defined as the 002 peak height to background ratio, was determined. As expected, the number of stacked graphene layers increased with temperature. Future efforts will be directed toward fabricating electrodes made from these carbons and assessing their electrochemical performance.

Publications, Reports, Intellectual Property or Patent Application Filed this Quarter.

None during this period

TASK 1

Battery Cell Materials Development

Project Number: CPS Project 18502, CPS Agreement 23060, ORNL FWP CEVT110 (ES164)

Project Title: Overcoming Processing Cost Barriers of High Performance Lithium Ion Battery Electrodes

Project PI, Institution: David Wood, Oak Ridge National Laboratory

Collaborators: Argonne National Laboratory, Sandia National Laboratories

Project Start/End Dates: 10/1/11 to 9/30/14

Objectives: Electrode suspensions for lithium ion batteries are currently formulated using expensive polyvinylidene fluoride (PVDF) binder and toxic, flammable n-methylpyrrolidone (NMP) solvent. It is desirable to replace these components with water and water-soluble binders, but methods of mass production of these suspensions are currently underdeveloped. The major problems with aqueous electrode dispersions are: 1) agglomeration of active phase particles and conductive carbon additive; 2) poor wetting of the dispersion to the current collector substrate; and 3) cracking of the electrode coating during drying. NMP based processing also has the inherent disadvantages of high solvent cost and the requirement that the solvent be recovered or recycled. Initial projections of the minimum cost savings associated with changing to water and water-soluble binder are 70-75%, or a reduction from \$0.210/Ah to \$0.055/Ah. The objective of this project is to transform lithium ion battery electrode manufacturing with the reduction or elimination of costly, toxic organic-solvents.

Approach: Fabrication of composite electrodes via organic (baseline) and aqueous suspensions will be completed. A focus will be placed on the effect of processing parameters and agglomerate size on the aqueous route cell performance and microstructure of the composite electrode. Several active anode graphite and cathode (NMC, LiFePO₄, etc.) materials will be selected with various water-soluble binders. The conductive carbon additive will be held constant. Rheological (viscosity) and colloidal (zeta potential) properties of the suspensions with and without dispersant will be measured with a focus on minimization of agglomerate size. These measurements will show the effects of agglomerate size and mixing methodology on suspension rheology and help determine the stability (i.e. ion exchange processes across the surfaces of various crystal structures) of active materials in the presence of water. Composite electrodes will be made by tape casting and slot-die coating, and the drying kinetics of the electrodes will be measured by monitoring the weight loss as a function of time and temperature. Solvent transport during drying will also be monitored as a method to control electrode morphology, porosity, and tortuosity. Electrode microstructure and surface chemistry will be characterized and correlated with cell performance. Electrochemical performance of electrode coatings made from the various suspensions

will be supplied to ORNL's strategic industrial partners for external validation in large cell formats.

Improved cell performance with reduced processing and raw material cost will be demonstrated using pilot-scale coatings. At ORNL coin cells will be tested and evaluated for irreversible capacity loss, AC impedance, capacity vs. charge and discharge rates, and long-term behavior through at least 500 charge-discharge cycles. Half cells, coin cells, and pouch cells will be constructed and evaluated. The coin cells will be used for screening and coarse evaluation of different suspension chemistries and coating methodologies. A fine tuning of these research areas will be completed using ORNL pouch cells and large format cells with ORNL's industrial partners. Electrode coatings will be produced on the ORNL slot-die coater and supplied in roll form to the industrial partners for assembly into large format cells.

Electrode morphology will be characterized by scanning electron microscopy (SEM) and TEM. The bulk structure and surface of the active materials will be characterized using XRD and XPS, respectively. In addition, in-situ TEM will be performed to investigate real-time SEI layer formation as a function of the different suspension chemistries.

Milestones:

- a) Development of an aqueous formulation for cathodes (March 2012); complete.
- b) Development of an aqueous formulation for anodes (May 2012); delayed.
- c) Coating technique and drying protocol for anodes and cathodes (July 2012); delayed.
- d) Development of porosity control in thin electrodes (September 2012); on schedule.
- e) Match cell performance in terms of initial capacity, irreversible capacity loss, and cyclability through 100 cycles of aqueous suspension and water-soluble binder to NMP/PVDF based suspensions (Sept. 2012); on schedule.

Financial data: \$300k/year for FY12

PROGRESS TOWARD MILESTONES

Summary of work in the past quarter related to milestones (a), (b), and (c).

Milestones (b) and (c) have been delayed due to equipment moving, installation, and commissioning in the new ORNL Battery Manufacturing Facility (BMF). The new target completion dates for these milestones are September 2012. Rheological properties of aqueous NMC532 suspensions with various CMC concentrations were investigated. Baseline coatings of both NMC532 and graphite A12 using NMP as solvent were performed with electrode balancing; however, the solid loading was too high for round robin testing at ANL. A second baseline coating was delayed due to the movement of coating equipment and will be performed shortly.

1. Rheological properties of aqueous NMC532

Aqueous NMC532 (Toda America) suspensions with various CMC (Fisher Scientific, M.W.=250,000 g/mol, DS=0.7) concentrations were prepared by mixing CMC solution in water for 10 min followed by dispersing NMC532 in the resulting solution for 10 min. Mixing process will carried out by a high-shear mixer (model 50, Netzsch). The CMC concentration was based on NMC mass. NMC and water ratio was 1:2.5.

Rheological properties of aqueous NMC532 with various CMC concentrations were investigated using a controlled stress Rheometer (AR-G2, TA Instruments) and shown in Figure 1. The NMC532 suspensions exhibited shear thickening behavior with CMC concentration below 0.5 wt%. The rheological behavior switched to Bingham plastic/Newtonian behavior and shear thinning at shear rate below 1000 s⁻¹ with 1.0 wt% and 2.0 wt% CMC, respectively. The critical shear rate (>1000 s⁻¹) was relatively high, which was above the operating window of most common coating methods. For instance, coating using a doctor blade with 200 μm gap and a

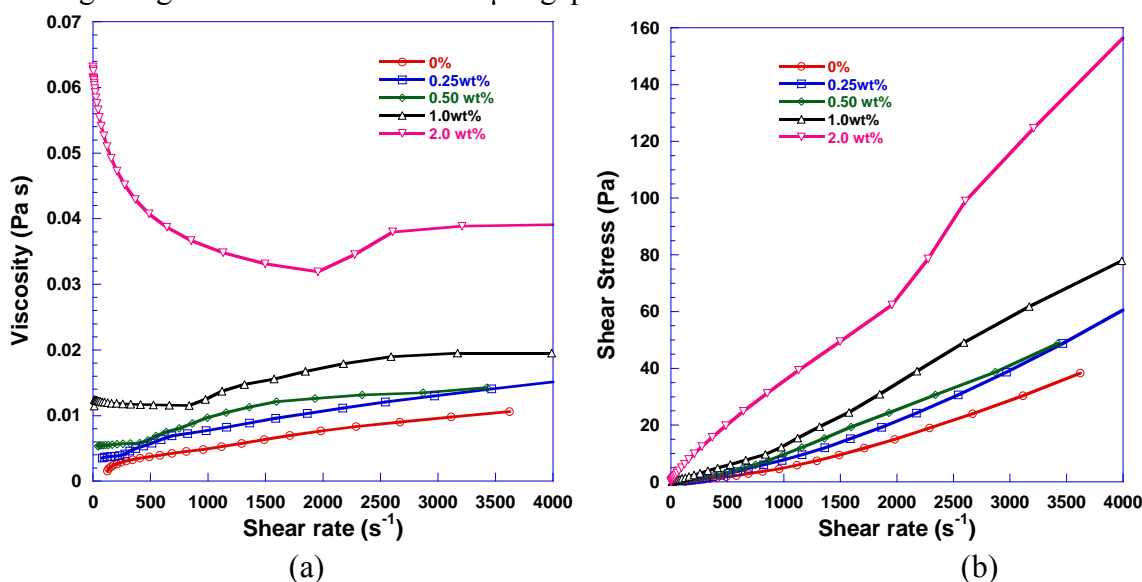


Figure 1. Rheological properties of aqueous NMC532 suspensions with various CMC concentrations a) viscosity vs shear rate and b) shear stress vs shear rate.

Table 1 Parameters from H-B model for the NMC532 suspensions

CMC concentration	0.0%	0.25%	0.50%	1.00%	2.00%
Power-law Index, n	1.57	1.51	1.64	1.05	0.83

shear rate of 750 s⁻¹ translates to coating speed of 12 m min⁻¹, which is higher than the industrial coating speed (~20 ft min⁻¹) in manufacturing LIB electrodes. Therefore, the low shear rate region is more interesting and will be focused in the following discussion. The rheological behavior change was further evidenced by the shear stress and shear rate plot as shown in Figure 1 (b), which could be fitted with Herschel–Bulkley (H–B) model.

The fitting power-law indices were listed in Table 1. The H–B equation is one of the most employed models for situations where a nonlinear dependence exists of shear stress on shear rate. It is described by the power law equation and is stated as the following:

$$\tau = \begin{cases} \tau_0 + K\dot{\gamma}^n & \text{if } \tau > \tau_0 \\ 0 & \text{if } \tau \leq \tau_0 \end{cases} \quad (1)$$

where τ , τ_0 , K , $\dot{\gamma}$ and n are the shear stress, yield stress (stress needed to initiate the flow), consistency index, shear rate and power-law index, respectively. If $n = 1$, this function reduces to the classical Bingham plastic equation. If $\tau_0 = 0$ and $n = 1$, this function describes Newtonian behavior.

The power-law index was 1.05 with 1.0 wt% CMC, demonstrating the best suspension stability. In addition, NMC532 suspension exhibited higher viscosity with increasing CMC concentration. This suggested that CMC not only acted as a dispersant in aqueous NMC532 suspension but also a binder.

Median agglomerate size, D_{50} , of aqueous NMC532 suspension was measured by laser diffraction (Partica LA-950 V2, Horiba Scientific) and shown in Figure 2. D_{50} was relatively constant and not a significant function of CMC concentration.

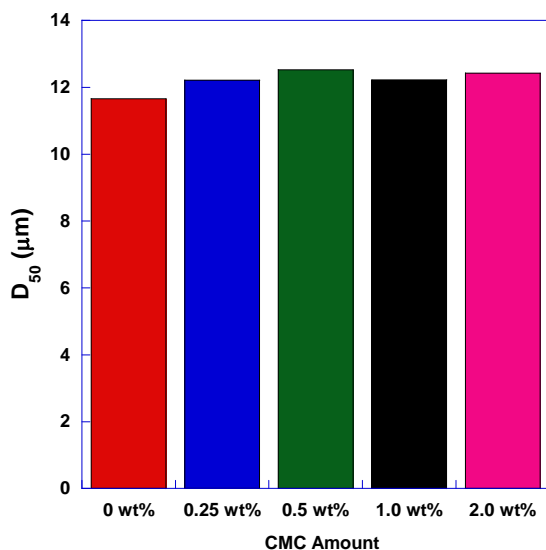


Figure 2. Agglomerate size of aqueous NMC532 suspensions with various CMC concentrations.

2. Future work:

Rheological properties of aqueous NMC532 with carbon black as well as various solid loading will be investigated to optimize electrode formulation. NMC532 electrodes will be fabricated through aqueous processing and their performance will be investigated. Similar formulation optimization and coating trials will be performed for the ConocoPhillips A10/A12 anode. A second set of coating trials will be subsequently completed for the round robin testing between ANL, SNL, and ORNL.

Publications, Reports, Intellectual property or patent application filed this quarter.

1. J. Li, B.L. Armstrong, J. Kiggans, C. Daniel, and D.L. Wood, "Performance Enhancement of Aqueous LiFePO₄ Cathode Dispersions Using Polyethyleneimine," *Journal of Power Sources*, Under Review, 2012.
2. J. Li, C. Rulison, J. Kiggans, C. Daniel, and D.L. Wood, "Superior Performance of LiFePO₄ Aqueous Dispersions via Corona Treatment and Surface Energy Optimization," *Journal of The Electrochemical Society*, **159**, A1152–A1157 (2012).
3. J. Li, B. Armstrong, J. Kiggans, C. Daniel, and D. Wood, "Dispersant and Mixing Sequence Effects in LiFePO₄ Processing," 221st Meeting of The Electrochemical Society, Seattle, Washington, Abstract No. 164, May 6-11, 2012.

TASK 1

Battery Cell Materials Development

Project Number: ES162

Project Title: Development of Industrially Viable Battery Electrode Coatings

Project PI, Institution: Robert Tenent and Anne Dillon (co-PI), NREL

Collaborators (include industry): Chunmei Ban (NREL), Steven George (University of Colorado, Boulder), Chris Orendorff (Sandia National Laboratory), Bryant Polzin (Argonne National Laboratory)

Project Start/End Dates: December, 2012 – September, 2016

Objectives: (1) Demonstration of Al₂O₃-based Atomic Layer Deposition coatings for improved cycling durability and abuse tolerance using standard electrode materials currently employed within the ABR program. (2) Design of an in-line atmospheric pressure atomic layer deposition (AP-ALD) system to demonstrate a process that may easily and inexpensively be integrated into the existing industrial Li-ion electrode fabrication lines.

Approach: Previously obtained results indicate that atomic layer deposition (ALD) can be used to form thin and conformal coatings on electrode materials that lead to both increased cycling lifetime, especially at high-rate, as well as abuse tolerance (e.g. stable cycling at high temperature and/or high voltage). This project will initially focus on using existing deposition capabilities to demonstrate an Al₂O₃-based ALD protective coating process for materials that are already commercially available at large-scale or are under advanced study within the VTP-EERE programs. This will include both anode and cathode materials in order to facilitate full cell testing and abuse studies. Initially, testing will be performed at the coin cell level to establish a stable baseline for comparison to existing data. In a later phase of the project larger format electrodes will be coated for testing in both pouch and 18650 cells. Coatings will be demonstrated on electrode materials produced at NREL as well as from outside parties. Finally, testing will be conducted both at NREL as well as within collaborating laboratories via a “round robin” process to ensure quality of data and the development of robust and transferrable processes.

In addition to small-scale exploratory research on various possible coating/electrode combinations, design work will be conducted for the development of a deposition system that will allow in-line coating at atmospheric pressure using an “ALD-like” process. The ultimate goal is to demonstrate a process that can be inexpensively integrated into existing industrial Li-ion battery electrode fabrication lines.

Milestones:

- a) Demonstration of an Al₂O₃ ALD coating showing improved durability and abuse tolerance performance for a commercially viable cathode material
Due: May, 2012

Status: On Schedule

- b) Design and initiate construction of a deposition system capable of in-line AP-ALD on commercially relevant substrate sizes.

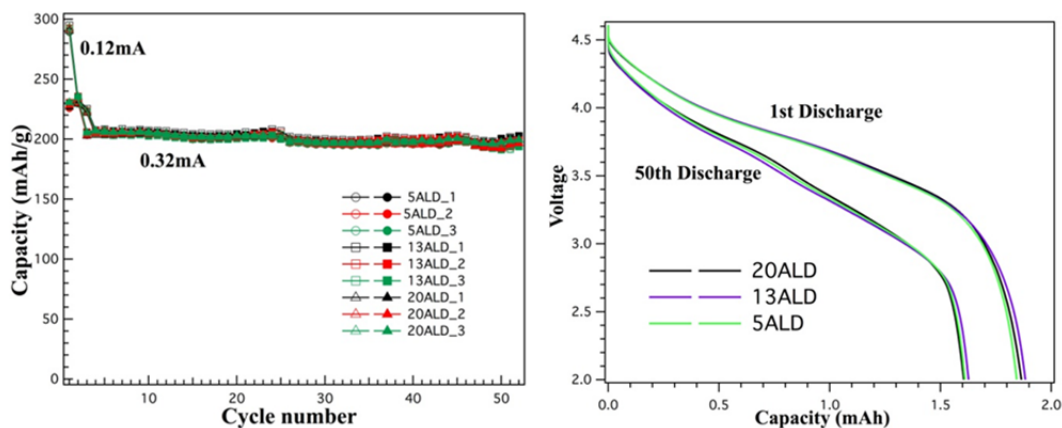
Due: September 2012

Status: On Schedule

Financial data: Current Funding \$300K/year

PROGRESS TOWARD MILESTONES

- a) Varied electrode materials were obtained from Argonne's cell fabrication facility including Toda HE5050, NCA and ANL made LiNiMnO both in powder and electrode forms. In addition, Sandia NL provided Toda NMC 111 and 523 materials both in powder and electrode formats. Currently, the Argonne provided Toda HE5050 material is under test in a coin cell format with varied thicknesses of ALD alumina coatings which were performed on-electrode. Additional samples are being placed under test at this time including as received materials and control samples that were processed through an identical environment and thermal processing profile to the alumina coated samples. These preliminary tests are being performed in a half-cell configuration to ensure that any effects on performance are attributable to the cathode coatings.



The above figure shows capacity data for all coated samples tested. Coatings of five, thirteen and twenty cycles of alumina were tested. All electrodes appear to show identical capacity as well as voltage profile up to 50 cycles including voltage fade behavior. Control samples for comparison are currently being tested and will be compared to this data to assess any effect of the ALD coating on performance. If reasonable performance enhancement is verified coated samples will also be provided back to ANL for independent testing. Similar experiments are currently planned for both the Toda NCA and ANL LiNiMnO and testing is expected to commence on these materials in the next quarter.

In addition to the Argonne supplied materials testing, earlier reported work in conjunction with Sandia showed that ALD alumina coatings lead to improved thermal performance, however, damage to electrodes during the coating process led to issues with cell performance. We are currently preparing to coat powders of the NMC111 and NMC 523 materials that can be fabricated into 18650 cells by the Sandia team and subjected to further thermal tests. We expect this to limit the potential for damage to the electrode system. Preliminary powder coatings for both materials are being conducted both at NREL and at CU-Boulder to determine the optimal ALD alumina coating thickness for further thermal testing samples to be sent to Sandia.

- b) Further discussions have been held with collaborators at CU-Boulder to develop our in-line ALD processing capabilities. We earlier demonstrated the ability to perform atmospheric pressure alumina ALD with an in-line format on a silicon wafer. In the next quarter, early demonstration depositions are planned on formed electrodes using this prototype deposition system. In addition, we have developed a preliminary design that should allow for improved film penetration as compared to earlier processing methods and are currently in the process of hiring a post-doctoral fellow who will be dedicated to construction and testing of our in-line ALD systems.

Publications, Reports, Intellectual property or patent application filed this quarter. (Please be rigorous, include internal reports--invention records, etc.)

We anticipate one forthcoming publication on the results of ALD alumina coating on the Toda HE5050 material within the next quarter.

TASK 2

Calendar & Cycle Life Studies

Project Number: 2.1B (ES030)

Project Title: Fabricate PHEV Cells for Testing & Diagnostics in Cell Fabrication Facility

Project PI, Institution: Andrew Jansen and Bryant Polzin, Argonne National Laboratory

Collaborators (include industry):

Dennis Dees, Argonne National Laboratory
Steve Trask, Argonne National Laboratory
Wenquan Lu, Argonne National Laboratory
Chris Orendorff, Sandia National Laboratory
Claus Daniel and David Wood, Oak Ridge National Laboratory

Project Start/End Dates: October 2008 / September 2014

Objectives: The objective of this work is to speed the evaluation of novel battery materials from the ABR and BATT programs, as well as from universities and the battery industry. The main objective in FY12 is to fabricate in-house pouch and 18650 cells in Argonne's new dry room facility using advanced energy storage materials.

Approach: Promising new exploratory materials are often developed in small coin cells, which may or may not scale up well in large PHEV battery designs. For this reason, pouch cells or rigid cells such as 18650's will be used for proofing of new battery materials in the capacity range of 0.4 to 2 Ah.

Pouch cells will be used for initial evaluations of long-term exploratory materials. Pouch cells are an efficient method of determining the stability of a cell system during calendar and cycle life aging. If the chemistry is not stable, it is likely that gassing will occur inside the cell. This will result in the pouch cell bulging or rupturing if the gassing is significant. More established materials and chemistries (or those that pass the pouch cell evaluation) will be used in rigid cells (e.g. 18650s).

Milestones:

- (a.) Optimize electrode slurry process using new Ross Mixer, March, 2012
(Completed)
- (b.) Evaluate materials from MERF scale-up of Argonne's cathode, May, 2012
(Completed)
- (c.) First cell build using 18650 cell making equipment, June 2012
(Delayed)

Financial data: \$1,100K

PROGRESS TOWARD MILESTONES

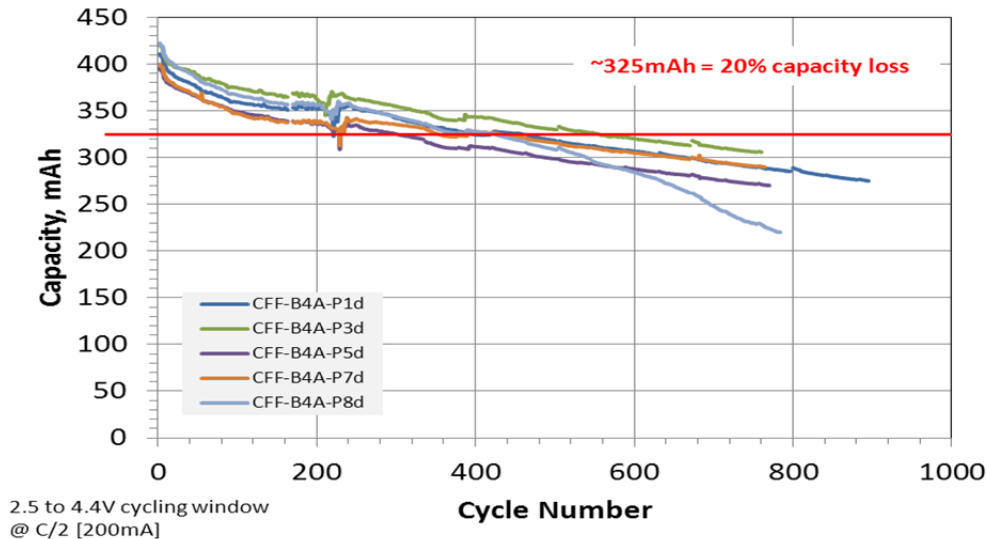
(a) Summary of work in the past quarter related to milestone (a)

The ability to make cells with long cycle life and good electrochemical performance is dependent on making high quality electrodes. Key to this is the ability to make homogeneously dispersed electrode slurries with intimate contact between active particles and conductive additives. To accomplish this step, a high energy/shear planetary mixer was purchased from Ross with a 2 liter chamber capacity. This relatively small capacity size is ideal for the typical electrode builds made with the pilot scale coater, where supply of novel materials is often limited. Installation of this mixer was completed in October, 2011.

Numerous slurry batches were made using ConocoPhillips CGP-A12 graphite and Toda' high energy cathode material HE5050 ($\text{Li}_{1.2}\text{Ni}_{0.15}\text{Co}_{0.10}\text{Mn}_{0.55}\text{O}_2$) to gain experience with the mixer and to optimize the mixing parameters and process steps. It was estimated that the minimum slurry volume is near 300 mL; below that amount resulted in insufficient mixing due to splatter from the high shear blade and not fully engaging the high shear blade. Single-sided and double-sided electrodes were made with both anode and cathode slurries. Pouch cells (xx3450 format) were made using these electrodes, and with electrodes made with a small supply of an exploratory high-energy NMC cathode ($\text{Li}_{1.2}\text{Ni}_{0.3}\text{Mn}_{0.6}\text{O}_{2.1}$) made by Argonne researchers in several batches.

A quick summary is provided here of the cell build using A12 graphite and Toda HE5050. After formation and characterization cycles were conducted, the pouch cells were placed on a cycle life profile, which consisted of repeated units of 40 cycles at C/2 rate followed by an HPPC test at the 5C discharge pulse. Based on earlier Diagnostic results, the upper voltage was limited to 4.4 V to enhance life. These cells have achieved nearly 800 cycles and are still under test (at 30°C).

High Energy Cathode (Toda HE5050) vs. Graphite (ConocoPhillips A12)



From the HPPC data it was determined that the ASI increases significantly before cycle 50 and then gradually rises with cycling. The 1-hour rest open circuit voltage from the HPPC tests showed some evidence of voltage fading below 40% DoD early in the life of the cells.

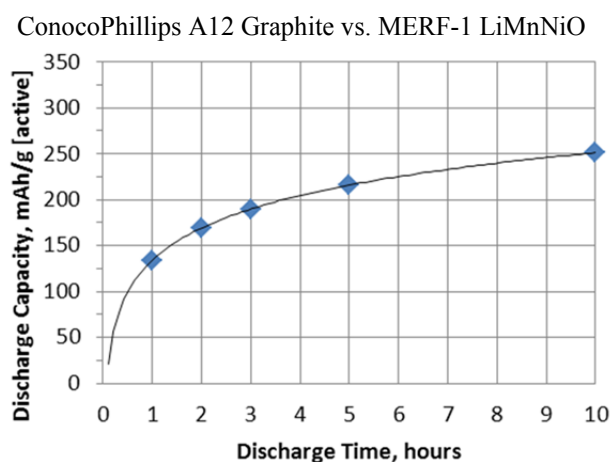
A summary of the rate capability for the first four pouch cell builds using high energy cathodes is shown in the table at right. Cell builds 1 and 4 used Toda HE5050 as the cathode, while cell builds 2 and 3 used small batches of R&D made cathode materials. Cell builds 3 and 4 were made with the new Ross mixer. The significant improvements in performance between cell builds 1 and 4, which have identical compositions, shows the level of expertise gained from repeated cell builds. Note that no electrolyte additives were used in these cell builds, which was done so that a baseline could be established for each class of materials. Future cell builds with these materials will include additives and variations in electrode composition, formation process, and test conditions.

Rate	Capacity of Cell Builds (mAh/g cathode)			
	1	2	3	4
C	146	196	150	198
C/2	163	205	193	213
C/3	172	209	203	217
C/5	183	217	215	227

(b) Summary of work in the past quarter related to milestone (b)

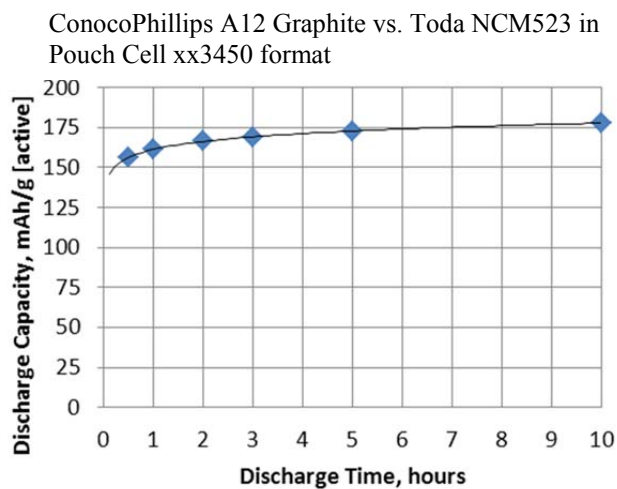
The Materials Engineering Research Facility (MERF) has scaled up their capability to make tens of kilograms of advanced cathode materials in their 20 L reactor – many of these cathode materials were discovered by researchers in the ABR Program. The first cathode material MERF scaled up is a high-energy NMC cathode ($\text{Li}_{1.2}\text{Ni}_{0.3}\text{Mn}_{0.6}\text{O}_{2.1}$) developed by Argonne researchers, and referred to here as MERF-1. The MERF made a 10 kg cathode batch that was validated in initial testing at the coin

cell level. One kg of this batch was then delivered to CFF in early March. Single-sided and double-sided electrodes were made with this cathode for further testing, after which a pouch cell build was conducted. The initial slow discharge capacity of this cathode is impressive at 250 mAh/g, but the delivered capacity at higher rates is less than desired (see figure). The capacity faded significantly during cycle life testing. An SEM analysis of the electrode showed that the cathode particles have signs of fracturing during the calendaring process. This observation was also made for the original cathode powders made by the ABR researchers, which appears to be a common problem for cathodes powders made via the carbonate precursor route. The MERF has made another batch of cathode that is undergoing validation at the MERF. If this material is deemed good, it will be forwarded onto CFF for incorporation into a pouch cell build.



(c) Summary of work in the past quarter related to milestone (c)

Effort was directed toward fabricating 18650 cells with commercially available materials and exploratory materials. It is anticipated that making 18650 cells will require significantly more material than pouch cell fabrication. For this reason, a commercial source was sought willing to supply openly at least 20 kg of advanced NCM material. Toda Kogyo agreed to supply Argonne with 40 kg of their NCM 5:2:3 cathode ($\text{Li}_{1.1}(\text{Ni}_{0.5}\text{Co}_{0.2}\text{Mn}_{0.3})_{0.9}\text{O}_2$). This material arrived in March of 2012 and was shared with Sandia and Oak Ridge for their cell builds. Enough double-sided electrodes were made to conduct a build with the 18650 format. A pouch cell build was performed first with these graphite and NCM523 electrodes to establish its rate capability (see figure) and its cycle life. These pouch cells are performing well with over 500 cycles completed at the C/2 rate. The first cell build in the 18650 format was expected to begin at the end of May, but was delayed a couple months due to delays in relocation of the electrode slitter and problems in slitting parallel edges. The electrodes tend to curve as they exit the slitter. Modifications are being made to the slitter to yield a straight cut and high precision templates are being made to check the quality of the electrodes dimensions.



**Publications, Reports, Intellectual property or patent application filed this quarter.
(Please be rigorous, include internal reports--invention records, etc.)**

“Overcharge Effect on Morphology and Structure of Carbon Electrodes for Lithium-Ion Batteries”, Wenquan Lu, Carmen M. L’opez, Nathan Liu, John T. Vaughey, Andrew Jansen, and Dennis W. Dees, *Journal of the Electrochemical Society* **159**(5), A566-A570 (2012).

TASK 2 Calendar & Cycle Life Studies

Project Number: 2.2B (ES031)

Project Title: Model Cell Chemistries (Electrochemistry Cell Model)

Project PI, Institution: Kevin Gallagher, Argonne National Laboratory

Collaborators (include industry):

Dennis Dees, Argonne National Laboratory
Daniel Abraham, Argonne National Laboratory
Andrew Jansen, Argonne National Laboratory
Wenquan Lu, Argonne National Laboratory
Bryant Polzin, Argonne National Laboratory
Kevin Gering, Idaho National Laboratory

Project Start/End Dates: October 2008 / September 2014

Objectives: The objective of this work is to correlate analytical diagnostic results with the electrochemical performance of advanced lithium-ion battery technologies for PHEV applications.

- Link experimental efforts through electrochemical modeling studies.
- Identify performance limitations and aging mechanisms.

Approach: Electrochemical modeling studies are utilized to elucidate transport, reaction, and thermodynamic phenomena in advanced lithium-ion cell chemistries. This work builds on earlier successful characterization and modeling studies in extending efforts to new PHEV technologies. The challenges center on expansion of the data base and enhancement of the modeling capabilities.

Milestones:

- (f.) Complete initial parameter estimation of high-energy LMR-NMC/graphite system. September 2012, (On schedule)
- (g.) Advance development of PHEV focused electrochemical models in support of programmatic goals. September 2014, (On schedule)
- (h.) Complete integration of new differential algebraic equation solver package with enhanced capabilities and complete conversion of existing models to newly adopted package. September 2012, (On schedule)
- (i.) Complete implementation and initial testing of full SEI growth model. December 2012, (Delayed)

Financial data: \$400K/year

PROGRESS TOWARD MILESTONES

(a) Summary of work in the past quarter related to milestone (a)

The Electrochemical Impedance Spectroscopy (EIS) cell model⁽¹⁾ was used to examine the impedance characteristics of the LMR-NMC positive electrode. Many of the initial results were presented in the previous quarterly report. Recent feedback on these early results has suggested a need for a more detailed explanation of the parameter development. Generally the electrolyte transport effects are small, but not insignificant. The electrolyte transport and thermodynamic parameters are supplied by Kevin Gering using his Advanced Electrolyte Model. The diffusion coefficient for the lithium diffusion through the oxide is obtained from fitting the low frequency Warburg impedance. As in earlier intercalation oxide based cathode studies, a distribution of characteristic lengths must be used to fit the impedance curve. It should also be noted that there is nothing special in the model to account for the complex LMR-NMC material. Probably the most difficult parameters to establish are the interfacial parameters, which is especially true for a single impedance sweep at one state of charge.

The interfacial impedance for each electrode typically consists of two circular arcs (i.e. a high frequency and mid frequency arcs). Ideally, the interfacial parameters can best be determined by fixing the active material and examining a wide variety of impedance studies including variations in state-of-charge, temperature, electrolyte composition, and electrode formulation. Lacking an extensive data set, we must rely on past studies to help guide the present effort. The relative time constant (i.e. fastest to slowest) of the individual interfacial phenomena are listed below.

- Electronic resistance between carbon additive and active material if carbon additive has a significant capacitance
- Ion migration through surface film on active material (i.e. SEI resistance)
- Lithium ion diffusion through surface film on active material
- Electrochemical reaction (i.e. Butler Volmer kinetics)
- Lithium diffusion through active material surface layer

It was assumed that the transport through the SEI was similar to earlier studies, except that the SEI was thicker. This assumption concerning the transport through the SEI, combined with the size of the high frequency circular arc required the electronic contact resistance between the active material and the carbon to be a major part of the interfacial impedance. This was discussed at the AMR and in the previous quarterly. Probably the best argument that this assumption is correct comes out of limited electrode formulation optimization studies that significantly reduced the size of the high frequency arc by increasing the electrode carbon content. The relative size of the kinetics and the diffusion through the active material surface layer are determined by the impedance curve and their assumed relative time constant. All the interfacial phenomena are significant, but only the electronic contact resistance dominates the interfacial impedance.

The LMR-NMC positive electrode impedance growth with aging is given in Figure 1. The change in impedance is dominated by the high frequency interfacial arc, but the mid frequency interfacial arc and the low frequency Warburg impedance also increases. The interfacial impedance shifts to lower frequencies as the cell ages. This is generally the case for parallel RC circuits or Warburg diffusive phenomena where there is a significant increase in impedance. Based on the initial assumption that the majority of the high

frequency arc impedance is associated with the electronic contact resistance between the oxide and the conductive carbon it is also the likely source of the increasing high frequency interfacial arc impedance. It should be noted that because of the high characteristic frequency (~ 10 kHz) of the arc it is possible that an electronic contact resistance at the electrode/current collector interface is responsible, at least partially, for the increase in impedance.

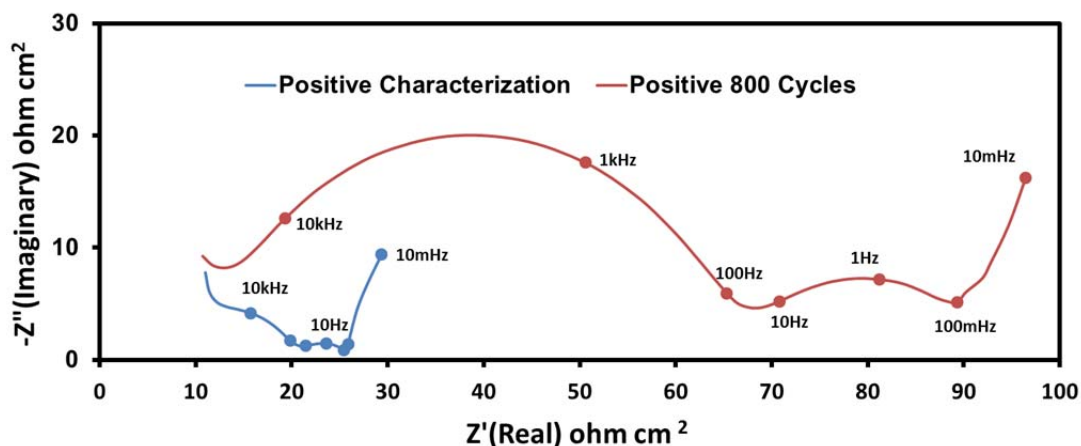


Figure 1. EIS aging of LMR-NMC positive electrode impedance (100 kHz-10 mHz) taken at a cell voltage of 3.75 volts and 30°C.

The three physical processes that can directly affect the mid frequency interfacial arc are lithium diffusion through the SEI (D_+), electrochemical kinetics (i_0), and lithium diffusion through the oxide surface layer (D_{si}). The impact on the cathode impedance from reducing the respective parameters by a factor of 5 is given in Figure 2. Some combination of a decrease in any or all these parameters could account for the increase in interfacial impedance, but not the increase in the Warburg impedance. Changes in Warburg impedance could derive from possible changes in the bulk oxide material or a loss in electrochemical active surface area.

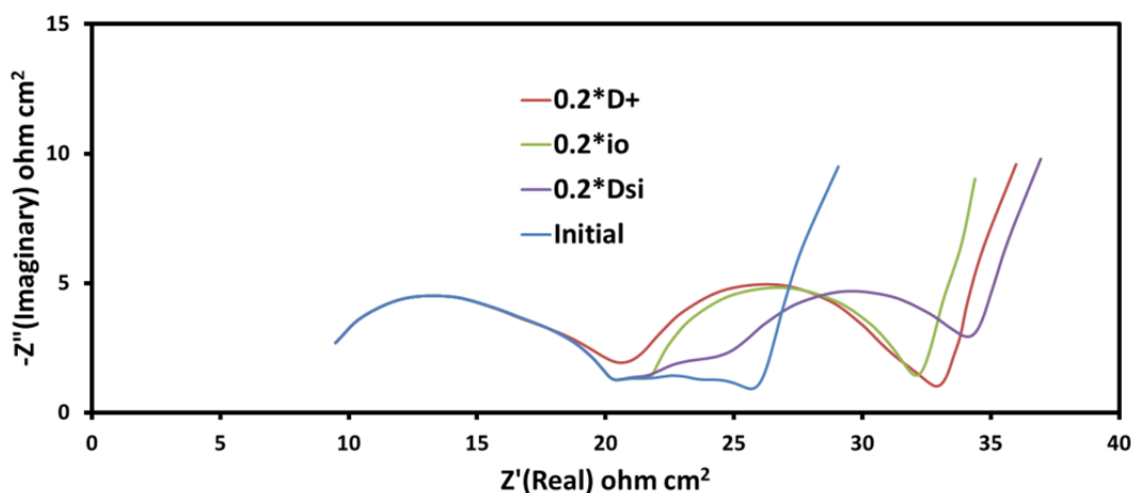


Figure 2. EIS model simulation of LMR-NMC positive electrode impedance data (100 kHz-10 mHz) taken at a cell voltage of 3.75 volts and 30°C.

(b) Summary of work in the past quarter related to milestone (b).

Some of the discussion in the previous quarterlies this year has focused on the hysteresis (i.e. very slow charge vs. discharge) observed in the open circuit voltage curve for the LMR-NMC materials. Understanding the source and modeling this hysteresis continues to be an important task. As described previously a combined experimental and theoretical study is underway.

(c) Summary of work in the past quarter related to milestone (c)

This project has been continually challenged by finding efficient ways to solve increasingly complex electrochemical cell models. A new differential algebraic equation solver package (PSE gPROMS) is being adopted to solve a wide variety of cell studies at the required level of complexity. Parameter estimation is always a serious challenge when dealing with the complex phenomenological modeling being used in this project. Previous effort used a “hand-fit” approach where the modeler systematically varied parameters to find a “best-fit” to the eye of the user. The new software package being implemented has parameter estimation algorithms and statistical assessment of the solution. Efforts this period continue to focus on integrating and improving the phase change model for electrode active materials. The importance of including phase change into the electrochemical model for electrodes like graphite has been well established, and recent work on the LMR-NMC electrode material indicates that more complex models will be needed for that electrode also. Further, the parameter estimation capabilities for the DC model are continuing to be utilized and improved.

(d) Summary of work in the past quarter related to milestone (d)

Implementation of the SEI growth model for the negative graphite electrode has been deemphasized because of the challenges the high energy LMR-NMC positive electrode are presenting.

(1) D. Dees, E. Gunen, D. Abraham, A. Jansen, and J. Prakash, *J. Electrochem. Soc.*, **152** (7) (2005) A1409.

Publications, Reports, Intellectual property or patent application filed this quarter. (Please be rigorous, include internal reports--invention records, etc.)

No publications, reports, or patents were submitted this quarter.

TASK 2

Calendar & Cycle Life Studies

Project Number: 2.3A (ES032)

Project Title: Diagnostic Evaluations - Electrochemical

Project PI, Institution: Daniel Abraham, Argonne National Laboratory

Collaborators (include industry): M. Bettge, Y. Li, Y. Zhu, D. Dees, A. Jansen, Argonne National Laboratory; Prof. A. Wei, Purdue University; Prof. I. Petrov, University of Illinois

Project Start/End Dates: October 2011/September 2012

Objectives: Electrochemical couples containing various positive and negative electrodes are being examined in the ABR program. The baseline electrolyte in these cells is EC:EMC (3:7, by wt.) + 1.2M LiPF₆. The main objective of this study is to use electrochemical diagnostic tools to identify factors that determine cell performance and performance degradation (capacity fade, impedance rise) on long-term storage and on extensive deep-discharge cycling. The electrochemical data obtained from these measurements are used in ABR's phenomenological modeling studies. A secondary objective of this study is to recommend and implement solutions that improve the electrochemical performance of materials and electrodes so that the PHEV cells may meet their 15y life criterion.

Approach: Our electrochemical measurements are conducted in various cell configurations that include coin cells, pouch cells, and reference electrode (RE) cells. Our investigations are conducted both on as-prepared single-sided electrodes, and on double-sided electrodes harvested from pouch- and 18650- cells. Our research includes the following components: (i) Studies in Reference Electrode cells – Data from these cells help identify causes of impedance rise and concomitant capacity fade; this knowledge will help us target the development of solutions to reduce cell performance degradation; (ii) development of electrolyte additives – these form surface films that protect the electrode components from further degradation; (iii) development of electrode coatings – modification of the electrode-electrolyte interfaces by these coatings have been shown to improve cell life.

Milestones:

- (a) Determine sources of impedance rise/capacity fade during extensive cycling of cells containing various electrochemical couples; September 2012 (on schedule)
- (b) Identify at least one electrolyte additive that improves cell life by 50% at 30°C and 25% at 55°C; September 2012 (on schedule).
- (c) Identify at least one electrode coating that improves cell life by 50% at 30°C and 25% at 55°C; September 2012 (on schedule)

Financial data: \$450 K (subcontracted \$30K to Purdue University)

PROGRESS TOWARD MILESTONES

(a) Summary of work in the past quarter related to milestone (a).

The ABR-1 positive electrodes contain 86 wt% $\text{Li}_{1.2}\text{Mn}_{0.55}\text{Ni}_{0.15}\text{Co}_{0.1}\text{O}_2$ (HE5050), 4 wt% SFG-6 graphite (Timcal), 2 wt% SuperP (Timcal) and 8 wt% PVdF (Solvay 5130). The ABR-1 negative electrodes contain ~ 90 wt% graphite (Conoco Philips A12), 6 wt% PVdF (Kureha KF-9300) and 4 wt% SuperP (Timcal). In previous reports we have shown that cell impedance rise is mainly governed by the positive electrode; the impedance rise at the negative electrode is relatively small. We have also noted that cell capacity fade is mainly governed by lithium trapping in the negative electrode SEI.

(b) Summary of work in the past quarter related to milestone (b)

Our colleagues (Kang Xu et al.) from the Army Research Lab have shown that the PFBP: Tris(perfluoro-t-butyl) phosphate electrolyte additive significantly improves capacity retention in 4.6 V $\text{LiNi}_{0.5}\text{Mn}_{1.5}\text{O}_4$ / Graphite Full Cells. We acquired some PFBP from Dr. Xu and examined its effect in ABR-1 cells that contained $\text{Li}_{1.2}\text{Mn}_{0.55}\text{Ni}_{0.15}\text{Co}_{0.1}\text{O}_2$ (HE5050)-based positive electrodes, Graphite (A12)-based negative electrodes, Celgard 2325 separator, and EC:EMC (3:7, by wt.) + 1.2M LiPF_6 (baseline) electrolyte; small amounts of PFBP (0.5 and 1 wt%) were added to the baseline electrolyte. The capacity and impedance data are shown in Figures 1 and 2, respectively.

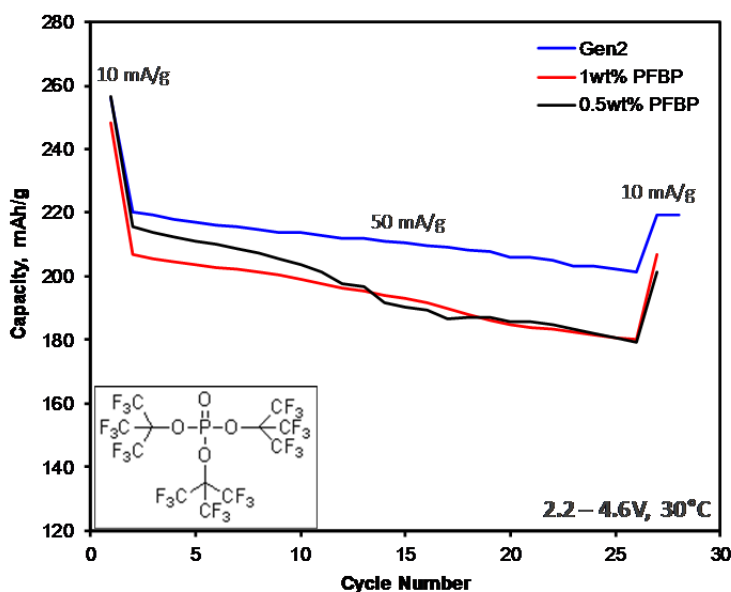


Fig. 1. Capacity as a function of cycle number showing effect of 0.5 and 1 wt% PFBP additive in the baseline Gen2 electrolyte. The inset shows the structure/composition of PFBP.

Figure 1 contains capacity as a function of cycle number data showing the effect of 0.5 and 1 wt% PFBP added to the baseline electrolyte; the Gen2 electrolyte data is shown for reference. The first and last cycle in the plot were carried out with a 10 mA/g current, whereas the intermediate cycles were conducted with a 50 mA/g current. The cells with the PFBP additive show slightly lower initial capacity, and also somewhat faster capacity fade relative to the baseline Gen2 electrolyte. The lower initial capacity is due to higher electrode impedance; half-cell data show that the PFBP increases impedance at both positive and negative electrode. The faster fade is also due to higher electrode impedances on cycling/aging.

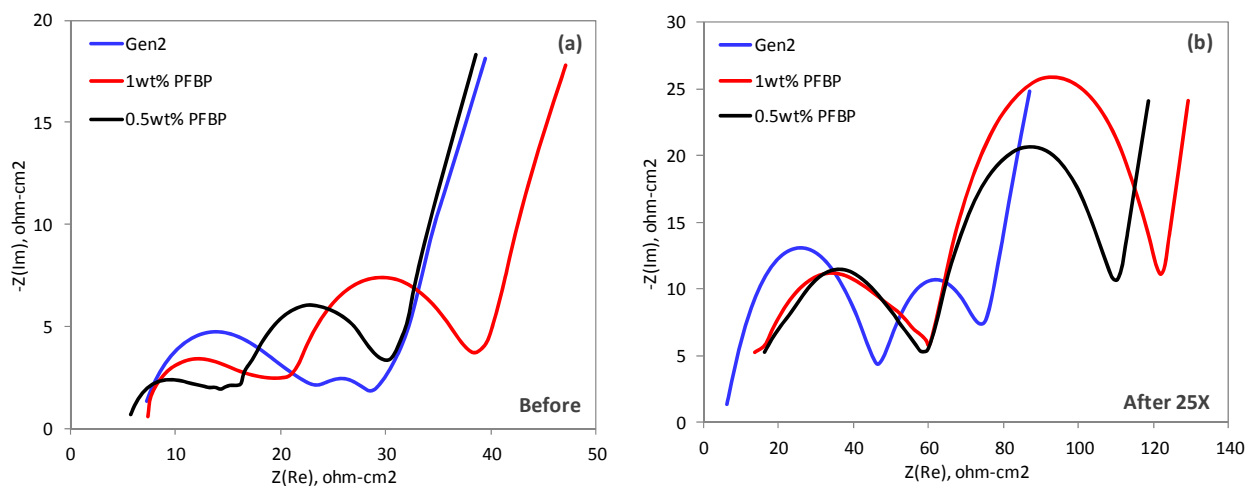


Fig.2. EIS data (3.75V, 30°C, 100 kHz-0.01 Hz) from full cells showing effect of PFBP additive.

Figure 2 contains EIS data from full cells containing the baseline Gen2 electrolyte, and with 0.5 and 1 wt% PFBP additive in the baseline electrolyte, (a) before, and (b) after 25 cycles at 30°C in the 2.2 to 4.6V voltage window. The “before” data is after formation cycling, which includes 3 initial 2–4.1V cycles, followed by two 2–4.6V cycles. The impedance of the additive-containing cells is higher than that of the baseline cell both before and after cycling. This higher impedance affects cell capacity values especially at higher rates. The higher electrode impedances suggest that the PFBP forms surface films on both the positive and negative electrodes which are, however, ineffective at inhibiting cell capacity fade and/or impedance rise.

(c) Summary of work in the past quarter related to milestone (c)

We conducted electrochemical cycling experiments and impedance measurements on cells with the as-prepared ABR-1 positive electrodes and with ABR-1 negative electrodes that were ALD coated to various nm-size thicknesses. All cells contained the EC:EMC(3:7, by wt.)+1.2M LiPF_6 electrolyte. The data from these tests are shown in Figures 3 and 4.

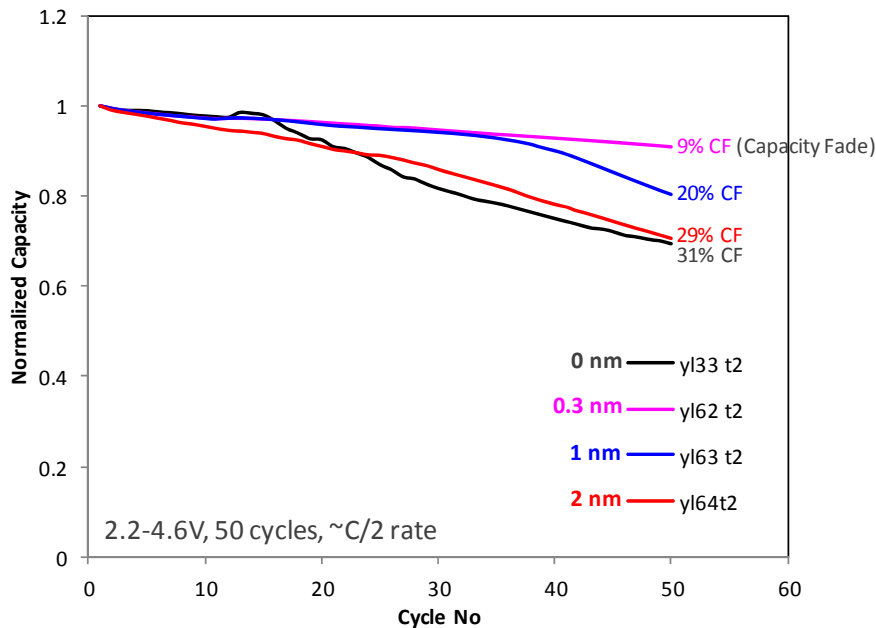


Fig. 3. Normalized Capacity as a function of cycle number showing effect of Alumina ALD coating (0, 0.3, 1, 2 nm thick) of the graphite-based negative electrodes.

Figure 3 shows that after 50 cycles the cell containing the as-prepared electrode shows the highest capacity fade (31%), whereas the cell containing the 0.3 nm alumina coated negative electrode shows the lowest capacity fade (9%). Cells containing the thicker (1 nm, 2 nm) negative electrode coatings show intermediate levels of capacity fade – the data indicate that thin negative electrode alumina coatings improve cell capacity retention.

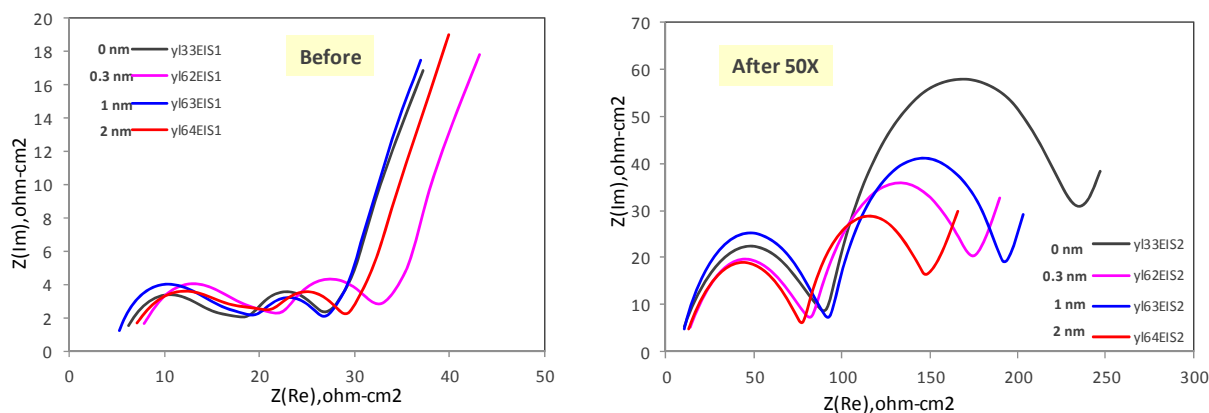


Fig.4. EIS data (3.75V, 30°C, 100 kHz-0.01 Hz) from full cells before and after 50 cycles in the 2.2-4.6V voltage window.

Figure 4 contains EIS data from full cells containing the as-prepared negative electrodes and with negative electrodes ALD-coated with 0.3, 1, and 2 nm thick alumina. The initial impedances of the as-prepared and ALD-coated samples are quite similar. All samples show a high-frequency arc (arising from the oxide-carbon interface) and a mid-frequency arc (arising from the oxide-electrolyte interface). After 50 cycles, the as-prepared

electrode shows the highest impedance. The cell impedances do not show a clear trend with alumina coating thickness; however, the 2 nm coated electrode shows the lowest impedance. Note that the coating appears to have the biggest impact on the mid-frequency arc (oxide-electrolyte interface). The high-frequency impedance increases even for the 2 nm coated sample. Other data have shown that (i) cell impedance rise arises primarily at the positive electrode, and (ii) thin alumina coatings mitigate impedance rise at the positive electrode. The cell impedance improvement maybe due to the transport of some Al/alumina to the positive electrode – this possibility will be examined in future experiments.

**Publications, Reports, Intellectual property or patent application filed this quarter.
(Please be rigorous, include internal reports--invention records, etc.)**

None

TASK 2

Calendar & Cycle Life Studies

Project Number: 2.3B (ES032)

Project Title: Diagnostic Evaluations - Physicochemical

Project PI, Institution: Daniel Abraham, Argonne National Laboratory

Collaborators (include industry): M. Bettge, Y. Li, M. Balasubramanian, D. Miller, Argonne National Laboratory; Prof. I. Petrov, University of Illinois; Prof. B. Lucht, University of Rhode Island; Prof. P. Guduru, Brown University

Project Start/End Dates: October 2011/September 2012

Objectives: Various lithium-ion chemistries are being examined for use in cells for PHEV applications. The main objective of this study is to use physicochemical characterization tools and techniques to explain the electrochemical performance and performance degradation mechanisms of ABR cells. The physicochemical data are used to guide development of electrochemical models that relate material and electrode chemistry to observed changes in cell performance during cycling and accelerated aging. Determining degradation mechanisms is an important step towards modifying the cell chemistry to attain the 15y life goal for these cells.

Approach: Our physicochemical examinations employ a combination of spectroscopy, microscopy, diffraction, and chemical analysis techniques. Our investigations are conducted on components harvested from small cells (1 to 50 mAh), and from pouch and 18650 cells subjected to characterization and long-term aging. Our research includes the following three components: (i) studies of the electrode-electrolyte interface using various techniques that include X-ray photoelectron spectroscopy; (ii) electrode studies using techniques that include X-ray diffraction, X-ray absorption spectroscopy (XAS), and Electron Microscopy (AEM); and (iii) stress evolution studies using techniques that include the “wafer curvature method”.

Milestones:

- (a) Performance degradation mechanisms in HE5050(+)/A12(-) cells, September 2012 (on schedule)
- (b) Initial information on performance degradation mechanisms in $\text{Li}_{1.14}\text{Mn}_{0.57}\text{Ni}_{0.29}\text{O}_2$ bearing cells, September 2012 (on schedule)
- (c) Stress evolution data on oxide and graphite electrodes during electrochemical cycling, September 2012 (on schedule)

Financial data: \$450 K (subcontracted \$30K to Brown University; \$50K to University of Illinois)

PROGRESS TOWARD MILESTONES

(b) Summary of work in the past quarter related to milestone (a).

X-ray photoelectron spectroscopy (XPS) studies were conducted on positive electrode samples harvested from ABR-1 Full Cells to examine the effect of cell aging on electrode degradation; the cells were discharged and held at 2V before electrode extraction. The samples were lightly rinsed in DMC to remove electrolyte residue before examination. An as-prepared (Fresh, no electrolyte exposure) sample was examined to provide baseline information. The data were obtained on a Kratos Axis Ultra X-ray photoelectron spectrometer under ultrahigh vacuum (10^{-9} Torr) conditions, and with monochromatic Al K α ~1486.6 eV radiation as the primary excitation source. Peak fits of all spectra were performed using the Shirley background correction and Gaussian-Lorentzian curve synthesis. The energy scale was adjusted based on the graphite peak in the C1s spectrum at 284.5 eV. Typical data are shown in Figure 1.

For the as-prepared sample, the C1s spectrum contains contributions from graphite (284.5 eV), SuperP carbons (285 eV), and the PVdF [-(CH₂CF₂)_x] binder (286.4 eV, 290.9 eV). The F1s spectrum shows a strong peak at 687.8 eV from the PVdF binder. The O1s spectrum shows a peak at 529.6 eV from the Li_{1.2}Ni_{0.15}Mn_{0.55}Co_{0.1}O₂, and a weak, broad peak centered at 532 eV that may be from a Li₂CO₃ impurity that is known to form on these oxides. Other peaks shown observed in the data include Mn3p, Ni3p, Co3p and Li1s.

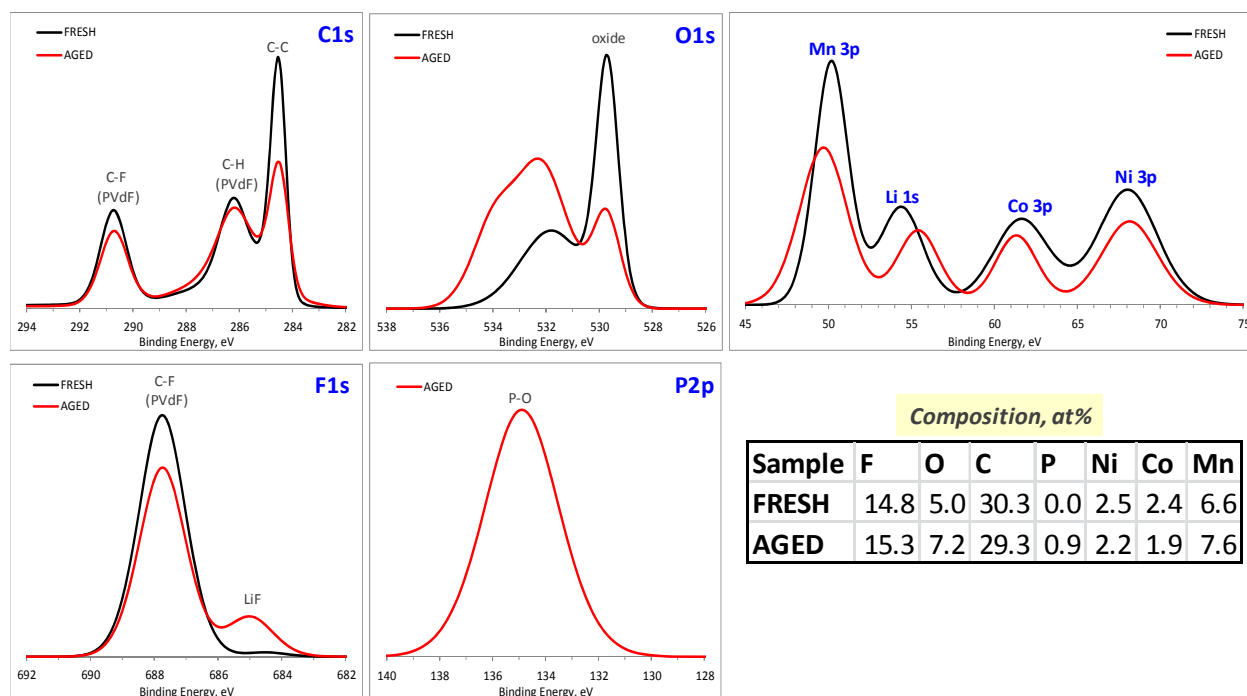


Figure 1: XPS data from ABR-1 positive electrode samples from FRESH (no exposure to electrolyte) and AGED (after 1500 cycles) cells.

For the aged sample (from a cell cycled 1500 times between 2.5 and 4.4V at 30°C), the C1s spectrum shows a reduction in the graphite/superP, and PVdF peak intensities on electrochemical cycling; the peak fits also indicated an additional weaker peak centered at 286.8 eV (C-O). Reduction in the binder (C-F) peak intensity is also seen in the F1s spectrum, which also shows a peak that arises from LiF. The P2p spectrum indicates peaks near 135 eV that arise from P-O functional groups. The O1s spectrum shows the most significant changes that include an intensity reduction of the oxide peak, which is consistent with the observed reduction in the Mn3p, Co3p, and Ni3p peak intensities; additional peaks with intensities centered at 532.4 eV (C=O) and 534.2 eV are also observed. The C 1s intensity at 286.8 eV (C*O(O)C=O), along with intensities at 532.4 eV (CO(O)C=O*) and 533.5 eV (CO*(O)C=O) suggest the presence of alkyl carbonates. The 534.2 eV also includes contributions from phosphate compounds. The XPS data indicate the presence of films on the surface of the cycled electrodes. The suggested compounds, LiF, $\text{Li}_x\text{PO}_y\text{F}_z$, alkoxides, and alkyl carbonates, are consistent with observations on other lithium-based metal-oxide compounds.

(b) Summary of work in the past quarter related to milestone (b)

The performance degradation trends of $\text{Li}_{1.14}\text{Mn}_{0.57}\text{Ni}_{0.29}\text{O}_2$ -bearing cells are very similar to those observed for the $\text{Li}_{1.2}\text{Ni}_{0.15}\text{Mn}_{0.55}\text{Co}_{0.1}\text{O}_2$ -bearing cells. The physicochemical data, and the mechanisms that govern cell performance degradation, are hence expected to be very similar.

(c) Summary of work in the past quarter related to milestone (c)

Real-time stress evolution in the ABR-1 positive-electrode during electrolyte wetting and electrochemical cycling is being measured using the wafer-curvature method. The ABR-1 positive electrodes contain 86 wt% $\text{Li}_{1.2}\text{Mn}_{0.55}\text{Ni}_{0.15}\text{Co}_{0.1}\text{O}_2$ (HE5050), 4 wt% SFG-6 graphite (Timcal), 2 wt% SuperP (Timcal) and 8 wt% PVdF (Solvay 5130). A preliminary dataset is shown in Fig. 2.

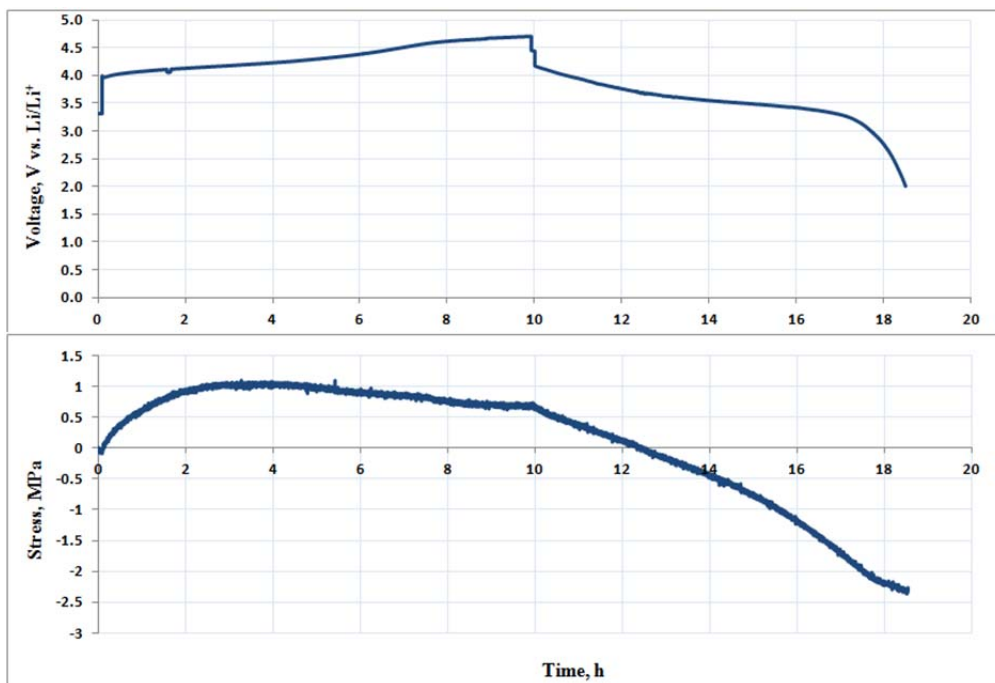


Fig. 2: Stress evolution in an ABR-1 positive electrode during the first cycle.

Upon electrolyte addition, the composite electrode rapidly develops compressive stresses of the order of 0.1 MPa because of binder swelling – this value is much smaller than the 1 to 2 MPa reported previously for the negative electrode. On oxide delithiation, the electrode develops a tensile stress, reaching a maximum of about 1 MPa; on further delithiation, the stress decreases but remains tensile. At high levels of delithiation (>250 mAh/g), the electrode stress becomes compressive (data not shown). The reasons for this behavior are yet to be determined. Oxide lithiation creates compressive stresses in the electrode – there is a significant hysteresis in stress values between the charge and discharge cycles. Further experiments are underway to validate and determine the reproducibility and persistence of the tensile-compressive stress transition behavior.

Publications, Reports, Intellectual property or patent application filed this quarter. (Please be rigorous, include internal reports--invention records, etc.)

None.

TASK 2

Calendar & Cycle Life Studies

Project Numbers: 1.1.1 and 2.4 (ES033)

Project Title: Strategies to Enable the Use of High-Voltage Cathodes (1.1.1) and Diagnostic Evaluation of ABRT Program Lithium Battery Chemistries (2.4)

Project PI, Institution: Robert Kostecki and Thomas Richardson, Lawrence Berkeley National Laboratory

Collaborators (include industry): None.

Project Start/End Dates: LBNL carried out diagnostics in the ATD Program since its 1999 inception, and the ABRT Program began October 2008.

Objectives: Task 1.1.1: To enable increased energy density by addressing the impact of high-voltage cathodes on the conducting carbon matrix. Task 2.4: (i) Determine the key factors that contribute to the degradation mechanism in the PHEV test cells and individual cell components. (ii) Characterize SEI formation on model electrode surfaces to improve understanding of key interfacial phenomena in PHEV cells.

Approach: Task 1.1.1: (i) determine the mechanisms for carbon damage and retreat at high potentials. (ii) Investigate mitigating treatments, additives, and procedures. Task 2.4: Use in situ and ex situ advanced spectroscopic and microscopic techniques in conjunction with standard electrochemical methods to characterize components harvested from fresh and tested PHEV cells, model thin-film cells, and special cells used to evaluate SEI formation processes.

Milestones: Determine interfacial degradation mechanism CBs in high-voltage cathodes (July 2012). On schedule. Synthesize a new type of CB with improved interfacial properties (September 2012). On schedule. Attend review meetings and present diagnostic results obtained in collaboration with ABRT Program participants. On schedule.

Financial data: FY 2012 funding \$600K

PROGRESS TOWARD MILESTONES

The focus of the work in the third quarter was on the characterization of the decomposition of the electrolyte on carbon black upon exposure to higher potentials. Because cyclic voltammetry is not representative of the behavior of an *in operando* Li-ion cell, a new investigation technique was developed and applied. Potentiostatic step methods have the advantage of separating signals from the electrochemical double layer that dominate the current signal in the first few ms or seconds and diffusion-controlled processes, including electrolyte decomposition reactions.

Figure 1 depicts a scheme of potentiostatic step measurements of a pristine commercial carbon black composite electrode in 1M LiPF₆, EC:DEC (1:2 vol.) electrolyte. Polarization begins at the open-circuit potential, and then 60-min constant-potential steps of 125 mV are applied and the current response is recorded. The current at the beginning

of each voltage pulse can be attributed to a capacitive behavior of the carbon black. To evaluate the electrochemical reactions two different parameter values were used: (i) the overall charge consumed during the entire potentiostatic step, and (ii) the current value at the end of the 60-min step. Figure 1B shows typical $i(t)$ behavior of an untreated carbon black/PVdF electrode. The current spike at the beginning is followed by a rapid relaxation and current plateau. In the final phase the current can be directly correlated to electrolyte decomposition and possibly PF_6^- intercalation/insertion into CB.

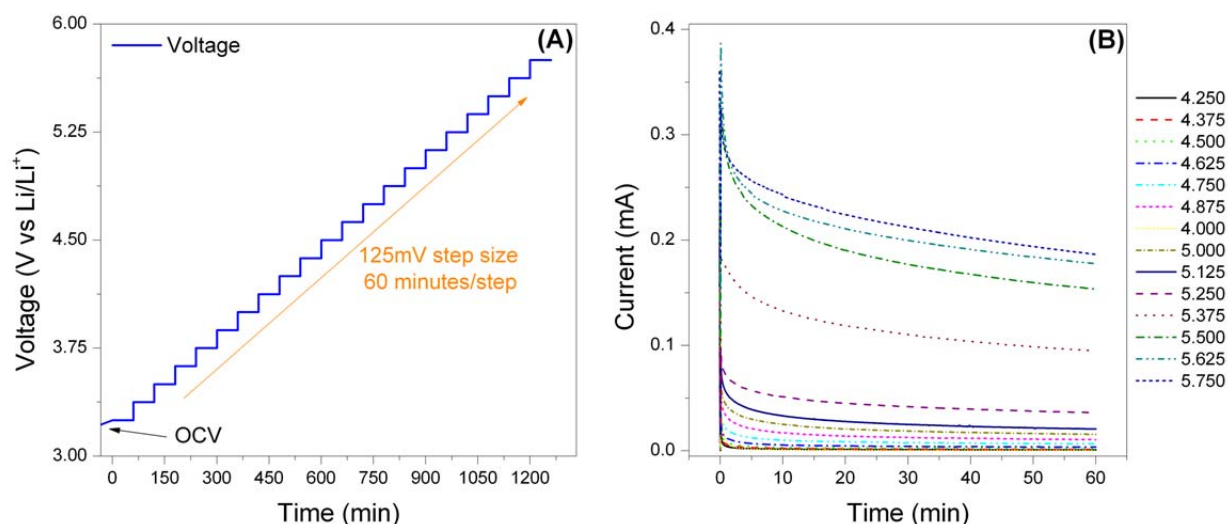


Figure 1. Scheme of the potentiostatic step method (A), and typical current response of an untreated commercial carbon black sample in EC:DEC 1:2 1M LiPF₆ (B)

The total charge consumed during each 60-min potentiostatic polarization at different potentials for a pristine and a heat-treated sample (see FY2012 2nd quarterly report) is displayed in Figure 2. The threshold of electrolyte decomposition reactions at carbon black is located at ~4.25 V, and their rates rise significantly at potentials above 4.5 V.

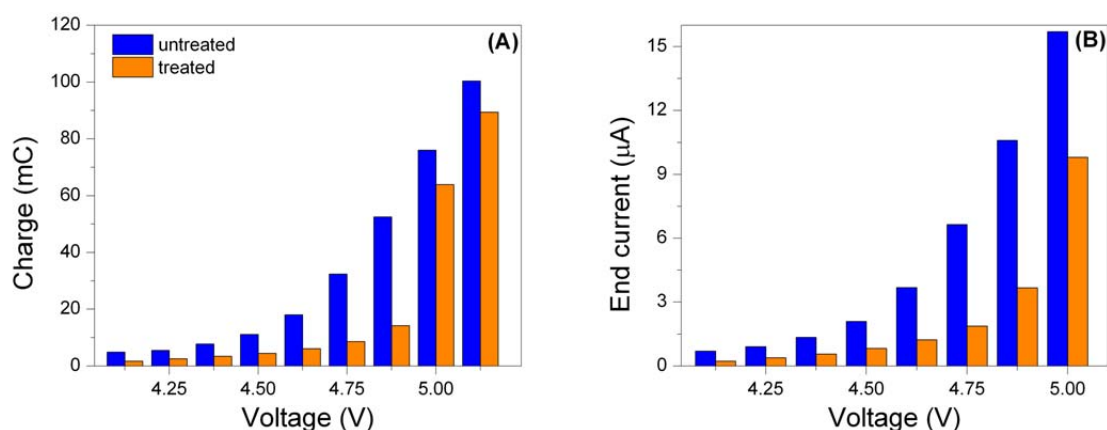


Figure 2. Charge consumed during potentiostatic measurements at each 60-min step (a) and the the end current of each step (b) for pristine and HT samples of pyrolyzed KaptonHN

These results clearly indicate the positive influence of the treatment and the limited electrolyte decomposition occurring at the modified amorphous carbon black samples at potentials up to 4.9 V. In collaboration with Dr. Battaglia (LBNL), new high-voltage composite cathodes with HT carbon black additive were prepared and are currently undergoing electrochemical cycling following the test protocol provided by Dr. Bryant Polzin (ANL). These measurements should provide a rapid validation in the electrochemical performance of modified composite cathodes and help determine possible plans for scale-up synthesis and testing efforts.

We continued our studies of the interfacial degradation mechanisms in Li-ion cells. The impedance of the symmetric cathode or anode cells displays no significant rise even after several hundreds of cycles, whereas the full electrochemical cell shows a continuous increase of the internal resistance. A diagnostic evaluation of these cells by vibrational spectroscopy and atomic force microscopy is underway.

TASK 2

Calendar & Cycle Life Studies

Project Number: 2.4 and 3.3 (ES034)

Project Title: Life and abuse tolerance diagnostic studies for high energy density PHEV batteries

Task 2.4: Life Diagnostics, Task 3.3: Abuse Behavior Modeling and Diagnostics

PI, Institution: Kyung-Wan Nam and Xiao-Qing Yang, Brookhaven National Laboratory

Barrier: Calendar and cycling life, Abuse tolerance

Objectives: The primary objectives of the efforts at BNL are: to determine the contributions of electrode materials changes, interfacial phenomena, and electrolyte decomposition to cell capacity power decline, and abuse tolerance; to develop new diagnostic techniques (in situ and ex situ) for lithium-ion batteries; to help other ABR teams and the battery developers to understand the technical barriers by using these new techniques; to explore new techniques to improve the abuse tolerance. The other objective is to design, synthesize and characterize new electrolyte for PHEV oriented lithium-ion and Lithium-air batteries with better performance and safety characteristics. Special attention will be given to the capabilities of electrolytes in improving the high voltage cycling of lithium-ion batteries.

Approach: Our approach is to use a combination of *in situ*, *ex situ* and time-resolved synchrotron based x-ray techniques to characterize electrode materials and electrodes taken from baseline ABR Program cells. *Ex situ* soft X-ray absorption spectroscopy (XAS) will be used to distinguish the structural differences between surface and bulk of electrodes using both electron yield (EY) and fluorescence yield (FY) detectors. Time-resolved X-ray diffraction technique will also be used to understand the reactions that occur in charged cathodes at elevated temperatures in the presence of electrolyte. In situ x-ray diffraction will be used to monitor the structural changes of the electrode materials during charge-discharge cycling at different conditions. A combination of time resolved X-ray diffraction (XRD), in situ soft and hard X-ray absorption (XAS), in situ transmission electron microscopy (TEM) techniques during heating will be applied to study the thermal stability of the electrode materials. The atomic layer deposition (ALD) technique will be used for the surface modification of new cathode materials, which will be studied using time resolved X-ray diffraction (XRD) for the effects of surface modification on the thermal stability. These approaches developed at BNL will be available to other members of ABR projects through extended collaboration. We will continue to develop new synchrotron based x-ray techniques such as combined in situ x-ray diffraction and mass spectroscopy during heating for the thermal stability of cathode material studies. We will continue to develop TEM based in situ diagnostic tools to study

the structural changes at both surface and bulk of the electrode particles with high spatial resolution.

Milestones:

(a) By April 2012, complete the study of thermal decomposition of charged $\text{Li}_x\text{Ni}_{0.8}\text{Co}_{0.15}\text{Al}_{0.05}\text{O}_2$ (NCA) cathode materials during heating using combined Time-Resolved XRD and Mass Spectroscopy. **Completed.** (b) By April 2012, complete the Time resolved r-ray diffraction (TRXRD) studies of ALD coated Al_2O_3 on $\text{Li}_{1.2}\text{Ni}_{0.17}\text{Co}_{0.07}\text{Mn}_{0.56}\text{O}_2$ new cathode material during heating. **Completed.** (c) By September 2012, complete the study of charged $\text{Li}_x\text{Ni}_{1/3}\text{Co}_{1/3}\text{Mn}_{1/3}\text{O}_2$ (NCM) cathode material for thermal decomposition during heating using combined Time-Resolved XRD and Mass Spectroscopy. **On schedule.** (d) By September 2012, complete the in situ XRD studies of $\text{Li}_{1.2}\text{Ni}_{0.15}\text{Mn}_{0.55}\text{Co}_{0.1}\text{O}_2$ (Toda HE5050) cathode material during charge-discharge cycling. **On schedule.**

Progress toward milestones for the 3rd quarter of FY2012:

(c) Summary of work in the past quarter related to milestone (c)

Progress has been made in studies of charged $\text{Li}_x\text{Ni}_{1/3}\text{Co}_{1/3}\text{Mn}_{1/3}\text{O}_2$ (NCM) cathode material using TR-XRD and MS. The thermal runaway has been ascribed to the reactions between the charged electrodes and the electrolyte. Therefore, in-depth understanding of the structural changes of the charged cathode material during thermal decomposition, with or without the presence of electrolytes and their relationship to the thermal stability of the cathode material is very important. In order to understand thermal degradation of the electrodes in Li-ion cells, we have developed techniques using the combination of the *in situ*-time resolved X-ray diffraction (TR-XRD) technique and the mass spectroscopy to study the structural changes and gas evolution during the thermal decomposition of charged cathode materials here we report our new studies on the structural changes of layered nickel based cathode materials (e.g., $\text{Li}_{1-x}\text{NiO}_2$, $\text{Li}_{1-x}\text{Ni}_{0.8}\text{Co}_{0.15}\text{Al}_{0.05}\text{O}_2$ and $\text{Li}_{1-x}\text{Ni}_{0.33}\text{Co}_{0.33}\text{Mn}_{0.33}\text{O}_2$) during thermal decomposition. The combined result from TR-XRD coupled with mass spectroscopy technique can provide valuable information for the development of new cathode materials as well as for the improvement of thermal stability of the materials being used currently.

Figure 1 shows the comparison of combined TR-XRD patterns with oxygen release from MS for $\text{Li}_{0.1}\text{Ni}_{0.33}\text{Co}_{0.33}\text{Mn}_{0.33}\text{O}_2$ (left) and $\text{Li}_{0.1}\text{Ni}_{0.8}\text{Co}_{0.15}\text{Al}_{0.05}\text{O}_2$ (right) in the absence of electrolyte as a function of heating temperature. The $\text{Li}_{0.1}\text{Ni}_{0.33}\text{Co}_{0.33}\text{Mn}_{0.33}\text{O}_2$ sample shows a clear phase transition from O1 structure to the Co_3O_4 type structure starting at about 170 °C and remained in this structure until 550 °C. During this phase transition, the oxygen release from MS shows a quite broad peak. In contrast, for the $\text{Li}_{0.1}\text{Ni}_{0.8}\text{Co}_{0.15}\text{Al}_{0.05}\text{O}_2$ sample, the phase transition from a hexagonal layered structure with $R\bar{3}m$ space group at room temperature to the LiMn_2O_4 -type spinel phase (space group of $Fd\bar{3}m$) only covers a narrow temperature between 160 to 200 °C, and then quickly changed to the MO-type rock-salt structure. As can be seen in the right panel of Fig. 1, the phase transitions of $\text{Li}_{0.1}\text{Ni}_{0.8}\text{Co}_{0.15}\text{Al}_{0.05}\text{O}_2$, especially the transition to

the rock-salt structure are accompanied with a very sharp oxygen release, indicating a poor thermal stability.

(d) Summary of work in the past quarter related to milestone (d)

The in situ XRD studies of $\text{Li}_{1.2}\text{Ni}_{0.15}\text{Mn}_{0.55}\text{Co}_{0.1}\text{O}_2$ (Toda HE5050) cathode material during charge-discharge cycling are underway.

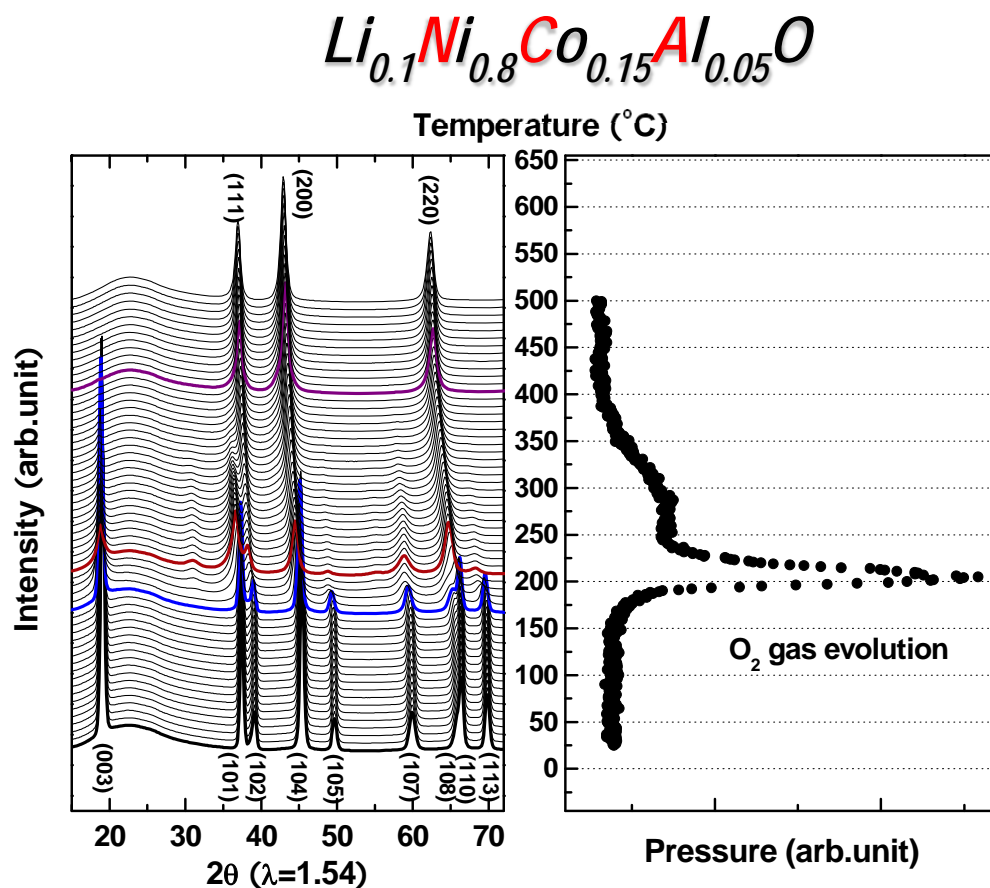


Fig. 1 Comparison of structural changes and oxygen release of overcharged $\text{Li}_{0.1}\text{Ni}_{0.33}\text{Co}_{0.33}\text{Mn}_{0.33}\text{O}_2$ (left) and $\text{Li}_{0.1}\text{Ni}_{0.8}\text{Co}_{0.15}\text{Al}_{0.05}\text{O}_2$ (right) by TR-XRD and MS during heating from 25 °C to 600 °C

TASK 2

Calendar & Cycle Life Studies

Project Number: CPS Project 18502, CPS Agreement 23060, ORNL FWP CEVT110 (ES165)

Project Title: Online and Offline Diagnostics for Advanced Lithium Secondary Battery Electrodes

Project PI, Institution: David Wood, Oak Ridge National Laboratory

Collaborators: Argonne National Laboratory, Keyence, Solar Metrology, Ceres Technologies

Project Start/End Dates: 10/1/11 to 9/30/14

Objectives: Due to high scrap rates of 10-20% or more associated with lithium secondary cell production, new methods of quality control (QC), which have been successful in other industries, must be implemented. Often flaws in the electrodes are not detected until the formation cycling when the entire series of manufacturing steps has been completed, and the associated scrap rates drive the costs of lithium secondary cells to an unacceptable level. If electrode flaws and contaminants could be detected in line near the particular processing steps that generate them, then the electrode material could be marked as unusable and the processing equipment could be adjusted to eliminate the defects more quickly. ORNL is considering in line analysis methods such as X-ray fluorescence spectroscopy (XRF) for electrode component uniformity and metal particle detection and laser thickness sensing of the electrode wet thickness measurement. In addition, on-line laser thickness measurement and IR imaging of wet and dry electrode coatings will be implemented for thickness uniformity and coating flaw detection. These methods have been effectively utilized in other industries such as photovoltaic, flexible electronics, and semiconductor manufacturing, but the equipment and measurement methods must still be tailored for lithium secondary cell production. The object of this project is to raise the production yield of lithium secondary battery electrodes from 80-90% to 99% and reduce the associated system cost by implementing in line XRF and laser thickness control. In addition, ORNL is providing its diagnostics capabilities and expertise to address materials issues with ABR cathode materials.

Approach:

Online diagnostics: Solar Metrology has been identified as a top manufacturer of in line XRF instruments for roll-to-roll applications and has a great deal of experience with the photovoltaics industry. ORNL will work closely with them to establish this technology for the lithium secondary battery industry. ORNL will produce tape casted and slot-die coated electrode rolls (anodes and cathodes) with deliberately introduced flaws to test the appropriateness of the method and the equipment modifications to the standard model. All key process parameters, such as line speed, coating thickness range, metal particle density, elemental homogeneity, etc., will be examined. In-line XRF data will also be

correlated with ex-situ XCT data to gain a complete chemical and structural picture of the electrode as it is coated and dried.

Keyence has been selected as the partner for developing a laser thickness sensor, or set of sensors, for lithium secondary battery electrode production. ORNL has a single-sided slot-die coating system, so only single-sided electrode coatings will be evaluated. ORNL will rent the sensors from Keyence and integrate them directly into ORNL's slot-die coating line for the proof-of-concept experiments.

The output data from the wet layer thickness measurements using the laser sensor(s) will be correlated with the thickness measurement capability by marking the regions that are out of specification during the coating process. The coated electrode rolls with markings will be fed into the in line XRF equipment to determine if wet regions out of specification match with dry regions that are determined to be out of specification. A feedback mechanism will be designed that considers whether the wet or dry thickness is a better input for adjusting the dispersion flow rate into the slot-die coater. The IR imaging QC will be correlated with thickness variation data to determine any further systematic flaw formation mechanisms.

ORNL characterization capabilities and offline diagnostics consisting of acoustic emission detection, in-situ and ex-situ X-ray diffraction, neutron scattering, and magnetic property determination will be utilized to investigate cathode materials issues with ABR developed materials, specifically Toda HE5050.

Milestones:

- a) Obtain in-line IR imaging data where different types of electrode coating flaws (pinholes, blisters, etc.) are identified (May 2012); delayed.
- b) A method of correlating wet and dry thickness using laser thickness measurement and in line XRF, respectively (June 2012); delayed.
- c) An in line XRF prototype(s) designed by Solar Metrology that measures electrode component uniformity, metal particle position, and dry electrode thickness (Sept. 2012); on schedule.
- d) A new or modified model of Keyence laser thickness sensor(s) specially designed for lithium secondary battery electrode dispersion deposition control (Sept. 2012); on schedule.
- e) Provide characterization and analysis for ABR developed HE5050 material provided by ANL (September 2012); on schedule.

Financial data: \$300k/year for FY12

PROGRESS TOWARD MILESTONES

Milestones (a) and (b) have been delayed due to equipment moving, installation, and commissioning in the new ORNL Battery Manufacturing Facility (BMF). The new target completion dates for these milestones are September 2012.

Task 1: Investigating the phase transformation pathways in TODA-HE5050 ($\text{Li}_{1.2}\text{Ni}_{0.15}\text{Mn}_{0.55}\text{Co}_{0.55}\text{O}_2$ or $0.5\text{Li}_2\text{MnO}_3 - 0.5\text{LiNi}_{0.375}\text{Co}_{0.25}\text{Mn}_{0.375}\text{O}_2$) cathode during electrochemical cycling; an in-situ XRD study.

Goal:

- Study the major structural changes in HE5050 cathode during electrochemical lithiation and delithiation between voltage window of 2.4V-4.8V.
- Determine lattice parameters and change in phase percentages as a function of charge/discharge cycles.
- Correlate the results with the electrochemical performance (voltage/ capacity fade).

Results

Summary from previous report (Q2):

1. In-situ XRD experiments were performed for as assembled, after 16 and 36 cycles and lattice parameters were calculated
2. Result showed the different trend in c- and a-lattice parameters cycled cells as compared to the fresh cell
3. This suggests different lithiation and delithiation mechanism in cycled cells that may lead to voltage/capacity fade

Results from this quarter (Q3):

In order to investigate the change in lattice parameter, the displacement of (003), (101), (102), (104), and (113) peak positions were analyzed for as assembled, cycled (after 36cycles). Those results are plotted as isoplots along with the electrochemical profile and shown in figure 1. The change in peak position of these planes are in agreement with change in lattice parameter values.

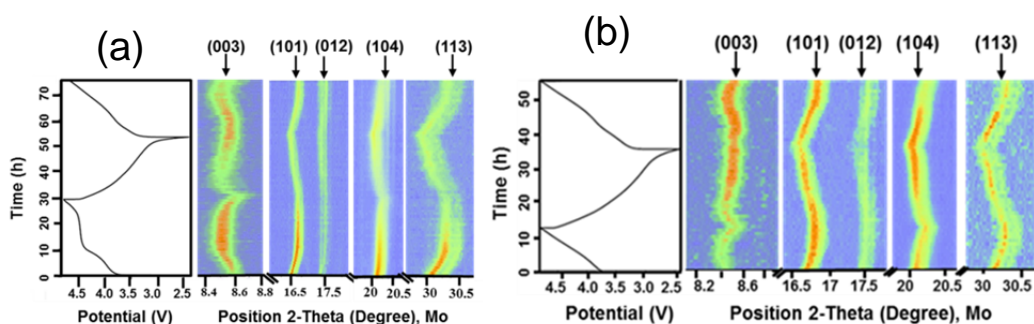


Figure 1: Isoplots of (003), (101), (012), (104), and (113) peak positions along with the electrochemical profile. These plots were collected from as assembled cell (a) and after 36 cycles (b).

Figure 2 represents the voltage profiles (electrode potential vs. capacity) of the material under investigation collected during 1st, 16th, and 36th cycles in the voltage window of 2.4 - 4.8 V. The cell shows 1st cycle charge capacity of 303 mAhg⁻¹ and discharge capacity of 232 mAhg⁻¹ at 10 mAh/g rate. First cycle irreversible capacity of ~70 mAhg⁻¹ with 1st cycle efficiency of ~77% was observed. After subsequent cycles (16 and 36 cycles), the discharge capacity decreased to 223 mAhg⁻¹ and 206 mAhg⁻¹ respectively. After 36 cycles, ~10% discharge capacity loss was observed as compared to the first cycle discharge capacity. However, the discharge voltage plateau shifts towards the lower voltage profile. This phenomenon is often termed as voltage decay/fade. To

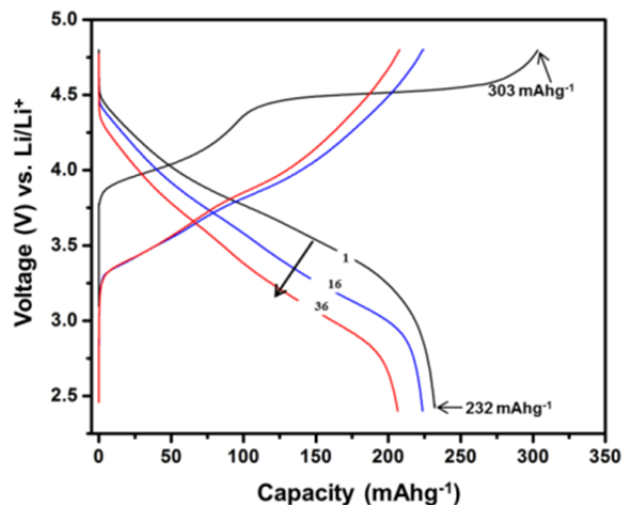


Figure 2: Galvanostatic charge/discharge profiles of Toda HE5050.

understand this behavior the XRD plots were carefully examined and explained as follows. The closer look at two theta range degree 27.5-29.5 degree is represented in figure 3. Interestingly, new peaks at ~28.32 degree 2-theta appear after 16 and 36 cycles (highlighted in dotted circle) during low voltage discharge (3.5-2.4 V) which are absent in the first 1.5 cycles (fig. 3a). These peaks remain during low voltage charging (2.4 - 3.5 V) and then disappear when charging beyond that voltage. These reflections are characteristic (440) peak of spinel phase (JCPDS # 00-018-0736) possibly due to presence of LiMn₂O₄ spinel phase. The whole structure still maintains remains as layered, it is anticipated that smaller size spinel domains may have been created in the crystals and locally integrated into the layered framework. This is also noted that the monoclinic (13 $\bar{3}$) peak disappears after subsequent cycling (figure 3). The disappearance of monoclinic phase after subsequent cycles is in agreement with the quantitative phase percentage values, where decrease in monoclinic phase was observed (64% trigonal and 36% monoclinic after 16 cycles, 72% trigonal and 28% monoclinic after 36 cycles). Therefore, it is believed that the spinel phase must have been formed at the expense of the monoclinic phase. The structural evolution from layered to spinel in the layered oxygen frame network in this lithium-rich oxide material may alter the lithium deintercalation/intercalation process. Therefore, after 16 (36) cycles, the lithium extraction/insertion should occur at different potential (voltage) as compared to the first cycle where only layered structure is present. This might be the reason for voltage drop/fade after subsequent cycling.

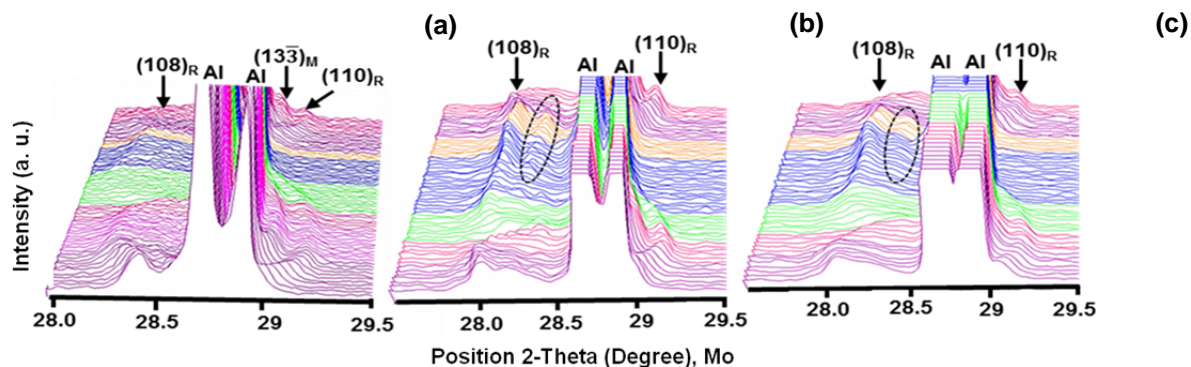


Figure 3: (108), (110), ($13\bar{3}$) reflection during first 1.5 cycles (a), after 16 cycles (b) and after 36 cycles (c). The R and M subscripts designate the rhombohedra (trigonal) phase and monoclinic phase respectively. The appearances of new peaks are highlighted in a dotted region.

Project 2: Investigating the structural changes in TODA-HE5050 ($\text{Li}_{1.2}\text{Ni}_{0.15}\text{Mn}_{0.55}\text{Co}_{0.55}\text{O}_2$ or $0.5\text{Li}_2\text{MnO}_3 - 0.5\text{LiNi}_{0.375}\text{Co}_{0.25}\text{Mn}_{0.375}\text{O}_2$) cathode during high-voltage hold via magnetic and transmission electron microscopy study.

Goal:

- Investigate the structural changes in TODA- HE5050 cathode materials during high-voltage hold.
- Correlate those structural changes with the impedance rise during high voltage hold.

Experimental

The electrochemical cycling was performed in a half cell (vs. Li^+/Li^0). Cells containing HE5050 cathode material were first charged to 4.6 V and discharged to 3.0 V followed by a second cycle charge up to 4.5 V at a rate of 20 mA/g. Consequently, the cells were held for required time interval. Separate cells were built for each experiments and electrochemical reaction was stopped at particular time of interest; before hold, after 90 h of hold to observe the effect of high voltage hold on the $\text{Li}_{1.2}\text{Ni}_{0.15}\text{Mn}_{0.55}\text{Co}_{0.55}\text{O}_2$ cathode oxide. Consequently, the cells were disassembled and cycled cathodes were retrieved, washed with PEC for several times and dried overnight. The ex-situ XRD pattern were collected on a PANalytical X'Pert Pro system. Transmission electron microscopy (TEM) was performed by using Cs- corrected Hitachi HF3300 TEM at 300kV. For pristine material, the powder was dispersed in the ethanol and few drops were added to a holy TEM copper grid. For cycled cathode, (after high-voltage hold) the material was obtained from the electrode by scratching off from the electrode. The material was ground by an agate mortar and the powder was dispersed in ethanol and sonicated for 10-15 minutes. Few drops from the solution were added to the holy Cu grid. Selected area electron diffraction was simulated by using WebEMAPS. The magnetic measurement was performed in a Super conducting Quantum Interface Design (SQUID) under field cooling (FC) and zero field cooling (ZFC) at Magnetic field = 100 Oe.

Results

Summary from previous report (Q2):

1. From in-situ XRD the contraction of unit-cell along c-axis was observed during prolonged hold period.
2. The decrease in c-lattice parameter and increase in a-lattice parameter was observed at constant voltage (4.5 V).

Results from this quarter (Q3):

To investigate those unusual effect during voltage hold, ex-situ XRD and selected area electron diffraction (SAED) along with high resolution transmission electron microscopy (HRTEM) experiments were performed for pristine material, before hold, and after 90 h of hold. The ex-situ XRD results show very much similar trend compared to the in-situ XRD. The (003) peak positions shifts towards the higher 2θ angle indicating the decrease in c-lattice parameter and contraction of unit cell along c-axis during high-voltage hold. To understand this behavior, transmission electron microscopy (Figure 4) and magnetic susceptibility experiments (Figure 5) were performed.

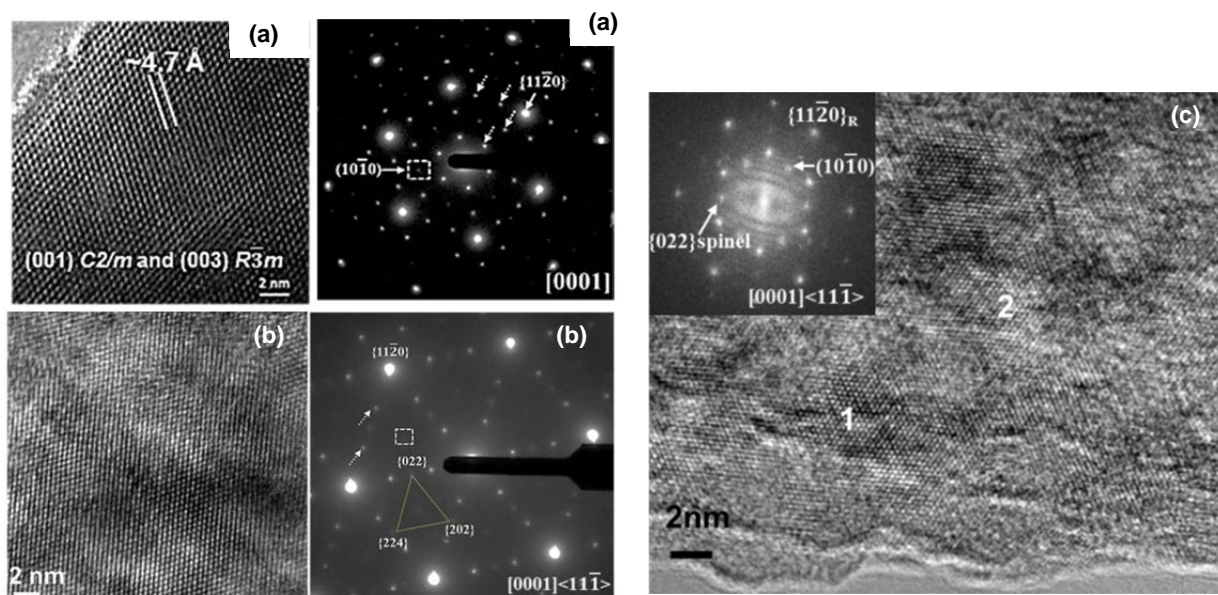


Figure 4. The HRTEM image and selected area electron diffraction from pristine HE5050 (a), charged at 4.5 V (b), and after hold for 90h (c).

The SAED from pristine material shows fundamental O3, $\{11\bar{2}0\}$ reflections (solid arrow) with monoclinic phase as superlattice reflections (dotted arrow). Faint forbidden $(10\bar{1}0)$ reflections (marked in a square) were also observed indicating some degree of Ni/Li interchange in the pristine material. After electrochemical delithiation, the monoclinic phase as well as O3 phase remains in the crystal however, the intensity of monoclinic phase is less compared to the pristine

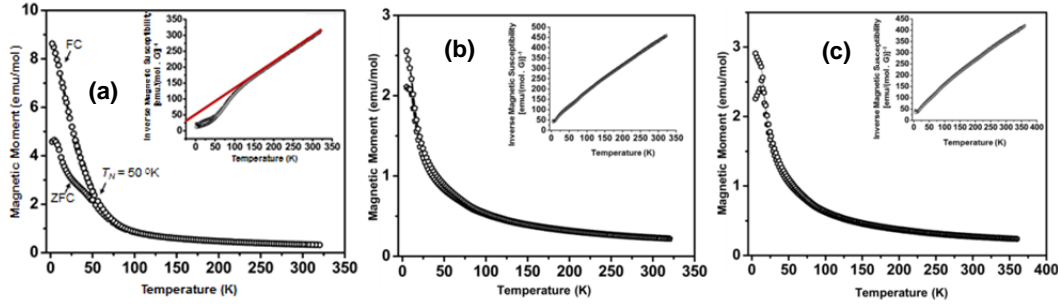


Figure 5. Variation of magnetic susceptibility with temperature for pristine HE5050 cathode (a), charging to 4.5 V(b), and after holding at 4.5 V for 90h (c).

material. After long term holding at 4.5 V, a spinel type reflection (022) could be visible from the particle surface. The HRTEM also shows spinel like domain on different areas of particle.

In Figure 5, the variation of magnetic moment with temperature and inverse magnetic susceptibility data (in set) are presented. The starting material shows magnetic ordering at lower temperature region which was suppressed during the charging. The ZFC curve after prolonged hold shows different trend as compared to other materials. This type of behavior may be related as “magnetic frustration” effect and originates due to simultaneous presence of ferro and ferri/anti-ferro magnetic domains in the unit cell. The calculated effective magnetic moment from the inverse magnetic susceptibility data along with Curie-Weiss temperature Θ (K) are represented in the table 1. It can be seen that the effective magnetic moment changes for the material undergone prolonged hold at 4.5 V which clearly establishes the fact that the average oxidation states of the material has been changes. The detailed analysis is in progress and will be presented in next quarterly report.

Table1: Effective magnetic moments and Curie-Weiss temperature of the pristine HE5050 cathode, after charging and after hold for 90h

Materials	μ_{eff} (μ_{B}) (Experimental)	μ_{eff} (μ_{B}) (Theoretical) Model	Θ (K)
Starting electrode	3.08 ± 0.0035	3.072 0.15Ni ⁺² (HS/LS) 0.55Mn ⁺⁴ (HS/LS) 0.1Co ⁺³ (LS)	-41 ± 0.7609
After 1.5 cycles charged up to 4.5 V	2.53 ± 0.0030	Ni must be oxidized to Ni ⁺⁴ (S=0)	-76 ± 0.6207
After 1.5 cycles charged up to 4.5 V, hold for 90 h	2.84 ± 0.0039	Oxidation state changes	-55 ± 0.8639

Planned Publications for next quarter.

4. D. Mohanty, S. Kalnaus, R. Meisner, A. Safa-Sefat, J. Howe, J. Li, D.L. Wood, C. Daniel, A. Payzant, and D.P. Abraham, "Investigating Phase Transformation Pathways During High-Voltage Hold of a Lithium-Rich $\text{Li}_{1.2}\text{Co}_{0.1}\text{Mn}_{0.55}\text{Ni}_{0.15}\text{O}_2$ Cathode by In-Situ X-Ray Diffraction," *Journal of Power Sources*, To Be Submitted, 2012.
5. D. Mohanty, S. Kalnaus, R. Meisner, K.J. Rhodes, J. Li, D.L. Wood, C. Daniel, A. Payzant, and D.P. Abraham, "Structural Transformation of a Lithium-Rich $\text{Li}_{1.2}\text{Co}_{0.1}\text{Mn}_{0.55}\text{Ni}_{0.15}\text{O}_2$ Cathode Resolved by In-Situ X-Ray Diffraction During High Voltage Cycling," *Journal of Power Sources*, To Be Submitted, 2012.

TASK 2

Calendar & Cycle Life Studies

Project Number: 2.2A (ES111)

Project Title: Battery Design Modeling (PHEV Battery Cost Assessment)

Project PI, Institution: Kevin Gallagher, Dennis Dees, and Paul Nelson, Argonne National Laboratory

Collaborators (include industry):

Ira Bloom, Argonne National Laboratory

Dan Santini, Argonne National Laboratory

Project Start/End Dates: August 2010/ September 2014

Objectives: The objective of this task is to develop and utilize efficient simulation and design tools for Li-ion batteries to predict precise overall (and component) mass and dimensions, cost and performance characteristics, and battery pack values from bench-scale results. Through these means, researchers and manufacturers will be able to better understand the requirements in the material and battery design to reach DOE cost and specific energy goals.

Approach: Our approach is to design batteries based on power and energy requirements for any chosen cell chemistry and then feed this design into a cost calculation that accounts for materials & processes required. Coupling design and cost allows the user to quantify the impact of underlying properties on the total battery pack cost (cell chemistry, parallel cells, electrode thickness limits, P/E). Furthermore, the efficient nature of these calculations means that various scenarios may be characterized in a short time span – analysis limited by the user not the model.

Milestones:

- (a.) Produce version 2.0 of the Battery Performance and Cost model (BatPaC) with documentation. October 2012 (On schedule)
- (b.) Implement liquid and air thermal management and evaluate role in design and cost. May 2012 (Complete)
- (c.) Support EPA and NHTSA use of BatPaC for 2017-2025 GHG regulation and CAFE standards rule making. March 2012 (Complete)
- (d.) Support the public distribution of the model and report. October 2012 (On schedule)
- (e.) Evaluate design and cost modeling of advanced Li-ion electrochemical couples. October 2012 (On schedule)

Financial data: \$300K/year

PROGRESS TOWARD MILESTONES

(a) Creation of battery performance and cost model BatPaC v2.0: BatPaC v2.0 is targeted for public distribution of late FY2012. Recent additions to the model include a separate worksheet that allocates the overhead directly onto the manufacturing processes and materials costs to directly evaluate the impact of each step in the battery process to the overall total cost to the original equipment manufacturer (OEM). Table 1 shows a simplified demonstration of how a cost is amplified by overhead tied to that material or process. For instance, the total cost of capital equipment is 3.9x the equipment cost while materials are only 1.07x purchase price. Figure 1 below shows a comparison between a traditional cost breakdown and the alternative approach with overhead distributed to the various manufacturing steps. The capital equipment is lumped under depreciation (8%) in Fig 1a) while in 1b) it is clear that electrode processing, cell fabrication and formation cycling are the most significant manufacturing steps and account for 20% of the total price to the OEM. Thus, the elimination or dramatic simplification of one of these manufacturing steps may be analyzed in a more direct fashion than in previous versions of the model.

Table 1. Overhead multipliers

Basic Cost Factors	Multiplier
Materials and purchased items, \$/pack	1.0666
Direct labor, \$/pack	1.8665
Capital equipment (100K packs/yr*)	3.8764
Building, land, utilities (100K packs/yr*)	1.5325

*For other production rates multiply by 100,000/rate

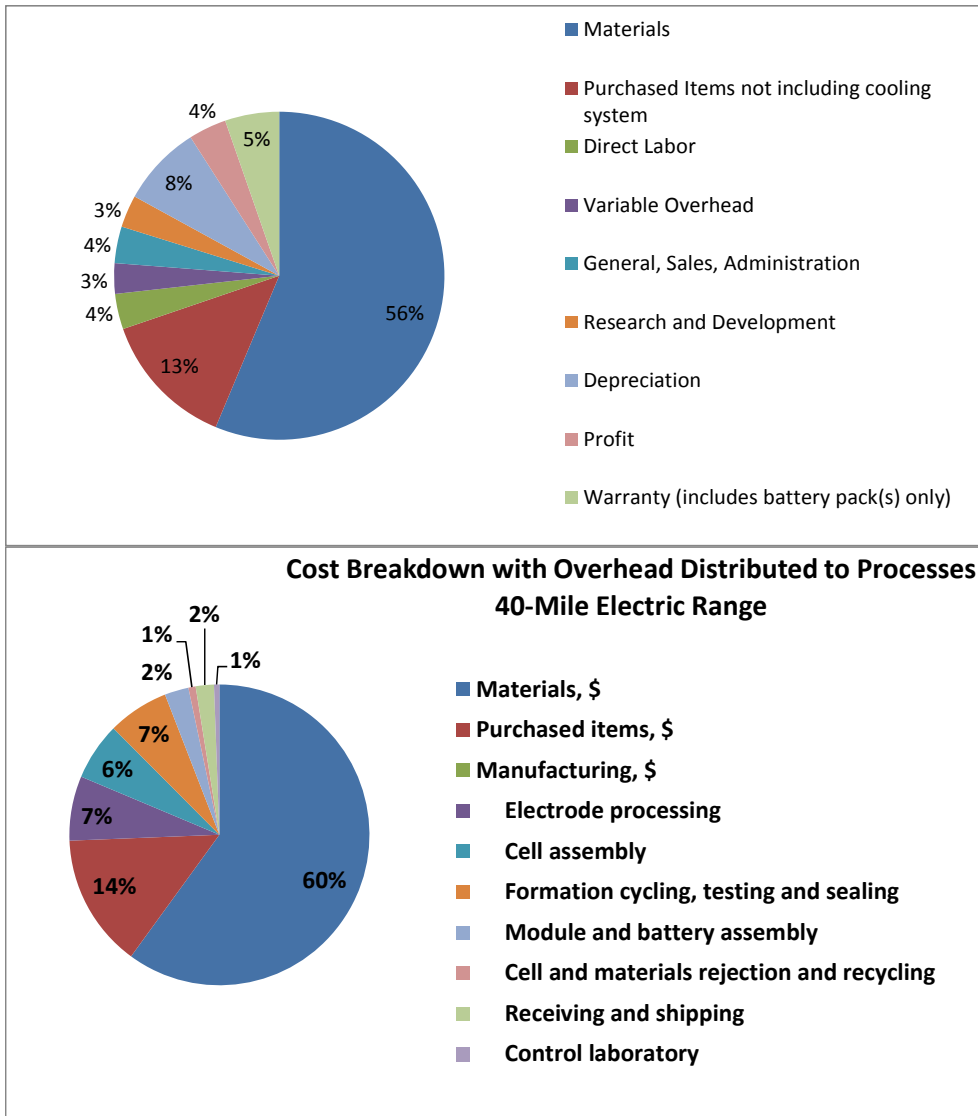


Figure 1. Cost breakdowns for a PHEV40 NCA-Gr a) traditional and b) with overhead allocated to manufacturing processes and materials.

(b) Implement thermal management options: Complete

(c) Support EPA 2017-2025 rule making: Complete. We will continue to support if new requests are made.

(d) Support public distribution: Interacted with multiple small and large companies to discuss BatPaC v1.0 availability, results of the model and some initial tips for use.

(e) Design & cost of advanced Li-ion: On-going.

**Publications, Reports, Intellectual property or patent application filed this quarter.
(Please be rigorous, include internal reports--invention records, etc.)**

Kevin G. Gallagher, J. Croy, M. Balasubramanian, D. Dees, D. Kim, S.-H. Kang and M.M. Thackeray, "Promises and Challenges of LMR-NMC Cathodes ($x\text{Li}_2\text{MnO}_3 \cdot (1-x)\text{LiMO}_2$, M = Ni, Co, Mn)" 221st ECS Meeting, Seattle, WA May 8th (2012)

Kevin G. Gallagher, Dennis Dees, and Paul Nelson, "PHEV Battery Cost Assessment" 2012 DOE Annual Merit Review presentation given

TASK 3

Abuse Tolerance Studies

Project Number: 3.1 (ES035)

Project Title: Develop & evaluate materials & additives that enhance thermal & overcharge abuse

Project PI, Institution: Zonghai Chen & Khalil Amine, Argonne National Laboratory

Collaborators (include industry): Yang Ren, Yan Qin, Chi-Kai Lin

Project Start/End Dates: 10/01/2008~09/30/2014

Objectives: Identify the role of each cell material/components in the abuse characteristics of different cell chemistries; Identify and develop more stable cell materials that will lead to more inherently abuse tolerant cell chemistries; Secure sufficient quantities of these advanced materials (and electrodes) & supply them to SNL for validation of safety benefits in 18650 cells.

Approach: Three-phase strategy is adopted for the thermal property improvement, including securing material, tests on cell components, and validation at cell level. In-house synthesis, commercial source and partners are used to secure materials, and various electrochemical and thermal analysis are conducted at cell components level in the second phase, and finally the thorough validation is executed at cell level. At the second and third phase, certain feedbacks can be obtained to phase one. For overcharge study, similar strategy is applied but in the first phase organic synthesis is the major source to secure materials. In addition, when feedbacks go to phase one, new design can be achieved using organic knowledge to improve the performance in certain aspect.

Milestones

- (a) Investigating the impact of electrolyte components on thermal stability of composite high energy cathode (HE5050) (finished);
- (b) Investigating the impact of upper limit potential on thermal stability of composite high energy cathode (HE5050) (ongoing);

Financial data: \$325K/FY2012, part of the fund was allocated to voltage fade project.

PROGRESS TOWARD MILESTONES (1 page)

(a) Summary of work in the past quarter related to milestone (a).

Figure 1a shows the physical setup of in situ high energy X-ray diffraction (HEXRD) during the thermal abuse of electrode materials. Figure 1b shows a picture of a special design of sample holder to maintain the electrode material in the detection zone of high energy X-ray during thermal abuse, as well as an exemplary HEXRD pattern of

delithiated $\text{Li}_{1-x}[\text{Ni}_{1/3}\text{Mn}_{1/3}\text{Co}_{1/3}]_{0.9}\text{O}_2$ (charged to 4.1 V vs. Li^+/Li). The diffraction peaks of layered materials can be clearly indexed as shown with red labels in Figure 1b. Figure 2a shows a comparison of HEXRD patterns for delithiated HE5050 ($0.5\text{Li}_2\text{MnO}_3 \bullet 0.5\text{LiNi}_{0.375}\text{Mn}_{0.375}\text{Co}_{0.25}\text{O}_2$, charged to 4.6 V vs. Li^+/Li) after being thermally abused at different chemical environments. The composition is further summarized in Table 1. When no solvent or electrolyte was added to the delithiated HE5050 sample, the material converted to M_3O_4 spinel structure after the thermal abuse, and M_3O_4 type structure was maintained up to 400°C . However, rock-salt type $\text{M}_x\text{Ni}_y\text{Co}_{1-x-y}\text{O}$ ($\text{M}=\text{Mn}$ and Co) and MnCO_3 was detected when an equivalent amount of solvent (EC/EMC 3:7 by weight) was added to the sample. With the presence of electrolyte (1.2 M LiPF_6 in EC/EMC, 3:7 by weight), the final product is $\text{M}_x\text{Ni}_{1-x}\text{O}$, MnCO_3 and MnF_2 . Figure 2b shows the in situ HEXRD profile of the sample with the presence of non-aqueous electrolyte and during the thermal abuse. It was found that the layered structure converted to regular spinel structure (LiM_2O_4) at about 206°C and that the regular spinel structure converted to M_3O_4 type spinel at about 234°C . At 310°C , the material finally decomposed into MnCO_3 , $\text{M}_x\text{Ni}_{1-x}\text{O}$ and MnF_2 . This mechanism is further summarized in Figure 2c.

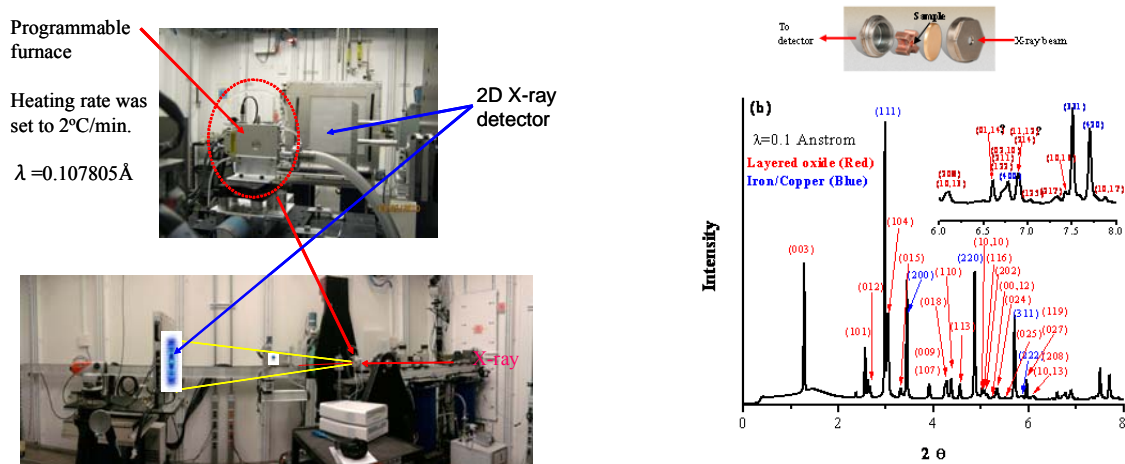


Figure 1 (a) Picture of in situ XRD set up at APS; and (b) Image of the sample holder used for in situ high energy X-ray diffraction, and an exemplary high energy X-ray diffraction pattern that was fully indexed with sample holder and layer lithium transition metal oxide.

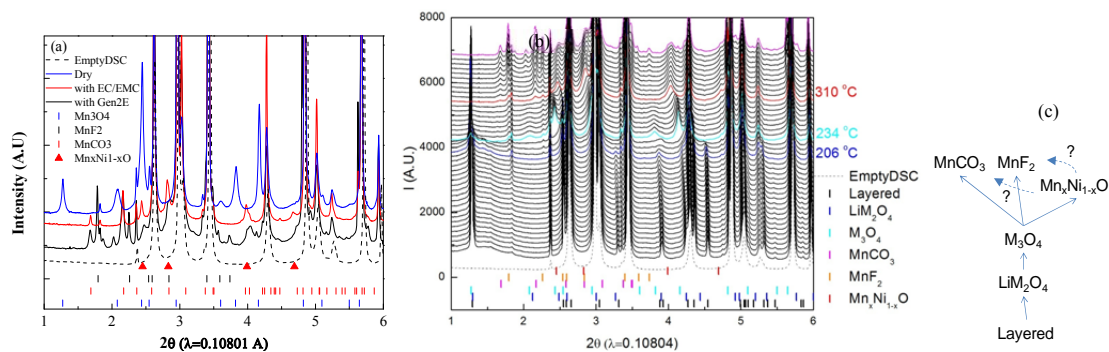


Figure 2(a) Comparison of HEXDRD patterns of abused delithiated HE5050 (charged to 4.6 V vs. Li^+/Li) showing that the decomposition pathway strongly depended on the chemical environmental it was exposed to, (b) in situ HEXRD pattern of delithiated HE5050 with the presence of electrolyte, and (c) proposed decomposition pathway for delithiated HE5050 with the presence of electrolyte.

Table 1 Decomposition products of delithiated HE5050 (charged to 4.6 V vs. Li^+/Li) after thermal abuse.

	$\text{M}_x\text{Ni}_{1-x}\text{O}$	MnCO_3	MnF_2	M_3O_4 -type
With Gen2E	Yes	Yes	Yes	No
With EC/EMC	Yes	Yes	No	No
Dry	No	No	No	Yes

(b) Summary of work in the past quarter related to milestone (b)

HE5050 is considered as high energy cathode material because it can be charged to a relatively high potential (up to 4.6 V vs. Li^+/Li) to deliver a higher specific capacity. It is also important that the safety of batteries will not be compromised for the higher energy density. Therefore, the chemical and thermal stability of will also be investigated against the upper cutoff potential. The in situ HEXRD experiments for materials charged up to 4.4, 4.5, 4.6 and 4.8 V vs. Li^+/Li have been carried out in this quarter, and the detailed data analysis and the kinetics of decomposition reactions will be reported in the coming quarter. In addition, the electrochemical compatibility of HE5050 with non-aqueous electrolyte as a function of the upper cutoff potential is under investigating, and the results are also expected to be reported in the coming quarter.

Publications, Reports, Intellectual property or patent application filed this quarter. (Please be rigorous, include internal reports--invention records, etc.)

1. Zonghai Chen, Yang Ren, Andrew N. Jansen, Chi-kai Lin, Wei Weng, and Khalil Amine, $\text{Li}_2\text{B}_{12}\text{F}_{12-x}\text{H}_x$ -Based Non-aqueous Electrolytes for Long Life and Safe Lithium-Ion Batteries, to be submitted to *Nature Communications.*, (2012).
2. Zonghai Chen, Yang Ren, Eungje Lee, Christopher Johnson, Yan Qin, and Khalil Amine, Study of Thermal Decomposition of $\text{Li}_{1-x}(\text{Ni}_{1/3}\text{Mn}_{1/3}\text{Co}_{1/3})_{0.9}\text{O}_2$ Using In situ

- High Energy X-ray Diffraction, to be submitted to *Advanced Energy Materials*, (2012).
3. Nam-Soon Choi, Zonghai Chen, Stefan A. Freunberger, Xiulei Ji, Yang-Kook Sun, Khalil Amine, Gleb Yushin, Linda F. Nazar, Jaephil Cho, and Peter G. Bruce, Current Issues in Energy Storage Materials and Devices, submitted to *Angew. Chem. Int. Ed.*, (invited, revision), (2012).
 4. Yang-Kook Sun, Zonghai Chen, Hyung-Joo Noh, Dong-Ju Lee, Hun-Gi Jung, Yan Ren, Steve Wang, Chong S. Yoon, Seung-Taek Myung, and Khalil Amine, Nano-Structured High-Energy Cathode Materials for Advanced Lithium Batteries, submitted *Nature Materials*, (revision), (2012).
 5. Zonghai Chen, Ilias Belharouak, Y.-K. Sun, and Khalil Amine, Titanium-Based Anode Materials for Safe Lithium-Ion Batteries, submitted to *Advanced Functional Materials*, (in press), (2012).

TASK 3 Abuse Tolerance Studies

Project Number: 3.2 (ES036)

Project Title: Abuse Tolerance Improvements

Project PI, Institution: Chris Orendorff, Sandia National Laboratories

Collaborators (include industry): ANL, INL, BNL, ORNL, NREL, Binrad Industries, Physical Sciences Inc., A123

Project Start/End Dates: 10/1/2011-9/30/2012

Objectives: The objective of this work is to develop inherently abuse tolerant lithium-ion cell chemistries. This involves understanding the mechanisms of cell degradation and failure, determining the effects of new materials & additives on abuse response, and cell level abuse testing and cell characterization to quantify improvements

Approach: Materials to full cell characterization to determine inherent safety and reliability of the most advanced lithium-ion chemistries. Approaches include a suite of battery calorimetry techniques (microcal, DSC, TGA/TDA, isothermal, ARC), abuse tests (electrical, mechanical, thermal), and analytical diagnostics (electrochemical characterization, optical spectroscopy, mass spectrometry, computed tomography, electron microscopy, etc.)

Milestones:

- (a) LiF/ABA electrolyte development (ON GOING, on schedule)
- (b) Cell prototyping optimization & collaboration with other Labs (ON GOING, on schedule)
- (c) Overcharge shuttle evaluation in full cells (DUE 9/30/2012, on schedule)
- (d) Support INL phosphazene electrolyte development (DUE 9/30/2012, on schedule)
- (e) Ionic liquid electrolyte development (ON GOING, on schedule)

Financial data: Total budgeted \$1.0M; received \$1.0M (from SNL); \$45K subcontract to Binrad Industries (ABA), \$10K subcontracted to Physical Sciences Inc. (phosphate-coated NMC)

PROGRESS TOWARD MILESTONES

(a) LiF/ABA electrolyte development. FY12 will focus on (1) developing new ABA molecules with improved voltage stability and (2) characterization of the degradation mechanisms of ABAs that lead to cathode passivation during runaway. As noted in Q2, SEI formation using LiF/ABA appears to be problematic as shown by the significant capacity fade in graphite anode half cells (Figure 1, left panel). The addition of VC appears to improve the capacity fade by stabilizing the anode interface, but additional

experiments are in progress to confirm this behavior and will be reported in Q4. XPS of NMC cathodes at elevated temperature show a change in the Co-O phase in the presence of the ABA (Figure 1, right panel, green trace). Results suggest a more oxidized surface (shoulder at 787 keV) with ABA electrolytes compared to LiPF₆ which is consistent with calorimetry results (less oxygen release, less combustion, and reduced specific heat output). The synthesis of 5 g of the second generation ABA was completed in Q3. After preliminary electrochemical and cell-level characterization in Q4, we will initiate discussion with the ANL Scale-Up Facility to make kilogram quantities of candidate ABAs. The objective of the new ABA is to provide improved high voltage stability for use with high voltage cathodes.

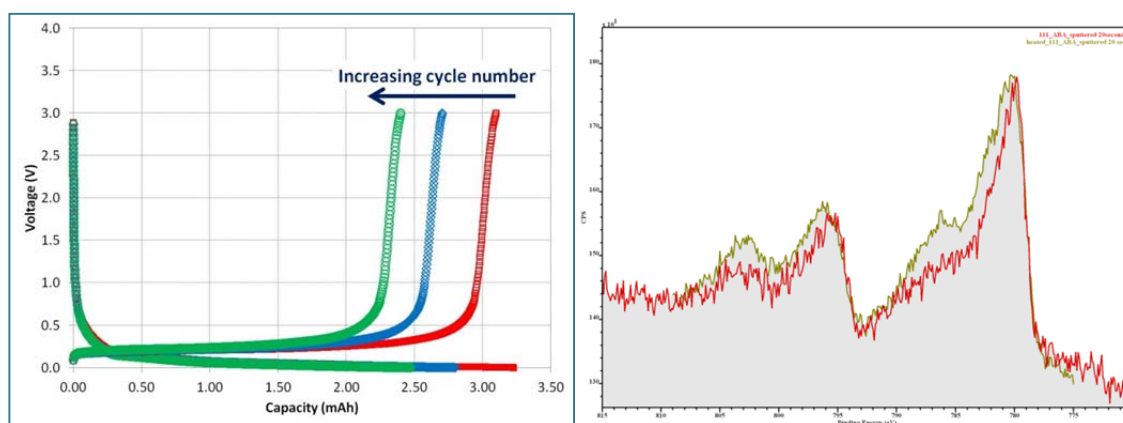


Figure 1. D/C capacity of anode ½ cells in 1.0 M LiF/ABA in EC:EMC (3:7) (left panel) and XPS of the Co region of NMC111 with ABA at ambient temperature (red) and after exposure to 250 °C (green) (right panel).

(b) Cell prototyping optimization & collaboration with other Labs. The electrode processing standardization effort between ANL/ORNL/SNL is underway with an electrode formulation of Toda 523 NMC:Denka carbon:Solvay binder (90:5:5). Electrodes have been cast at Sandia giving 157 mAh/g and the round robin testing activity is in progress (Figure 2). SNL has delivered the NMC523 (and NMC111) electrodes and powders to ANL for screening and to NREL for ALD coating. SNL will build cells for the JPL electrolyte and the high voltage materials projects in Q4.

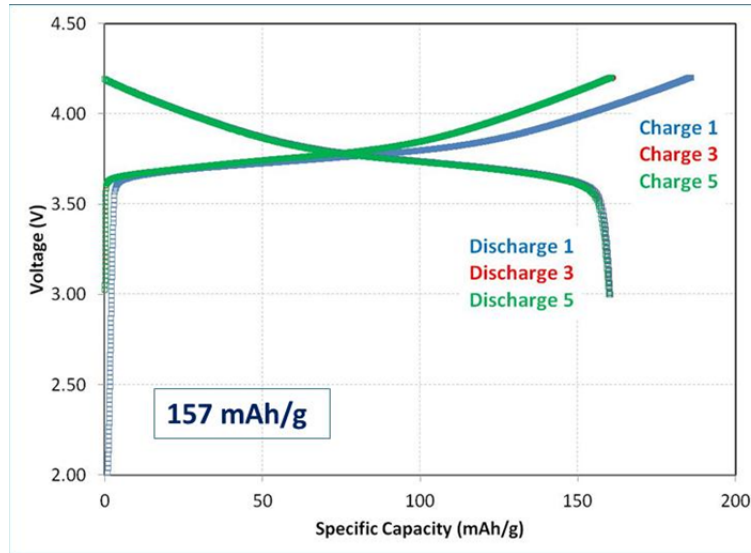


Figure 2. Charge and discharge capacity of NMC523

(c) Overcharge shuttle evaluation in full cells. The bulk of the RS2 shuttle work was completed in Q2 FY12. Q3 focused on tying up a few loose ends including (1) cell balancing experiments (5-10% imbalance) and (2) cell characterization post-overcharge. Figure 3 shows the time it takes for cells to be balanced at C/5 charge rate for two cells that are 10 and 50% out of balance. For the 50% imbalanced case, it takes 4.5 h for the cells to be balanced at a constant charge rate, while at 10% imbalance the cells are balanced in approx. 45 min. In both cases, the temperature rise is < 10 °C.

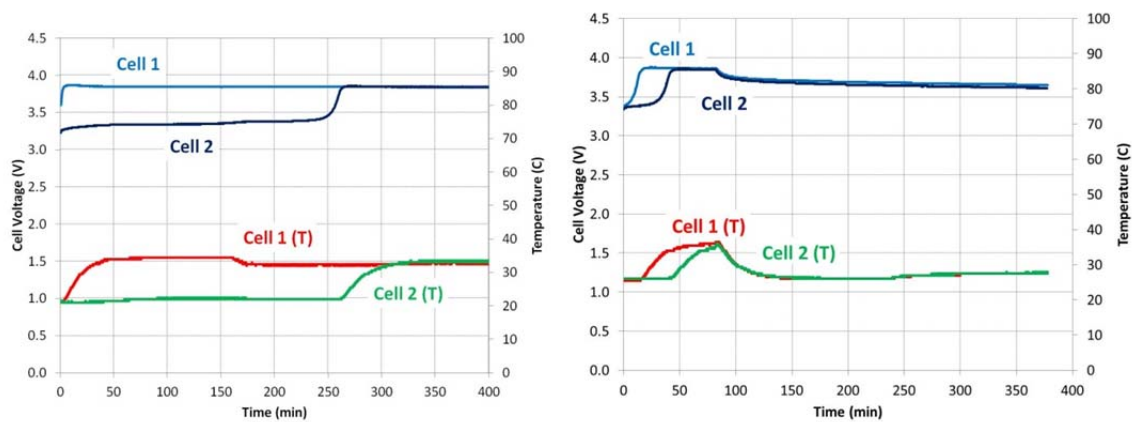


Figure 3. Cell voltage and skin temperature during cell balancing at 200 mA (C/5) for cells 50% (right) and 10% (left) out-of-balance.

As reported in Q2, cells with and without the shuttle were subjected to overcharge abuse at a 1C charge rate (Figure 4). After the abuse test, the measured capacity of the RS2 cell was 0.95 Ah, compared to 1.01 Ah for the fresh cell prior to the test. This is additional support for the utility of this shuttle not only to prevent a catastrophic failure of a cell

during overcharge, but to maintain cell functionality. In Q4 we plan on repeating this experiment and sending tested cells to ANL's Post-Test Facility for characterization.

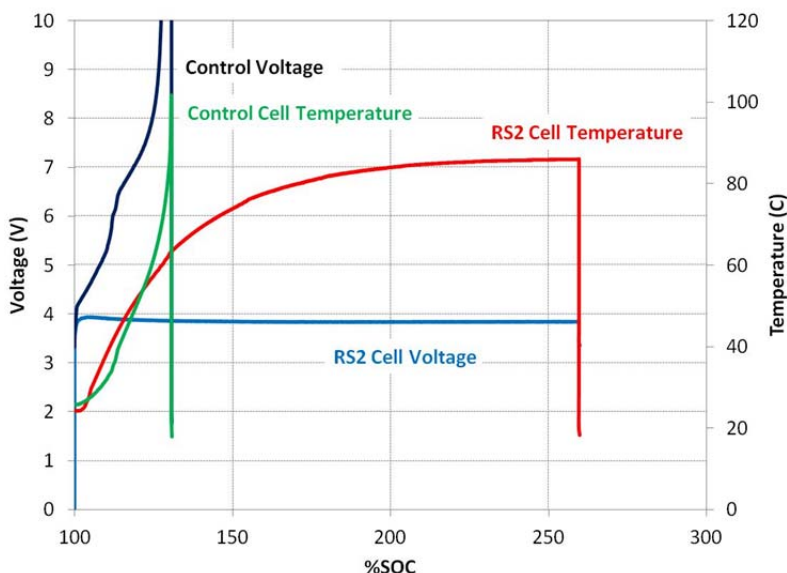


Figure 4. Cell voltage and skin temperature during a 1 A overcharge abuse test for cells with and without the redox shuttle

(d) Support INL phosphazene electrolyte development. Electrolytes were received from INL in early Q1 FY12. These include a control (1.2 M LiPF₆ in EC:EMC (2:8)) and phosphazene containing electrolytes SM-6, FM-2, and PhIL-1 (up to 3% by wt). Flammability measurements were made by sealing 5 mL of each electrolyte in an 18650 can and heating the sample until it ruptures the burst disk and vents into a spark ignition source placed 2 in. above the sample, as reported previously by our Laboratory (G. Nagasubramanian; C. J. Orendorff, *J. Power Sources*, 196 (2011) 8604). Flammability measurements are underway and will be reported in Q4.

(e) Ionic liquid electrolyte development. In parallel with characterizing IL-2 (from Q2), we have synthesized another candidate ionic liquid for use in lithium-ion cells (IL-3) in order to continue improving the voltage stability (both for low and high voltage stability). The chloride electrolyte and the sulfonimide show excellent stability up to 5V (vs. Li/Li⁺) shown in Figure 5.. Work in Q4 will continue on cell-level evaluation of IL-2 and IL-3 to determine their utility as lithium-ion cell electrolyte solvents.

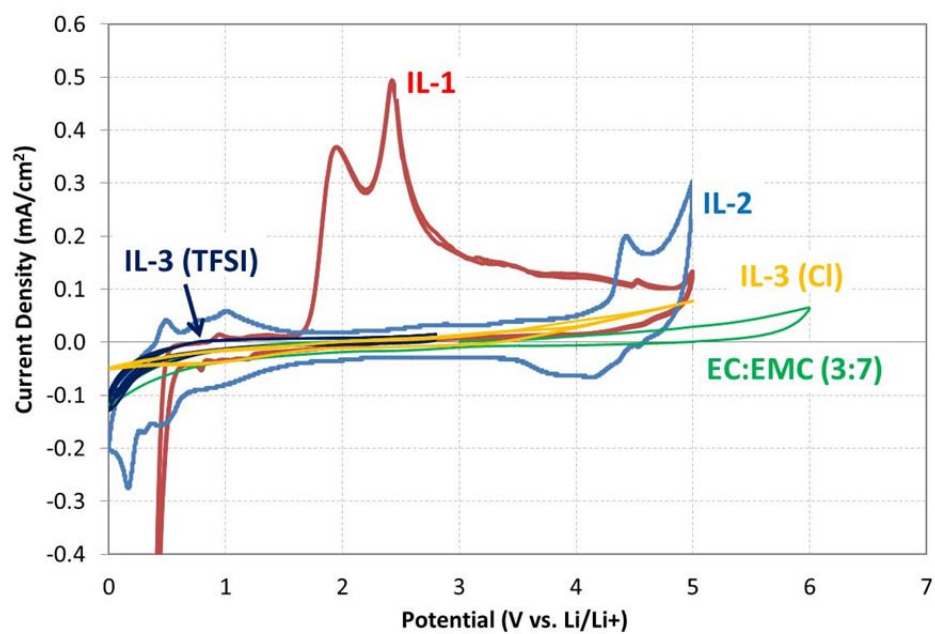


Figure 5. Current density as a function of potential (vs. Li/Li+) measured by cyclic voltammetry for candidate ionic liquids as electrolytes for lithium ion cells

TASK 3

Abuse Tolerance Studies

Project Number: 3.3 (ES037)

Project Title: Overcharge Protection for PHEV Batteries

Project PI, Institution: Guoying Chen and Thomas Richardson, Lawrence Berkeley

Collaborators: Robert Kostecki, John Kerr, Vince Battaglia, Marca Doeff, Gao Liu, Yuegang Zhang (Molecular Foundry)

Project Start Date: March 2009

Objectives: Develop a reliable, inexpensive overcharge protection system. Use electroactive polymers for internal, self-actuating protection. Minimize cost, maximize rate capability and cycle life of overcharge protection for high-energy Li-ion batteries for PHEV applications.

Approach: Our approach is to use electroactive polymers as self-actuating and reversible overcharge protection agents. The redox window and electronic conductivity of the polymer will be tuned to match the battery chemistry for non-interfering cell operation. Rate capability and cycle life of the protection will be maximized through the optimization of polymer composite morphology and cell configuration.

Milestones:

- a) Investigate overcharge protection performance of polymer fiber incorporated composite separators (Jun. 2012). **Complete**
- b) Evaluate the property and performance of new high-voltage electroactive polymer candidates (Jul. 2012). **On Schedule**
- c) Report overcharge protection for pouch and other large-scale battery cells (Sep. 2012). **On Schedule**

Financial data: \$190K (FY2009), \$190K (FY2010), \$250K (FY2011)

PROGRESS TOWARD MILESTONES

We have demonstrated that electrospinning is capable of producing non-woven electroactive-fiber-composite mats with high porosities and open pore structures. Despite the dilution of electroactive polymer within an inert polymer matrix, *in situ* optical experiments confirmed that charge carriers propagate rapidly within the fibers and across the interconnected fibers. Synthesis conditions can be varied to prepare uniform fiber composites with a varying degree of fiber-level mixing between the electroactive and supporting polymers. Figure 1a shows the SEM image of a composite consisting of poly(3-butylthiophene) (P3BT) and poly(ethylene-oxide) (PEO) in a weight ratio of 3:1. The fibers have an average diameter of 1 μm , and solvent evaporation produced 100 nm pores on the fiber surfaces. Energy dispersive X-ray spectroscopy (EDS) elemental mapping of O and S, which located PEO and P3BT, respectively, indicated that the two polymers in this composite are intimately mixed at the individual fiber level (Fig. 1b). The even distribution of the electroactive polymer should improve its utilization and reduce the cost for overcharge protection separators.

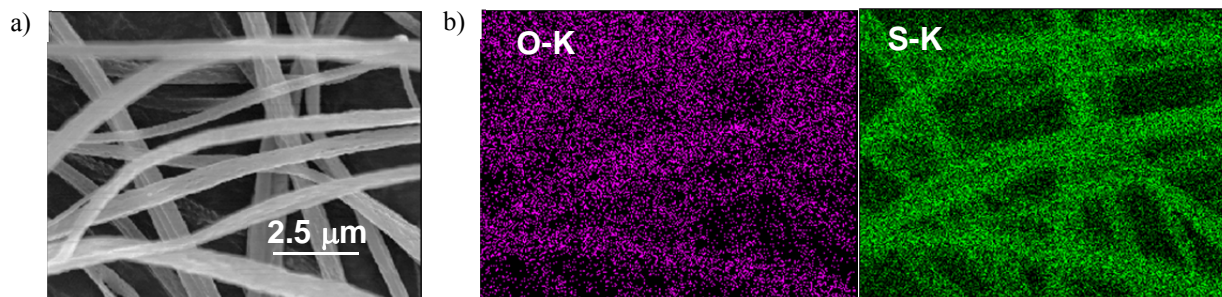


Figure 1. a) SEM image of the P3BT and PEO composite prepared by electrospinning and b) EDS maps of oxygen and sulfur.

Dense electroactive-fiber membranes, suitable for use as lithium battery separators, were prepared by electrospinning. Fig. 2a shows a 25 μm -thick composite membrane composed of poly[(9,9-dioctylfluorenyl-2,7-diyl)] (PFO) and PEO in a weight ratio of 1:3. Initial results for a $\text{Li}_{1.05}\text{Mn}_{1.95}\text{O}_4$ half-cell protected by a bilayer separator consisting of the PFO/PEO fiber membrane and a P3BT-glass fiber composite are shown in Fig. 2b. When cycled at a C/3 rate and 50% overcharge, a steady state was reached at 4.6 V, and the cell maintained its discharge capacity for more than 50 cycles. Compared to previous composites prepared with a microporous Celgard membrane, these nonwoven membranes provided electronic and dendritic barriers with lower ionic resistance, enabling faster charge and discharge for increased power density. The study suggests that electrospinning can be a cost-effective way to produce lithium-ion battery separators capable of voltage-regulated shunting. In May 2012, this technology was filed in U.S. Patent Application 61/647,389, titled “High-Rate Overcharge-Protection Separators for Rechargeable Lithium-ion Batteries and the Methods of Making the Same”.

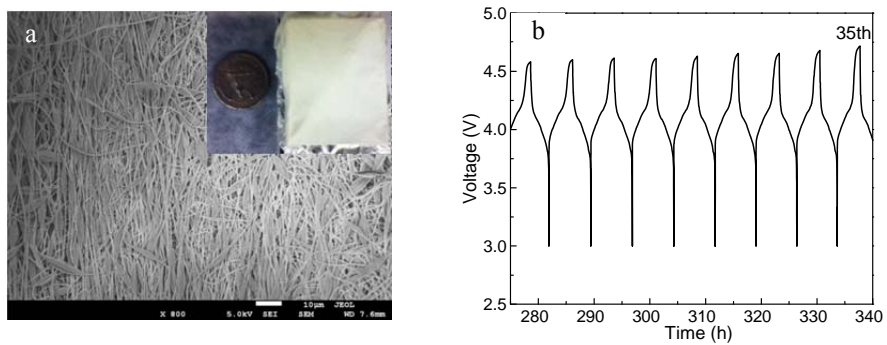


Figure 2. a) Digital (inset) and SEM images of the PFO and PEO composite separator and b) cycling voltage profiles of the protected $\text{Li}_{1.05}\text{Mn}_{1.95}\text{O}_4$ half-cell.